Michèle Corrigan, B.Sc.

Deciphering the Molecular Mechanisms of Stem Cell Mechanotransduction: A New Avenue for the Development of Therapeutics for Osteoporosis

Trinity College Dublin 2019

A thesis submitted to the University of Dublin in partial fulfilment of the requirements for the degree of

Doctor of Philosophy

Supervisor: Prof. David A. Hoey

Internal examiner: Prof. Bruce Murphy

External examiner: Prof. Alicia El Haj

Declaration

I declare that this thesis has not been submitted as an exercise for a degree at this or any other university and is entirely my own work. I agree to deposit this thesis in the University's open access institutional repository or allow the library to do so on my behalf, subject to Irish Copyright Legislation and Trinity College Library conditions of use and acknowledgement

X

Michele Corrigan

Summary

Osteoporosis is characterised by reduced bone density and weakened bone architecture leading to high fracture risk. The changes in bone tissue result from an imbalance in the bone remodelling cycle whereby the rate of resorption via osteoclasts increases along with a decrease in bone formation by MSC derived osteoblasts. The most common treatments for osteoporosis inhibit resorption and have adverse side effects including atypical fractures and limited efficacy. Bone tissue adapts to the surrounding mechanical environment, increasing bone formation in response to loading which requires the osteogenic differentiation of MSCs. It is appreciated that MSCs respond to mechanical stimuli but the mechanisms by which loading is transduced into MSC lineage commitment lacks understanding. The delineation of these mechanotransduction mechanisms is sought to identify novel anabolic therapeutic targets to correct net bone loss in osteoporosis.

The first objective of this thesis was to delineate the molecular mechanisms mediating the biophysical induction of MSC osteogenesis leading to bone formation. In Ch 3, the role of the mechanosensitive channel TRPV4 in mediating a calcium influx and downstream osteogenesis in response to fluid shear was demonstrated in MSCs. Furthermore, a protocol to biochemically activate TRPV4 to mimic the MSC response to fluid shear was developed. In Ch 4, the influence of primary cilium activity on MSC mechanotransduction was investigated and a protocol to elongate the primary cilium to enhance mechanosensitive osteogenic responses was established. A second objective was to determine the suitability of mechanotherapeutics as an anabolic treatment in osteoporotic MSCs. In Ch 5 the diminished migration, proliferation and differentiation capacity of osteoporotic MSCs were determined and benchmarked to healthy counterparts. Finally, in Ch6 the effect of activating, TRPV4 and the cilium, in terms of MSC osteogenesis was investigated in the setting of osteoporosis.

In the first study, it was shown that fluid shear induced calcium signalling in MSCs is dependent on the transmembrane channel TRPV4. Furthermore, the fluid shear induced upregulation of the osteogenic gene expression is abrogated by antagonising TRPV4. Treating MSCs with the specific TRPV4 agonist, GSK101, can mimic the fluid shear induced calcium signal and upregulation of early osteogenic matrix deposition, demonstrating the importance of TRPV4 in MSC osteogenic lineage commitment. Although TRPV4 is expressed through the MSC membrane, it is heavily localised to the primary cilium. MSCs where the cilium is abrogated show an altered response to biochemical TRPV4 activation suggesting an important role for the cilia-localised TRPV4.

The second study sought to enhance primary cilium mediated MSC osteogenesis. Three known ciliotherapies were investigated of which both lithium chloride (LiCl) and fenoldopam

enhanced MSC cilium incidence and length. However, LiCl increased Hedgehog and decreased Wnt activity while fenoldopam did not. Moreover, LiCl negatively affected osteogenic markers while fenoldopam maintained or increased expression. Both treatments increased the fluid shear induced *Cox2* upregulation demonstrating enhanced mechanosensitivity. Cell proliferation significantly decreased in LiCl. Fenoldopam upregulated mechanically stimulated calcium deposition and was determined as the optimal ciliotherapy to enhance osteogenic differentiation of MSCs.

In the third study MSCs were isolated from the bone marrow aspirates of healthy and osteoporotic human donors and their bone regeneration capacity evaluated. Osteoporotic MSCs display an inhibited migration to FBS, diminished basal expression of *COX2* and an inhibited upregulation of *COX2, OPN* and *RUNX2* in response to fluid shear as well as diminished proliferation. Furthermore, calcium deposition under biochemically induced osteogenic differentiation was decreased and the quality of osteogenic matrix was compromised in osteoporotic MSCs. Surprisingly, osteoporotic MSCs also showed diminished formation of adipogenic matrix. Outlining deficits in the bone forming capacity of osteoporotic MSCs especially the reduced mechanoresponse in osteoporotic MSCs highlight potential targets for therapeutic design to support bone formation.

The final study applied the protocols developed for the biochemical activation of the TRPV4 and primary cilium mediated mechanotransduction mechanisms to healthy and osteoporotic MSCs. Initially, healthy and osteoporotic MSCs were evaluated for TRPV4 and primary cilium activity. This revealed a loss in the fluid shear induced upregulation of *TRPV4* in osteoporotic MSCs. It was also demonstrated that in osteoporosis, cilium incidence and length are significantly diminished. Applying GSK101 maintained but did not enhance TRPV4 expression in healthy or osteoporotic MSCs. The fenoldopam protocol developed earlier elongated osteoporotic MSC primary cilia and displayed a similar trend in healthy counterparts. Moreover, GSK101 increased the fluid shear induced collagen formation of osteoporotic MSCs, while fenoldopam increased the fluid shear induced calcium formation in healthy MSCs. Together these results suggest that with further development targeting TRPV4 and the cilium could enhance the osteogenic response of MSCs to mechanical stimuli.

In conclusion, this thesis has delineated two mechanotransduction mechanisms facilitating the MSC response to fluid shear experienced during physical activity leading to osteogenic lineage commitment. TRPV4 is the principal channel mediating calcium signalling in MSCs experiencing fluid shear and mediates osteogenic gene expression and matrix deposition. TRPV4 can be biochemically activated to mimic the effect of fluid shear. The primary cilium can be biochemically elongated using fenoldopam to enhance MSC mechanosensitivity in terms

of fluid shear induced increases in gene expression and osteogenic matrix deposition. The discovery of a mechanosensitivity deficit in osteoporotic MSCs as well as reduced migration, proliferation and impaired differentiation will inform future therapeutic development. Finally, it was shown that these new mechanotherapeutics show promise in correcting this defect in MSC behaviour, and with further optimisation, could be used to enhance bone formation, correcting net bone loss in osteoporosis.

Acknowledgements

Over the long road of preparing and writing this thesis I have been supported, guided and encouraged by the most wonderful of people. For inspiring the very nerdy discussions between the brilliant Lab Techs of Scoil Mhuire, I want to sincerely thank Ms. Kiernan and Ms. Nulty for the work they do for so many students. For the sharing of woeful tales of university and everything else I want to thank Alanna, Doireann, Cliona, Aoibheann, Sarah, Clodagh, Sarah, Lorna, Catherine, Deirdre and Jenna. For a steady supply of encouragement and wise words I want to thank my partners in postgraduate research Shelly and Áine and more recently the wonderful David Tierney.

There was an unwavering source of spirit raising laughs, smiles, Holas and constant supply of scientific advice from the researchers of Trinity Centre for Bioengineering and Centre for Applied Biomedical Research. I started my PhD research as part of the first research group under Dr. Hoey's lead and I was lucky to be a part of our ambitious team. I got to spend an incredible couple of months at Prof. Christopher Jacobs lab in Columbia University and feel very lucky to have learnt from him and his lab group. Dr. Marie-Noëlle Labour taught me more than I could quantify about running a lab, molecular and cellular biology techniques and science communication, Dr. Mohamed Noor was another incredibly talented teacher who I am so grateful to have worked with. I would not have been able to complete this work without the hard work of research interns Thaïs and Emily, thank you, your papers are in the works! Thanks to Dr. Cairnan Duffy, Dr. Nian Shen, Dr. Ian Woods and Dr. Siobhán Coyle for all the guidance and good company in the lab. To the people I worked most closely with, you are very dear friends who have seen me at my worst! Dr. Kian Eichholz, Dr. Jilly Johnson- thanks for the chats, sharing your knowledge so generously and helping me

out and Dr. Elena Stavenschi Toth my desk buddy and best friend throughout this whole journey, I'm so glad to have learnt so much from you and with you. I want to give special thanks to Dr. Mathieu Riffault who has guided me through multiple existential crises and brought direction to my research. I wish to sincerely thank Dr. David Hoey's who has been so generous, thorough and patient in his supervision and guidance and it's at this stage that an appreciation for that really grows. Thank you for facilitating in every way possible, the completion of my PhD.

Without the constant support and care of my family I would never have started this and they've been very important in its completion too. Mum, Dad, Jennifer, William, Clara, Odhran, Woodie and Len, thanks for listening to long rants, visiting for tea, understanding when I was late or absent and making me happy. Lastly, I want to thank Ivor who is always there to lend a skilled hand in the lab, to give perspective on where my research fits into the literature and to pick up the pieces with endless patience.

Contents

List of Figures 13

List of Tables 24

Nomenclature 25

Conference Abstracts 27

Publications 28

Chapter 1: 29

Introduction 29

1.1 Osteoporosis 29

1.2 Bone formation and mechanoadaptation 31

1.3 Stem cell-mediated bone formation 32

1.4 Stem cell-mediated bone formation in osteoporosis 33

1.5 Mechanotransduction 34

1.6 Mechanotransduction in the setting of osteoporosis 35

1.7 Thesis Objectives 38

Chapter 2: 39

Literature Review 39

2.0 Introduction 39

2.1 The structure and function of bone 39

2.2 Bone formation and remodelling 44

2.3 Mesenchymal stem cells and their role in bone formation 47

2.4 Osteoporosis and the current therapeutic approach 52

2.5 Bone formation in osteoporosis 56

2.6 Loading-induced bone formation 59

2.7 Mechanosensing by mesenchymal stem cells 61

2.8 Mechanotransduction in mesenchymal stem cells 63

2.8.1 TRPV4 mediated mechanotransduction 67

2.8.2 Primary cilium mediated mechanotransduction 69

2.9 Summary 73

Chapter 3: 75

TRPV4-mediates oscillatory fluid shear mechanotransduction in mesenchymal stem cells in part via the primary cilium 75

3.1 Introduction 75

3.2 Methods 79

3.2.1 Mesenchymal Stem Cell Culture 79

3.2.2 Gene expression 80

3.2.3 Parallel Plate Flow Chambers 80

3.2.4 Calcium Imaging 81

3.2.5 Immunocytochemistry 82

3.2.6 Biochemical targeting of TRPV4 83

3.2.7 Extracellular matrix stain and extraction 84

3.2.8 Inhibition of primary cilia formation 84

3.2.9 Data Analysis 85

3.3 Results 86

3.3.1 Mesenchymal stem cells respond to oscillatory fluid shear with a rapid increase in cytosolic calcium and osteogenic gene expression 86

3.3.2 TRPV4 is expressed by mesenchymal stem cells and is found at mechanosensitive sites across the membrane 88

3.3.3 TRPV4 is required for oscillatory fluid shear mediated calcium signaling in MSCs 90

3.3.4 TRPV4 is required for oscillatory fluid shear mediated increases in osteogenic gene expression 92

3.3.5 Biochemical activation of TRPV4 induces a calcium response that mimics that produced by oscillatory fluid shear 93

3.3.6 TRPV4 activation induces an increase in osteogenic gene expression that mirrors that seen with mechanical stimulation 94

3.3.7 Biochemical modulation of TRPV4 activity influences bone matrix deposition 96

3.3.8 Mesenchymal stem cells with defective intraflagellar transport display 97

an altered response to TRPV4 activation 97

3.4 Discussion 100

3.5 Conclusion 104

Chapter 4: 106

Ciliotherapy Treatments to Enhance Biochemically- and Biophysically-Induced Mesenchymal Stem Cell Osteogenesis: A Comparison Study 106

4.1 Introduction 106

4.2 Methods 110

4.2.1 Mesenchymal stem cell culture 110

4.2.2 Biochemical modulation of cilium length 110
4.2.3 Immunocytochemistry 111
4.2.4 Measurement of primary cilium incidence and length 111
4.2.5 Measurement of β-catenin nuclear localisation 112
4.2.6 Gene expression 112
4.2.7 Mechanical stimulation 113
4.2.8 Extracellular matrix deposition 113
4.2.9 DNA Quantification 114
4.2.10 Data analysis 115
4.3 Results 115
4.3.1 The effect of ciliotherapy treatment on mesenchymal stem cell primary cilia incidence and length. 115
4.3.2 The effect of ciliotherapy treatment on cilia-associated signalling in MSCs. 118
4.3.3 The effect of ciliotherapy treatment on early MSC osteogenesis. 120
4.3.4 The effect of ciliotherapy treatment on biochemical induction of MSC osteogenic lineage commitment 122
4.3.5 The effect of ciliotherapy treatment on biophysical induction of MSC osteogenic lineage commitment. 125
4.4 Discussion 128
4.5 Conclusion 132
Chapter 5: 133
Human bone marrow MSCs isolated from osteoporotic patients demonstrate abnormal recruitment, mechanosensitivity, and osteogenic matrix deposition. 133
5.1 Introduction 133
5.2 Methods 136
5.2.1 Human bone marrow sample acquisition 136
5.2.2 Human bone marrow mesenchymal stem cell (hMSC) isolation and culture 137
5.2.3 Validation of hMSC Isolation 137
5.2.4 hMSC Migration 138
5.2.5 hMSC gene Expression 139
5.2.6 Mechanical Stimulation 140
5.2.7 Proliferation 140
5.2.8 Quantification of osteogenic matrix deposition 140
5.2.9 Quantification of adipogenic matrix deposition 141
5.2.10 Data Analysis 141
5.3 Results 142

5.3.1 Human bone marrow mesenchymal stem cells were isolated from healthy and osteoporotic donors 142
5.3.2 Osteoporotic hMSCs have defective chemotaxis 145
5.3.3 Osteoporotic hMSCs have reduced mechanosensitivity when compared to healthy controls 146
5.3.4 Osteoporotic hMSCs exhibit reduced cell growth when compared to healthy controls 148
5.3.5 Osteoporotic MSCs deposit abnormal and reduced osteogenic matrix when compared to controls 149
5.3.6 Defective hMSC osteogenic differentiation in osteoporosis does not lead to a shift to enhanced adipogenesis 153
5.4 Discussion 155
5.0 Conclusion 159
Chapter 6: 161
Targeting primary cilia and associated mechanosensitive channels as a therapeutic strategy to enhance human MSC osteogenesis in osteoporosis. 161
6.1 Introduction 161
6.2 Methods 163
6.2.1 Bone marrow mesenchymal stem cell isolation and culture 163
6.2.2 Biochemical treatments to promote TRPV4 activity and primary ciliogenesis 164
6.2.3 Immunocytochemistry 164
6.2.4 Measurement of primary cilium incidence and length 165
6.2.5 Measurement of TRPV4 intensity 166
6.2.6 Gene expression 166
6.2.7 Mechanical Stimulation 167
6.2.8 Staining and quantification of osteogenic matrix deposition 167
6.2.9 DNA Quantification 168
6.2.10 Data Analysis 168
6.3 Results 169
6.3.1 Osteoporotic hMSCs demonstrate similar TRPV4 expression but inhibited TRPV4 mechanoregulation when compared to healthy controls 169
6.3.2 Osteoporotic hMSCs have reduced cilium incidence and cilium length when compared to healthy controls 170
6.3.3 The effect of TRPV4 agonist (GSK101) and ciliotherapy (fenoldopam) treatment on TRPV4 expression and primary cilia structure in healthy and osteoporotic hMSCs 172
6.3.4 The effect of GSK101 and fenoldopam treatment on early osteogenesis in healthy and osteoporotic hMSCs 174

6.3.5 The effect of GSK101 and fenoldopam treatment on proliferation in healthy and osteoporotic hMSCs 176
6.3.6 The effect of GSK101 and fenoldopam treatment on the osteogenic lineage commitment and matrix deposition of healthy and osteoporotic hMSCs 177
6.4 Discussion 183
6.5 Conclusion 186
Chapter 7: 188
Discussion and Conclusion 188
7.1 Summary 188
7.2 Delineation of MSC mechanotransduction mechanisms 191
7.3 Human osteoporotic MSC treatment 193
7.4 Limitations and future directions 196
7.5 Conclusion 200
Supplementary Material: 202
Supplementary Figure 3.1 202
Supplementary Table 3.1: 202
Supplementary Figure 4.1 203
Supplementary Figure 4.2 204
Supplementary Table 4.1 205
Supplementary Table 5.1: 206
Supplementary Methods 5.2: 206
Supplementary Figure 5.1: 207
Supplementary Figure 5.2: 208
Supplementary Table 6.1: 209
References: 211

List of Figures

Figure 1.1: Overview of the mechanisms researched in this thesis and their application for therapeutic design. Initially the mechanical environment of bone marrow during physical activity will be modelled *in vitro* and the mechanisms mediating the mechanotransduction response leading to osteogenic differentiation will be delineated. Next, protocols to biochemically activate the mechanisms identified will be designed and applied to human MSCs to enhance bone modelling activity(Aoki et al., 2019). 37

Figure 2.1: Structure of bone A Gross anatomical features of a femur, B Cross sectional view of the osteon, a unit of cortical bone (Betts et al., 2018) 41

Figure 2.2: Structural features for mechanical efficiency in the head of the femur A illustration of the principal stresses experienced by the femur during physiological loading (Forsyth and Davey, 2008) B x-ray image showing pronounced trabeculae formation at 1 and 2 along the regions experiencing greatest tension and compression (Rudman et al., 2006) 43

Figure 2.3: The differentiation capacity of MSCs characterised according to ISCT guidelines on surface marker expression. Each lineage is marked by black arrows with the blue arrows and text indicating the transcription factors regulating the differentiation towards each lineage (Giuliani et al., 2013) 49

Figure 2.4 The bone and bone marrow interface describing the cells populating mature bone, osteocytes and osteoblasts, and the marrow, HSC (hematopoietic stem cell) which gives rise to osteoclasts and the MSC (mesenchymal stem cell) which gives rise to osteoblasts, adipocytes and chondrocytes (Castillo and Jacobs, 2010) 59

Figure 2.5: a-c Representation of the transmission electron microscopy informed structured of TRPV4 with each of the four subunits represented in a different colour. d Representation of the mechanism of action of ion channels stimulated by mechanical stimulus, illustrated by the red arrows (Huse, 2017, Deng et al., 2018) 68

Figure 2.6 Schematic of the primary cilium structure, illustration of the regulation of hedgehog signalling using the ciliary axoneme, (Singla and Reiter, 2006, Adams, 2010) 71

Figure 3.1: (A) Representative calcium profiles of individual MSCs during No Flow (green) and oscillatory fluid shear (OFS) generating 1Pa, 1Hz shear stress (blue). Stimulus begins at t=0s. Baseline values calculated from 20 seconds prior to the

application of OFS. The dashed black line at 1.2 fold change marks the value above which cells are considered to be responsive. (B) Fold increase in calcium at first peak during No Flow and OFS, Median ± Interquartile range, No Flow, n=17; OFS, n=21, Mann-Whitney test, ***p<0.001. (C) Frequency of cells eliciting a response or showing no response in static (green) and OFS (blue) conditions, N=3, n=36, Fisher's exact test, **p<0.01. (D) Time from onset of flow (t=0s) to first peak, Median ± Interquartile range, NF n=17, OFS n=21. (E) (F) Expression of early osteogenic markers in MSCs following application of 1Pa, 1Hz OFS for 2 hours, Mean ±SEM (E) *Cox2* N=4, n=8-13, (F) *Opn* N=4, n=14-20, student's t-test, *p<0.05, ** p<0.01 87

Figure 3.2: (A) Expression of *Trpv4* in cells exposed to 1Pa 1Hz OFS for 2 hours, Mean ±SEM N=3, n= 9-10, student's t-test, p>0.05. (B) Quantification of cell wide Trpv4 stain intensity under OFS, Median ± Interquartile range n=18-21, Mann Whitney test, **p<0.01. (C, D) Immunofluorescent staining of MSCs showing TRPV4 expression and the cytoskeleton (F-actin) (scale bar=10µm) following 2 hours at (C) static conditions and (D) 1Pa, 1Hz oscillartory fluid flow. (E, F) Immunofluorescent staining of MSCs showing TRPV4 expression and (E) focal adhesions using vinculin (scale bar=10µm, inset 1µm) and (F) primary cilia using acetylated alpha tubulin (scale bar =10µm, inset 1µm). (G) (H) Fluorescence intensity at region marked by arrow, along dashed white line in inset of (G) focal adhesion and (H) primary cilium. 89

Figure 3.3: (A) Representative calcium profile of individual MSCs responding to OFS generating 1Pa, 1Hz. OFS begins at t=0s. Cells treated with vehicle alone, DMSO, represented in the solid green; those treated for 1 hour pre mechanical stimulation with 10µM GSK205 are in the purple dashed line. Baseline values calculated from the 20 seconds prior to the application of OFS. The dashed black line at 1.2-fold change marks the value above which cells are considered to be responsive. (B) Median ± Interquartile range fold increase in calcium at first peak following application of treatment. Vehicle: N=4, n= 9; GSK205: N=4, n=22, Mann Whitney test, ***p<0.001. (C) Frequency of cells responding to the stimulus. Median ± Interquartile: Vehicle: N=4, n=22; GSK205: N=4, n=11, Fisher's exact test, *p<0.05. (D) Time to first peak for individual cells following application of stimulus at time 0s. Bars mark Median ± Interquartile, Vehicle: N=4, n=9; GSK205: N=4, n=22 ND= None determined, no responsive cells observed. 91

Figure 3.4: Basal gene expression in MSCs treated with vehicle control or 10µM GSK205 for 3 hours. (B) (D) Gene expression following 2 hours of 1Pa 1Hz OFS in each group. (A)(B) *Cox2* and (C)(D) *Opn*, represented as Mean ±SEM, N=4-6. n=12-

21; (A) (C) student's t-test (B)(D) 2 way ANOVA with Bonferroni post test; NS p>0.05, *p<0.05, **p<0.01, ***p<0.001 in comparison to the no flow control within the same treatment group, & p<0.05 significantly different effect of flow stimulus on the vehicle and antagonist treatment groups. 93

Figure 3.5: (A) Representative calcium profile of individual MSCs responding to OFS generating 1Pa, 1Hz shear stress. OFS begins at t=0s. Cells treated with equal amounts of the vehicle, DMSO and exposed to OFS are in solid green, those treated with 1nM GSK101 are represented by dashed blue line and 10nM GSK101 by the dark blue dotted line. All biochemical treatments are applied only from the onset of fluid shear. Baseline values were calculated from the 20 seconds prior to the application of OFS. The dashed black line at 1.2 fold change marks the value above which cells are considered to be responsive. (B) Median and interquartile range of fold increase in calcium at first peak following application of treatment. Control N=4, n= 9, 1nM GSK101 N=4, n=14, 10nM GSK101 N=4, n=19, Kruskal-Wallis test with Dunn's multiple comparisons post test, *p<0.05, NS p>0.05. (C) Frequency of calcium response in MSCs exposed to stimulus, OFS N=4, n=9, 1nM GSK101 N=4, n=31, 10nM GSK101 N=4, n=27, Chi-square test, NS p>0.05. (D) Time to first peak for individual cells following application of stimulus at time 0s. Bars mark Median and interquartile range, Control N=4, n=9, 1nM GSK101 N=4, n=14, 10nM GSK101 N=4, n=19. Kruskal Wallis test with Dunn's post-test, NS p>0.05. (E) *Cox2* and (F) *Opn* expression in MSCs treated with DMSO only, Vehicle, 1nM and 10nM GSK101 for 2 hours, Mean ±SEM N=2-3, n=7-13, 1 way Anova with Bonferroni post-test, *p<0.05, ***p<0.001. 95

Figure 3.6: Representative images of (A) picrosirius red and (B) alizarin red s staining of MSCs following 21 days treatment with vehicle (DMSO), GSK101 and GSK205 at 2x (scale bar=500µm, inset at 10x, scale bar=100µm). Quantification of (C) picrosirius (collagen) and (D) alizarin (calcium) stains extracted from each group in (A) and (B) n=6, statistical analysis One-way ANOVA with Dunnett's multiple comparisons post test *p<0.05, **p<0.01, p<0.001. 97

Figure 3.7: (A) Validation of inhibition of *Ift88* gene expression, N=4, student's t-test with Welch's correction, * p<0.05. (B) Frequency of primary cilium formation following transfection with siRNA, N=4-6, n=286-293, Fisher's exact test, ***p<0.001. (C) (D) Immunostaining of cells transfected with either off target control (C) or *Ift88* targeted siRNA (D) stained with acetylated α-tubulin, (primary cilium, red; arrows) and

pericentrin (centrioles, green; arrow head). Nuclei are counterstained with DAPI (blue). Scale bars represent 5μm and 1μm (insert). (E) (G) Basal gene expression in MSCs transfected with siRNA targeting *Ift88* or scrambled control, t-test, NS=Not significantly different. (F) (H) Gene expression following 2 hours of treatment with 10nM GSK101 in each group. (E)(F) *Cox2* and (G)(H) *Opn*, represented as Mean ±SEM, N=3, n=5-8, 2 way ANOVA with Bonferroni post-test, ***p<0.001 significant in comparison to the no flow control of each treatment group, && p<0.01, &&& p<0.001 significant effect of the treatment on the response to OFS. 99

Figure 4.1: Representative images of MSCs following treatment with A Forskolin or vehicle, DMSO, B Lithium Chloride (LiCl) or vehicle, H_2O and C Fenoldopam or vehicle, DMSO, for 1 hour and 24 hours at 100x fluorescence (red channel- acetylated alpha tubulin, green channel- pericentrin and DAPI) (scale bar 10μm), inset shows zoom on cilium (scale bar 1μm). D, F, H Percentage of cells in each group with a primary cilium N=3, n=194-275. Bars illustrate % ciliated cells, mean±SEM, statistical analysis, two-way ANOVA, +p<0.05, ++p<0.01 effect of time in culture, &p<0.05 different effect of treatment at different time points, *p<0.05 significant difference between treatments in the 1-hour time point group. E, G, I Length of cilium following each treatment, N=3, n=194-275. Box plot illustrates 25th and 75th percentile values, whiskers represent 5th and 95th percentile values, line at median, black dots represent points outside of the 5th and 95th percentile, statistical analysis, one-way ANOVA with Bonferroni post-test, *p<0.05, *p0.01, ***p<0.001, significant difference between labelled groups. 117

Figure 4.2:Effect of biochemical primary cilium elongation on Hedgehog and Wnt pathway activity. A, B *Ptch1* and *Gli1* expression following 24 hours of A 100mM LiCl or B 50μM Fenoldopam treatment, N=3, n=7-10. Bars illustrate mean±SEM, NS, not significant, statistical analysis, unpaired two tailed t-test. C, F Representative images of immunofluorescent staining of βcatenin in MSCs at 100x fluorescence (red channel- β-catenin, green channel- phalloidin and DAPI) (scale bar 10μm) D, G fold change intensity of β- catenin in the nucleus of MSCs (N=3, n=36-37), E, H *Axin2* expression (N=2, n=3-6) following 24 hours of C-E 100mM LiCl and F-H 50μM Fenoldopam treatment, bars illustrate mean±SEM, NS, not significant, statistical analysis, unpaired two tailed t-test. 119

Figure 4.3: Effect of biochemical primary cilium elongation on osteogenic gene expression. *Cox2, Opn, Runx2* and *Dlx5* expression following 24 hours of A 100mM

LiCl or B 50µM Fenoldopam treatment, N=3, n=4-6. Bars illustrate mean±SEM, NS, not significant, *p<0.05, statistical analysis, unpaired two tailed t-test. 120
Figure 4.4: Osteogenic marker expression following 2 hours of 2Pa 2Hz OFF in each group A-D Lithium Chloride or vehicle, H2O and E-H Fenoldopam or vehicle, DMSO represented as Mean ±SEM, N=3, n=5-12, statistical analysis, 2 way ANOVA with Bonferroni post-hoc test; $$p<0.01, $$$p<0.001 effect of flow on gene expression, #p<0.05, ###p<0.001 effect of treatment on gene expression, *p<0.05, **p<0.01 effect of flow within individual treatment groups. 122
Figure 4.5: Quantification of DNA content following treatment with A 100mM LiCl or vehicle, H2O and B 50µM Fenoldopam or vehicle, DMSO for 21 days with full osteogenic supplements under static conditions. N=1, n=5-6, Mean±SEM, *p<0.05, student's t-test with Welch's correction. C, D, G, H Representative images of extracellular matrix staining C, D Picrosirius and G, H Alizarin Red, following treatment with C, G LiCl or vehicle, H2O and D, H Fenoldopam or vehicle, DMSO after 21 days culture in full osteogenic supplements, scale =500µm and 100µm in the inset. E, F, I, J Quantification of matrix staining E, I total collagen and collagen normalized to DNA content and F, J total calcium and calcium normalized to DNA content from each group, student's t-test, *p<0.05, **p<0.01, ***p<0.001. 124
Figure 4.6: A, Quantification of DNA content following treatment with LiCl or vehicle, H2O for 21 days cultured in either static, No Flow, or mechanically stimulated, Flow. B, C Representative images of extracellular matrix staining B Picrosirius, C Alizarin Red staining, following treatment, scale =500µm and 100µm in the inset. D-G Quantification of matrix staining D, E total collagen and calcium concentration extracted from each group. F, G Extracellular matrix normalized to DNA quantification F collagen and G calcium, two-way ANOVA, $p<0.05, effect of flow on collagen and calcium concentration. ###p<0.001 effect of treatment, *p<0.05, ***p<0.001 Bonferroni post test, effect of flow on individual treatment groups, &p<0.05, &&p<0.01 difference between the effect of flow in each treatment. 126
Figure 4.7: A, Quantification of DNA content following treatment with Fenoldopam or vehicle, DMSO for 21 days cultured in either static, No Flow, or mechanically stimulated, Flow. B, C Representative images of extracellular matrix staining B Picrosirius, C Alizarin Red staining, following treatment, scale =500µm and 100µm in the inset. D-G Quantification of matrix staining D, E total collagen and calcium concentration extracted from each group. F, G Extracellular matrix normalized to DNA

quantification F collagen and G calcium, two-way ANOVA, $p<0.05, $$p<0.01, effect of flow on collagen and calcium concentration.*p<0.05, **p<0.01 Bonferroni post test, effect of flow on individual treatment groups, &p<0.05, difference between the effect of flow in each treatment. 127

Figure 5.1: Details of MSC donors and immunophenotypic analyses of extracted MSCs A Donor age and orthopaedic health. B Representative forward and side scatter dot plot illustrating the selection of a gate to define the MSC population. C-E Representative plots of phycoerythrin fluorescence magnitude against the count of events, gated for healthy 3 defined in B. C IgG control to quantify background fluorescence of the cells, marked by vertical red line, D CD73 positive events detected in 99.7% overall, E CD45 positive events detected in 0.7% of the gated population. F Percentage population expressing stem cell specific surface markers, negative markers (shaded orange) should not exceed 2.0% expression in an MSC population and positive markers (shaded green) should exceed 95.0% expression to adhere to International Society for Cellular Therapy guidelines for defining an MSC population. n=3. Blue dashed line highlights readings outside of ISCT guidelines. 144

Figure 5.2: Migratory capacity of hMSC samples in the presence of 10% FBS. A Number of cells in each individual samples migrating upon exposure to 10% FBS, Mean±SEM, n>3, students unpaired t-test comparing 0% to 10% FBS in each sample, lowest p values, less than 0.1 listed. B Number of cells migrating to 10% FBS pooled from the healthy and osteoporotic groups, Mean±SEM, student's unpaired t-test, *p<0.05. 145

Figure 5.3: Expression of genes associated with early osteogenic differentiation in each sample A *COX2* B *OPN* C *RUNX2* relative to *18S*, Mean ± SEM, n=3-7, student's t-test, p values <0.15 are shown. Fold change gene expression response to 2Pa, 2Hz fluid shear applied for 2 hours. D, E, F Response of individual patients, Mean ±SEM, n=3-5, two-way ANOVA, not significant. G, H, I Comparison of healthy or osteoporotic samples pooled, Mean±SEM, n=3, two-way ANOVA comparing effect of flow and effect of MSC health, &p<0.05 effect of flow is different in healthy and osteoporotic, Bonferroni post test showing effect of flow in individual groups, +p<0.05, +++p<0.001, students t-test comparing fold change expression in healthy and osteoporotic MSCs, p values <0.15 are shown. 147

Figure 5.4: Quantification of proliferative activity, at 7 day intervals for 3 weeks, via picogreen assay for DNA content. A Individual patients DNA content, Mean±SEM,

n=3-4, two-way ANOVA *p<0.05, **p<0.01 significant increase between day 7 and 14, &&p<0.01 significant increase between day 14 and 21. B Average DNA content in samples of healthy and osteoporotic patients, Mean±SEM, N=3, n=12, two-way ANOVA with Bonferroni post test, +p<0.05 significant effect of health on DNA content, p<0.05 significant difference between days (not shown), *p<0.05 significant increase at day 14 in healthy samples. 148

Figure 5.5: A Quantification of DNA content following 21 days in growth medium or osteogenic medium, Mean±SEM, n=4, two-way ANOVA with Bonferroni post test B, C Representative images of Picrosirius Red stained monolayers of B Healthy and C Osteoporotic samples following 21 days culture in growth or osteogenic differentiation medium, 2x scale bar=1000µm, inset at 10x scale bar=200µm, n=3. D-G Quantification of osteogenic matrix in each sample D, E concentration of collagen extracted from D individual samples and E samples pooled based on health (µg/ml), Mean±SEM, n=4, two-way ANOVA with Bonferroni post test, ***p<0.001, differentiation medium effects the samples differently p<0.001 (interaction effect. F, G Collagen concentration normalized to DNA content (ng/ml) for F each sample and G pooled concentration of collagen in healthy and osteoporotic samples, N=3, two-way ANOVA with Bonferroni post test, ***p<0.001, **p<0.01,*p<0.05. 151

Figure 5.6: A, B Representative images of Alizarin Red stained monolayers of A Healthy and B Osteoporotic samples following 21 days culture in growth or osteogenic differentiation medium, 2x scale bar=1000µm, inset at 10x scale bar=200µm, n=3. C-F Quantification of osteogenic matrix in each sample C, D concentration of calcium extracted from C individual samples and D samples pooled based on health (µg/ml), Mean±SEM, two-way ANOVA with Bonferroni post test, ***p<0.001, differentiation medium effects the samples differently p<0.001 (interaction effect), n=4. E, F Calcium concentration normalized to DNA content (ng/ml) for E each sample and F pooled concentration of calcium in healthy and osteoporotic samples, N=3. 152

Figure 5.7: A Quantification of DNA content following 21 days in growth medium or adipogenic, Mean±SEM, n=4, two-way ANOVA with Bonferroni post test B, C Representative images of Oil Red O stained monolayers of B Healthy and C Osteoporotic samples following 21 days culture in growth or adipogenic differentiation medium, 2x scale bar=1000µm, inset at 10x scale bar=200µm, n=3. D-G Quantification of adipogenic matrix in each sample D, E concentration of lipid extracted from D individual samples and E samples pooled based on health (µg/ml), n=4. F, G Oil Red O

concentration normalized to DNA content (ng/ml) for F each sample and G pooled concentration of collagen in healthy and osteoporotic samples, N=3, Mean±SEM, two-way ANOVA with Bonferroni post test, *p<0.05, ***p<0.001, differentiation medium effects the samples differently &p<0.05, &&&p<0.001 interaction effect.

Figure 6.1: Expression of TRPV4 in healthy and osteoporotic MSCs. A TRPV4 relative to 18S, Mean± SEM, n=3-7, student's t-test. B Representative images of TRPV4 expression on healthy and osteoporotic hMSCs at 100x fluorescence (red channel- F-actin, green channel- TRPV4 and DAPI) (scale bar 10µm). C Quantification of cell wide TRPV4 intensity in individual hMSC samples, 25-75th percentile shown in box, whiskers mark 5-95 percentile, outliers marked in black points, one way anova shows healthy 1 is significantly more intense than all other samples, ***p<0.001. D Pooled TRPV4 intensity for healthy and osteoporotic samples, Mean ±SEM, n=3, student's t-test, not significant. E, F Fold change TRPV4 expression in response to 2Pa, 2Hz fluid shear applied for 2 hours. E Response of individual patients, Mean ±SEM, n=3-6, two-way ANOVA, +p<0.05 effect of osteoporosis. F Comparison of healthy and osteoporotic samples pooled, Mean±SEM, n=3, two-way ANOVA with Bonferroni post test, comparing effect of flow and effect of MSC health, &&p<0.01 effect of flow is different in healthy and osteoporotic, +p<0.05 effect of flow in healthy compared to no flow healthy.

Figure 6.2: Expression of IFT88 in healthy and osteoporotic MSCs. A IFT88 relative to 18S, Mean± SEM, n=3-7, student's t-test. B Representative images of the primary cilium on healthy and osteoporotic hMSCs at 100x fluorescence (red channel- acetylated alpha tubulin, green channel- pericentrin and DAPI) (scale bar 10µm), inset shows zoom on cilium (scale bar 1µm). C % ciliation in individual samples shown as Mean ±SEM, n=3, two-way ANOVA, p<0.05 the variation in cilium incidence is significantly different in osteoporosis. D Pooled % ciliation for healthy and osteoporotic patients, Mean ±SEM, n=3, student's t-test, p<0.05. E Cilium length 25-75th percentile shown in box, whiskers mark 5-95th percentile, outliers marked in black points, one way anova shows each healthy sample is significantly different to each osteoporotic sample p<0.001, healthy 1 and healthy 3 are significantly different p<0.05, osteoporotic 3 is significantly shorter than osteoporotic 1 and 2 p<0.05. F Pooled cilium length, Mean ±SEM, n=3, student's t-test, p<0.001. G, H Fold change IFT88 expression in response to 2Pa, 2Hz fluid shear applied for 2 hours. G Response of individual patients, Mean ±SEM, n=3-6, two-way ANOVA, not significant, t-test to compare No flow to

Flow for each individual sample, *p<0.05. H Comparison of healthy and osteoporotic samples pooled, Mean±SEM, n=3, students t-test, not significant. 171
Figure 6.3: Characterisation of short term treatment of healthy and osteoporotic hMSCs with vehicle (DMSO), GSK101, Fenoldopam or Fenoldopam and GSK101 on TRPV4. A Fold change TRPV4 expression relative to vehicle control, Mean ±SEM, n=3-8, two-way ANOVA, not significant. B Representative images of TRPV4 on healthy and osteoporotic hMSCs at 100x fluorescence (red channel- F-actin, green channel- TRPV4 and DAPI) (scale bar 10µm). C Quantification of cell wide TRPV4 intensity in treated healthy and osteoporotic hMSCs, 25-75th percentile shown in box, whiskers mark 5-95th percentile, outliers marked in black points, n=52-59, one-way ANOVA p<0.001 healthy hMSCs treated with GSK101 express significantly more TRPV4 than Fenoldopam treated samples. Osteoporotic hMSCs treated with GSK101 express more TRPV4 p<0.05, relative to fenoldopam, those treated with fenoldopam express less TRPV4 compared to vehicle controls, p<0.01. Treatment with Fenoldopam & GSK101 decreases TRPV4 relative to DMSO, p<0.001 and relative to GSK101, p<0.01. 173
Figure 6.4: Characterisation of short term treatment of healthy and osteoporotic hMSCs with vehicle (DMSO), GSK101, Fenoldopam or Fenoldopam and GSK101 on primary cilia. A Fold change IFT88 expression relative to vehicle control, Mean ±SEM, n=3-8, two-way ANOVA, not significant. B Representative images of the primary cilium on healthy and osteoporotic hMSCs at 100x fluorescence (red channel- acetylated alpha tubulin, green channel- pericentrin and DAPI) (scale bar 10µm), inset shows zoom on cilium (scale bar 1µm). C % Ciliation Mean ±SEM, n=3, two-way ANOVA, ***p<0.01 effect of health. D Cilium length 25-75th percentile shown in box, whiskers mark 5-95 percentile, outliers marked in black points, n=81-124, one way anova shows GSK101 induces a significant increase in length in healthy (p<0.05) and in osteoporotic (p<0.01) hMSCs compared to Fenoldopam treatment , Fenoldopam & GSK101 treatment induces a significant increase in osteoporotic hMSCs, p<0.05. 175
Figure 6.5: Gene expression following short term treatment with vehicle (DMSO), GSK101, Fenoldopam or Fenoldopam and GSK101 in a healthy and osteoporotic hMSCs. A COX2 B OPN C RUNX2 fold change expression relative to vehicle control, Mean ±SEM, n=3-8, two-way ANOVA, with Bonferroni post test, COX2 effect of treatment p=0.0821, *p<0.05 significant effect of Fenoldopam & GSK101 on COX2 expression. 177

Figure 6.6: Quantification of DNA content in A Healthy and B Osteoporotic samples following 21 days culture in osteogenic differentiation medium containing either vehicle (DMSO), GSK101, Fenoldopam or Fenoldopam & GSK101 and exposed to static (No Flow) or mechanical stimulation (Flow), ng DNA/well, Mean±SEM, n=4-6, two-way ANOVA with Bonferroni post test, ***p<0.001, *p<0.05 significant difference between vehicle and treatment. Representative images of Picrosirius Red stained monolayers of C Healthy and D Osteoporotic samples following 21 days culture in osteogenic differentiation medium containing either vehicle (DMSO), GSK101, Fenoldopam or Fenoldopam & GSK101 and exposed to static (No Flow) or mechanical stimulation (Flow) 2x scale bar=1000µm, inset at 10x scale bar=200µm, n=4-6. C-F Quantification of osteogenic matrix in each sample E, F concentration of collagen extracted from E Healthy and F Osteoporotic samples (µg/ml), Mean±SEM, n=4-6. G, H Collagen concentration normalized to DNA content (ng/ml) for G Healthy and H Osteoporotic samples n=4-6, two-way ANOVA $$$ p<0.001 effect of flow, & p<0.05 effect of treatment is different under the influence of flow, with Bonferroni post test, ***p<0.001, **p<0.01, *p<0.05 significant difference between vehicle and treatment. 180

Figure 6.7: Representative images of Alizarin Red stained monolayers of A Healthy and B Osteoporotic samples following 21 days culture in osteogenic differentiation medium containing either vehicle (DMSO), GSK101, Fenoldopam or Fenoldopam & GSK101 and exposed to static (No Flow) or mechanical stimulation (Flow) 2x scale bar=1000µm, inset at 10x scale bar=200µm, n=4-6. C-F Quantification of osteogenic matrix in each sample C, D concentration of calcium extracted from C Healthy and D Osteoporotic samples (µM), Mean±SEM, n=4-6. E, F Calcium concentration normalized to DNA content (ng/ml) for E Healthy and F Osteoporotic samples n=4-6, two-way ANOVA with Bonferroni post test, ***p<0.001, **p<0.01, *p<0.05 significant difference between vehicle and treatment; &&p<0.01, &&&p<0.001 interaction effect. 182

Figure 7.1: Overview of the mechanisms researched in this thesis and their application for therapeutic design. Initially the mechanical environment of bone marrow during physical activity was modelled in vitro and two MSC mechanotransduction mechanisms were delineated, calcium signalling via TRPV4 and primary cilium mediated osteogenesis. Protocols developed to biochemically activate the mechanisms identified were applied to human MSCs to enhance bone modelling activity (Aoki et al., 2019). 191

Supplementary Figure 3.1: (A) Median and interquartile range of fold increase in calcium at first peak following application of GSK101 in cells transfected with scrambled siRNA or siRNA targeting IFT88, Mann Whitney test, NS p>0.05. (B) Frequency of calcium response in MSCs exposed to GSK101, Fisher's exact test, NS p>0.05. (C) Time to first peak for individual cells following application of GSK101 at time 0s. Bars mark Median and interquartile range, Scrambled N=4, n= 20, IFT88 KD N=4, n=12, Mann Whitney test, NS p>0.05. 202
Primer sequences and concentrations employed in quantitative PCR analysis 202
Supplementary Figure 4.1: Representative images of MSCs following treatment with A Forskolin, B LiCl or C Fenoldopam or vehicle, DMSO or H2O, control for 1 hour and 24 hours in 4x phase contrast (scale bar 200µm). 203
Supplementary Figure 4.2: Positive Control for β-catenin localization to the nucleus A representative images of immunofluorescent staining at 100x fluorescence (red channel- β-catenin, green channel- phalloidin and DAPI (scale bar 10µm) following treatment with 2ng/ml TGF-β1 or vehicle, 4mM HCl 1mg/ml BSA, control for 2 hours. B Quantification of nuclear intensity of β-catenin in each condition, statistical analysis, two-tailed t-test, *p<0.05. 204
The sequences of the primers used to quantify gene expression in MSC 205
The sequences of the primers used to quantify gene expression in MSCs 206
Supplementary Figure 5.1: Representative images of Alcian blue stained pellet cultures of each sample following 21 days culture in chondrogenic differentiation medium, 4x scale bar =500µm, inset is at 10x, scale bar =100µm, n=2-4. 207
Supplementary Figure 5.2: % of the surface area covered by Picrosirius (top) and Alizarin (bottom) stained monolayer in healthy and osteoporotic MSCs in growth or osteogenic medium, n=3, Mean +/-SEM. 208
The sequences of the primers used to quantify gene expression in MSC 209
Supplementary Table 6.2: 210
Comparison of the performance of each MSC sample characterized in terms of migration, osteogenic gene expression under fluid shear, proliferation, collagen and calcium deposition in osteogenic supplements for 21 days 210

List of Tables

Supplementary Table 3.1: Primer sequences and concentrations employed in quantitative PCR analysis

Supplementary Table 4.1: The sequences of the primers used to quantify gene expression in MSC

Supplementary Table 5.1: The sequences of the primers used to quantify gene expression in MSCs

Supplementary Table 6.1: The sequences of the primers used to quantify gene expression in MSC

Supplementary Table 6.2: Comparison of the performance of each MSC sample characterized in terms of migration, osteogenic gene expression under fluid shear, proliferation, collagen and calcium deposition in osteogenic supplements for 21 days

Nomenclature

ALP	Alkaline phosphatise
BMU	Bone modelling unit
BMP	Bone morphogenetic protein
BSA	Bovine serum albumin
COX2	Cycloxygenase 2
CXCL7	Pro-platelet basic protein
CXCR4	C-X-C motif chemokine receptor 4
DVT	Deep vein thrombosis
ECM	Extracellular matrix
EDTA	Ethylenediaminetetraacetic acid
ERK	Extracellular signal regulated kinase
FAK	Focal adhesion kinase
FBS	Fetal bovine serum
FRET	Fluorescence resonance energy transfer
GSK101	GSK1016790A
HT	Hormone therapy
IGF	Insulin-like growth factor
ISCT	International society for cellular therapy
LiCl	Lithium Chloride
MEK	Mitogen activated protein kinase
MSC	Mesenchymal stem cell
NBF	Neutral buffered formalin
OFS	Oscillatory fluid shear
OPN	Osteopontin
OP	Osteoporosis
OSX	Osterix
PDGF	Platelet derived growth factor
PGE_2	Prostaglandin E2
PTH	Parathyroid hormone
qPCR	Quantitative polymerase chain reaction
RANKL	Receptor activator of nuclear factor kappa-β ligand

ROCK	Rho associated protein kinase
RUNX2	Runt-related transcription factor 2
SDF	Stromal cell derived factor
SERM	Selective estrogen receptor modulator
TNFα	Tumor necrosis factor alpha
TGFβ	Transforming growth factor beta
TRPV4	Transient receptor potential vanilloid 4

Conference Abstracts

- Corrigan, M. A., Johnson, G. P., Riffault, M., Stavenschi, E., Labour, M-N.,Hoey, D.A., TRPV4 mediates oscillatory fluid shear mechanotransduction in mesenchymal stem cells in part via the primary cilium. *World Congress in Biomechanics,* Dublin, Ireland, 2018
- Corrigan, M. A., Johnson, G. P., Ferradaes, T., Hoey, D.A., Can modulating the primary cilium influence bone formation: A comparison of ciliotherapy treatments on stem cell osteogenesis. *In: Proc. of the Orthopaedic Research Society*, New Orleans, USA, 2018
- Corrigan, M. A., Ferradaes, T., Hoey, D.A., Can modulating the primary cilium influence bone formation: A comparison of ciliotherapy treatments on stem cell osteogenesis. *24th Annual Conference of the section of Bioengineering of the Royal Academy of Medicine in Ireland,* Dublin, 2018
- Corrigan, M. A., Johnson, G. P., Riffault, M., Stavenschi, E., Labour, M-N.,Hoey, D.A., TRPV4 mediates oscillatory fluid shear mechanotransduction in mesenchymal stem cells in part via the primary cilium. *Matrix Biology Ireland,,* Dublin, Ireland, 2017
- Corrigan, M. A., Johnson, G. P., Riffault, M., Hoey, D.A., Targeting of TRPV4 mimics the mechanotransduction response to fluid shear in mesenchymal stem cells. *23rd Annual Conference of the section of Bioengineering of the Royal Academy of Medicine in Ireland,* Belfast, Northern Ireland, 2017
- Corrigan, M. A., Riffault, M., Labour, M-N.,Hoey, D.A., Fluid shear induces TRPV4 mediated calcium influx contributing to osteogenic responses in MSCs. *In: Proc. of the Orthopaedic Research Society*, San Diego, USA, 2017
- Corrigan, M. A., Johnson, G. P., Stavenschi, E., Labour, D.A., TRPV4 is required for flow mediated calcium signalling and osteogenic lineage commitment of mesenchymal stem cells. *22nd Annual Conference of the section of Bioengineering of the Royal Academy of Medicine in Ireland*, Galway, Ireland, 2016
- Corrigan, M. A., Lee, K. L., Labour, M-N.,Jacobs, C. R., Hoey, D.A., Calcium signalling through the primary cilium regulates mechanotransduction of

mesenchymal stem cells. *In: Proc. of the Orthopaedic Research Society*, Las Vegas, USA, 2015

- Corrigan, M. A., Lee, K. L., Labour, M-N.,Jacobs, C. R., Hoey, D.A., Fluid flow-induced bending of the primary cilium triggers a distinct intraciliary calcium flux in mesenchymal stem cells. *21st Annual Conference of the section of Bioengineering of the Royal Academy of Medicine in Ireland,* Maynooth, Ireland, 2015
- Corrigan, M. A., Lee, K. L., Labour, M-N.,Jacobs, C. R., Hoey, D.A., Fluid flow-induced bending of the primary cilium triggers a distinct intraciliary calcium flux in mesenchymal stem cells. *Cilia*, Paris, France, 2014

Publications

E Stavenschi, MA Corrigan, GP Johnson, M Riffault, DA Hoey, Physiological cyclic hydrostatic pressure induces osteogenic lineage commitment of Human Bone Marrow Skeletal Stem Cells: A Systematic Study, ***Stem Cell Research and Therapy*** 9:276, 2018

MA Corrigan, GP Johnson, E Stavenschi, M Riffault, MN Labour, DA Hoey, TRPV4-mediates oscillatory fluid shear mechanotransduction in mesenchymal stem cells in part via the primary cilium. ***Sci Rep***, 8**,** 3824, 2018.

GP Johnson, E Stavenschi, KF Eichholz, MA Corrigan, S Fair, DA Hoey, Mesenchymal stem cell mechanotransduction is cAMP dependent and regulated by adenylyl cyclase 6 and the primary cilium. ***Journal of Cell Science,*** 131, 2018.

MA Corrigan, TM Ferradaes, M Riffault, DA Hoey, Ciliotherapy treatments to enhance biochemillay and biophysically-induced mesenchymal stem cell osteogenesis: A comparison study. ***Cellular and Molecular Bioengineering***, 12, 53-67, 2019.

MA Corrigan, S Coyle, KF Eichholz, M Riffault, B Lenehan, DA Hoey, Aged osteoporotic bone marrow stromal cells demonstrate defective recruitment, mechanosensitivity, and matrix deposition. ***Cells, Tissues and Organs,*** (Submitted for review).

Chapter 1:

Introduction

1.1 Osteoporosis

Worldwide as many as 1 in 3 women and 1 in 5 men over 50 will suffer an osteoporotic fracture in their lifetime (Melton et al., 1992, Melton et al., 1998). Osteoporosis is a disease characterised by the significant loss in bone density which leads to fracture fragility (Kanis et al., 1994). In osteoporotic patients, a fall from a standing height can result in a hip fracture resulting in agonising pain and often necessitating surgical intervention. Furthermore, patients suffering fragility fractures have particularly complex needs, a hip fracture can prevent independent walking, washing and dressing, and as a result there is a 20-24% increase in patient mortality in the year following hip fracture (Cooper et al., 1993). Moreover, the risk of fracture following the first break rises by 86% (Kanis et al., 2004). In 2013 it was estimated that the osteoporotic fractures sustained by the 22 million women and 5.5 million men in the European Union cost 37 billion euro. The loss of bone density with aging and increasing life expectancy indicates that the economic burden of osteoporosis will grow by a further 25% by 2025 (Hernlund et al., 2013).

Originally osteoporosis was defined solely by a reduction in bone density but the importance of the tissue microarchitecture has been recognised more recently (Armas and Recker, 2012). The loss in bone density occurs because there is an increased rate of bone remodelling, the process by which bone tissue is resorbed by osteoclasts and replaced with new mineralised matrix by osteoblasts. Throughout our lifetime bone

remodelling occurs which maintains bone strength and fracture resistance, however the decrease in estrogen following menopause increases the activity of osteoclasts (Armas and Recker, 2012). With aging, increases in Haversian canal and osteon diameter also indicate upregulated resorption, however changes in the bone marrow content are also an important factor in aging related bone loss (Compston, 2011). Over time the fat content of the marrow increases and there is a greater propensity for progenitors in the marrow to undergo adipogenic differentiation (Pino et al., 2012b, Duque and Troen, 2008). This inhibits the supply of osteoblast progenitors which are required to replace the bone during remodelling. The decrease in the supply of osteoblasts impairs bone formation leading to an imbalance in the bone remodelling cycle. Therefore, a potential avenue to treat osteoporosis, may be to target the replenishment of the osteoblast, promoting bone formation, and correcting the imbalance in bone remodelling.

Currently, treatment options consist mainly of bisphosphonates which inhibit bone resorption to rebalance the bone remodelling system. However these have limited efficacy, especially since the diagnosis of osteoporosis usually occurs at the time of the first fragility fracture when bone density has substantially decreased (Tella and Gallagher, 2014). There is only one bone anabolic therapy currently on the market, a recombinant parathyroid hormone called teriparatide, which increases osteoblast activity but this has shown some increased osteoclastic activity and side effects including osteosarcoma in rat models (Minisola et al., 2017). The increasing burden of osteoporosis and lack of efficient treatment options indicates the need for more effective therapies and to enable this, novel therapeutic targets are required.

1.2 Bone formation and mechanoadaptation

In order to develop new treatments for osteoporosis a better understanding of the mechanisms of bone formation is required. Bone adaptation is also facilitated by the process of remodelling, which occurs in discrete regions called bone multicellular units (BMU). The cycle consists of 3 steps, resorption, reversal and formation, which coordinate the access of cells with opposing functions to the bone surface. Osteoclasts are large multinucleated cells which originate from hematopoietic stem cells and have a strong lysosomal capacity. They digest the bone matrix through a process of acidification and proteolysis. Next, the resorbed surface is cleared in preparation for bone formation in the reversal phase. Bone formation occurs via secretion and mineralisation of a collagen rich matrix by osteoblasts, which arise from mesenchymal stem cells (MSCs), the progenitors of osteoblasts. In the reversal phase, osteoblasts, form clusters on the bone surface where they secrete osteogenic matrix. Remodelling finishes when bone lining cells cover the surface of the new matrix (Hadjidakis and Androulakis, 2006, Delaisse, 2014).

Bone also adapts to the mechanical environment it experiences, building strength through increased deposition in response to physical activity and supporting bone resorption to reduce weight following unloading such as bed rest. This is evident through the examination of the limbs of an athlete, for example, the radius of a tennis player's serving arm has greater bone mineral content than the opposite less loaded radius (Ducher et al., 2005). Similarly, an astronaut can lose 10-15% bone density at the hip and spine following long duration spaceflight (Sibonga, 2013). Bone formation can occur directly via stimulation of osteoblasts or their progenitors, or indirectly via stimulation of osteocytes which in turn signal to these bone forming cells. Under

physiological loading bone experiences strain, which builds pressure differences, that drives fluid shear within the embedded osteocyte lacuna-canalicular network and throughout the tissue (Klein-Nulend et al., 2012). Osteocytes respond by secreting osteogenic factors such as BMPs and $PGE_{2,}$ promoting bone formation at the site of loading (Klein-Nulend et al., 2012). MSCs similarly sense fluid shear and respond with increased proliferation and differentiation towards the osteogenic lineage (Li et al., 2004).

1.3 Stem cell-mediated bone formation

As the osteoblast progenitor, the differentiation of MSCs down the osteogenic lineage represents an integral part of the bone forming process. MSCs are multipotent self-renewing stromal cells responsible for supplying osteoblasts in addition to adipocytes and chondrocytes in the maintenance of the adult musculoskeletal system. They were first defined in bone marrow, where they compose 0.001-0.01% of the cells (Pittenger et al., 1999). MSC-like cells have also been found in adipose, intrapatellar fat pad and umbilical cord among other tissues (Via et al., 2012). However, recent advances in cell tracking techniques have sparked a debate on the definition of an MSC, the frequent perivascular localisation of MSCs has led to their liking to pericytes, yet not all pericvtes are multipotent (Guimarães-Camboa et al., 2017, Sacchetti et al., 2016). It is now appreciated that a stem cell with universal differentiation potential is not present in the mature skeleton but pools of stem cells develop with tissue specific multipotency to sustain the surrounding environment (Robey, 2017). Markers for the human skeletal stem cell originating from periosteum, bone and marrow tissue, have been delineated recently (Chan et al., 2018), however the guidelines established by the International

Society for Cellular Therapy are still commonly used and will be used throughout this thesis (Dominici et al., 2006). The ISCT definition of an MSC includes adipogenic, chondrogenic and osteogenic lineage commitment capacity which confirms these cells can contribute as skeletal stem cells. The adipogenic, chondrogenic and osteogenic potential of MSCs has been demonstrated *in vitro* (Pittenger et al., 1999) and the bone and cartilage forming capacity demonstrated *in vivo*. In orthopaedic research, understanding the molecular mechanisms by which this population commits to the osteogenic lineage over chondrogenic or adipogenic can help identify targets for therapeutic intervention to prevent bone loss and/or promote formation.

1.4 Stem cell-mediated bone formation in osteoporosis

With regards to osteoporosis, an imbalance in the bone remodelling cycle is a significant factor in the loss of bone mass. This disease is marked by a decoupling of the resorption and formation rates where osteoclast activity increases but osteoblast matrix deposition rate can no longer replace the quantity of bone removed (Nordin et al., 1981, Eastell et al., 1993). Although mineralisation has been predicted to increase in osteoporosis, in the absence of collagen this leads to a more brittle bone structure and overall the rate of bone formation decreases (Mulvihill et al., 2008, de Vernejoul, 1989). The marrow of osteoporotic patients contains more adipocytes than healthy counterparts (Verma et al., 2002, Pino et al., 2012b), furthermore the smaller population of MSCs have a greater propensity for adipogenic differentiation but there is a lack of knowledge on osteogenic capacity in these patients (Astudillo et al., 2008, Hess et al., 2005). Clinical studies of the effect of weight bearing exercise display a weakened mechanoresponse in osteoporotic MSCs compared to healthy counterparts (Harding and

Beck, 2017). The mechanical environment and mechanobiological response of osteocytes becomes altered in osteoporosis, however there is little knowledge of the effect of osteoporosis on osteoblast and osteoprogenitor function (Verbruggen et al., 2015). Maintenance of healthy bone tissue requires a sufficient population of osteoblasts as well as an adequate rate of matrix deposition from individual osteoblasts (Parfitt, 1982). As such osteoblastogenesis is a prime therapeutic target for the restoration of healthy bone density in osteoporosis.

1.5 Mechanotransduction

In healthy skeletal tissue, MSCs are mechanoresponsive and the mechanical stimuli generated by physical activity upregulates osteogenic differentiation (Arnsdorf et al., 2009, Li et al., 2004). The conversion of biophysical signals to changes in cellular behaviour is termed 'mechanotransduction'. To understand the molecular mechanisms by which osteogenesis is regulated the forces experienced at the cellular level in the bone and marrow interface have been investigated, particularly hydrostatic pressure and fluid shear stress (Gurkan and Akkus, 2008, Metzger et al., 2015b). Organelles along the cell membrane form the first point of contact between the cell and the surrounding environment and thus are important sites for mechanotransduction (Ingber, 2006). Ion channels play an essential role in this process in a variety of tissues including kidney (Delmas, 2004), cartilage (Pingguan-Murphy B. and M.M., 2008) and bone (el Haj et al., 1999). There are a number of mechanisms by which ion channels can be activated including membrane stretching; hydrostatic pressure and fluid shear and which facilitate the generation of a specific stimulus dependent response (Martinac, 2004). Furthermore, ion channels have selective permeability, transporting a specific signal,

commonly calcium, which initiates a signalling cascade capable of changing gene and protein expression (Clapham, 2007). Another key player in mechanotransduction is the primary cilium, a microtubule based extension of the cell membrane (Hoey et al., 2012a). The cilium is a singular appendage which is present on most mammalian cells and protrudes into the extracellular environment where it is ideally placed to intercept intercellular signalling and changes in the extracellular biochemical and biophysical environment (Satir et al., 2010). In addition, the rod like structure of the ciliary axoneme forms a membrane enclosed compartment, partially removed from the cytosol where signalling components can interact in a concentrated volume. In this way it is ideally placed to mediate mechanotransduction as has been shown in cell types that experience fluid flow induced shear stress including kidney epithelia (Nauli et al., 2003), osteocytes (Lee et al., 2015c) and MSCs (Hoey et al., 2012d).

1.6 Mechanotransduction in the setting of osteoporosis

The adaptive response of MSCs to mechanical loading represents an important factor in the maintenance of bone health. In the osteoporotic disease state there is a requirement for a greater bone forming response; however, MSCs are known to have a greater propensity for the adipogenic lineage in osteoporosis (Pino et al., 2012b). Current treatments for osteoporosis can improve bone density and prevent bone loss temporarily, however once treatment ceases the bone density is not maintained (Naylor et al., 2018). This along with an increase in the resorption activity implies that the threshold load which would generate osteoblast or osteoclast activity are altered in the disease state (Seefried, 2010). The delineation of the pathways by which mechanical signals are transduced into a biochemical change in cell behaviour could highlight novel

drug targets to influence the osteogenic differentiation of MSCs and improve bone formation in osteoporosis. In summary, osteoporosis is a growing problem in our aging population and more efficient treatment options are urgently needed. Healthy bone tissue is influenced by the mechanical environment experienced by the skeleton and can induce a bone modelling response to loading to maintain fracture resilience (Frost, 2003). While a small number of clinical studies have investigated the effect of weight bearing exercise on osteoporotic patients, the results are difficult to compare given the differences in the mode of exercise and load experienced by the skeleton as well as the methods of quantifying bone (Cavanaugh and Cann, 1988, Krølner et al., 1983, Prince et al., 1991). Of the studies available there are inconsistent results, some trials result in improved bone geometry, others don't elicit a detectable change. As such, there is a requirement to evaluate the mechanoadaptation of osteoporotic bone. Loading induced bone formation requires a supply of MSCs, as the precursors of osteoblasts, to sense and osteogenically differentiate in response to mechanical stimuli (Chen et al., 2016a). The molecular mechanisms involved in MSC mechanotransduction remain elusive; delineating these could identify targets to therapeutically mimic the proosteogenic effect of physical activity in osteoporosis.

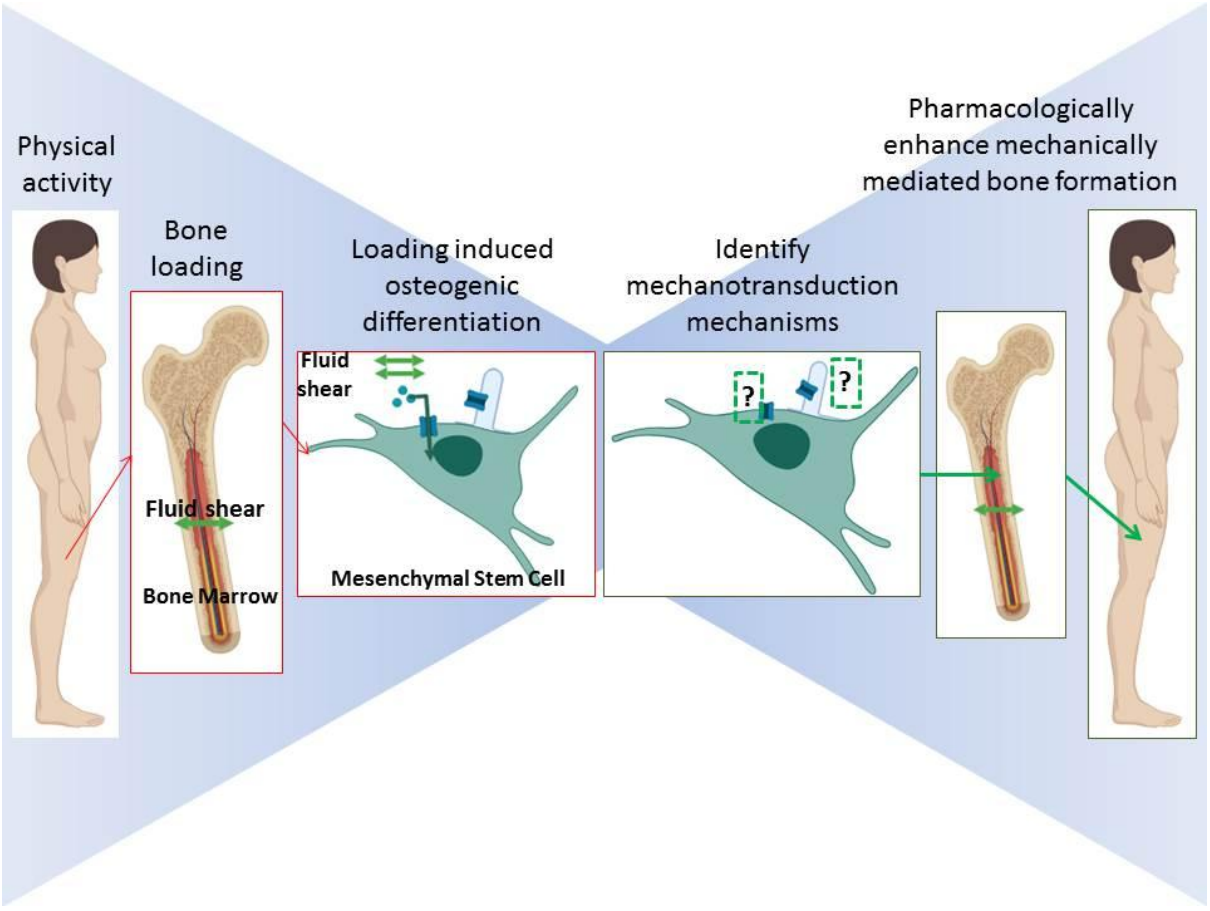

Figure 1.1: Overview of the mechanisms researched in this thesis and their application for therapeutic design. Initially the mechanical environment of bone marrow during physical activity will be modelled *in vitro* and the mechanisms mediating the mechanotransduction response leading to osteogenic differentiation will be delineated. Next, protocols to biochemically activate the mechanisms identified will be designed and applied to human MSCs to enhance bone modelling activity(Aoki et al., 2019).

1.7 Thesis Objectives

This thesis pursues the principal objective of determining the mechanisms underlying the biophysical induction of MSC osteogenic differentiation leading to bone formation. Through the discovery of this fundamental information, a second core objective of this thesis is to target these mechanisms therapeutically to enhance MSC osteogenesis and bone formation as a potential novel therapy for osteoporosis. The following is proposed to accomplish these objectives:

1. Determine the molecular mechanisms of MSC mechanotransduction and target these pharmacologically to mimic the osteogenic effect of loading

    1.1 Investigate the role of the mechanosensitive calcium channel, TRPV4, in MSC mechanotransduction and determine whether this channel can be targeted therapeutically.

    1.2 Given the role of the primary cilium in MSC mechanotransduction, determine whether this organelle can be targeted therapeutically.

2. Determine whether these novel mechanotherapeutics can be utilised to enhance the osteogenic potential of human osteoporotic MSCs.

    2.1 Investigate whether the recruitment, proliferation and osteogenic potential (biochemical and biophysical induction) of MSCs is defective in osteoporosis

    2.2 Determine whether novel mechanotherapeutics developed above can be utilised to enhance the osteogenic potential of human osteoporotic MSCs.

Chapter 2:

Literature Review

2.0 Introduction

This thesis sets out to investigate the molecular mechanisms mediating the change in behaviour in MSCs when exposed to mechanical stimuli with the overall goal of developing a pharmacological target to induce the bone forming effects seen with physical activity. To inform the reader on the background to this work the mechanobiology of bone will be summarised. In addition, the role of the MSC particularly in bone formation will be explained. A second objective of this thesis is to investigate the behaviour of MSCs in osteoporosis and the potential to influence mechanotransduction mechanisms to improve the osteogenic activity of patients. With this in mind, the current understanding of osteoporosis, the impact on the bone formation process and the mechanisms of current treatments will be reviewed. Finally, the role of mechanical loading in the bone formation process and the known mechanisms of transducing these stimuli into changes in behaviour in skeletal cells are detailed.

2.1 The structure and function of bone

Bone is the strong yet flexible tissue which provides a stable frame for the musculoskeletal system while also protecting vital organs, facilitating movement and storing calcium and phosphate for endocrine regulation. The human adult skeleton is categorised into long, short, flat, irregular and sesamoid bones, the characteristics of

each type assist in different aspects of the musculoskeletal system functionality. While long bones such as the femur and humerus are pillars of support during movement, short bones such as the carpals and tarsals provide support in the wrist and ankle. Contrastingly, flat bones such as the cranium or ribs and irregular bones such as vertebrae or facial bones form a protective casing around vital organs. Sesamoid bones form within tendons; they help in the transmission of muscular forces, for example the patella at the large hinge joint between the femur and the tibia (Kaufmann et al., 2018, Huse, 2017). The largest bone in the skeleton is the femur, the head of which is ball shaped to fit into the hip socket joint, the opposite end lies on the knee. Long bones are cylindrical in shape surrounding a lumen which is filled with marrow which facilitates an additional skeletal function, the site of cell production (Standring, 2015). As a composite of collagen fibres and calcium phosphate crystals, bone is both elastic and tough, providing a dynamic structure which can resist multiaxial loading (Fyhrie and Christiansen, 2015).

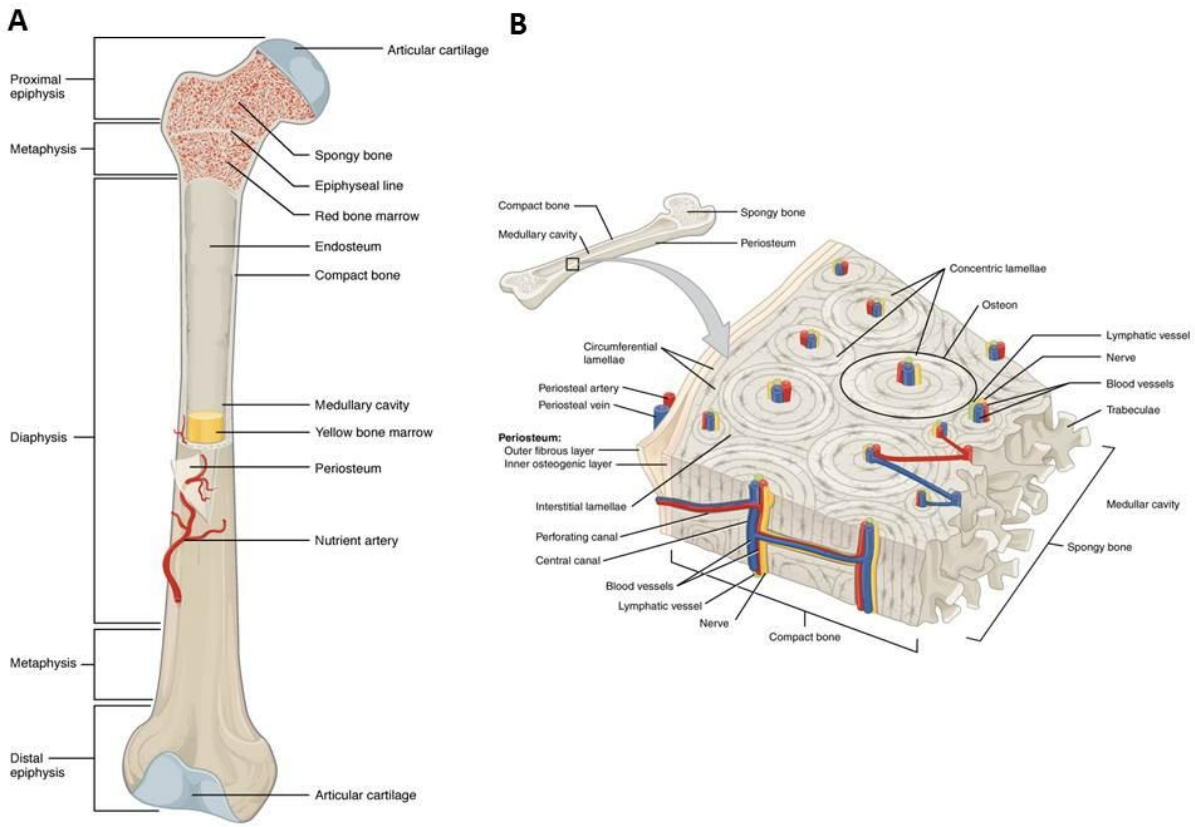

Figure 2.1: Structure of bone A Gross anatomical features of a femur, B Cross sectional view of the osteon, a unit of cortical bone (Betts et al., 2018)

The structures of bone, from the macro to the nano scale, provide functionality to facilitate the complex roles of the skeleton. Bone is surrounded by an outer membrane, periosteum, which forms a protective barrier against exfoliation of the tissue and is the site of entry of vessels into bone. There are two main forms of bone tissue, the outermost is dense and compact, known as cortical bone and the innermost is a porous lattice structure known as trabecular bone. These layers form a cylindrical shape which is covered on the innermost layers by another membrane called endosteum. Within the lumen of bones, lies a spongy, viscous fluid, bone marrow, which is not constrained to this cylindrical shape but overflows into the space between trabeculae. Marrow is composed of a red component which includes the vast majority of the marrow cellular contents and a yellow component which primarily provides a store of adipose as well as

a central artery and vein and surrounding arterioles and sinusoids. While the yellow marrow content increases with age, red marrow content, containing mature blood cells, haematopoietic stem cells and mesenchymal stem cells, decreases as the skeleton matures (Gurkan and Akkus, 2008). Examining bone structure at the micro scale reveals a series of building blocks known as osteons in cortical bone while trabecular bone is composed of connected rods and plates. Osteons are also known as Haversian systems and consist of a series of circular layers of tissue surrounding a canal which contains the blood and lymphatic vessels as well as nerve tissues. The concentrically arranged lamellae surrounding the Haversian canal contain a network of spaces, lacunae, which house cells, osteocytes (Rho et al., 1998). The interaction of osteocytes with each other and the central haversian canal is made possible by a network of submicron wide channels known as canaliculi. These facilitate the stretching of dendrites from osteocytes for cell to cell communication through compact bone (Schaffler and Kennedy, 2012).

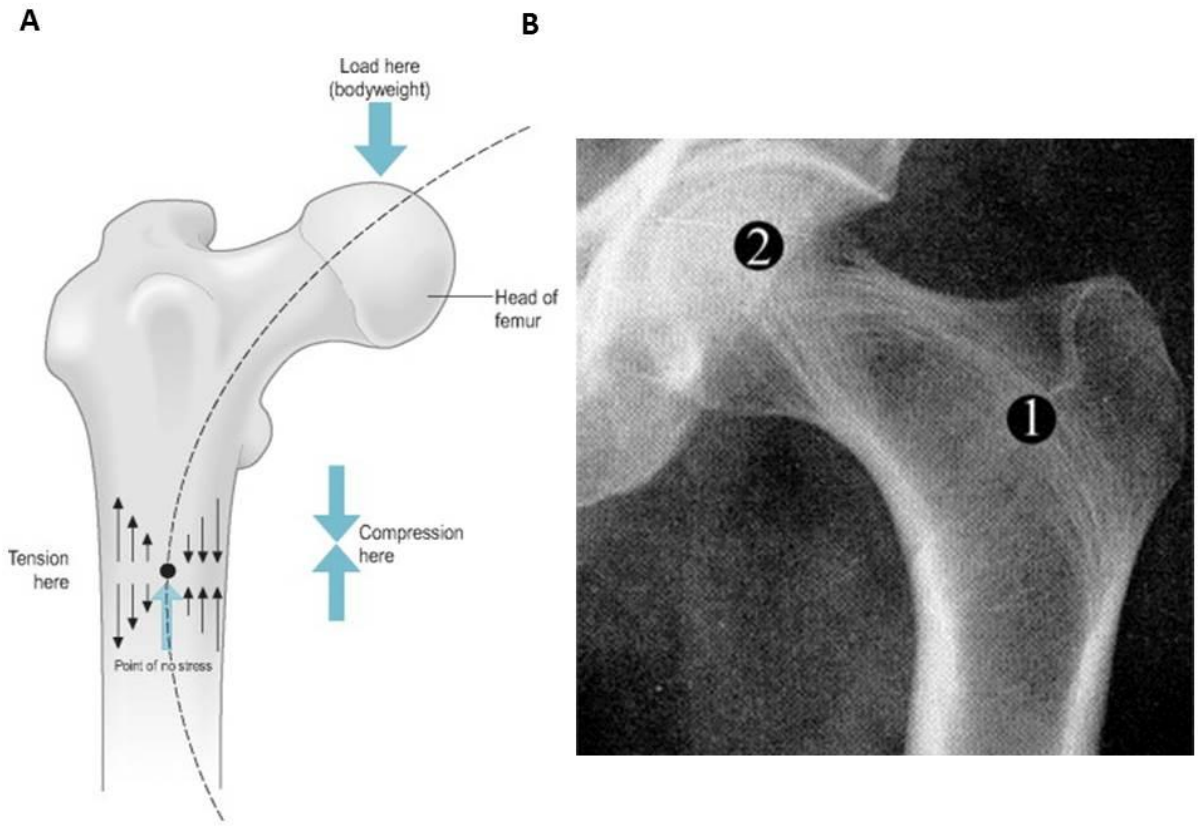

Figure 2.2: Structural features for mechanical efficiency in the head of the femur A illustration of the principal stresses experienced by the femur during physiological loading (Forsyth and Davey, 2008) B x-ray image showing pronounced trabeculae formation at 1 and 2 along the regions experiencing greatest tension and compression (Rudman et al., 2006)

The resilience of bone to mechanical loading during the range of loads encountered in physiological activity is facilitated by the combined capabilities of both cortical, withstanding stresses greater than 150MPa, and cancellous (trabecular), withstanding strains of greater than 50% (Hart et al., 2017). The combination of cortical and spongy bone enables the weight bearing capacity of the human skeleton. Cortical bone is stiff to provide a strong structural framework for the skeleton whereas trabeculae are arranged to follow the stresses that bones frequently experience in support of the denser outer layers (Cowin, 1986). The composition of cortical bone in discrete units allows loading induced deformation to be spatially limited. The proportion of cortical to cancellous

bone develops to accommodate the most frequently experienced loads particular to each region of the skeleton. This is facilitated by bone's mechanoadaptive abilities which were summarised by Frost's 'mechanostat' hypothesis in 1987. In summary, Frost proposes that bone adapts to alteration in mechanical loading both positive and negative (Frost, 1987). There is a threshold above which bone modelling is activated to increase bone mass whereas loading below a second set point triggers bone remodelling in maintenance. Despite some updates over the years to define the theory in the context of new analytical techniques the conclusion remains the same (Frost, 2003). Moreover, the demands for greater insight into the molecular mechanisms which influence the mechanoadaptation remain, to aid in our understanding of tissue homeostasis and disease progression.

2.2 Bone formation and remodelling

The structural adaptation of bone to its mechanical environment is made possible by the processes of remodelling and adaptive modelling. Whereas most long bones are formed through the process of endochondral ossification some bony regions including the skull and jaw are developed through intramembranous ossification. Endochondral ossification originates as a hyaline cartilage template which is gradually mineralised and this facilitates the increase in bone length via the growth plate, a region where mineralisation is delayed and chondrocytes continue to proliferate (Mackie et al., 2008). Intramembranous ossification describes the differentiation of mesenchymal stem cells to osteoblasts where an initial cluster of differentiating MSCs deposit mineral, creating an initial ossification centre (Kaufmann et al., 2018). Over time the mature skeleton is renewed in a similar process to intramembranous ossification, this occurs in discrete regions known as bone multicellular units (BMU) in a cyclical process known as

remodelling. Remodelling begins when osteoclast progenitors near the bone surface become stimulated. These originate from hematopoietic stem cells, located within the marrow, which are differentiating down the macrophage or monocyte lineage. When osteoclasts attach to the surface of bone they secrete vesicles of acidic material which break down the components of bone. This activity followed by proteolysis completes bone resorption and is recognised in histological staining by a ruffled border of the active osteoclast (Teitelbaum, 2000, Hadjidakis and Androulakis, 2006). The resorbed surface is then prepared for new bone formation via reversal, the second step of remodelling. Reversal is important for the coupling of resorption and formation phases, in fact osteoclasts release signals which stimulate the migration of osteoprogenitors from the bone surface and MSCs from the bone marrow to the BMU (Hadjidakis and Androulakis, 2006, Delaisse, 2014). The third and final step in remodelling is formation, where new osteogenic matrix is deposited. Formation requires clusters of osteoblasts to produce matrix, these originate as mesenchymal stem cell derived osteoblast precursors which increase in size and become cuboidal ALP expressing cells. Osteoblastogenesis is highly regulated by transcription factors such as RUNX2 and OSX, growth factors such as PDGF and TGF and hormones including progesterone and prolactin (Crockett et al., 2011). Initially osteoblasts produce matrix which is deposited along the resorbed surface and matured before being mineralised. The collagenous template is composed primarily of type I collagen, whereas mineralisation is composed of phosphate and calcium. Hydroxyapatite crystals are formed by osteoblasts, they secrete membrane bound vesicles containing phosphates into the immature matrix and derive calcium from extracellular fluid (Crockett et al., 2011). An imbalance in the coupling of the resorption and formation steps of the remodelling cycle leads to impaired skeletal strength, particularly in old age when MSC mediated

osteoblastogenesis is commonly impaired. This highlights the importance of a supply of healthy MSCs and it has been suggested that decreased availability of pre-osteoblasts contributes to impaired remodelling (Demontiero et al., 2012).

In addition, bone resorption and formation activities occur independently and at separate sites to facilitate the adaptation of the skeleton to environmental conditions. This can be observed during skeletal maturation as the bones of the appendicular skeleton grow in length and diameter and throughout adulthood when bone density increases and shape adapts to better support the loading experienced during physiological activities. Originally bone modelling was conceptualised following the observation of abnormal bone shape and a deficit in bone quality seen in infants with foot paralysis due to spina bifida. The bone modelling phenomenon was studied in rat models by paralysing a single limb while the contralateral limb experienced normal loading, here the bone formation due to loading could be observed independent of postnatal growth (Frost, 1990, Rális et al., 1976). The bone forming response to loading was first quantified in the humeri of tennis players where the cortical thickness of the serving arm was found to be significantly higher, 28.4% in women and 34.9% in men, than the opposite arm (Jones et al., 1977). In the decades since, with the development of experimental models which can apply a defined load *in vivo,* the response of MSCs to mediate the bone forming response have become appreciated. Furthermore, MSCs in osteoporotic models become less responsive to mechanical loading (Frost, 1992, Li et al., 2013). Although the strain ranges that drive modelling and remodelling are different the process of bone formation remains the same and requires a ready source of MSCs and regulated osteoblastic differentiation.

2.3 Mesenchymal stem cells and their role in bone formation

The maintenance of healthy bone requires a continued supply of mesenchymal stem cells (MSCs) of adequate quantity and with sufficient osteogenic capacity. *In vitro* and *in vivo* examination of the bone forming surface has identified marrow tissue as the principal source of osteoblast precursors with some contribution from the periosteum and bone lining cells (Kristensen et al., 2014, Matic et al., 2016, Moore et al., 2018b). Mesenchymal stem cells (MSCs) are multipotent self-renewing cells residing primarily in the bone marrow of the mature skeleton. Originally MSCs were described from marrow, periosteum and muscle connective tissue with the potential to form adipocytes, chondrocytes and osteocytes *in vitro* given lineage specific culture conditions and growth factors (Caplan, 1991). Furthermore, early investigations demonstrated the ability to form adipose and bone *in vivo* (Caplan, 1991, Pittenger et al., 1999). Other potentialities including myoblasts and neurons have only been proposed in non-native culture conditions (Robey, 2017). Recently questions have been raised about the definition of the MSC, with some suggesting it has been confused with a pericyte or lineage specific precursor (Sacchetti et al., 2016, Guimarães-Camboa et al., 2017, Worthley et al., 2015, Zhou et al., 2014). Recent analyses of the transcriptome of multipotent progenitors from different tissues concludes that there is not one universal multipotent MSC but tissue specific stem cells which are primed to differentiate into the cellular components of their tissue origin (Sacchetti et al., 2016). With the advancement of cell tracing technologies, seminal studies have attempted to identify the specific markers of a skeletal stem cells (Chan et al., 2018, Chan et al., 2015). In mouse, a $CD45^{-}Ter119^{-}Tie2^{-}AlphaV^{+}Thy^{-}6C3^{-}CD105^{-}CD200^{+}$ skeletal stem cells has been identified that can self-renew and form cartilage, bone and stromal tissue. Interestingly, proliferation is induced at sites of fracture and lineage commitment influence by

surrounding progenitors and growth factors such as BMP2 indicating a healing mechanism (Chan et al., 2015). Moreover, a human skeletal stem cell has been recently defined as $PDPN^{+}CD146^{-}CD73^{+}CD164^{+}$ in adult bone, can self-renew and can form cartilage, bone and stromal tissue (Chan et al., 2018). However, the term MSC remain widely used in orthopaedic research as defined by the position paper of the International Society for Cellular Therapy (Dominici et al., 2006). These guidelines are likely to isolate a mixed population of skeletal stem cells and lineage specific progenitors but understanding the molecular mechanisms by which this population commits to the osteogenic lineage over chondrogenesis or adipogenesis can help identify targets for therapeutic intervention in bone loss. Although significant advances have been made in defining the progenitors of skeletal tissues the term 'MSC' will be used in this thesis to describe the multipotent progenitor of adipose, cartilage and bone which can self-renew *in vitro* and fulfils the criteria set out by the ISCT.

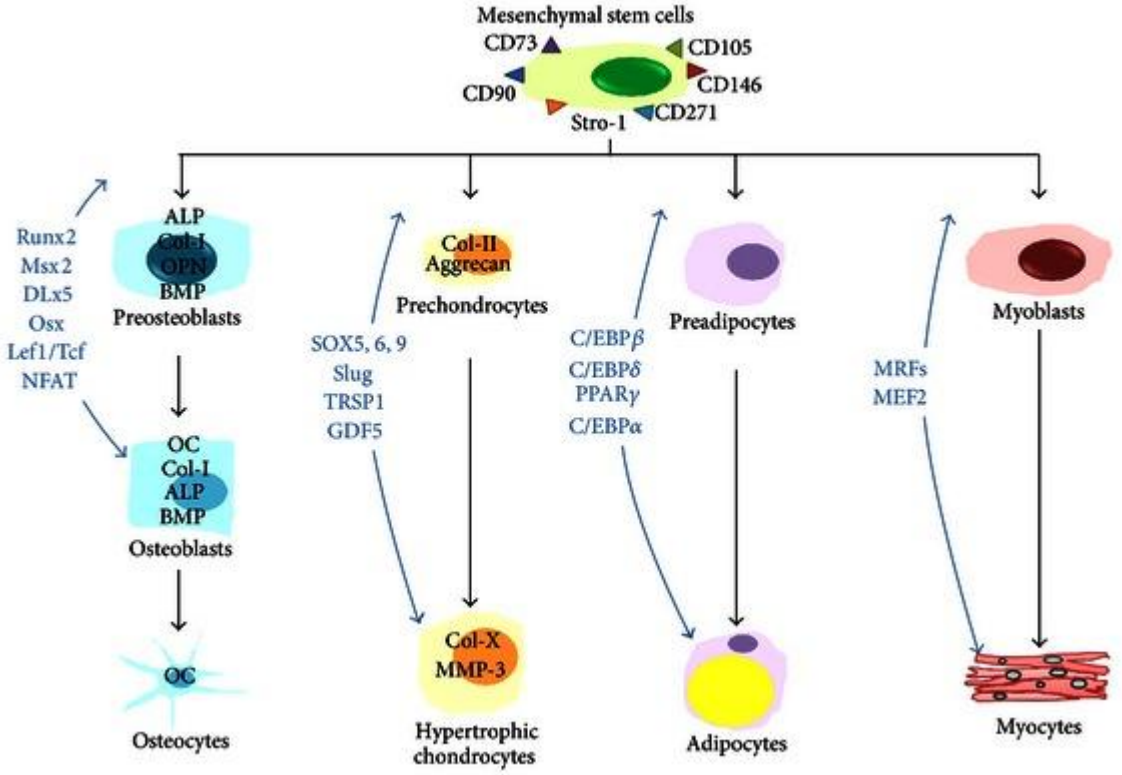

Figure 2.3: The differentiation capacity of MSCs characterised according to ISCT guidelines on surface marker expression. Each lineage is marked by black arrows with the blue arrows and text indicating the transcription factors regulating the differentiation towards each lineage (Giuliani et al., 2013)

For bone formation skeletal progenitors must migrate, proliferate and differentiate as required by the modelling activity cycle. Knowledge of the mechanisms by which MSCs migrate during uncoupled bone formation is lacking although the study of fracture healing and bone formation during development demonstrate possible routes of regulation. While proinflammatory cytokines including TNFα and CXCL7 have an important role in fracture repair, growth factors such as BMP and PDGF are important in endochondral and intramembranous ossification (Su et al., 2018). In addition, numerous growth factors such as TGFβ released from bone during the remodelling cycle, along with PDGF, IGF and BMP expressed in the marrow environment, trigger MSC migration to sites of remodelling (Fiedler et al., 2002, Tang et al., 2009).

The bone modelling process requires adequate MSC proliferation to supply sufficient numbers of osteoid producing osteoblasts. Although the mechanism regulating proliferation during loading induced bone formation remains elusive, applying physiologically relevant mechanical stimuli to MSCs *in vivo* induces an upregulation in MSC proliferation (Delaine-Smith and Reilly, 2012). Several of the pathways involved in MSC migration and indeed lineage commitment have also been linked to proliferation including Wnt and BMP families. In particular BMP3 promotes the proliferation of MSCs through a pathway involving TGFβ and activin, while the ligand LPS drives proliferation by binding to TLR4 on the MSC membrane and directing Wnt signalling through Wnt3a and Wnt5a (Stewart et al., 2010, He et al., 2016). The cytokine IL-17 mediates proliferation of MSCs through the production of reactive oxygen species and the MEK-ERK pathway, this activity also influences MSC migration and osteoblastic differentiation (Huang et al., 2009).

The osteoblastic differentiation of MSCs has been studied extensively *in vitro* but *in vivo* investigations are only beginning to emerge as technological advancements enable cell labelling and lineage tracking. The differentiation of MSCs requires lineage specific growth factors and an appropriate cell density and distribution (Gregory et al., 2005). Studying the process of osteoblastogenesis, 3 distinct stages have been identified covering the initial 96 hours of differentiation; stage 1 occurs within the first 3 hours of differentiation, stage 2 within hours 6-24 and stage 3 at hours 48-96. In each stage a different set of genes are modified, initially transcriptional regulation marks the main activity, in the second stage apoptosis, cell adhesion and matrix protein production are altered and in the third stage the cell cycle and DNA replication are altered (van de Peppel et al., 2017). Microarray gene expression profiling at these specific early time points determined an ordered series of changes beginning immediately upon the

introduction of growth factors. Analysis of osteogenic matrix production *in vitro* determines a 3 stage process for mineralisation of MSCs over 28 days. Initially proliferation dominates the activity of MSCs during the first 2 days, days 5 to 14 see the production of early osteogenic proteins including alkaline phosphatase and collagen type 1, followed finally by the production of mature osteogenic matrix proteins such as calcium, phosphate, osteocalcin and osteopontin (Birmingham et al., 2012).

Osteogenic differentiation is a highly regulated process controlled by several well studied signalling pathways some of which interact. The most studied pathways include TGFβ/BMP, which supports early stages of differentiation and regulates the late stage activities, WNT/β-catenin, which activates bone formation and suppresses resorption and PTH, which acts in a regulatory role for anabolic activity in low doses but supports catabolism over long term activation (Zuo et al., 2012). One of the first responses seen when MSCs are exposed to physiological loads is an upregulation of COX2, which is required for the production of prostaglandins , the activity of COX2 specifically is important for strain induced lamellar bone formation in rats (Hoey et al., 2012d, Forwood, 1996). Furthermore, fluid shear induced osteogenic matrix production in murine MSCs is preceded by an upregulation in *Cox2*, *Opn* and *Runx2* (Stavenschi et al., 2017). The most important transcription factor for osteogenic differentiation is RUNX2, mediating the expression of genes necessary for extracellular matrix production including type 1 collagen, osteopontin, bone sialoprotein (BSP) and osteocalcin by binding to DNA at an osteoblast specific promoter. The induction of RUNX2 expression is regulated in part by SMADs produced by the BMP pathway and kinases produced by the MAP, ERK and PI3K pathways (WITKOWSKA-ZIMNY et al., 2010). Downstream of RUNX2, Osterix expression becomes activated, although the molecular mechanisms by which it acts are not fully understood knockout studies have

determined the essential nature of its role (Huang and Olsen, 2015). Furthermore it is specific to osteoprogenitors in the marrow and cells expressing osterix exhibit the characteristics found on Nestin^{+} cells, a novel marker identified through *in vivo* cell tracking to define the skeletal progenitors portion of multipotent marrow cells (Mizoguchi et al., 2014). Although more *in vivo* analyses are required, bioluminescent imaging has recently shown that osteogenic progenitors maintain their MSC characteristics for 1 week at a segmental bone defect, where the production of type 1 collagen determines they are undergoing osteogenic differentiation (Corn et al., 2013). Overall, MSC osteogenic lineage commitment is precisely regulated at the gene level but further investigation is required to delineate the activation of specific mechanisms. Knowledge of the molecular mechanisms of osteoblastic differentiation is an essential tool in designing new therapies to improve bone health, especially in disease states such as osteoporosis.

2.4 Osteoporosis and the current therapeutic approach

Osteoporosis is a disease characterised by a systemic loss in bone density and quality leading to low impact fractures. Osteoporotic fractures commonly occur as a result of a fall from standing height because the bone structure can no longer support physiological loads. While the loss in bone density is progressive, osteoporosis often remains undetected until the first fragility fracture is sustained. None the less bone mineral density can be measured using dual energy x-ray absorptiometry, whereby a T-score is generated which compares the quantity of bone to that of the average healthy adult population (Kanis et al., 1994). The World Health Organisation defines osteoporosis as a T score 2.5 standard deviations below that of the average healthy population, however

a second category between 1 and 2.5 standard deviations below normal is diagnosed as osteopenic (Brown et al., 2002). Osteopenia is a less severe reduction in bone density than osteoporosis. The diagnosis of osteoporosis fits into three major categories primary type 1 or postmenopausal, primary type 2 or senile and secondary osteoporosis. Primary type 1 occurs because of an increase in the rate of remodelling following a change in estrogen levels whereas primary type 2 occurs because of low rates of bone turnover and reduced osteoblastic activity, leading to a gradual decrease in bone density with age; both are more common in women (Hammett-Stabler, 2004). Secondary osteoporosis occurs due to complications from another condition, most commonly endocrine, nutritional, haematological and autoimmune illnesses such as diabetes mellitus, celiac disease, multiple myeloma and rheumatoid arthritis result in bone loss (Mirza and Canalis, 2015).

Women are affected by osteoporosis more often than men due to the loss in calcium during pregnancy and lactation and the changes in estrogen levels at the menopause. In fact worldwide, post-menopausal women have approximately a 12% risk of osteoporotic fracture, greater than their risk of breast cancer. In Western Europe the fracture risk is approximately 40%, a similar risk level to coronary heart disease (Kanis et al., 2000, Kanis, 2007). Furthermore, approximately 1 in 8 men over the age of 55 experience osteoporosis (Schuit et al., 2004). The most common sites of fracture are the spine, hip, distal forearm and proximal humerus and fracture incidence leads to chronic pain and often a loss in the ability to live independently. Moreover, between 20 and 40% of patients sustaining a hip fracture die within 12 months (Ballane et al., 2014). In addition to debilitating human costs, managing the financial burden of osteoporosis is a growing challenge. It requires orthopaedic post fracture treatment, often including surgery, additional daily care requirements as a result of a fracture, and pharmaceutical

intervention to prevent the progression of bone loss. In the European Union in 2010 these costs amounted to 37 billion euro but these costs are expected to rise with our aging population (Hernlund et al., 2013). In fact by 2050 the cost of osteoporosis is expected to rise approximately 2-fold to 76.7 billion euro (Kanis and Johnell, 2005).

There are several FDA approved drugs for the treatment of osteoporosis which have shown reductions in fracture incidence. However, in a number of patients these have been associated with considerable side effects which are resulting in real concerns on behalf of the clinician and patient when prescribing, leading to a crisis in the treatment of osteoporosis (Khosla and Shane, 2016). The latest guidelines for clinicians suggest that the current pharmacologic treatment options be employed only when hip or vertebral fractures have been sustained and the T-score is <-2.5 or in the case of females over 50 when the T-score is <-1 at the femoral neck or other fracture prone locations (Cosman et al., 2014). The most commonly prescribed treatments are bisphosphonates which bind to hydroxyapatite and inhibit resorption (Drake et al., 2008). There are four major types of bisphosphonates which successfully reduce vertebral fracture incidence in postmenopausal osteoporotic patients by between 41-70% following 3 years of use. Reduction of fracture incidence at the hip, spine and other non-vertebral sites is less effective, 25-50%. However, the incidence of side effects make it challenging to decide when to prescribe and to ensure patient compliance. More common side effects include gastrointestinal upset but renal function can also be compromised and usage over 5 years or more comes with a risk of osteonecrosis of the jaw and atypical femur fractures (Cosman et al., 2014). A second class of osteoporosis treatment is calcitonin, a hormone which destabilises the ruffled border in osteoclasts and prevent it attaching to the bone surface for resorption. Vertebral fracture incidence reduction of 30% is achieved with calcitonin treatment but it also leads to a slightly increased risk of malignant cancers

(Mehta et al., 2003). Other classes of anti-resorptive therapies are selective estrogen receptor modulators and hormone therapy which have similar efficacy to calcitonin at 30-34%. They function in preventing bone resorption by binding to estrogen receptors to regulate the action of osteoclasts. SERMs are associated with an increased risk of deep vein thrombosis among other side effects such as hot flushes and leg cramps; HT is associated with stroke and DVT and with myocardial infarction in patients post menopause for several years (Gennari et al., 2010, Cosman et al., 2014). For this reason they must be prescribed cautiously, close to the age of menopause and at the lowest, shortest dosage effective. The antibody Denosumab, a RANKL inhibitor, is administered with greater fracture reduction efficacy, 68% at vertebral sites, but it often leads to rapid bone loss at the cessation of treatment requiring a second therapy to prevent further bone loss. Furthermore, its side effects include hypocalcemia, serious skin infection and atypical fractures (Zaheer et al., 2015). More recently, advances have been made in the design of therapies to target and enhance the bone forming response which have great efficacy on fracture incidence. Teriparatide is a replacement for parathyroid hormone which is given at a low dose to activate osteoblast formation and inhibit osteoblast apoptosis. With promising rates of fracture incidence reduction, 65% at vertebral sites and 53% at non-vertebral sites treated for 18 months, it provides a favourable alternative. However, the end of treatment is associated with rapid bone loss, necessitating a second line of treatment and approved duration of treatment is limited by osteosarcoma incidence in longer term treatments of rat models (Bodenner et al., 2007). In addition, an antibody targeting sclerostin has been developed to promote osteoblast function; sclerostin is produced by osteocytes and prevents the activity of Wnt/βcatenin. A phase 3 clinical trial of romosozumab, administering romosozumab for 12 months followed by denosumab for a further 12 months, showed promising effects,

reducing non-vertebral fracture risk and increased bone mineral density. However, a phase 3 trial of a second antibody targeting sclerostin, blosozumab, has not gone ahead due to more frequent serious injection site reactions. Interestingly, the drop in the bone formation effects of romosozumab over time is hypothesised to be partially due to a lack of osteoprogenitors (McClung, 2017). Overall, there is a range of therapies on the market for osteoporosis but they come with substantial risks and limited improvements in bone health. Treatments are usually started when the first fracture occurs which is when OP is often diagnosed however this limits their effectiveness as currently bone density can be maintained but there is little progress in increasing bone density. Furthermore, the fact that treatment currently takes the smallest portion of costs associated with osteoporosis indicates that novel therapies are needed to improve bone health in a safer way and reduce the burden of osteoporosis on orthopaedic care (Hernlund et al., 2013).

2.5 Bone formation in osteoporosis

In osteoporosis, the loss in bone density is caused by a number of factors including changes in the material components of bone and their structural organisation. Osteoporotic bone is associated with changes in both collagen and mineral, while collagen crosslinking is decreased in fracture prone sites, mineralisation increases making the tissue more brittle. With age, microdamage accumulates, especially in women, which drives an increase in the remodelling rate. Consequentially, bone porosity increases, from approximately 12% at 60 years of age to about 50% in the most elderly cases studied. The additional pores increase the surface area which osteoclasts are exposed to and where remodelling can take place (Osterhoff et al. 2016, Injury). As the bone remodelling rate increases in the osteoporotic disease state, bones become

prone to fracture because the osteoid formation rate becomes insufficient to replace the resorbed bone. Bone tissue level changes are mediated by cellular behaviour, within the bone remodelling cycle with osteoclasts, osteoblasts and their progenitors contributing to this (McNamara, 2010). In osteoporosis, osteoclast activity is promoted, their maturation is altered and apoptosis is diminished. This is mediated in part by increased RANKL signalling, mRNA levels of RANK are increased in osteoclasts of human osteoporotic bone (Tsangari et al., 2004). RANKL, the ligand expressed by osteoblasts and required for osteoclast activity, is positively influenced by cytokines and parathyroid hormone (Duque and Troen, 2008) and estrogen deficiency leads to increased cytokine secretion (McNamara, 2010). Similarly, PTH increases in the low calcium, low vitamin D environment supporting osteoblasts role in osteoclast differentiation (Duque and Troen, 2008). Moreover, low estrogen environments support hematopoietic progenitors and prolong resorption, unbalancing the bone remodelling cycle, one of many detrimental effects of estrogen deficiency on bone (McNamara, 2010).

While delineation of the molecular mechanisms driving bone resorption has informed the development of the current therapies for osteoporosis, a more complete understanding of bone formation could facilitate better anabolic therapeutic design. Both senile and post-menopausal osteoporosis show altered expression of genes responsible for osteoblast development (Duque and Troen, 2008, McNamara, 2010). Recent data suggests that TGFβ1 and osteoprotegerin are increased and TGFβ2 is decreased in post-menopausal osteoporosis although the role of TGFβ family members is complex and requires further investigation (Wu et al., 2013, Faraji et al., 2016). Similarly mutations in lamin A/C have been posited to play a role in decreased osteoblastic activity and increased RANKL signalling in osteoporosis (Rauner et al.,

2009). Furthermore, osteoblast proliferation is inhibited in osteoporosis as a result of impaired IGF-1 signalling, the expression of which is also negatively affected in oestrogen deficient patients (Perrini et al., 2008). However, a more striking change is found in the marrow of osteoporotic patients which provides the progenitors for the osteoblast population. With age the properties of bone marrow change and the fat content increases, where in osteoporosis the number of adipocytes in the marrow is greater compared to controls of a similar age (Duque and Troen, 2008, Pino et al., 2012b). The presence of adipocytes inhibits osteoblastogenesis whereby it is believed the common progenitor of the lipid and bone lineages becomes imbalanced towards adipogenic activity. One of the main mediators of adipogenic differentiation in MSCs, leptin, becomes dysregulated in osteoporosis, furthermore in osteoporosis MSCs become less responsive to leptin (Astudillo et al., 2008, Hess et al., 2005, Zheng et al., 2015). Although the osteogenic differentiation of osteoporotic MSCs is less understood, it is appreciated that the reaction to osteogenic stimuli is suppressed in osteoporosis (Rodríguez et al., 2004). Additional changes in osteoporotic MSCs are seen upon observation of migration, an impaired chemotactic response has been linked to integrin formation, BMP signalling and Wnt activity (Haasters et al., 2014, Donoso et al., 2015). The lack of adaptation of the bone forming response to the demands of increased resorption could be addressed by the progenitors of osteoblasts and this encourages further investigation into the molecular mechanisms driving osteogenic differentiation in the setting of osteoporosis.

2.6 Loading-induced bone formation

The adaptation of bone tissue to its mechanical environment is widely appreciated and understanding how the cellular components of bone sense and respond to mechanical stimuli informs therapeutic design and tissue engineering in orthopaedic medicine. The forces which bone cells experience vary spatially; the osteocytes are embedded deep within cortical bone tissue while preosteoblasts can be resident on the bone surface or within the viscous marrow in the bone lumen.

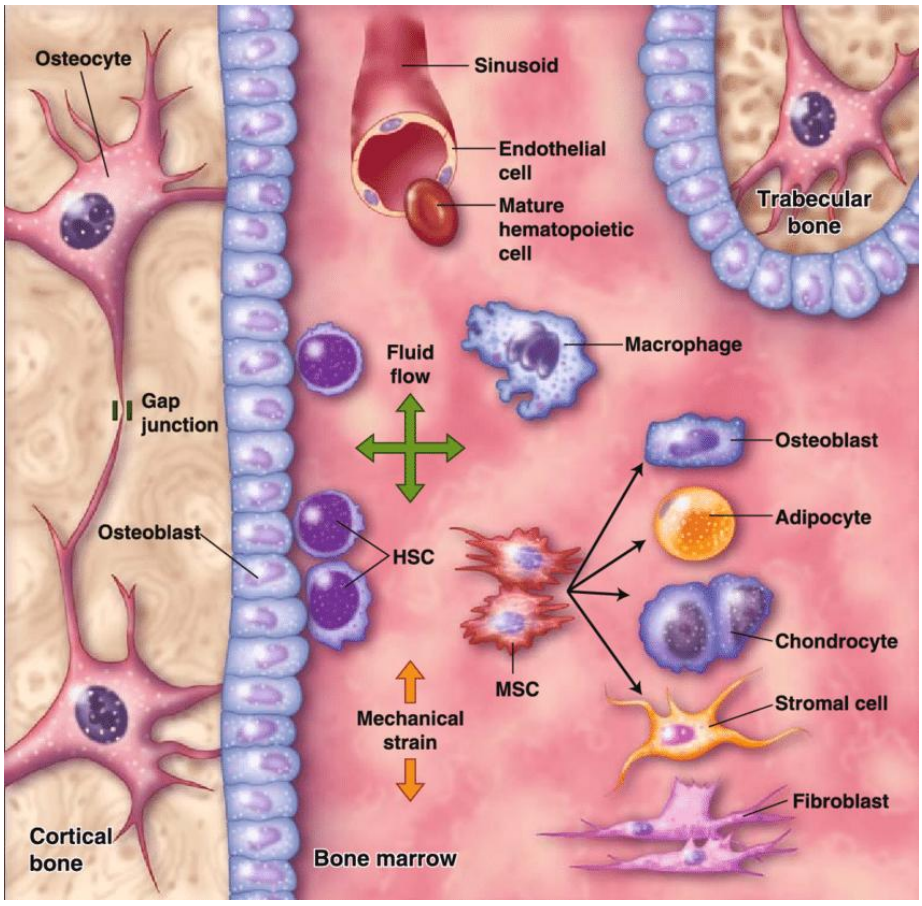

Figure 2.4 The bone and bone marrow interface describing the cells populating mature bone, osteocytes and osteoblasts, and the marrow, HSC (hematopoietic stem cell) which gives rise to osteoclasts and the MSC (mesenchymal stem cell) which gives rise to osteoblasts, adipocytes and chondrocytes (Castillo and Jacobs,

The osteocyte cell body is housed within lacunae and cell processes extend out from the cell body into mineralised bone through surrounding canaliculi. When bone experiences strain during physiological loading osteocytes feel this stimulus, this can act directly on the cell membrane by initiating signalling at the transmembrane connections between cells and their surroundings such as the gap junction connexion 43 (Cherian et al., 2003, Cherian et al., 2005). Furthermore, the strain induces pressure in the canaliculi, cyclic hydraulic pressure effects microtubule organisation and induces oscillations in intracellular calcium (Liu et al., 2010a). More frequently studied is fluid flow induced shear stress which becomes amplified by the matrix surrounding the cell process and can open ion channels to mediate calcium signalling (Klein-Nulend et al., 2012, Wang et al., 2007, Lee et al., 2015c). The magnitude of the shear experienced depends on the load experienced and the frequency of loading, furthermore a dynamic load will induce a greater response than similar static loads (Weinbaum et al., 1994).

In contrast to osteocytes, osteoblasts sit on the surface of bone tissue and are exposed to the strain incident on the mineralised matrix they are attached to. During intense physical exercise the bone is exposed to up to 3000 μstrains and applying this magnitude of strain at 1Hz for 1 minutes induces a biochemical osteogenic response in osteoblasts, including prostaglandin mediated collagen synthesis (Binderman et al., 1988, Jones et al., 1991). In addition, osteoblasts at the endosteum lie adjacent to bone marrow which is displaced during physical exercise generating a shear stress on the membrane of the osteoblast. Fluid shear stress induces a range of robust biochemical signals in osteoblasts including prostaglandin synthesis and intracellular calcium fluxes. Similar to osteocytes, the response depends on shear stress magnitude and frequency but at levels which modelling predicts to occur physiologically, 2Pa, 1Hz, shear stress

causes a greater osteogenic response than strain in osteoblasts (Jacobs et al., 1998, Reich and Frangos, 1993, You et al., 2000).

Consideration of the mechanical environment is an important balancing act in osteoporosis where exposure to exercise presents a risk of fall and fracture to fragile, brittle bones but physical activity is important in maintaining optimal bone density. In addition, higher strains will be experienced by bone as tissue density decreases yet physiological loads remain similar. This increased mechanical stimulus is hypothesised to induce an altered response in osteocytes altering the mineral content of the osteoid deposited (McNamara, 2010). Moreover, estrogen deficiency can impair osteoblast mechanosensitivity and trigger the apoptosis of osteocytes which contribute to the increased mineral content (Sterck et al., 1998, Tomkinson et al., 1997). Considering these effects it is important to understand the mechanoresponse of bone cells in designing therapies to improve bone quality.

2.7 Mechanosensing by mesenchymal stem cells

Considering the bone marrow as the source of MSCs, the mechanical environment of MSCs consists of the marrow cavity and the bone forming surface. Marrow is contained within the medullary cavity and exists under a pressure even in static conditions; this intramedullary pressure is influenced by blood pressure and skeletal location but is estimated to be approximately 4kPa and muscular contractions enhance this (Kumar et al., 1979, Gurkan and Akkus, 2008). Furthermore, during physical activity the bone is strained and pressure generated in the marrow cavity displace the viscous fluid in an oscillating fashion and this fluid flow is more pronounced in the smaller volume found

between trabeculae. While the location of the marrow makes it is difficult to measure the pressure experienced *in vivo*, measurements of intact sheep tibiae and human femora *ex vivo* estimate it is less than 50kPa (Bryant, 1983, Downey et al., 1988). The application of cyclic hydrostatic pressure to human MSCs results in an upregulation *COX2* as well as increased deposition of osteogenic matrices, both collagen and calcium (Liu et al., 2009). Although pressures between 10 and 300kPa influenced matrix deposition, early gene expression changes were more robust at higher magnitudes of pressure, 100 and 300kPa (Stavenschi et al., 2018b). The application of much higher magnitudes of hydrostatic pressure, 1 and 10MPa at 1Hz, influence the differentiation of MSCs towards the chondrogenic lineage increasing the mRNA expression of aggrecan and *SOX9* as well as the production of proteoglycans (Wagner et al., 2008, Miyanishi et al., 2006). Thus, pulsatile pressure applications have a robust influence on MSC differentiation with pressure magnitude determining lineage commitment.

As the marrow is displaced during exercise the movement of the viscous fluid generates a shear stress on the MSCs within. The rate of fluid shear is highly dependent on marrow viscosity, which is inherently difficult to measure given the change in temperature and pressure once the marrow containing bone lumen is exposed (Gurkan and Akkus, 2008). However computational modelling, informed by µCT scans of porcine proximal femur, have aided in the understanding of the magnitude and influences on the shear stress experienced by MSCs. Shear stress increases with the strain rate and in trabecular bone where the marrow volume is more constrained (Metzger et al., 2015b). Although most studies to date have applied shear stress in the range of 0.1-2Pa in 2D systems and less than 0.03Pa in 3D constructs, modelling predicts that a viscous marrow can generate shear stress exceeding 5Pa (Coughlin and

Niebur, 2012, Delaine-Smith and Reilly, 2012). The application of shear stress *in vitro* is usually carried out using a parallel plate flow chamber via the exposure of cultured cells to a defined and controlled rate of fluid flow. Moreover, oscillating flow is considered to better model physiological activity compared to steady or pulsatile patterns given the dynamic nature of the gait cycle (Jacobs et al., 1998). Shear stress has a pro-osteogenic, anti-adipogenic effect on MSCs, upregulating early gene expression in a magnitude and frequency dependent manner and increasing the deposition of extracellular matrix optimally at 2Pa, 2Hz while reducing adipocyte formation (Stavenschi et al., 2017, Rubin et al., 2007). In addition, application of 1Pa shear stress at 1Hz induces MSC proliferation (Li et al., 2004).

Although there have been multiple attempts to model the mechanical environment of MSCs *in vitro* in 2D and 3D systems, the characteristics of the stimulus applied can be difficult to compare between studies and to *in vivo* models. Consideration of the role of biochemical components and the substrate the cells attach to is important in comparing studies. Overall, MSCs can sense and respond to their mechanical environment and the loading stimulus they experience is important in regulating their fate especially in terms of lineage commitment.

2.8 Mechanotransduction in mesenchymal stem cells

Once biophysical stimuli are detected, MSCs must transduce the signal into a biochemically driven behavioural response which will aid in cell functionality, this process is termed mechanotransduction. Mechanotransduction is primarily mediated by membrane bound proteins and the cytoskeleton as the mechanical load will impact them directly. These initial sites of reaction trigger a signalling cascade which will influence

gene and protein expression and the contribution made by MSCs to their surrounding tissues.

The cytoskeleton is composed of microtubules, actin filaments and intermediate filaments which each have distinct roles in supporting cell structure. Microtubules extend from the centrosomes and spatially organise organelles in the cytoplasm. Actin is arranged in long coiled chains and forms networks which support cell structure for motility and division, when these join into bundles and become crosslinked by other proteins such as actinin they are known as stress fibres (Pellegrin and Mellor, 2007). Intermediate filaments are generally tougher than actin filaments and increase the strength of the cytoskeleton. The extracellular matrix and cytoskeleton interact to maintain the structural properties of the cell; the ECM exerts compression on microtubules while tensile stress applied to filaments maintains stability. The deformation of the cytoskeleton observed upon cell loading supports the hypothesised roles of cytoskeletal components (Alenghat and Ingber, 2002). The cytoskeleton influences MSC differentiation where osteogenesis is promoted on a stiff substrate which causes the formation of stress fibres and greater F-actin expression. Adipogenic differentiation is induced when the actin components are biochemically disassembled and when grown on small, round micropatterns. The RhoA/ROCK pathway is activated by actin fibre formation and decreases in RhoA activity support chondrogenic and adipogenic activity in MSCs (Mathieu and Loboa, 2012). Changes in actin and microtubules can modulate nuclear activity through the LINC complex a family of proteins residing on the nuclear membrane and lamins within the nucleus to influence DNA replication and transcription (Steward and Kelly, 2015). While it is intermediate filaments that transduce the cyclic hydraulic pressure predicted to occur in bone marrow, disassembly of IF bundles is induced and they recoil to the perinuclear region

leading to the upregulation of osteogenic genes (Stavenschi and Hoey, 2018). The cytoskeleton plays an important role in communicating with the environment surrounding MSCs serving as a two-way signal transducer between nuclear activity and the extracellular matrix.

The first point of contact between the cell and the extracellular matrix are focal adhesions embedded in the cell membrane, because of this interaction they play important roles in mechanotransduction. An integrin is a glycoprotein composed of an alpha and beta subunit which is expressed on the cell membrane and binds to extracellular matrix proteins. Focal adhesions consist of a central dimer of an alpha and beta integrin component where the combination of subunits determines binding specificity; this core combines with intracellular proteins to communicate the signals detected in extracellular regions with various signalling pathways in the cytoplasm. Integrins transduce a number of mechanical stimuli in MSCs including dynamic compression, hydrostatic pressure and matrix stiffness. Focal adhesions facilitate cell spreading and their formation predicts MSC lineage commitment whereby more focal adhesions allow osteogenesis but minimal adhesions and a rounded phenotype promote adipogenesis and chondrogenesis (Mathieu and Loboa, 2012). A stiffer matrix results in increased α_2 integrin at the substrate interface and $\alpha_2\beta_1$ is primarily responsible for collagen binding. The binding of α_2 integrin to collagen is important in mediating ascorbic acid induced osteogenic gene expression and mineralised matrix production through the ROCK and FAK pathways (Shih et al., 2011). Moreover, the application of cyclic hydrostatic pressure or dynamic compression to MSCs leads to an upregulation in chondrogenic genes and this requires integrin binding to the pericellular matrix as indicated by blocking the integrin interaction with an RGDS peptide (Steward et al.,

2014). Overall, disturbing integrin activity hinders the cells ability to interact with the surrounding matrix.

The cell membrane is the site of ion channels which regulate the transfer K^+, Na^+ and Ca^{2+} between the cytosol and the extracellular environment. Transmembrane channels are directly impacted by physiological mechanical loading especially fluid flow induced shear stress which can induce a tenfold increase in intracellular calcium in MSCs (Liu et al., 2010b). In fact, intermittent application of 0.004-1.2Pa shear stress induces an influx of calcium. Stretch activated channels can be activated via diverse physiological loads on the MSC membrane including pressure and cyclic tensile strain (McMahon et al., 2008, Xiao et al., 2015). While $1g/cm^2$ pressure induced calcium signals activated osteogenesis similar to that seen with fluid shear, 10% cyclic stretch upregulated the synthesis of GAG. However, changes in the osmotic pressure and substrate mediated membrane tension are all capable of opening mechanosensitive channels in other tissues and may play a role in MSCs. A recent study poses the role of stretch activated calcium channels in activating calcium sensitive potassium channels (Martinac, 2004, Chubinskiy-Nadezhdin et al., 2017). Furthermore, the mechanosensitive potassium channel TREK1 plays a role in MSC mediated osteogenesis increasing the collagen production in co-cultured epiphyseal cells (Henstock et al., 2018). Moreover, calcium signalling has been linked to important roles in several pathways which mediate the proliferation and differentiation of MSCs. The mobilisation of calcium is involved in mediating the changes in vimentin seen in chondrogenic differentiation of MSCs in response to hydrostatic pressure via the second messenger's calmodulin and calcineurin (Steward et al., 2014). Fluid shear induced influx of calcium in MSCs is associated with phosphorylation of ERK, which leads to the transcription of RUNX2 and upregulation of early osteogenic markers osteopontin and osteocalcin (Li et al., 2004, Riddle et al.,

2006, Liu et al., 2010b). Fluid shear mediated calcium signalling also mediate the phosphorylation of kinases on the osterix pathway supporting osteogenesis (Liu et al., 2015). To further delineate the mechanisms by which mechanotransduction occur the expression of mechanosensitive calcium channels on MSCs will be necessary, then the specific role of these channels and their role in directing MSC fate can be investigated.

2.8.1 TRPV4 mediated mechanotransduction

The study of the mechanotransduction mechanisms in chondrocytes and osteocytes among other mechanosensitive cells outlines several mechanosensitive calcium channels with essential roles mediating the cell's response to loading. One such channel, TRPV4, is a calcium permeable, non-selective cation channel from the transient receptor potential vanilloid group. While TRPV4 can be activated by osmotic pressure, heat, pH it is also mechanosensitive and multiple specific biochemical agonists have been developed which enable further investigation into the precise stimulus required to activate it (White et al., 2016).

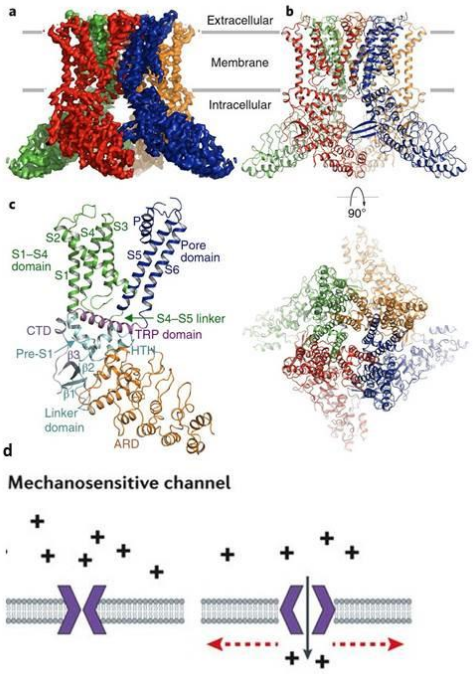

Figure 2.5: a-c Representation of the transmission electron microscopy informed structured of TRPV4 with each of the four subunits represented in a different colour. d Representation of the mechanism of action of ion channels stimulated by mechanical stimulus, illustrated by the red arrows (Huse, 2017, Deng et al., 2018)

Recently TRPV4 has come to light for its prominent role in chondrocyte mechanotransduction where it mediates a calcium signalling response to loading and aids in gene expression and PGE_2 production (Phan et al., 2009, O'Conor et al., 2014). In addition, TRPV4 plays an essential role in the osteocyte response to fluid shear, whereby the calcium influx mediates a decrease in sclerostin production (Lyons et al., 2017). Furthermore, attenuation of the TRPV4 mediated calcium signal in osteocytes exposed to fluid shear reduces the *Cox2* upregulation that the same mechanical stimulus induces in controls (Moore et al., 2018a, Lee et al., 2015c). Strikingly, TRPV4 is localised to the primary cilium in several cell types including osteocytes, chondrocytes and kidney epithelial (Lee et al., 2015c, Phan et al., 2009, Köttgen et al., 2008). Mechanosensitive calcium channels including TRPV4 play an important role in signal transduction particularly via the primary cilium which may provide a novel target to manipulate cell fate.

2.8.2 Primary cilium mediated mechanotransduction

Another key player in mechanotransduction, which has only become appreciated recently, is the primary cilium, an antenna like extension of the cell membrane. The primary cilium is non-motile and occurs as a single cilium on most mammalian cell types during growth arrest or non-dividing stages of the cell cycle. The rod-like shape is formed from a ring of nine microtubule doublets which begin at the basal body, formed from the mother centriole, extending away from the cytoplasm (Satir et al., 2010). The plasma membrane extends around these microtubules forming a microcompartment that is spatially distinct from the cytosol. Extension into the extracellular environment and the large surface to volume ratio of the ciliary membrane equip the cilium for encountering external stimuli and initiating signalling cascades. Although long regarded as a vestigial organelle the primary cilium is now appreciated as a mechanosensor and chemosensor playing an essential role in adaptation to environmental changes in developmental signalling but also in a range of mature tissues including kidney, liver, cartilage and bone (Satir et al., 2010, Hoey et al., 2012a). Quantifications from our lab and others have recorded cilium incidence at approximately 86-95% on human bone marrow derived MSCs, with ciliogenesis only occurring during cell cycle arrest (Hoey et al., 2012d, McMurray et al., 2013). *In vitro* studies suggest the average length of the cilium axoneme is approximately 3µm; however this can vary, from 1.7-6µm, with MSC donor, antibody staining and imaging technique (McMurray et al., 2013, Labour et al., 2016c, Dalbay et al., 2015). Although the available recording of primary cilium incidence in marrow tissue is low at 1% of cells, there is a need to study ciliogenesis *in vivo* given the consequence of cilium dysfunction on the skeletal system (Coughlin et al., 2015). More precise measures of cilium incidence require the comparison of cilium incidence at different skeletal locations, the current approximations account only for

ovine vertebrae models and more accurate methods have been developed to measure the length of cilia in different focus planes (Dummer et al., 2016).

Defects in cilium formation and function can result in a number of different syndromes collectively known as ciliopathies; the features depend on which ciliary protein is genetically mutated. Ciliopathies are typically associated with retinal degenerations, renal cystic disease and cerebral anomalies. A role for the primary cilia in musculoskeletal development is apparent from the occurrence of skeletal dysplasia in ciliopathies including Jeune asphyxiating thoracic dystrophy, Meckel–Gruber syndrome and Nephronophthisis (Waters and Beales, 2011, Huber and Cormier-Daire, 2012). Furthermore, mouse models deleting ciliary localised proteins in osteoblasts result in osteopenia and in chondrocytes result in abnormal differentiation and premature growth plate closure (Song et al., 2007, Yuan et al., 2015). Deletion of the cilium in MSCs *in vitro* impairs the differentiation capacity towards the adipo, chondro and osteogenic lineages through a reduction in transcription factor expression (Tummala et al., 2010). The critical role of the cilium in differentiation promotes research into the mechanisms by which it influences cell response as a potential mode of intervention in disease states.

Both the structure and location of the primary cilium facilitate mechanotransduction in many cell types including MSCs. Proteins are transported along the cilium axoneme via the intraflagellar transport system and multiple IFT proteins contribute to this function. Silencing genes such as *Ift80* and *Ift88* in murine MSCs has highlighted roles for the primary cilium in maturation along the chondrogenic and osteogenic lineages (Yuan et al., 2015). Receptors specific to the Hedgehog and Wnt pathway are expressed at the cilium and pathway activity is regulated by controlling the access of ligands to these receptors within the cilium. For example, the receptor Patched is expressed at the base

of the cilium, it inhibits the movement of smoothened onto the ciliary membrane, however when Hedgehog ligand binds to Patched then Smoothened is free to move. Smoothened is translocated to the tip of the primary cilium where Gli is activated and Gli induces the transcription of hedgehog targets in the nucleus. The primary cilium is essential for spatially removing Gli from Smoothened to regulate Hedgehog activity (Rohatgi et al., 2007). Hedgehog target genes including *Gli* negatively influence adipogenesis and hedgehog activity promotes activity of the BMP pathway mediating osteogenic differentiation (Chen et al., 2016b). The compartment existing within the ciliary membrane also enables the regulation of Wnt activity, whereby β-catenin is sequestered in the cilium axoneme until Wnt binds to the receptor Frizzled on the cilium and triggers β-catenin nuclear translocation, which influences transcription of osteogenic markers (Bodine and Komm, 2006).

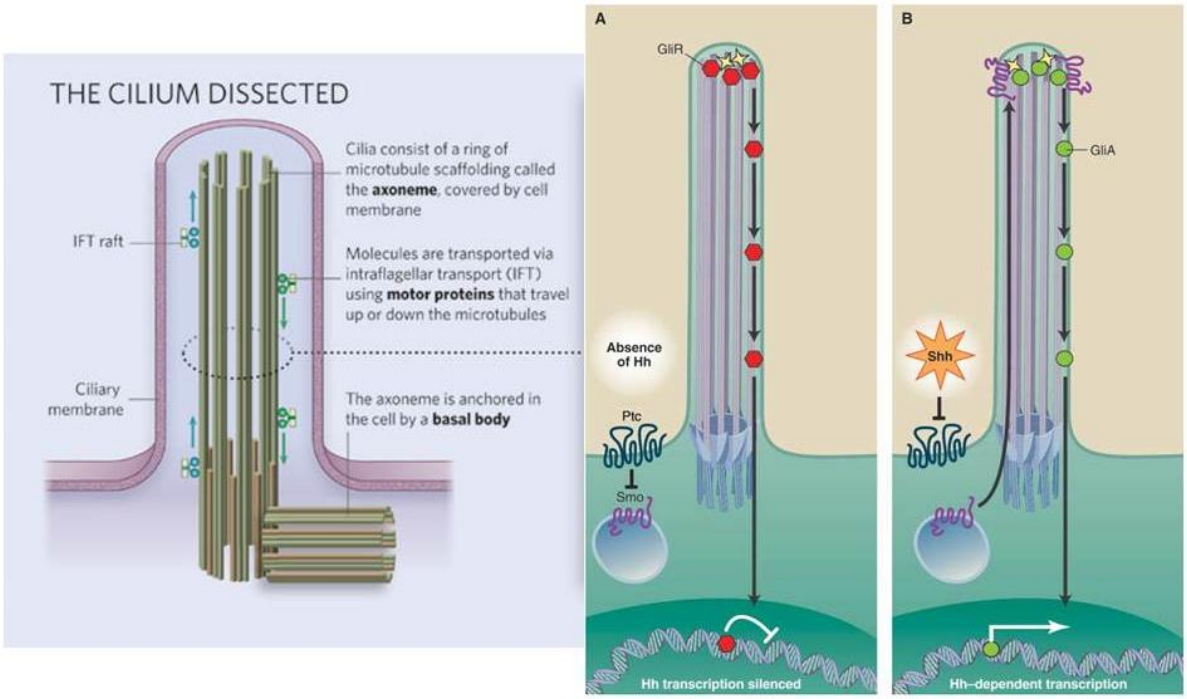

Figure 2.6 Schematic of the primary cilium structure, illustration of the regulation of hedgehog signalling using the ciliary axoneme, (Singla and Reiter, 2006, Adams, 2010)

The protrusion of the cilium axoneme into the extracellular space exposes it to the surrounding environment including interstitial fluid, adjacent cell membranes and matrices. The primary cilium is required to regulate Wnt signalling and in MSCs this is responsive to topographical changes in the local environment. During physiological loading the primary cilium plays a significant role in mediating the osteogenic response in skeletal progenitors. Knockdown of *Ift88* in human MSCs resulted in a loss in the upregulation of early osteogenic markers that are induced by oscillatory fluid flow inducing 1Pa shear stress. Furthermore, deletion of *Kif3a*, an essential component of the cilium, in the marrow cells of mice led to an impaired rate of bone formation in response to loading. In kidneys the cilium bends under the influence of extracellular fluid flow and this opens calcium channels (Praetorius and Spring, 2001, Praetorius and Spring, 2003). In osteocytes, a calcium signalling centre is formed at the primary cilium and it is responsive to physiologically predicted fluid shear rates (Lee et al., 2015c). These findings suggest that calcium signalling and potentially cilium localised calcium channels could form an important mechanotransduction partnership in MSCs.

The importance of the primary cilium in initiating and regulating signalling pathways highlights it as a therapeutic target. Moreover, the localisation of specific pathways to the cilium indicates a robust response could be achieved by influencing activity at the cilium. Recently, osteocytes have been treated with Fenoldopam and lithium chloride to elongate the cilium axoneme with the aim of promoting its mechanosensory capacity (Spasic and Jacobs, 2017). Furthermore, the progression of Hedgehog activity associated with osteoarthritis progression in chondrocytes is attenuated by disruption of ciliary traffic using lithium chloride (Thompson et al., 2016). There are promising results in manipulating cell activity in both osteocytes and chondrocytes which suggest

that therapeutically targeting the primary cilium activity could have promising results for cell fate manipulation.

2.9 Summary

The adaptation of the skeleton to its mechanical environment is essential in maintaining strength and fracture resilience throughout our lifetime. Bone is a hierarchical structure, the signals from osteocytes deep within mineral tissue and skeletal progenitors in the marrow and periosteum are involved in sensing and responding to the mechanical stimuli experienced. The multipotent skeletal progenitor, named MSC, supplies the osteoblast population that produce osteoid matrix for the formation of bone. There must be sufficient number of MSCs and the MSCs must be responsive to surrounding signals and capable of osteogenic lineage commitment to maintain skeletal health.

The consequences of an inadequate bone formation rate can be seen in osteoporosis, where bone density is decreased and patients become prone to fracture. Current therapies are inefficient and present serious side effects. New therapeutic development aims to increase bone density by increasing new bone formation. There are fewer MSCs in the marrow of osteoporotic patients and they have an increased tendency to towards adipogenesis however the osteogenic capacity of osteoporotic MSCs is not well understood. An understanding of how physical loading induces an osteogenic response could identify novel therapeutic targets for osteoporosis. Although it is understood that mechanical stimuli trigger a proliferative and osteogenic response in MSCs, the mechanisms by which MSCs sense mechanical signals and change their biochemical behaviour is unclear. Literature on the mechanisms that other skeletal cell types use in mechanotransduction informs hypotheses for MSC mechanotransduction. In particular

the role of calcium signalling and mechanosensitive calcium channels in fluid shear responses in osteoblasts poses the question of their role in the osteoblast progenitor. Moreover, the function of the primary cilium in mechanotransduction and recent advances in manipulating it to influence cell fate inform this work investigating the role that such mechanisms could have in MSCs.

Chapter 3:

TRPV4-mediates oscillatory fluid shear mechanotransduction in mesenchymal stem cells in part via the primary cilium

3.1 Introduction

Skeletal homeostasis and repair requires the continued replenishment of the bone forming osteoblast from a mesenchymal stem cell (MSC) population (Knight and Hankenson, 2013). This process of MSC differentiation has been shown to be mechanically regulated, with physical loading promoting MSC osteogenesis and bone formation (Chen et al., 2015, Stavenschi et al., 2017). However, the molecular mechanisms by which mechanical stimuli can induce a change in biochemical cellular signaling, termed mechanotransduction, is poorly understood. With aging and the onset of osteoporosis, the number and osteogenic potential of MSCs is diminished (Veronesi et al., 2011, Pino et al., 2012a), leading to a decoupling of the bone formation/resorption cycle and net bone loss (Sambrook and Cooper, 2006). Given the potent role of physical activity in regulating stem cell differentiation and bone formation, deciphering the mechanisms of mechanotransduction may provide novel targets to promote bone formation by mimicking the beneficial effects of loading at a molecular level (Komm et al., 2015).

During loading-induced deformation of bone, MSCs within the marrow are predicted to experience a complex array of mechanical stimuli that includes oscillatory fluid flow induced shear stress (Metzger et al., 2015a), which has been shown *in vitro* to drive MSC proliferation and differentiation (Li et al., 2004, Stavenschi et al., 2017, Riddle et al., 2006). Several studies have explored the role of fluid shear (FS) in driving osteogenic responses in MSCs, with varying magnitudes and durations of mechanical stimuli making direct comparisons challenging. Human MSCs (hMSCs) exposed to FS display an upregulation in bone morphogenetic protein 2 (BMP2) and osteopontin (OPN)(Yourek et al., 2010) after 24hrs stimulation or runt related transcription factor (RUNX2), alkaline phosphatase (ALPL), and OPN (Sonam et al., 2016) after 48hrs stimulation. A recent systematic study on the effect of oscillatory fluid shear (OFS) variables such as shear magnitude and frequency has demonstrated an increase in Cyclo-oxygenase 2 (Cox2), Opn and Runx2 expression at early time points, that over 21 days results in enhanced collagen and matrix mineralization (Stavenschi et al., 2017), which is an agreement with a number of studies demonstrating fluid shear induced MSC osteogenesis (Shamseer et al., 2012, Bancroft et al., 2002, Scaglione et al., 2008). Cytosolic Ca2+ is a primary second messenger in the control and regulation of a wide range of stem cell functions and is released from intracellular stores in response to fluid shear, with cytosolic calcium levels peaking within seconds of the application of flow (Riddle et al., 2006). The role of this initial calcium signaling in triggering downstream osteogenic transcriptional activity is widely appreciated, as demonstrated in osteoblasts where removal of the calcium flux within the cytosol prevents the fluid shear mediated upregulation in Opn (You et al., 2001). Furthermore, a loss of this calcium signal impairs the capacity of osteoprogenitors to proliferate and form mineralized tissue (Wen et al., 2012). Despite the well characterized effect of

OFS on calcium signaling and differentiation, the mechanisms by which MSCs sense this mechanical stimulus remains poorly understood.

The application of fluid shear to MSCs results in strain across the membrane that is concentrated at specific regions, such as focal adhesions and at the primary cilium (Vaughan et al., 2014). These sites of maximum strain have been shown to be important for stem cell fluid shear mechanotransduction (Shamseer et al., 2012, Riehl et al., 2015). Focal adhesions are large macromolecular assemblies that are the initial site of interaction between the cell and the extracellular matrix (ECM), via integrin attachments. Integrins facilitate increased cytoskeletal interaction and provide binding sites for a multitude of effectors, activating key mechanosignaling pathways (McMurray et al., 2015, Ross et al., 2013). The primary cilium is a solitary cellular organelle that extends from the cell membrane(Satir et al., 2010, Hoey et al., 2012b). Previous work in kidney epithelial cells and osteocytes suggests it is positioned apically and so exposed to fluid shear in the extracellular fluid between cells(Lee et al., 2015c). The cilium is composed of microtubules along which specialised motor proteins known as intraflagellar transport proteins function to transport cargo along the axoneme. Absence of a functional cilium including the IFT component IFT88 disrupts skeletal development (Irianto et al., 2014, Haycraft et al., 2007). Spatially removed from the cytoplasm, the ciliary microdomain is highly enriched in signaling molecules, receptors and ion channels (Hoey et al., 2012a, Hoey et al., 2012b, Labour et al., 2016a), and as such plays critical roles in stem cell function including mechanotransduction (Shamseer et al., 2012). Interestingly, both focal adhesions and the primary cilium have been linked to mechanically-induced calcium signaling. Mechanical stretch of integrins and/or bending of the cilium leads to a rapid increase in local and cytosolic calcium levels (Lee et al., 2015c, Matthews et al., 2010). Fluid shear induced strain has the

capacity to open stretch-activated calcium channels, motivating the identification of these specific channels which mediate calcium signals during MSC mechanotransduction.

The Transient Receptor Potential (TRP) family is a group of calcium permeable membrane spanning ion channels. Defined in 7 subgroups, they display diverse stimulatory mechanisms including mechanical activation(Nilius and Owsianik, 2011). Substantial evidence exists for the role of TRP subfamily V member 4 (TRPV4) in mechanosensation. TRPV4 is required for loading induced responses in committed cells such as chondrocytes (O'Conor et al., 2014), osteocytes (Lee et al., 2015c), epithelial (Pochynyuk et al., 2013) and endothelial cells (Thodeti et al., 2009). Furthermore, TRPV4 has been previously found to have a preferential spatial cellular organization to areas of high strain, such as at focal adhesions (Matthews et al., 2010) and along the primary cilium (Lee et al., 2015c, Phan et al., 2009). Mutations in TRPV4 have been linked to human skeletal pathologies (Kang et al., 2012) and TRPV4 KO mice do not lose bone in a hind limb suspension model (Mizoguchi et al., 2008), strongly indicating that TRPV4 plays a role in skeletal mechanobiology. Furthermore, MSCs isolated from TRPV4 KO mice demonstrate an inhibited osteogenic potential (O'Conor et al., 2013). Although the role of TRPV4 in mechanotransduction in mature cells of the musculoskeletal system is well demonstrated, in MSCs its subcellular spatial organization and potential role in mechanotransduction are poorly characterized.

As a precursor to loading-induced bone formation, deciphering the molecular mechanisms of MSC osteogenesis is a critical step in developing novel anabolic therapies to promote bone regeneration. Therefore, in this study we characterize the expression of TRPV4 in MSCs and demonstrate that TRPV4 localizes to areas of high strain, specifically the primary cilium, and show that this mechanosensitive channel is

required for stem cell mechanotransduction, mediating fluid shear induced calcium signaling and osteogenic gene expression. Furthermore, we demonstrate that TRPV4 can be activated pharmacologically eliciting an osteogenic response that mirrors both the flux in calcium signal and upregulation in early osteogenic genes activated by fluid shear, indicating mechanotherapy potential. Lastly, we show that TRPV4 localization to the primary cilium is functionally significant, with MSCs with defective primary cilia exhibiting an inhibited osteogenic response to TRPV4 activation. Collectively, this data demonstrates a novel mechanism of stem cell mechanotransduction, which can be targeted therapeutically, and further highlights the critical role of the primary cilium in stem cell biology.

3.2 Methods

3.2.1 Mesenchymal Stem Cell Culture

The murine mesenchymal stem cell line C3H10T1/2 was obtained from ATCC (LGC Standards, Teddington, Middlesex, UK, http://www.lgcstandards-atcc.org). MSCs were maintained in Dulbecco's modified Eagle's medium (DMEM) with low glucose (Sigma-Aldrich Ireland Ltd. Arklow, Ireland, http://www.sigmaaldrich.com/ireland.html) supplemented with 10% fetal bovine serum (FBS) (South American origin, Labtech International, Ltd. Heathfield, East Sussex, UK) and 1% Penicillin Streptomycin (P/S) (Sigma). All experiments were carried out using C3H10T1/2s at passage 12-17. This cell line has previously been shown to undergo both biochemical and biophysically induced osteogenic lineage commitment (Stavenschi et al., 2017). For extracellular matrix formation MSCs were supplemented with 10nM Dexamethasone (Sigma), 10mM β-glycerophosphate (Sigma) and 0.05mM

Ascorbic acid (Sigma) to provide the components necessary for osteogenic matrix formation.

3.2.2 Gene expression

TRI reagent (Sigma) was used to extract RNA per the manufacturer's protocol. The concentration of RNA in each sample was measured using a Nanodrop spectrophotometer and sample purity was checked via 260/280 and 260/230 absorbance ratios. 100-800ng of RNA was reverse transcribed to cDNA using the High-Capacity cDNA Reverse Transcription Kit (Applied Biosystems, Foster City, CA, USA, https://www.thermofisher.com). Quantitative polymerase chain reactions (qPCR) were prepared for all samples using SYBR Select Master Mix with ROX passive dye (Applied Biosystems, 4472903) and custom designed primers (Sigma) for *18s, Cox2* and *Opn*. *TRPV4* qPCR reactions were prepared using TaqMan Universal PCR Mix (Applied Biosystems, 4304437) with ROX passive dye and a pre-designed Taqman Gene Expression Assay (Applied Biosystems, 4331182) as outlined in supplementary table 1 for amplification using the ABI 7500 real time PCR machine (Applied Biosystems). The relative quantity of each sample was calculated with reference to *18s* and expressed as fold change normalized to the control group.

3.2.3 Parallel Plate Flow Chambers

Parallel plate flow chambers were designed in house as described previously (Stavenschi et al., 2017). Briefly, MSCs were seeded on fibronectin (10µg/ml) coated glass slides, assembled between two plates and attached to a programmable syringe pump (New Era Pump Systems Inc. Farmingdale, NY, USA, http://www.syringepump.com). Oscillating fluid shear (OFS) was applied through a

10ml syringe (Becton Dickinson and Company, Franklin Lakes, NJ, USA, www.bd.com) at 52.5ml/min and at a frequency of 1Hz subjecting cells to a shear stress of 1Pa. The no flow controls were similarly assembled within the chambers but were not subjected to fluid shear.

3.2.4 Calcium Imaging

Changes in calcium signaling were observed using the cell permeant calcium indicator Oregon Green 488 BAPTA-1AM (OGB) (Invitrogen, Carlsbad, CA, USA, https://www.thermofisher.com). OGB stock was prepared in DMSO at 2mM, all further dilutions were in phenol red free DMEM, 0.5% FBS. MSCs were seeded on fibronectin (Sigma) coated glass slides (No. 2- CN Technical, Wisbech, UK, http://www.cntech.co.uk) at a density of 3400/cm^2. After 48 hours in culture cells were incubated in 10μM OGB at room temperature for 45 minutes before rinsing twice in phosphate buffered saline (PBS) (Sigma). Slides were assembled in a parallel plate flow chamber (RC30- Warner Instruments, Hamden, CT, USA, https://www.warneronline.com) in phenol red free DMEM (Sigma), 0.5% FBS, and incubated for a further 15 minutes. Initially medium was perfused through the chamber at 0.028ml/min (0.01Pa shear stress) (New Era) for 2 minutes, followed in the case of OFS treatment by 2.8ml/min (1Pa) oscillating across the chamber at 1Hz for 5 minutes. The indicator was imaged using an Olympus IX83 epifluorescent microscope (Olympus, Hamburg, Germany https://www.olympus-europa.com/) at 40x (N.A. 0.60 Air). Exposure time was kept below 600ms and was kept constant between control and treatment groups, allowing image acquisition every 1.29s. Following each experiment, 10μM ionomycin (Alomone Labs, Jerusalem, Israel, http://www.alomone.com) was applied to the cells as a positive control for sensitivity of the indicator to calcium.

Response was calculated as fold change fluorescence over baseline levels where baseline was taken as the 30 seconds prior to treatment (t=0). Cells were only considered responsive if displaying a fold change over baseline greater than 1.2 in response to treatment as well as a greater than 1.2-fold change in calcium signal upon application of ionomycin. The peak is defined as the apex of the first fluctuation above 1.2 fold change fluorescence in responding cells. In figure 3.1B and 3.3B the fold change magnitude is taken from the highest fluctuation above baseline observed for comparison to the treatments plotted.

3.2.5 Immunocytochemistry

MSCs were seeded on fibronectin coated glass coverslips for 24 hours before serum starvation in DMEM low glucose, 0.5% FBS, 1% P/S for 48 hours. After fixation in neutral buffered formalin for 10 minutes (Sigma), coverslips were permeabilized in 0.1% Triton X-100 and non-specific binding sites were blocked using 1% w/v BSA (Sigma) in PBS for 2 hours at room temperature. The primary antibodies targeting the primary cilium (acetylated α tubulin, ab24610, Abcam, Cambridge, UK, http://www.abcam.com) or vinculin (ab18058, Abcam) were applied overnight at 4°C, diluted 1:1500 and 1:1000 respectively. Next, primary antibodies targeting TRPV4 (TRPV4, ab74738, Abcam) or centrioles (pericentrin, ab448, abcam) were applied for 1 hour at room temperature at a dilution of 1:1000 and followed by an Alexa Fluor 594 conjugated secondary antibody (A21203, Life Technologies, Carlsbad, CA, USA, https://www.thermofisher.com) for acetylated alpha tubulin and vinculin and an Alexa Fluor 488 conjugated secondary antibody (A11008, Life Technologies) for TRPV4 and pericentrin, both secondary antibodies were diluted at 1:500. Finally, DAPI (Sigma) was applied for 5 minutes in PBS prior to sample mounting on glass slides using

Prolong gold mounting medium (Invitrogen). Imaging was performed on an Olympus IX83 epifluorescent microscope with a 100W halogen lamp at 100x (N.A. 1.40 Oil)(Figure 2C) or the Leica SP7 (Leica Microsystems, Wetzlar, Germany, http://www.leica-microsystems.com) scanning confocal microscope at 63x (N.A. 1.40 Oil) (Figure 2D and E). For imaging the primary cilium, the confocal was set to a pinhole of 67µm and 701.33mAU. The focal adhesions were acquired using settings of 95.6µm pinhole size and 1.00AU. Controls in the absence of primary antibody were used to test for non-specific binding and background staining of the secondary antibodies. The line profile tool in LAS X software (Leica) was used to measure the intensity of each channel along manually defined regions of interest.

3.2.6 Biochemical targeting of TRPV4

The TRPV4 channel was inhibited via application of GSK205 antagonist (Merck Millipore, Billerica, MA, USA, http://www.merckmillipore.com) at 10µM diluted in cell culture medium. Cells were treated with GSK205 supplemented medium for 1 hour prior to application of mechanical stimulation and controls were incubated for the same time frame for calcium signaling and gene expression. TRPV4 was activated via the specific agonist GSK1016790A (Sigma). Cells were not pre-treated with GSK101; supplemented medium was only applied for the duration in place of the 1Pa mechanical stimulus. Vehicle controls consisted of <0.1% DMSO for each set up. For long term cell culture GSK205, GSK101 or DMSO were applied at the same concentrations and maintained throughout the culture period via supplementation to the medium which was changed every 3 days.

3.2.7 Extracellular matrix stain and extraction

To investigate extracellular matrix formation, cells were fixed in formalin following 21 days in culture. Collagen deposition was stained using 1% Picrosirius Red (Sigma) under gentle agitation at room temperature, after 1 hour all wells were rinsed twice in 0.5% acetic acid and distilled H_2O. Calcium staining was performed using Alizarin Red S at 1% for 20 minutes at room temperature and rinsed in distilled H_2O until the background was clear of stain. Images were acquired using 2x (NA 0.06) and 10x (NA 0.25) objectives. Collagen deposition was quantified by scraping picrosirius stain from each well in PBS and centrifuging at 14000g for 10 minutes. The pellet collected was dissolved in 0.5M NaOH and absorbance measured at 550nm. Calcium stain was extracted via incubation in 10% acetic acid for 30 minutes under gentle agitation followed by heating at 85°C for 10 minutes. Cell debris was collected by centrifugation at 20,000g for 15 minutes and the pH adjusted to pH4.1-4.5 before measuring absorbance at 405nm.

3.2.8 Inhibition of primary cilia formation

Intraflagellar transport protein 88 (IFT88) is a protein required for functional ciliogenesis and was targeted with siRNA. Lipofectamine RNAiMAX (Invitrogen) was diluted 1/135 in OptiMEM (Gibco, Foster City, CA, USA, https://www.thermofisher.com) reduced serum transfection medium. This was mixed 1:1 with predesigned Stealth RNAi siRNA targeting IFT88 (MSS211714, Invitrogen) at a dilution of 16.7µM in OptiMEM and incubated at room temperature for 15 minutes before application. The off-target control was Stealth RNAi siRNA Negative Control, Medium GC (12935300, Invitrogen). After 24 hours, additional medium was added to each transfection. 48 hours following transfection the transfected cells were seeded for

experimentation in DMEM (0.5% FBS, 1% P/S). Cells were cultured for an additional 24 hours before exposure to GSK101. Validation of the efficiency of siRNA knockdown was analyzed at the mRNA level using qPCR and at the protein level using immunocytochemistry (ICC) as described above.

3.2.9 Data Analysis

The relative expression of each gene with reference to *18s* was calculated and the results expressed as fold change gene expression relative to the control group along with the standard error of the mean. For all gene expression and stain extraction an unpaired two-tailed t-test (α=0.05) was used to analyze control to treatment conditions or in the case of more than one condition a one-way ANOVA and under multiple conditions a two-way ANOVA were used with a Bonferroni post-test (α=0.05). For fluorescence intensity measurements, the data sets did not follow a normal distribution and were tested via a Mann Whitney test except in the case of more than one treatment condition where a Kruskal Wallis was used with Dunn's post-test. The frequency of MSCs eliciting a calcium response to different stimuli was tested via a Fisher's exact test for comparison of two treatments or a Chi-square group for multiple treatments. Stringent parameters identifying a responsive cell in terms of calcium signaling, were defined based on the effect of the ionophore, ionomycin, on the activity of the indicator and the change in fluorescence seen in similar studies of osteoblasts, osteocytes and kidney collecting duct cells.

3.3 Results

3.3.1 Mesenchymal stem cells respond to oscillatory fluid shear with a rapid increase in cytosolic calcium and osteogenic gene expression

To characterize the response of MSCs to fluid flow induced shear stress, OFS was applied at 1Pa, 1Hz, mimicking physiological mechanics predicted to occur within the bone marrow (Shamseer et al., 2012). To determine the initial response to a mechanical stimulus, calcium levels within the cell were determined in real-time using a fluorescent indicator. MSCs were initially exposed to a laminar fluid flow-induced shear stress of 0.01Pa for 2 mins to equilibrate the system. No change in intracellular calcium levels was detected during this period when compared to No Flow controls demonstrating that this low level of mechanical stimulus is insufficient to induce a mechanoresponse. MSCs were then exposed to OFS at 1Pa and fold change fluorescence levels were quantified relative to no OFS. The application of 1Pa OFS elicits a 1.53-fold increase in cytosolic calcium demonstrating that this increased mechanical stimulus is transduced by MSCs eliciting a second messenger signaling response (Fig. 3.1A, B). Taking a cell that demonstrates a calcium peak greater than 1.2-fold in response to OFS as mechanoresponsive, 1Pa OFS induces a response in a significantly greater number of MSCs compared to static controls (Fig. 3.1C, $p<0.01$). Furthermore, the response to OFS was immediate (17.64 ±4.84 seconds) (Fig. 3.1D). To characterize a downstream response to mechanical stimuli, gene expression analysis was performed on cells exposed to 1Pa OFS for 2 hours. In response to OFS, the expression of the osteogenic markers *Cox2* and *Opn* was significantly upregulated (5.52-fold, $n\geq8$, $p<0.05$ and 4.35-fold, $n\geq14$, $p<0.01$ respectively) compared to No Flow controls (Fig. 3.1E, F). Previous studies have shown that increases in *Cox2* and *Opn* are early markers of full osteogenic commitment in MSCs (Stavenschi et al., 2017). This data therefore demonstrates that

OFS predicted to occur within the marrow elicits a positive mechanoresponse in MSCs in terms of second messenger calcium signaling and downstream osteogenic gene express ion.

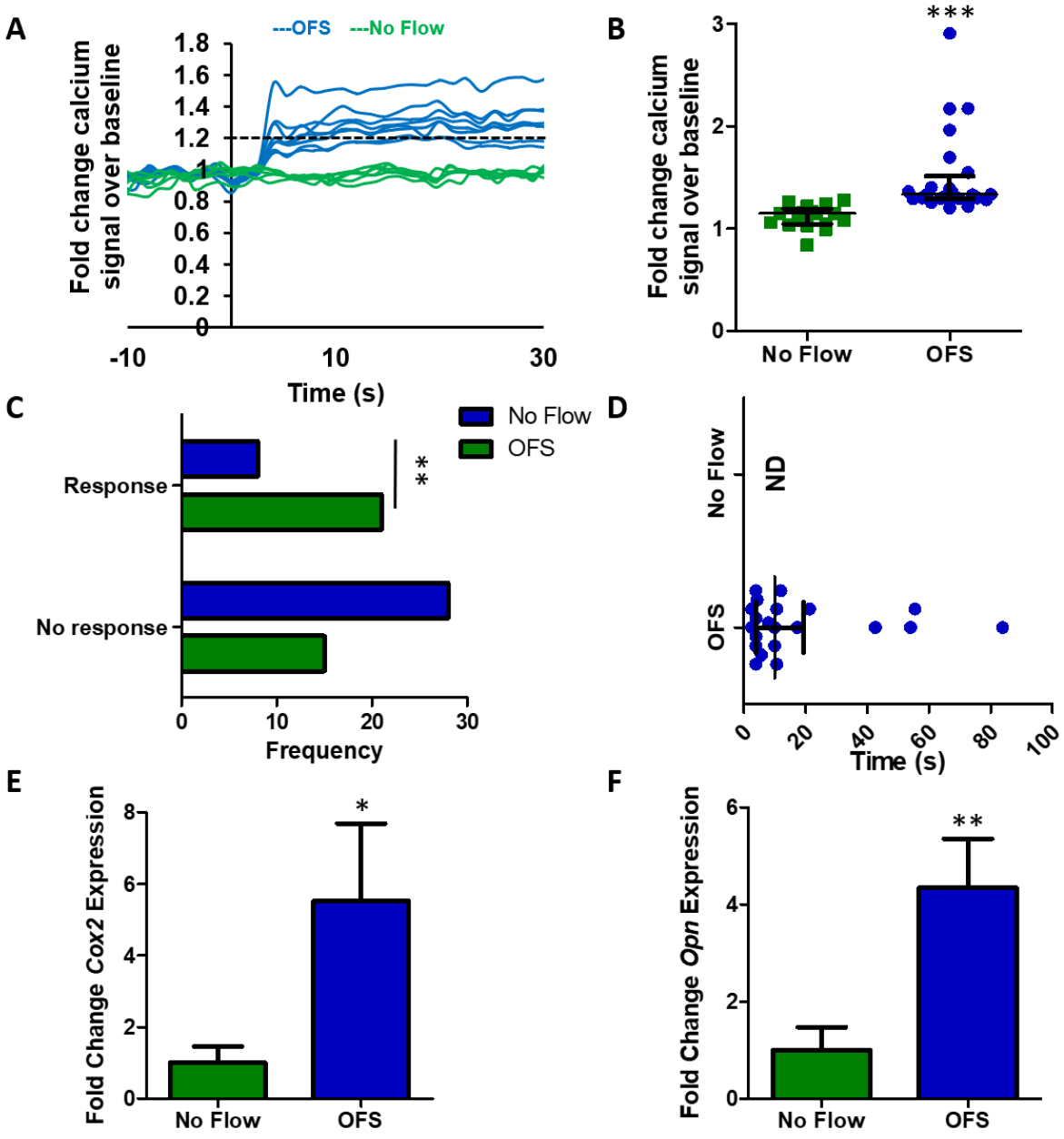

Figure 3.1: (A) Representative calcium profiles of individual MSCs during No Flow (green) and oscillatory fluid shear (OFS) generating 1Pa, 1Hz shear stress (blue). Stimulus begins at t=0s. Baseline values calculated from 20 seconds prior to the application of OFS. The dashed black line at 1.2 fold change marks the value above which cells are considered to be responsive. (B) Fold increase in calcium at first peak during No Flow and OFS, Median ± Interquartile range, No Flow, n=17; OFS, n=21, Mann-Whitney test, ***p<0.001. (C) Frequency of cells eliciting a response or showing no response in static (green) and OFS (blue) conditions, N=3, n=36, Fisher's exact test, **p<0.01. (D) Time from onset of flow (t=0s) to first peak, Median ± Interquartile range, NF n=17, OFS n=21. (E) (F) Expression of early

osteogenic markers in MSCs following application of 1Pa, 1Hz OFS for 2 hours, Mean ±SEM (E) *Cox2* N=4, n=8-13, (F) *Opn* N=4, n=14-20, student's t-test, *p<0.05, ** p<0.01

3.3.2 TRPV4 is expressed by mesenchymal stem cells and is found at mechanosensitive sites across the membrane

Given the role of the mechanosensitive calcium channel TRPV4 in cellular mechanotransduction in lineage committed cells, TRPV4 expression in MSCs was determined at the mRNA level using qRT-PCR and at the protein level using immunocytochemistry. Initially, to investigate the expression of TRPV4 and to determine whether TRPV4 is mechanically regulated, MSCs were exposed to 1Pa OFS for 2hrs. TRPV4 was successfully amplified and there was a non-significant trend of increased expression following mechanical stimulation compared to static controls (p=0.8254) (Fig. 3.2A). To further verify these findings at the protein level, immunofluorescence microscopy analysis was performed with antibodies against TRPV4 and F-actin (phalloidin; to detect cell area) following 1Pa OFS for 2hrs and fluorescence intensity per area was quantified. TRPV4 staining was present across the whole cell area and TRPV4 protein intensity is significantly increased 1.53-fold ($n \geq 18$, $p<0.01$) in response to OFS demonstrating thEt the expression of this channel is mechanoregulated (Fig. 3.2B, C, D). We next examined whether TRPV4 preferentially localizes to sites within the cell which are known to experience high strain under fluid shear and have been previously been shown to play a role in mechanotransduction (Whitfield, 2008, Tzima et al., 2001). Therefore, immunofluorescence confocal microscopy was performed in MSCs treated with antibodies against TRPV4, vinculin to identify focal adhesions (FAs) and acetylated-α-tubulin to identify the primary cilium. Vinculin staining clearly identified focal adhesions located along the periphery of the cell as demonstrated in Fig. 3.2E. TRPV4 staining was punctate throughout the cell area with faint co-localization identified at focal adhesions. This faint co-localization was

verified by fluorescent intensity readings along identified FAs (Fig. 3.2E, G). Acetylated-α-tubulin staining identified primary cilia as rod-like structures on the apical surface of MSCs located above or adjacent to the nucleus. Unlike at FAs, there was a striking co-localization of TRPV4 along the ciliary axoneme (Fig. 3.2F), particularly at the base which is predicted to experience the greatest membrane strain under fluid shear (Downs et al., 2014a). This was further verified by fluorescent intensity (Fig. 3.2H). This data therefore demonstrates that MSCs express TRPV4 and that this expression is mechanically regulated. Furthermore, TRPV4 is specifically localized to areas within the cell that experiences high strain under fluid shear, particularly at the primary cilium.

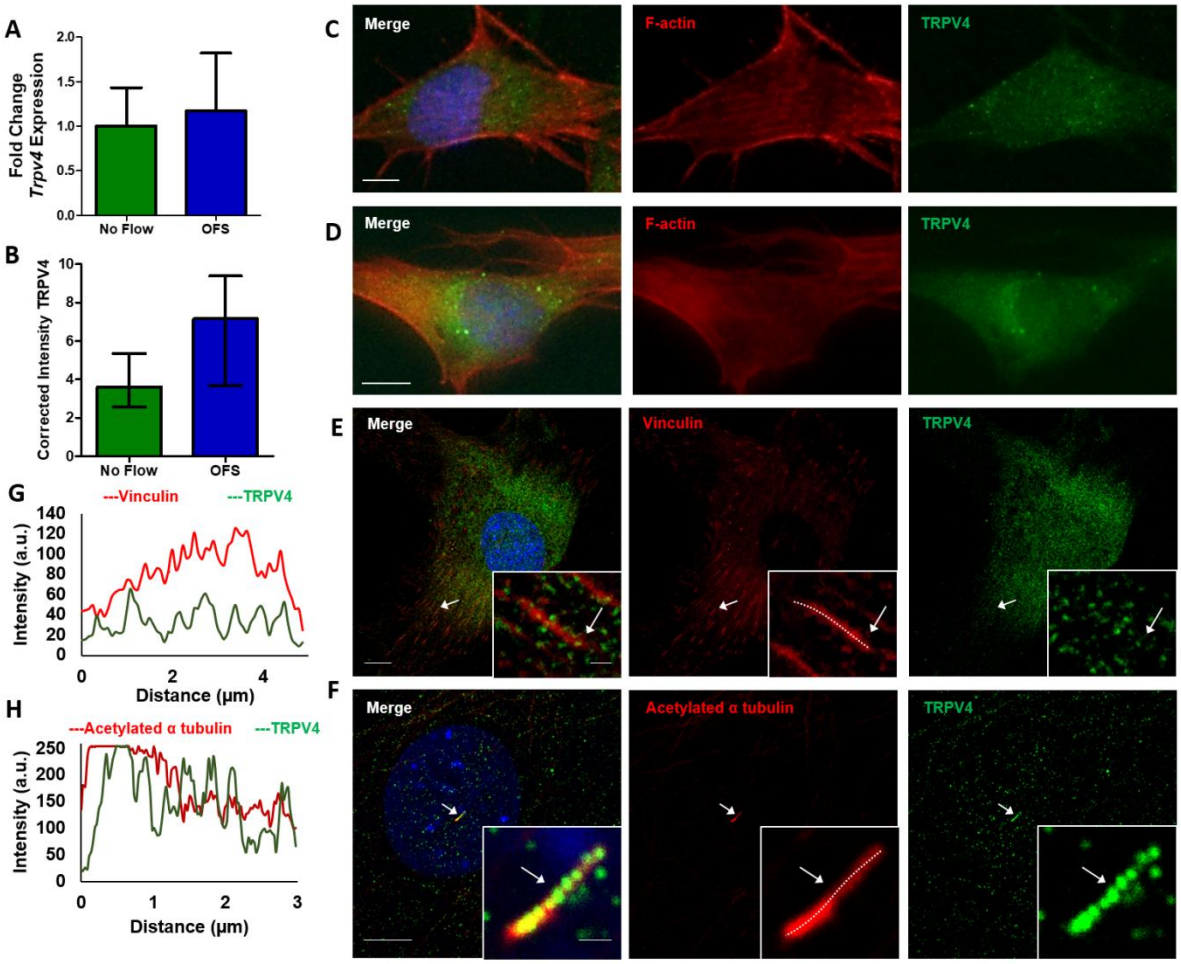

Figure 3.2: (A) Expression of *Trpv4* in cells exposed to 1Pa 1Hz OFS for 2 hours, Mean ±SEM N=3, n= 9-10, student's t-test, p>0.05. (B) Quantification of cell wide Trpv4 stain intensity under OFS, Median ± Interquartile range n=18-21, Mann Whitney test, **p<0.01. (C, D) Immunofluorescent staining of MSCs showing TRPV4 expression and the cytoskeleton (F-actin) (scale bar=10μm) following 2 hours at (C) static conditions and (D) 1Pa, 1Hz oscillartory fluid flow. (E, F) Immunofluorescent staining of MSCs

showing TRPV4 expression and (E) focal adhesions using vinculin (scale bar=10μm, inset 1μm) and (F) primary cilia using acetylated alpha tubulin (scale bar =10μm, inset 1μm). (G) (H) Fluorescence intensity at region marked by arrow, along dashed white line in inset of (G) focal adhesion and (H) primary cilium.

3.3.3 TRPV4 is required for oscillatory fluid shear mediated calcium signaling in MSCs

Employing the TRPV4 specific antagonist, GSK205, the role of TRPV4 in oscillatory fluid shear-induced calcium signaling was examined. MSCs were treated with GSK205 or DMSO vehicle control and exposed to 1Pa OFS and intracellular calcium levels were analyzed in real-time. Analysis of the calcium signal in MSCs treated with DMSO vehicle control demonstrated a similar response to that shown in Fig. 3.1A, with OFS inducing rapid calcium increases (17.54 seconds) averaging 1.40-fold in 40% of cells (Figure 3.3), demonstrating that DMSO treatment alone does affect mechanically-induced calcium signaling in MSCs. Interestingly, in the absence of TRPV4 functionality, a dramatic loss in calcium signal is observed. No cell met the criteria for mechanoresponsive cells, i.e. greater than 1.2-fold change fluorescence. These cells were responsive to ionomycin, a ionophore applied to the cells to empty stores of calcium and test the functionality of the calcium sensor in each cell. However, the average maximum calcium peak was significantly lower than the control group at 1.08 ±0.02-fold change in the GSK205 group. Therefore, specific antagonization of TRPV4 elicited a complete loss in oscillatory fluid shear induced calcium signaling in MSCs.

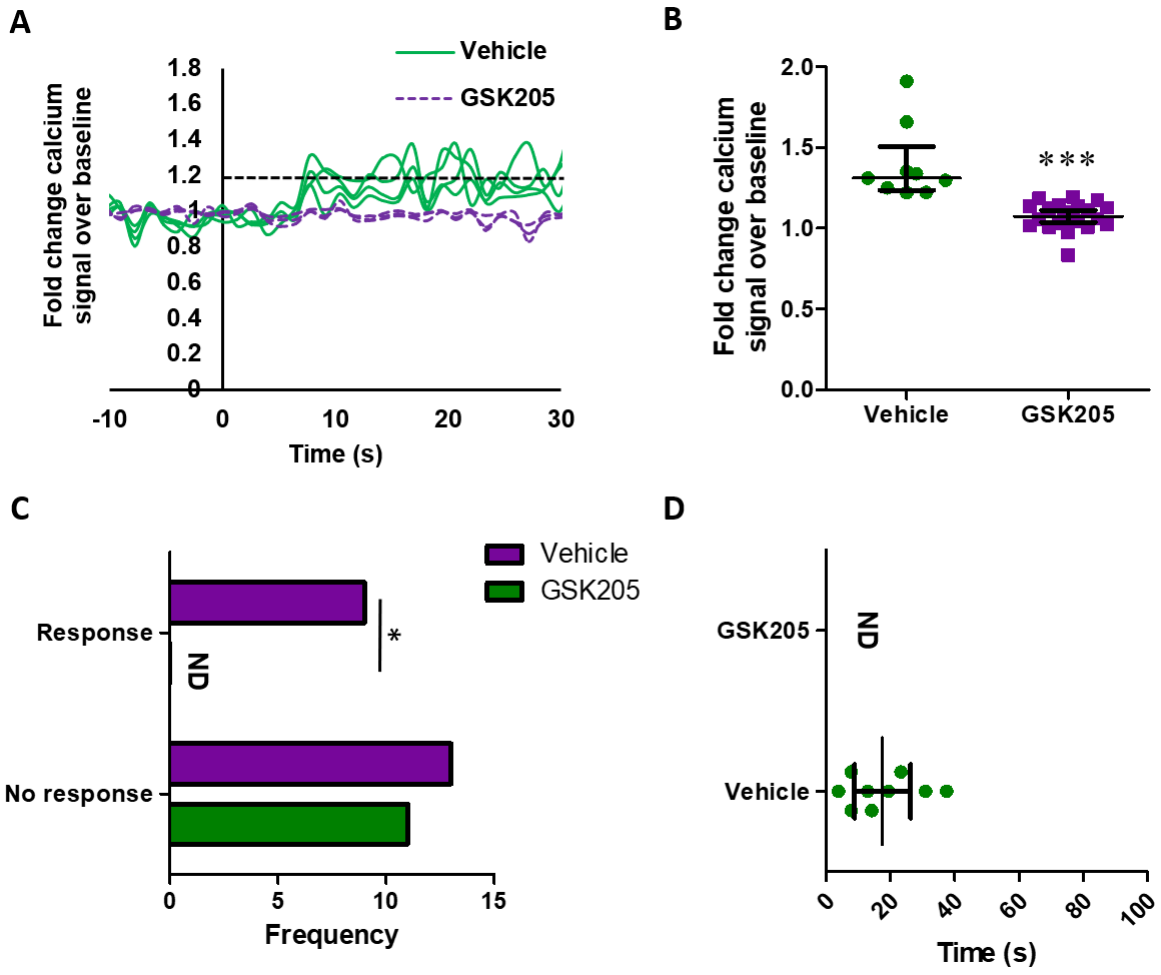

Figure 3.3: (A) Representative calcium profile of individual MSCs responding to OFS generating 1Pa, 1Hz. OFS begins at t=0s. Cells treated with vehicle alone, DMSO, represented in the solid green; those treated for 1 hour pre mechanical stimulation with 10µM GSK205 are in the purple dashed line. Baseline values calculated from the 20 seconds prior to the application of OFS. The dashed black line at 1.2-fold change marks the value above which cells are considered to be responsive. (B) Median ± Interquartile range fold increase in calcium at first peak following application of treatment. Vehicle: N=4, n= 9; GSK205: N=4, n=22, Mann Whitney test, ***p<0.001. (C) Frequency of cells responding to the stimulus. Median ± Interquartile: Vehicle: N=4, n=22; GSK205: N=4, n=11, Fisher's exact test, *p<0.05. (D) Time to first peak for individual cells following application of stimulus at time 0s. Bars mark Median ± Interquartile, Vehicle: N=4, n=9; GSK205: N=4, n=22 ND= None determined, no responsive cells observed.

3.3.4 TRPV4 is required for oscillatory fluid shear mediated increases in osteogenic gene expression

Considering the requirement for TRPV4 in oscillatory shear stress mediated calcium signaling, the role of TRPV4 activity in fluid shear induced gene expression was next investigated. As above, MSCs were treated with GSK205 prior to application of 1Pa fluid shear oscillating at 1 Hz for 2hrs. *Cox2* and *Opn* in the No Flow control group were unaffected by the antagonist treatment (Fig. 3.4A, C) demonstrating that TRPV4 activity does not influence basal osteogenic gene expression. Control MSCs treated with DMSO elicited a significant increase in both *Cox2* (5.5-fold, $n \geq 15$, $p < 0.001$) and *Opn* (4.35-fold, $n \geq 14$, $p < 0.01$) when compared to No Flow (Fig. 3.4B, D), as previously demonstrated in Fig.1. However, the osteogenic response of MSCs treated with GSK205 following OFS was inhibited, with a reduced increase in *Cox2* (4.4-fold, $n \geq 14$, $p < 0.05$) and a complete loss of the increase in *Opn* (1.33-fold, $n \geq 12$) gene expression (Fig. 3.4B, D). Thus, the mechanosensitive calcium channel TRPV4 is required for oscillatory fluid shear induced increases in early markers of osteogenesis.

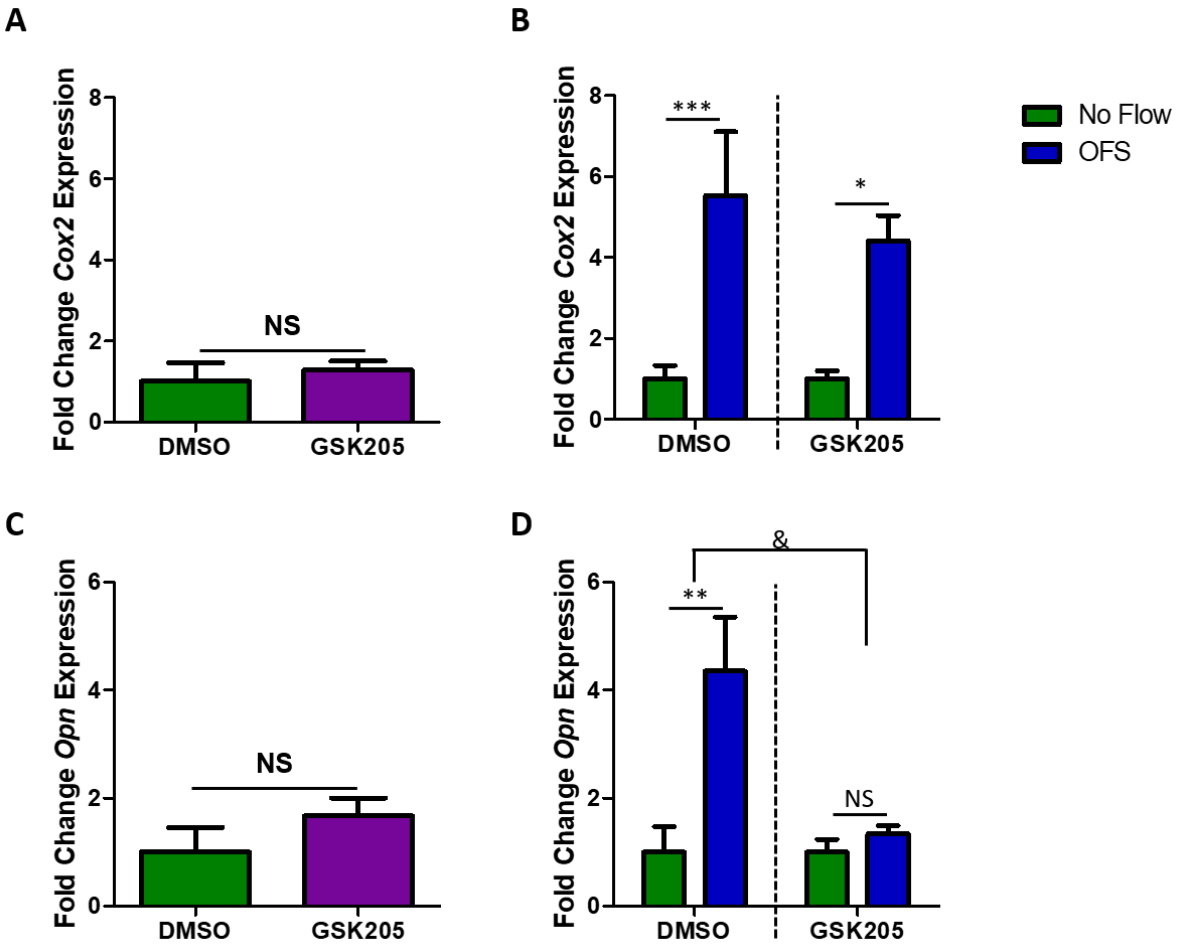

Figure 3.4: Basal gene expression in MSCs treated with vehicle control or 10µM GSK205 for 3 hours. (B) (D) Gene expression following 2 hours of 1Pa 1Hz OFS in each group. (A)(B) *Cox2* and (C)(D) *Opn*, represented as Mean ±SEM, N=4-6. n=12-21; (A) (C) student's t-test (B)(D) 2 way ANOVA with Bonferroni post test; NS $p>0.05$, *$p<0.05$, **$p<0.01$, ***$p<0.001$ in comparison to the no flow control within the same treatment group, & $p<0.05$ significantly different effect of flow stimulus on the vehicle and antagonist treatment groups.

3.3.5 Biochemical activation of TRPV4 induces a calcium response that mimics that produced by oscillatory fluid shear

Considering the demonstrated role of TRPV4 in MSC mechanotransduction, an approach to target this calcium channel to mimic the effect of OFS was examined using the TRPV4 specific agonist GSK101. Real time analysis of calcium signaling was performed in MSCs treated with increasing concentrations of GSK101 in the place of OFS as in previous experiments. The application of 1nM and 10nM GSK101 was promptly marked by a rise in calcium within the cytosol in the absence of mechanical

stimulation, at a similar frequency to those subjected to OFS (Fig. 3.5A, C). Notably, the calcium signal in response to both 1nM and 10nM GSK101 is similar to that elicited by OFS in terms of magnitude (1nM, 2.30-fold; 10nM, 1.86-fold, Fig.3.5B) and time (10nM, 19.85 ±2.19s, Fig. 5D), however the response to 1nM elicited a more variable response greater than that seen in response to fluid shear (1nM, 29.52 ±7.13s). Overall, the biochemical activation of TRPV4 can induce a calcium signal comparable to that elicited under oscillatory fluid shear.

3.3.6 TRPV4 activation induces an increase in osteogenic gene expression that mirrors that seen with mechanical stimulation

To further the potential of therapeutically targeting TRPV4 to mimic the effect of OFS, MSCs were treated with GSK101 for 2hrs and osteogenic genes *Cox2* and *Opn* were analyzed as before. Analysis of *Cox2* and *Opn* was carried out using qPCR and fold change was calculated against vehicle treated controls. 1nM GSK101 treatment resulted in an upward trend, but non-significant increase in *Cox2* (1.14-fold, $n \geq 6$, $p=0.7640$) and elicited no response in *Opn* gene expression (0.80-fold, $n \geq 7$, $p=0.5548$) (Fig. 3.5E, F). However, 10nM GSK101 treatment induced a significant 2.49-fold increase in *Cox2* ($n \geq 8$, $p<0.01$) and a 1.83-fold increase in *Opn* ($n \geq 7$, $p<0.05$). Both osteogenic responses with 10nM treatment compare favorably to that elicited in response to OFS (Fig. 3.1E, F), demonstrating that GSK101 can be utilized to therapeutically mimic the anabolic effect of mechanical loading.

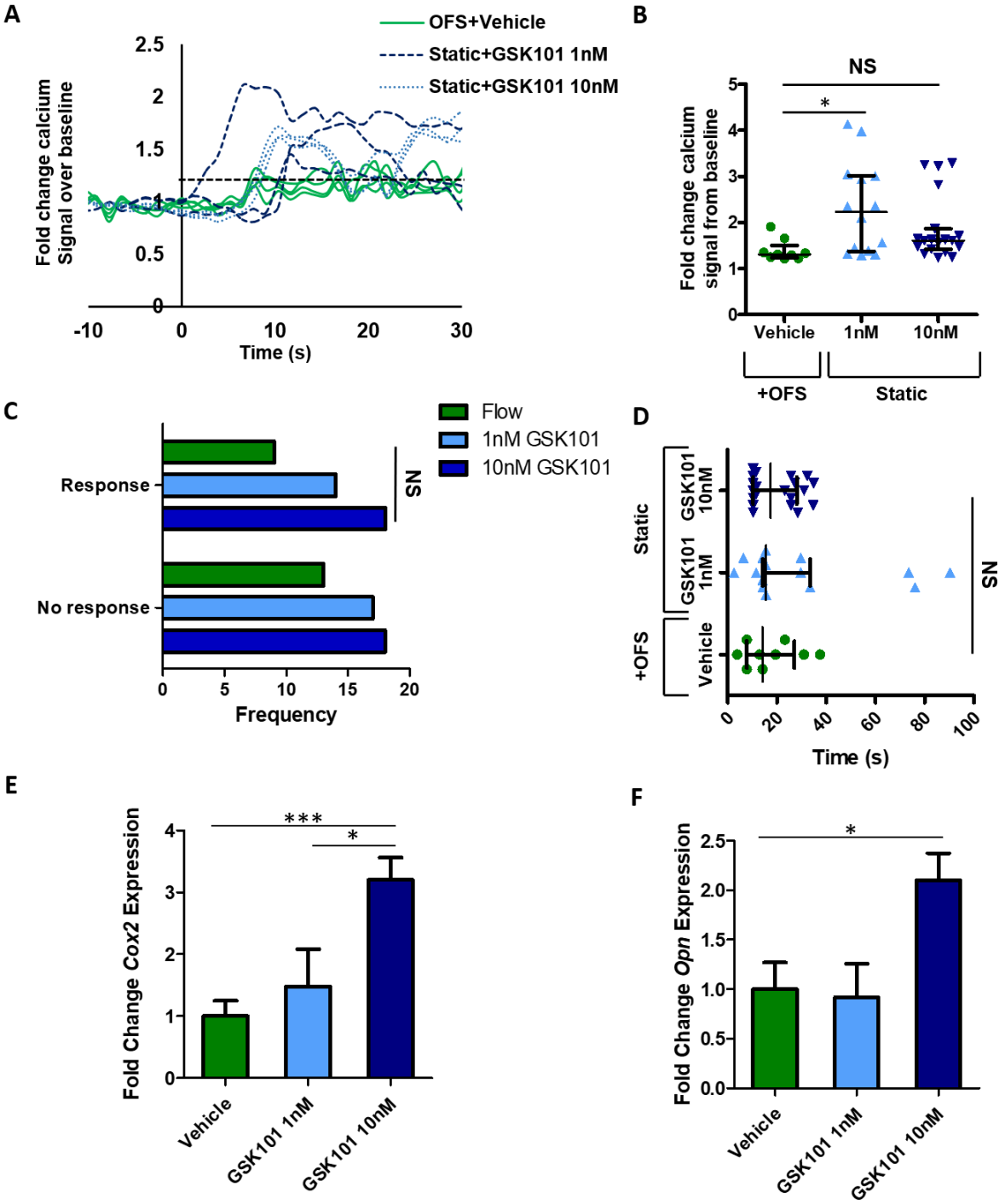

Figure 3.5: (A) Representative calcium profile of individual MSCs responding to OFS generating 1Pa, 1Hz shear stress. OFS begins at t=0s. Cells treated with equal amounts of the vehicle, DMSO and exposed to OFS are in solid green, those treated with 1nM GSK101 are represented by dashed blue line and 10nM GSK101 by the dark blue dotted line. All biochemical treatments are applied only from the onset of fluid shear. Baseline values were calculated from the 20 seconds prior to the application of OFS. The dashed black line at 1.2 fold change marks the value above which cells are considered to be responsive. (B) Median and interquartile range of fold increase in calcium at first peak following application of treatment. Control N=4, n= 9, 1nM GSK101 N=4, n=14, 10nM GSK101 N=4, n=19, Kruskal-Wallis test with Dunn's multiple comparisons post test, *$p<0.05$, NS $p>0.05$. (C) Frequency of calcium response in MSCs exposed to stimulus, OFS N=4, n=9, 1nM GSK101 N=4, n=31, 10nM GSK101 N=4, n=27, Chi-square test, NS $p>0.05$. (D) Time to first peak for individual cells following application of stimulus at time 0s. Bars mark Median and interquartile range, Control N=4, n=9, 1nM GSK101 N=4, n=14, 10nM GSK101 N=4, n=19. Kruskal Wallis test with Dunn's post-test, NS $p>0.05$.

(E) *Cox2* and (F) *Opn* expression in MSCs treated with DMSO only, Vehicle, 1nM and 10nM GSK101 for 2 hours, Mean ±SEM N=2-3, n=7-13, 1 way Anova with Bonferroni post-test, *p<0.05, ***p<0.001.

3.3.7 Biochemical modulation of TRPV4 activity influences bone matrix deposition

Given the demonstrated role of TRPV4 in mediating early biophysical and biochemical osteogenic responses in MSCs, we next investigated whether long term targeting of this channel could directly influence full osteogenic lineage commitment of progenitor cells. Therefore, MSCs were cultured with the TRPV4 antagonist GSK205 or agonist GSK101 over a 21 day period and bone matrix deposition in terms of collagen and calcium deposition was analysed. After 21 days of TRPV4 inhibition, GSK205 significantly inhibited the deposition of collagen and mineral by MSCs (0.28-fold Picrosirius, n=6, p<0.001 and 0.89 fold Alizarin, n=6, p<0.05) (Fig.3.6C). Moreover, significant cell death was evident in this group indicating a role for TRPV4 in cell viability. Interestingly, similar to that seen at early timepoints, TRPV4 activation over 21days resulted in a significant increase in collagen and mineral deposition (1.29-fold Picrosirius, n=6, p<0.05, 1.18-fold Alizarin, n=6, p<0.01) (Fig. 3.6D) further supporting the early evidence for the positive influence of GSK101 on osteogenesis and confirms a role for TRPV4 in the osteogenic differentiation of MSCs.

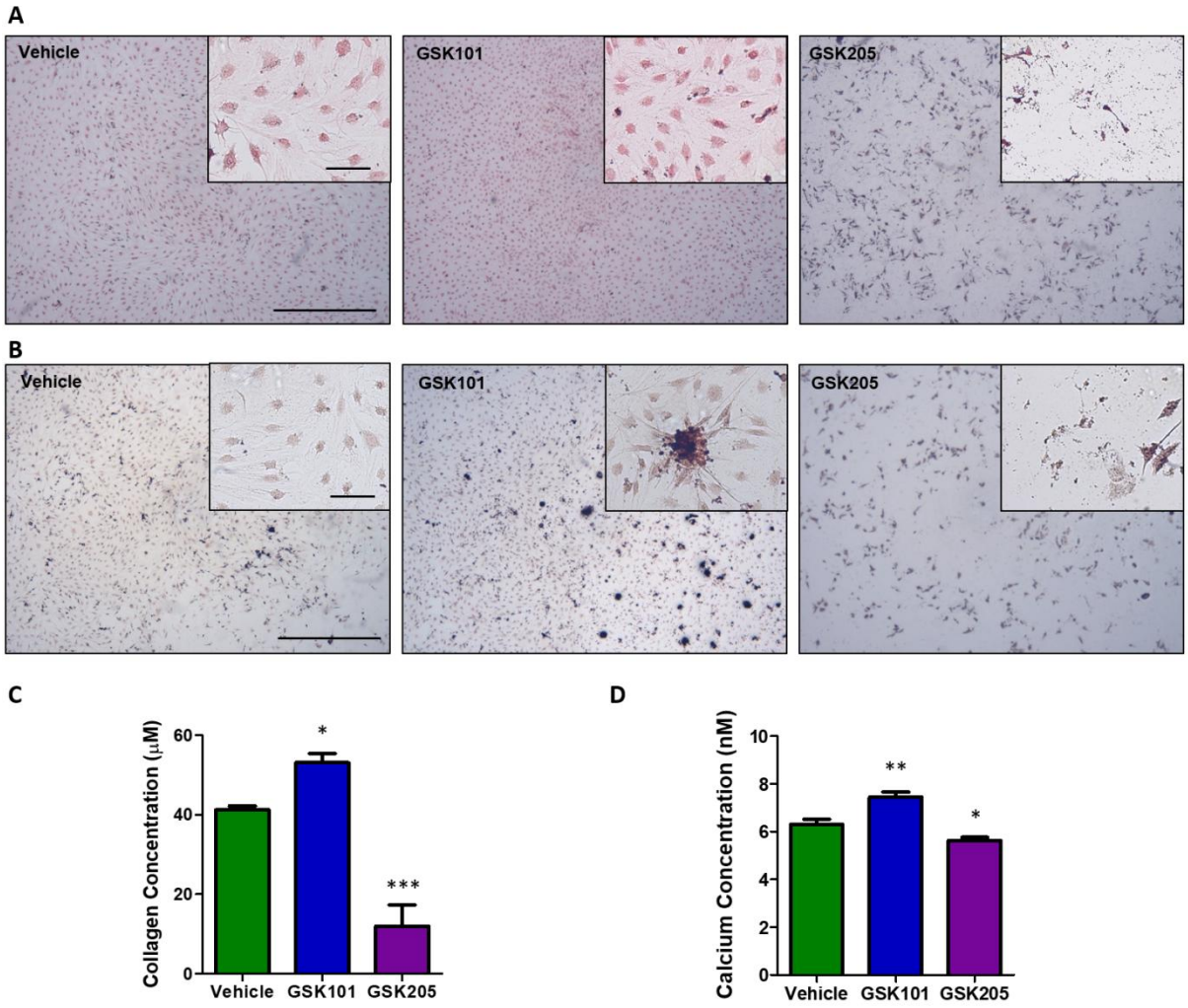

Figure 3.6: Representative images of **(A)** picrosirius red and **(B)** alizarin red s staining of MSCs following 21 days treatment with vehicle (DMSO), GSK101 and GSK205 at 2x (scale bar=500μm, inset at 10x, scale bar=100μm). Quantification of **(C)** picrosirius (collagen) and **(D)** alizarin (calcium) stains extracted from each group in **(A)** and **(B)** n=6, statistical analysis One-way ANOVA with Dunnett's multiple comparisons post test *p<0.05, **p<0.01, p<0.001.

3.3.8 Mesenchymal stem cells with defective intraflagellar transport display an altered response to TRPV4 activation

Given the localization of TRPV4 to the primary cilium, a known site of mechanotransduction, the role of the cilium in TRPV4-mediated osteogenic responses was further investigated. The formation of cilia was inhibited through the utilization of siRNA targeting IFT88. IFT88 is a principal motor protein required for ciliogenesis. The transfection resulted in significantly diminished *Ift88* mRNA expression and the

frequency of primary cilia was significantly reduced as demonstrated by immunocytochemistry (Fig. 3.7A-D). In the remaining cells, which still possessed a cilium, the axoneme length was stunted which is suggestive of defective IFT transport and cilia function. MSCs were transfected with siRNA targeting IFT88 (cilium knockdown) or scrambled siRNA and the calcium signal in response to 10nM GSK101 was measured. Global TRPV4-mediated calcium signaling was unchanged in MSCs with defective cilia. Transfected MSCs were also treated with 10nM GSK101 for 2 hours and the expression of osteogenic genes Cox2 and Opn was examined. TRPV4 activation via GSK101 treatment in MSCs transfected with scrambled control elicited a significant increase in *Cox2* (16.5-fold, $n \geq 5$, $p < 0.001$) and *Opn* (12.7-fold, $n \geq 5$, $p < 0.001$). However, in MSCs which do not possess a primary cilium, TRPV4 mediated increases in *Cox2* gene expression are significantly less than off target siRNA transfected controls (Fig.3.7F), suggesting that TRPV4 localization to the cilium is functionally important in terms of eliciting a *Cox2* response. Interestingly, deletion of IFT88 resulted in a slight but significant increase in the TRPV4-mediated *Opn* response (Fig.3.7H). Together, this data indicates that TRPV4 localization to the primary cilium is functionally important but the significance is potentially pathway dependent.

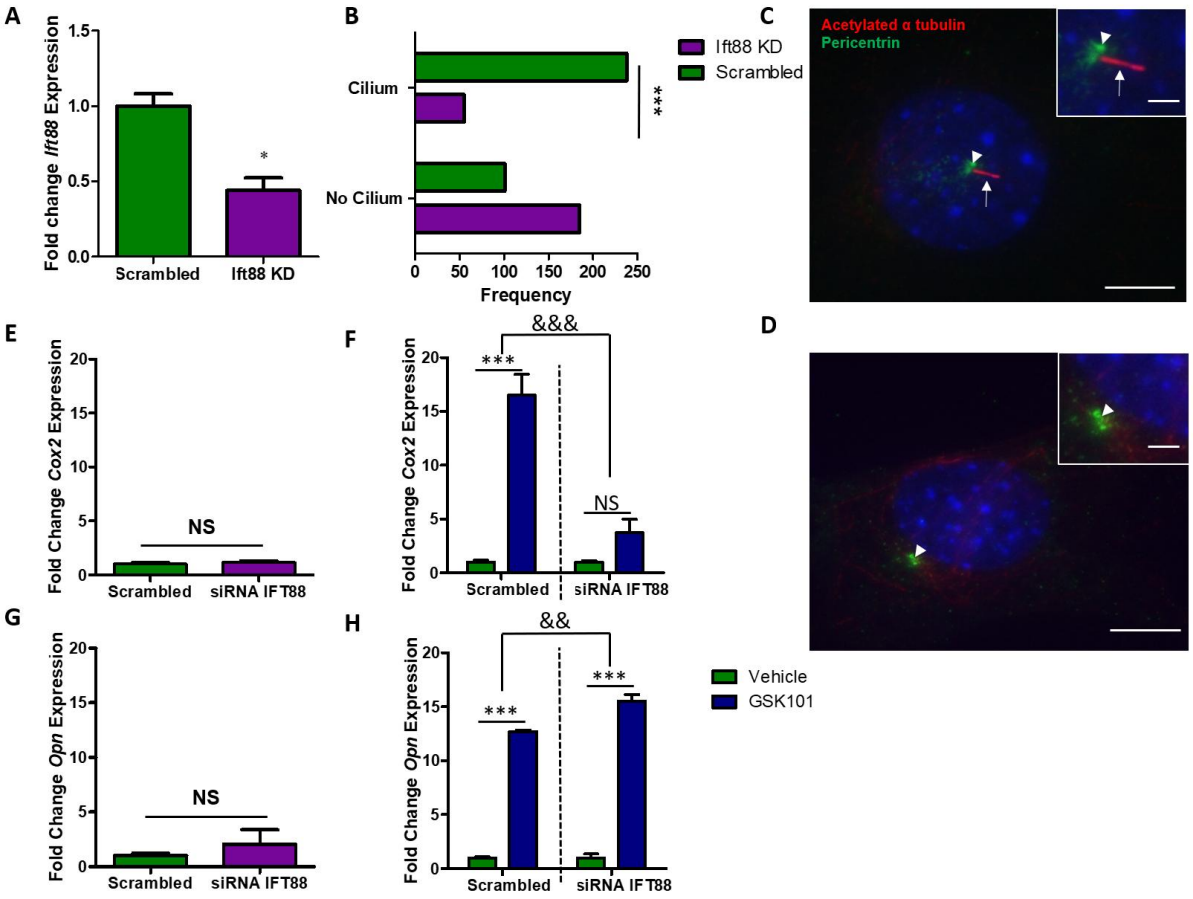

Figure 3.7: (A) Validation of inhibition of *Ift88* gene expression, N=4, student's t-test with Welch's correction, * $p<0.05$. (B) Frequency of primary cilium formation following transfection with siRNA, N=4-6, n=286-293, Fisher's exact test, ***$p<0.001$. (C) (D) Immunostaining of cells transfected with either off target control (C) or *Ift88* targeted siRNA (D) stained with acetylated α-tubulin, (primary cilium, red; arrows) and pericentrin (centrioles, green; arrow head). Nuclei are counterstained with DAPI (blue). Scale bars represent 5µm and 1µm (insert). (E) (G) Basal gene expression in MSCs transfected with siRNA targeting *Ift88* or scrambled control, t-test, NS=Not significantly different. (F) (H) Gene expression following 2 hours of treatment with 10nM GSK101 in each group. (E)(F) *Cox2* and (G)(H) *Opn*, represented as Mean ±SEM, N=3, n=5-8, 2 way ANOVA with Bonferroni post-test, ***$p<0.001$ significant in comparison to the no flow control of each treatment group, && $p<0.01$, &&& $p<0.001$ significant effect of the treatment on the response to OFS.

3.4 Discussion

A potent regulator of skeletal health is physical loading; with the application of an external mechanical stimulus known to enhance MSC osteogenesis and bone formation (Turner, 1998, Stavenschi et al., 2017). Therefore, understanding the mechanisms by which physical loading can drive stem cell osteogenic differentiation is pivotal to the development of novel anabolic therapies to promote bone formation in diseases such as osteoporosis through the targeting of this progenitor population (Pisani et al., 2016). In this study, we demonstrate that TRPV4 is a key component of MSC mechanotransduction, regulating oscillatory fluid shear-induced calcium signaling and osteogenic gene expression. Critically, we also demonstrate that TRPV4 can be targeted pharmacologically, eliciting an anabolic response that mirrors that seen with mechanical stimulation, demonstrating mechanotherapy potential. Interestingly, we also show that this mechanosensitive channel localizes to the primary cilium, a known site of MSC mechanotransduction (Hoey et al., 2012d), and demonstrate that the primary cilium is in part required for the TRPV4-mediated increases in *Cox2*. In summary, this data demonstrates a novel mechanism of stem cell mechanotransduction, which can be targeted therapeutically, and further highlights the critical role of the primary cilium in stem cell biology.

TRPV4 mediates OFS mechanotransduction in MSCs. By mimicking the marrow mechanical environment through the application of OFS, this study demonstrates that MSCs transduce a mechanical stimulus rapidly, resulting in a 1.53-fold increase in cytosolic calcium. This response is consistent with previous work in cells of the osteogenic lineage in response to OFS(Li et al., 2004, You et al., 2001, Hu et al., 2017, Lee et al., 2015c), and demonstrates the utilization of calcium signaling as an important

second messenger in MSC mechanotransduction. Interestingly, the complete loss of calcium signaling in MSCs treated with GSK205, an antagonist selective for TRPV4, suggests that TRPV4 is the principal mediator of calcium responsive mechanotransduction in MSCs. This finding is consistent with recent studies comparing the role of TRPV1 and TRPV4(Hu et al., 2017). Previous studies in chondrocytes, endothelial cells and osteocytes demonstrate a similar dependence on TRPV4 in terms of loading induced calcium signaling(O'Conor et al., 2014, Thodeti et al., 2009, Lee et al., 2015b), highlighting the role of this channel in the mechanobiology of multiple tissues in addition to progenitors. Interestingly, the inhibition of TRPV4 also diminished the osteogenic response to shear in terms of *Cox2* and *Opn* gene expression. *Cox2* is required for the production of PGE_2 and has roles in MSC osteogenesis, loading-induced bone formation and fracture repair (Zhang et al., 2002, Forwood, 1996). Although increases in *Cox2* were diminished following TRPV4 inhibition, a significant increase in *Cox2* was still achieved in response to OFS. Therefore, although TRPV4 plays a role in *Cox2* responses, alternate mechanotransduction mechanisms may compensate for the loss of TRPV4. For example, OFS-induced increases in *Cox2*, which have previously been linked to calcium signaling, have also been shown to be dependent on cAMP signaling (Kwon et al., 2010), and thus may be activated by multiple mechanisms. *Opn* has demonstrated diverse functions in osteogenic cells, acting as a chemoattractant and regulator of proliferation and mineralization (Giachelli and Steitz, 2000, Lund et al., 2009, Kahles et al., 2014). The complete loss of the *Opn* response to OFS following TRPV4 inhibition is consistent with increases in *Opn* being calcium dependent (You et al., 2001). A role for TRPV4 in modulating gene expression in response to mechanical load is similar to that demonstrated in chondrocytes (O'Conor et al., 2014) and osteocytes (Lee et al., 2015c) demonstrating that TRPV4 is an

important channel mediating mechanotransduction in progenitor cells through to lineage committed populations. Furthermore, modulation of TRPV4 activity effects the osteogenic differentiation of MSCs over a 21 day culture period. Inhibition of TRPV4 activity in long term culture is detrimental to cell health and this substantiates the importance of its role in cell survival and differentiation. In summary, TRPV4 is a critical component of MSC mechanotransduction and thus identifies this channel as a potential target to mimic the pro-anabolic effect of loading.

Biochemical activation of TRPV4 elicits a calcium second messenger and osteogenic response that mirrors that seen with oscillatory fluid shear in MSCs. The TRPV4 specific agonist GSK101, at either 1nM or 10nM, induced a calcium response of similar magnitude and timing to that elicited by oscillatory fluid shear. However, 1nM GSK101 elicited a more variable calcium response in terms of magnitude and time to peak suggesting that this is approaching the lower threshold for robust TRPV4 activation in MSCs. Furthermore, 1nM GSK101 did not induce an osteogenic response, but a significant increase in *Cox2* and *Opn* was achieved following 10nM treatment. This induced mechanoresponse is consistent with previous work by O'Conor *et al* which demonstrated that GSK101 elicits an increase in calcium and gene expression in chondrocytes, mirroring that seen with dynamic loading (O'Conor et al., 2014). While TRPV4 activation in chondrocytes promotes cartilage matrix deposition, in progenitor cells we have found GSK101 treatment increases the collagen and calcium produced by MSCs over a 21-day period and this influence on the osteogenic commitment of MSCs confirms the significance of the early gene expression changes in lineage commitment downstream. Together with our observations of an early anabolic response mediated by TRPV4 activation, this demonstrates that TRPV4 can be targeted therapeutically to elicit an osteogenic response that mimics that seen with physical loading.

TRPV4 is a mechanoregulated channel that specifically co-localizes to the primary cilium; an organelle which experiences high strain under fluid shear and is a known site of stem cell mechanotransduction(Hoey et al., 2012d). Despite previous evidence for TRPV4 co-localization with integrins in endothelial cells (Matthews et al., 2010, Thodeti et al., 2009), TRPV4 was only found to co-localize to the primary cilium, with intense staining evident towards the ciliary base. Interestingly, under fluid shear the deflection of the ciliary axoneme results in a concentration of strain at the base which may be sufficient to directly stretch open this channel (Downs et al., 2014a, Espinha et al., 2014, Battle et al., 2015, Rydholm et al., 2010). This specific localization to areas of high strain may potentially increase the mechanosensitivity of the cell. Furthermore, due to the discrete cylindrical microdomain of the cilium and the specific localization of a plethora of signaling molecules, localization of TRPV4 to this signaling center may amplify and enhance the rate of TRPV4-mediated mechanosignaling (Takao and Kamimura, 2017). This spatial organization of TRPV4 is consistent with observations in lineage committed cells such as osteocytes , chondrocytes and cells of the endothelium and the trabecular meshwork of the eye(Lee et al., 2015c, Kottgen et al., 2008, Luo et al., 2014, Phan et al., 2009). Intriguingly, in MSCs which do not possess a primary cilium, TRPV4 mediated increases in *Cox2* gene expression are decreased, indicating that the localization of TRPV4 to the cilium is functionally significant. This loss in TRPV4-mediated Cox2 upregulation in MSCs following cilia removal is consistent with the loss in OFS-mediated Cox2 upregulation in MSCs which do not possess a primary cilium (Hoey et al., 2012d). Therefore, the mechanism of cilia-mediated MSC mechanotransduction may include TRPV4. Interestingly, Ift88 knockdown did not result in a reduction in TRPV4-mediated cytosolic calcium signaling in MSCs (Supplementary Figure 3.1), despite previous work demonstrating

that chemical removal of primary cilia from chondrocytes, using chloral hydrate, leads to a significant reduction in TRPV4-mediated calcium signaling (Phan et al., 2009). Although the techniques to abrogate cilia in these two studies are different, it may suggest that TRPV4 localisation to cilia may play a more dominant role in calcium signalling in cartilage. However, any change in cilia-localized calcium signalling would be masked by the cytosolic flux in our approach. Further work to delineate cilia-localized TRPV4 signalling utilizing a genetically encoded cilia localized FRET sensors is required as employed by Lee *et al*(Lee et al., 2015c). Moreover, the loss of the cilium did not prevent the TRPV4-mediated increase in *Opn* gene expression but augmented it, suggesting that *Cox2* and *Opn* may be activated via alternate pathways downstream of TRPV4, with TRPV4-mediated *Opn* regulation being independent of the primary cilium. The increase in the *Opn* response in the presence of defective cilia indicates that this alternative pathway may be compensating for the loss in the *Cox2* response. In summary, the co-localization of TRPV4 to the primary cilium is significant and highlights the important role of the cilium in MSC biology.

3.5 Conclusion

This study presents evidence for the role of TRPV4 in MSC mechanotransduction, presenting a novel mechanism by which oscillatory fluid shear is transduced into a biochemical bone forming response in this progenitor population. This therefore highlights this channel as a therapeutic target and we have demonstrated that TRPV4 can be activated pharmacologically mimicking the anabolic effect of loading by activating second messenger calcium signaling, osteogenic gene expression and bone matrix deposition demonstrating mechanotherapeutic potential. Lastly, we demonstrate that the cilium plays a critical role in TRPV4-mediated signaling in MSCs likely

through the co-localization of this channel to the microdomain of this mechanosensory organelle.

Chapter 4:

Ciliotherapy Treatments to Enhance Biochemically- and Biophysically-Induced Mesenchymal Stem Cell Osteogenesis: A Comparison Study

4.1 Introduction

Osteoporotic patients are prone to low impact fractures because of the significant depletion in bone density and quality. This occurs due to an imbalance in the bone remodelling cycle where bone formation rates can no longer match the bone resorption activity. Most of the current therapies inhibit bone resorption to restore balance, however over 25% of patients don't respond well to treatment and rare but disabling side effects, such as osteonecrosis of the jaw, are associated with these treatment (Cairoli et al., 2014). To overcome limitations in anti-catabolic therapies for osteoporosis, anabolic bone forming therapies targeting the osteoblast and its progenitor, the mesenchymal stem cell (MSC), are emerging in the form of intermittent Parathyroid Hormone (PTH) and Sclerostin antibodies. PTH is currently the only clinically approved treatment but effectiveness plateaus at 2 years (Baron and Hesse, 2012). Sclerostin antibodies are showing promise in phase 3 clinical trials. However, there are concerns linking sclerostin to cardiovascular disease (Evenepoel et al., 2014). A key mediator of bone anabolism is physical loading and thus represents a novel avenue to enhance bone formation. The adaptation of bone tissue to mechanical loading requires sensation of the surrounding mechanical environment as well as transduction of these cues into changes in intracellular behaviour (Duncan and Turner, 1995). The

molecular mechanisms mediating environmental responses such as from physical activity could form novel therapeutic targets to enhance bone formation, as osteoporotic patients do not possess sufficient bone strength to withstand high impact exercise.

MSCs are multipotent cells which form the source of bone forming osteoblasts and are abundant within the marrow of long bones (Dominici et al., 2004). The adaptation of bone to mechanical loading requires the MSC population to differentiate to support the finite osteoblast population (Corral et al., 1998). Marrow is displaced during physical activity eliciting a shear stress on the cells predicted to be in the range of 0.5 and 8Pa, depending on viscosity and anatomical location (Metzger et al., 2015a). Fluid shear within the minimal values of physiological relevance and in particular, the oscillations that would be generated by daily ambulation support MSC osteogenesis (Kreke et al., 2005, Hoey et al., 2012d, Stavenschi et al., 2017). Understanding the mechanisms by which stem cells sense their microenvironment leading to a pro-osteogenic response is critical to the development of new anabolic therapies that target these mechanisms.

In recent years, the primary cilium has emerged as an important organelle involved in regulating cellular behaviour in responses to its extracellular environment, particularly in bone (Jansen et al., 2015, Hoey et al., 2012a). The primary cilium is a microtubule-based appendage that is present in singular form on the surface of most mammalian cells. Structural features equip the cilium for perceiving external changes, the rod-shaped appendage provides optimal contact between membrane bound receptors and biochemical cues present in the extracellular fluid. Moreover, the high surface to volume ratio of the ciliary microdomain and the close proximity of the ciliary microdomain as well as its location spatially removed from the rest of the cytosol facilitates rapid interaction of ligands and receptors inside the membrane (Hilgendorf et

al., 2016). In MSCs, primary cilia play a role in interpreting biochemical signals in osteogenic differentiation and lack of a functional primary cilium reduces the expression of early markers of differentiation (Kwon et al., 2010). Furthermore, the primary cilium regulates TGFβ induced recruitment in human MSCs (Labour et al., 2016b). In addition, the antenna like structure of the cilium protruding into the extracellular space exposes it to surrounding fluid movement. It was first shown in kidney epithelia that cilia deflection is dependent on the flow of urine (Singla and Reiter, 2006). The importance of the MSC primary cilium in the bone forming response to loading was demonstrated *in vivo* where murine bone marrow, including the stem cell population, were depleted of primary cilia. Here, the bone formation rate in response to ulna loading was inhibited in the presence of dysfunctional cilia (Chen et al., 2016a). Furthermore, the response of hMSCs to oscillating fluid shear *in vitro*, which characteristically results in enhanced osteogenic markers, is blunted in the absence of primary cilia (Hoey et al., 2012d). Given the potent role of the cilium in MSC osteogenesis, this cellular organelle represents an ideal target for therapeutic development.

Alteration in cilia structure have been associated with a plethora of diseases (Hildebrandt et al., 2011) and thus have fuelled several investigations on methods to alter cilia incidence and length as a potential therapy, known as ciliotherapies. The adenylyl cyclase activator forskolin can increase cilium length in kidney collecting duct, kidney epithelium and bone mesenchymal cells via an increase in PKA activity mediated through cAMP. Its alteration of cilium length requires solubilized tubulin (Sharma et al., 2011). Modulation of axoneme length is perceived to be a mechanism to regulate the cilium-mediated fluid shear response in the kidney which becomes defective in polycystic kidney disease (Besschetnova et al., 2010). Lithium chloride is

an FDA approved treatment for bipolar and manic depression which has been used to lengthen primary cilia in a range of cell types (Curran and Ravindran, 2014). The elongation of the cilium axoneme is mediated by inhibiting GSK3β in algae and human fibroblast studies where it was found to promote the acetylation of alpha tubulin (Miyoshi et al., 2011, Nakakura et al., 2015). However, in murine brain and neuron cells lithium was not associated with GSK3β interference but effects on the AC3-cAMP pathway (Ou et al., 2009, Miyoshi et al., 2011). Recent studies in a rat model validate the use of lithium *in vivo* as a cilium elongating agent and as a therapy to alter hedgehog signalling associated with progression of osteoarthritis (Thompson et al., 2016). Through the study of a well characterized ciliopathy, Polycystic Kidney Disease (PKD) where cilia are shortened, and patients experience hypertension, the drug fenoldopam has been discovered to alter cilia. Fenoldopam treatment ameliorates PKD associated hypertension in murine models (Kathem et al., 2014b). Interestingly, fenoldopam induced increases in cilium length heighten the sensitivity of kidney cells to fluid shear highlighting this approach as a potential option to increase the cilium-mediated osteogenic response in MSCs to fluid shear (Upadhyay et al., 2014).

Given the role of the primary cilium in signal transduction, both biochemical and biophysical, in MSCs this study set out to target this activity to promote MSC differentiation. The first objective was to optimize the length of the MSC primary cilium using known cilium-altering compounds Forskolin, Lithium Chloride and Fenoldopam and determine the impact of these treatments on MSC behavior. The second objective was to use the optimized treatments to increase the bone forming response of MSCs in the presence of physiologically relevant biochemical and biophysical signals.

4.2 Methods

4.2.1 Mesenchymal stem cell culture

The murine mesenchymal stem cell line C3H10T1/2 was obtained from ATCC (LGC Standards). MSCs were maintained in Dulbecco's modified Eagle's medium (DMEM) with low glucose (Sigma-Aldrich) supplemented with 10% fetal bovine serum (FBS) (Labtech) and 1% Penicillin Streptomycin (P/S) (Sigma). All experiments were carried out using C3H10T1/2s at passage 12-17. For long term studies MSCs were supplemented with 10mM β-glycerophosphate (Sigma) and 0.05mM Ascorbic acid (Sigma) as well as Dexamethasone (Sigma) at either 10nM (minimal supplements) to provide the components necessary for osteogenic matrix formation or 100nM (full supplements) to biochemically induce osteogenic differentiation as a positive control.

4.2.2 Biochemical modulation of cilium length

Three separate ciliotherapies known to increase the length of the cilium axoneme in various cell types were utilized in this study. Forskolin (Sigma) (Sharma et al., 2011), Lithium Chloride (Sigma) (Thompson et al., 2016) and Fenoldopam mesylate (Sigma) (Kathem et al., 2014b) treatments were compared in MSCs as detailed in Table 1. A time course study was conducted whereby each treatment was applied for either 1hr or 24hrs followed by fixation for cilia structural analysis. Cells were imaged at 4x (N.A. 0.13) phase contrast following each treatment to determine the overall effects on morphology and cell viability. For long term studies treatments were applied throughout the culture period.

4.2.3 Immunocytochemistry

MSCs were seeded on fibronectin coated glass coverslips for 24 hours before serum starvation in DMEM low glucose, 0.5% FBS, 1% P/S for 48 hours. After fixation in neutral buffered formalin for 10 minutes (Sigma), coverslips were permeabilised in 0.1% Triton X-100 for a further 10 minutes and non-specific binding sites were blocked using 1% w/v BSA (Sigma) in PBS for 2 hours at room temperature. The primary antibody targeting the primary cilium (acetylated α tubulin, ab24610, Abcam) or β-catenin (active beta catenin, 05-665, Merck Millipore) was applied overnight at 4°C, diluted 1:1500 in blocking solution. Next, the primary antibody targeting pericentrin (ab448, Abcam) was applied for 1 hour at room temperature at a dilution of 1:1000. Alexa 594 and Alex 488 secondary antibodies were applied in tandem for 1 hour at room temperature at 1:500. Finally, phalloidin (Alexa 488 phalloidin, A12370, Life Technologies) was applied to the β-catenin stained samples for 20 minutes. DAPI (Sigma) was applied for 5 minutes in PBS prior to sample mounting on glass slides using Prolong gold mounting medium (Invitrogen). Imaging was performed on an Olympus IX83 (Olympus) epifluorescent microscope at 100x (N.A. 1.40 Oil). Images were acquired as z-stacks, taking the first slice when the primary cilium came into focus and the last when the acetylated α tubulin stain was no longer in focus at any point along the axoneme. The distance between slices was maintained at 0.25µm.

4.2.4 Measurement of primary cilium incidence and length

Primary cilium incidence was defined as positive staining for acetylated α tubulin on a cord protruding from two centrosomes stained by pericentrin. The length of the cilium was calculated by constructing a right-angled triangle to capture the length that may lie within multiple planes between the coverslip and slide as outlined in Rowson *et al.*

(Rowson et al., 2016). Briefly, the number of slices in the z direction and the thickness of each slice were taken as one side, the length of the cilium in a maximum projection of all slices was taken as another side, the length of the cilium was calculated as the hypotenuse of the triangle formed by these two sides.

4.2.5 Measurement of β-catenin nuclear localisation

β-catenin intensity within the nucleus was measured by creating a mask around the nucleus limiting both the intensity and size of the object defined as a nucleus in the DAPI channel (Image J). The intensity of β-catenin within this region of interest was corrected for average background intensity for the same area in pixels. Average corrected nuclear intensity was compared to the vehicle control for each treatment.

4.2.6 Gene expression

TRI reagent (Sigma) was used to extract RNA per the manufacturer's protocol. The concentration of RNA in each sample was measured using a Nanodrop spectrophotometer and sample purity was checked via 260/280 and 260/230 absorbance ratios. A minimum of 100ng of RNA was reverse transcribed to cDNA using the High-Capacity cDNA Reverse Transcription Kit (Applied Biosystems). The efficiency of the reverse transcription was monitored by quantifying cDNA using a Qubit single stranded DNA assay (Invitrogen). Quantitative polymerase chain reactions (qPCR) were prepared for all samples using SYBR Select Master Mix with ROX passive dye (Applied Biosystems, 4472903) and custom designed primers (Sigma) for *18s*, *Cox2*, *Opn*, *Dlx5*, *Runx2*, *Gli1*, *Ptch1* and *Axin2* for amplification using the ABI 7500 real time PCR machine (Applied Biosystems) as outlined in Supplementary Table 1. The

relative quantity of each sample was calculated with reference to *18s* and expressed as fold change normalised to the control group.

4.2.7 Mechanical stimulation

Parallel plate flow chambers, designed in house as described previously, were used for short term fluid shear application (Stavenschi et al., 2017). Briefly, MSCs were seeded on fibronectin (10µg/ml) coated glass slides, assembled between two plates and attached to a programmable syringe pump (New Era Pump Systems). Oscillating fluid flow (OFF) was applied through a 10ml syringe (Becton Dickinson) at 104ml/min, subjecting cells to a shear stress of 2Pa, at a frequency of 2Hz. This stimulus was applied for 2 hours. The no flow controls were similarly assembled within the chambers but were not subjected to fluid shear. For long term studies an orbital shaker (Dragon Lab) was used to apply a spatiotemporal fluid shear of minimum 0.3Pa , exceeding 1Pa at the edge of the well, across the wells of a 6 well plate containing 1.8ml of medium as previously demonstrated in (Salek et al., 2012). Shear stress was applied for 2 hours/day, 5 days/week for 21 days.

4.2.8 Extracellular matrix deposition

To investigate extracellular matrix formation, cells were fixed in formalin following 21 days in culture. Collagen deposition was stained using 1% Picrosirius Red (Sigma) under gentle agitation at room temperature, after 1 hour all wells were rinsed twice in 0.5% acetic acid and distilled H_2O. Calcium staining was performed using Alizarin Red S at 1% for 20 minutes at room temperature and rinsed in distilled H_2O until the background was clear of stain. Images were acquired using 2x (NA 0.06) and 10x (NA

0.25) objectives. Collagen deposition was quantified by scraping picrosirius stain from each well in PBS and centrifuging at 14000g for 10 minutes. The pellet collected was dissolved in 0.5M NaOH and absorbance measured at 550nm. Calcium stain was extracted via incubation in 10% acetic acid for 30 minutes under gentle agitation followed by heating at 85°C for 10 minutes. Cell debris was collected by centrifugation at 20,000g for 15 minutes and the pH adjusted to pH4.1-4.5 before measuring absorbance at 405nm.

4.2.9 DNA Quantification

To monitor MSC proliferation the quantity of DNA following long term culture was measured using a Picogreen double stranded DNA assay (Invitrogen). Briefly, cells were rinsed twice in PBS and lysed in 0.2% v/v Triton X100, 10mM Tris pH 8, 1mM EDTA on ice for 20 minutes. Lysates were sonicated for 1 minute then vortexed for 1 minute and returned to ice for 5 minutes before repeating these mechanical disruption steps 4 times more at 5-minute intervals. Samples were then flash frozen in liquid nitrogen and homogenized by passing through a 21-gauge needle 10 times. Following the kit protocol 1xTE buffer was used to dilute the picogreen solution. DNA stock was diluted in 1xTE to form standards. picogreen solution was added to wells containing the standards and samples in triplicate. After shaking and a 3-minute incubation at room temperature, protected from light, fluorescence was excited at 480nm and read at 520nm. The concentration of samples in DNA/ml was calculated from the equation of the trendline fitted to the standard curve.

4.2.10 Data analysis

Box plots used for cilium length illustrate the 25th and 75th percentile values, whiskers represent 5th and 95th percentile values and the line is at the median, black dots represent points outside of the 5th and 95th percentile. A two-way ANOVA was used to test the effect of treatment on cilium formation, a one-way ANOVA was used to test the effect on cilium length. The mean fold change gene expression relative to the control group is presented along with the standard error of the mean. The nuclear intensity of β-catenin is presented as fold change relative to the vehicle control. The effect of treatment on *Gli1, Ptch1* and *Axin2* and basal *Cox2, Opn, Runx2* and *Dlx5* and β-catenin intensity was analysed using an unpaired t-test with Welch's correction in the case of unequal variance in the groups tested. The effect of treatment on MSCs in full osteogenic supplements was analysed via an unpaired t-test, with Welch's correction where the variances are unequal. The effect of treatment on the response of MSCs to fluid flow and the quantity of DNA, collagen and calcium was analysed with a two-way ANOVA and Bonferroni post-test.

4.3 Results

4.3.1 The effect of ciliotherapy treatment on mesenchymal stem cell primary cilia incidence and length.

Ciliotherapies Lithium Chloride and Fenoldopam, but not Forskolin, increase cilium incidence and length in mesenchymal stem cells. To determine an optimal cilium promoting treatment regime for MSCs, low and high concentrations of Forskolin (10μM and 100μM), Lithium Chloride (50mM and 100mM) and Fenoldopam (10μM and 50μM) were applied for 1 hour and 24 hours. Each treatment was not found to

affect cell morphology or viability at each time point and concentration (supplementary figure 4.1). Surprisingly, Forskolin treatment did not increase the % ciliation or cilium length as expected although there was a significant decrease in mean cilium length following low concentrations of Forskolin for one hour compared to vehicle control (23.28% decrease) and high concentration Forskolin (27.20% decrease) groups ($p<0.001$) (Figure 4.1E). Although there was an increase in the number of cilia in the 24-hour group ($p<0.01$) this was an effect of time in culture rather than treatment and time in culture increased % ciliation in all 3 treatments (Figure 4.1 D, F, H). Lithium Chloride treatment had a significant effect on % ciliation following 1 hour of treatment ($p<0.05$) but the effect was not significant following 24 hours culture. As expected, lithium chloride treatment increased cilium length at both concentrations and time points. Although the length percentage increases were highest after 1 hour at 50mM (138.24%, $p<0.001$), the changes were most consistent and the % ciliation was optimal after 24 hours 100mM treatment (130.96%, $p<0.001$) (Figure 4.1G). The effect of Fenoldopam was only seen at the 24-hour time point and in the 50μM treatment concentration where a significant increase in cilium length was witnessed (114.38%, $p<0.001$) (Figure 4.1 I). Therefore. two distinct treatments can elongate the MSC primary cilium significantly following 24 hours in culture, 100mM LiCl increases median length by 0.58μm, 50μM Fenoldopam increases median length by 0.41μm.

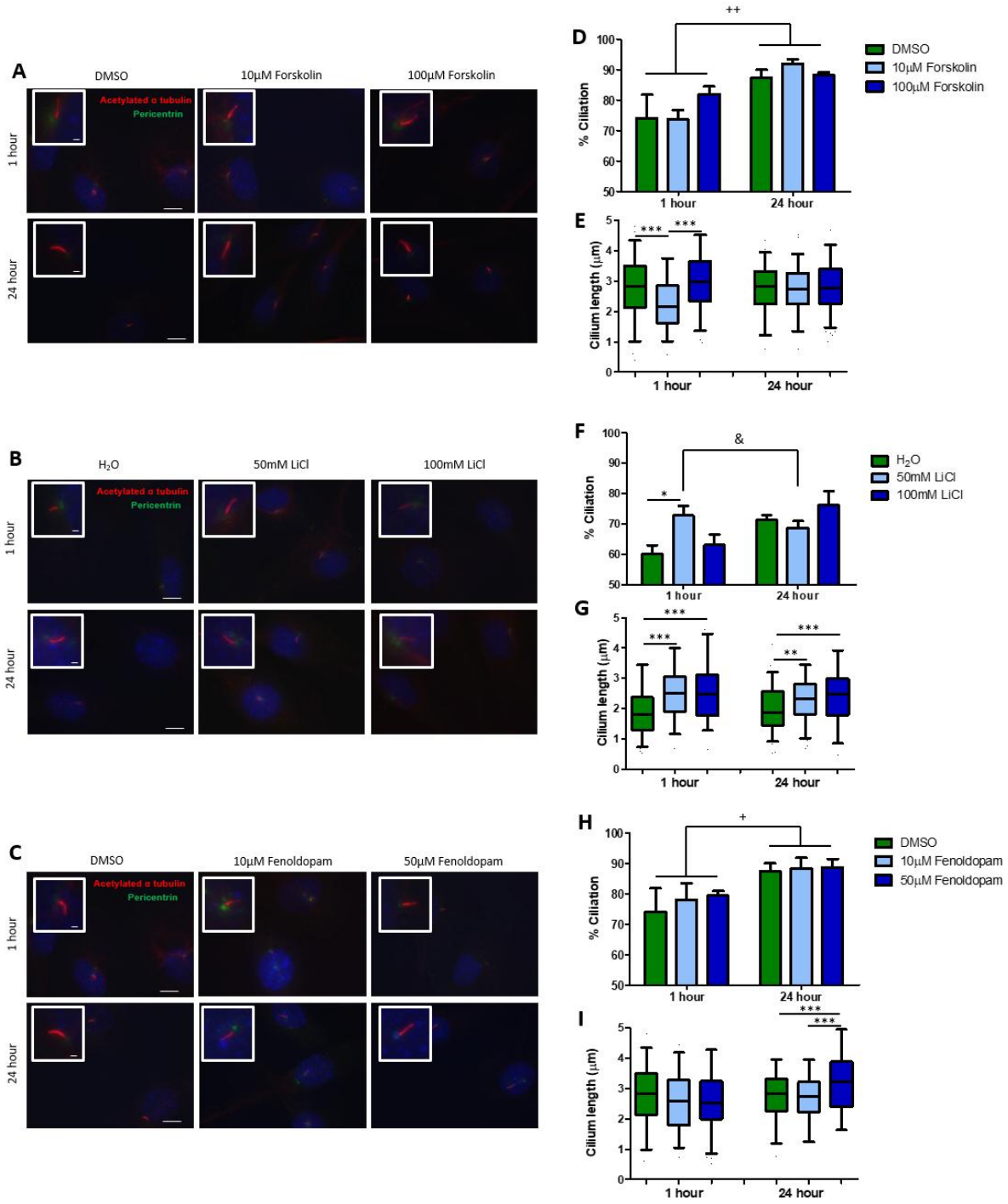

Figure 4.1: Representative images of MSCs following treatment with **A** Forskolin or vehicle, DMSO, **B** Lithium Chloride (LiCl) or vehicle, H_2O and **C** Fenoldopam or vehicle, DMSO, for 1 hour and 24 hours at 100x fluorescence (red channel- acetylated alpha tubulin, green channel- pericentrin and DAPI) (scale bar 10µm), inset shows zoom on cilium (scale bar 1µm). **D, F, H** Percentage of cells in each group with a primary cilium N=3, n=194-275. Bars illustrate % ciliated cells, mean±SEM, statistical analysis, two-way ANOVA, +p<0.05, ++p<0.01 effect of time in culture, &p<0.05 different effect of treatment at different time points, *p<0.05 significant difference between treatments in the 1-hour time point group. **E, G, I** Length of cilium following each treatment, N=3, n=194-275. Box plot illustrates 25th and 75th percentile values, whiskers represent 5th and 95th percentile values, line at median, black dots represent points outside of the 5th and 95th percentile, statistical analysis, one-way ANOVA with Bonferroni post-test, *p<0.05, *p0.01, ***p<0.001, significant difference between labelled groups.

4.3.2 The effect of ciliotherapy treatment on cilia-associated signalling in MSCs.

Given the positive effects of Lithium Chloride and Fenoldopam on cilium length, the impact of the optimised treatment regimens (24 hours treatment with 100mM LiCl or 50μM Fenoldopam) on cilia-associated signalling was investigated. To examine the effects on Hedgehog signalling the expression of mRNA encoding *Ptch1* and *Gli1* were quantified via qPCR. Lithium Chloride treatment leads to a decreasing trend of expression in both *Ptch1* (0.60±0.20-fold change) and *Gli1* (0.32±0.13-fold change), which is not seen in Fenoldopam (Figure 4.2A, B). Activity of the Wnt pathway was analysed via the localisation of beta catenin to the nucleus and the expression of *Axin2*. LiCl treatment elicits a considerable increase in beta catenin localisation to the nucleus ($p=0.0955$) and a significant increase in *Axin2* expression ($p<0.05$) (Figure 4.2C-E). Neither beta catenin localisation nor *Axin2* were changed following Fenoldopam treatment (Figure 4.2F-H). Therefore, both Hedgehog and Wnt signalling are altered by LiCl treatment, however Fenoldopam did not influence either pathway.

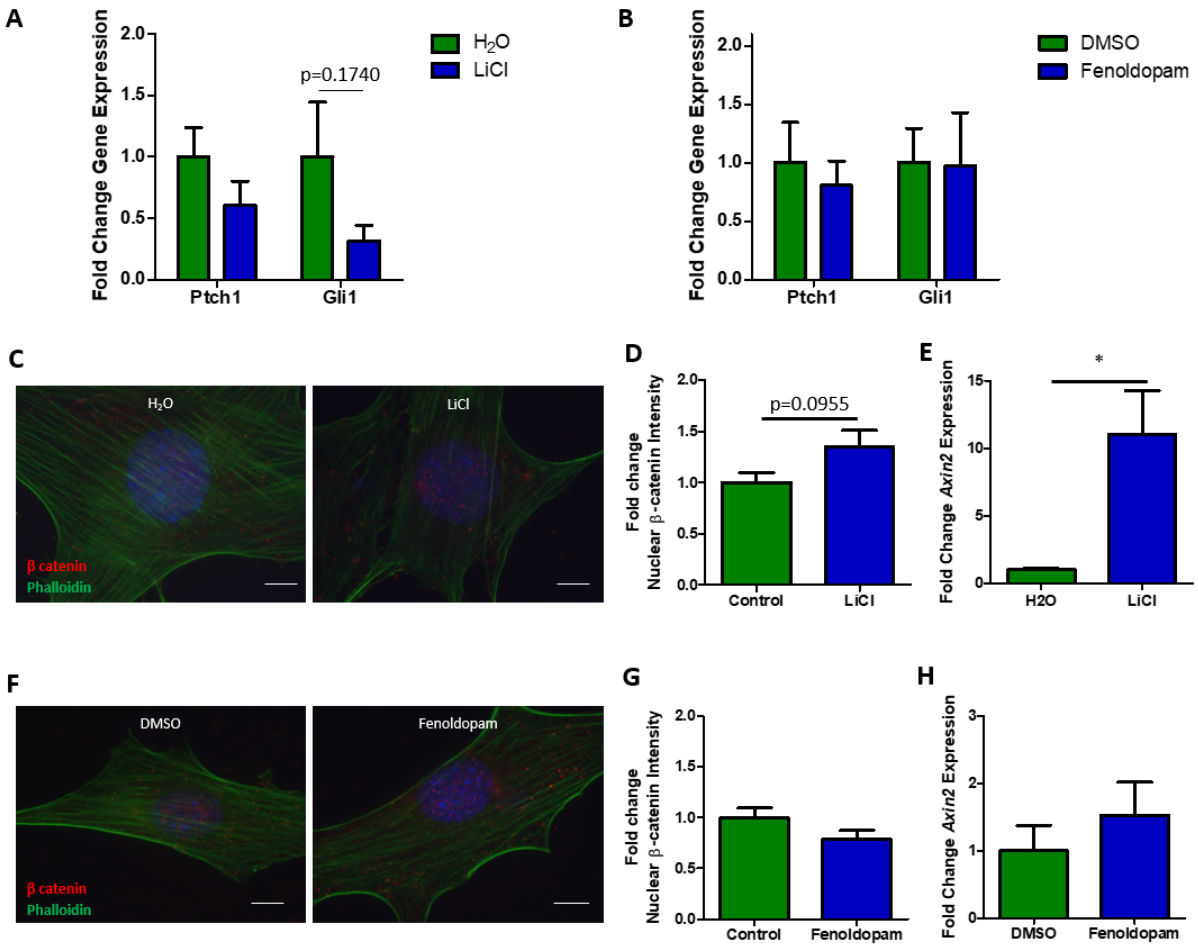

Figure 4.2:Effect of biochemical primary cilium elongation on Hedgehog and Wnt pathway activity. **A, B** *Ptch1* and *Gli1* expression following 24 hours of **A** 100mM LiCl or **B** 50µM Fenoldopam treatment, N=3, n=7-10. Bars illustrate mean±SEM, NS, not significant, statistical analysis, unpaired two tailed t-test. **C, F** Representative images of immunofluorescent staining of βcatenin in MSCs at 100x fluorescence (red channel- β-catenin, green channel- phalloidin and DAPI) (scale bar 10µm) **D, G** fold change intensity of β- catenin in the nucleus of MSCs (N=3, n=36-37), **E, H** *Axin2* expression (N=2, n=3-6) following 24 hours of **C-E** 100mM LiCl and **F-H** 50µM Fenoldopam treatment, bars illustrate mean±SEM, NS, not significant, statistical analysis, unpaired two tailed t-test.

4.3.3 The effect of ciliotherapy treatment on early MSC osteogenesis.

4.3.3.1 Basal osteogenic gene expression

Considering the role of the primary cilium in mediating MSC osteogenic differentiation under biochemical induction, the impact of ciliotherapy treatments on levels of osteogenic markers at the gene level were investigated. LiCl resulted in a decreasing trend of *Opn* ($p=0.1363$) expression, and a significant decrease in *Runx2* ($p<0.05$) and *Dlx5* ($p<0.01$) expression (Figure 3A). In contrast, Fenoldopam resulted in a significant 5.29±1.46-fold increase in *Cox2* and a 2.09±1.62-fold increase in *Runx2* (Figure 4.3B). In summary, LiCl treatment resulted in an anti-osteogenic effect whereas Fenoldopam treatment is supportive of osteogenic signaling, demonstrating a diverse effect on osteogenesis despite similar effects on cilia length.

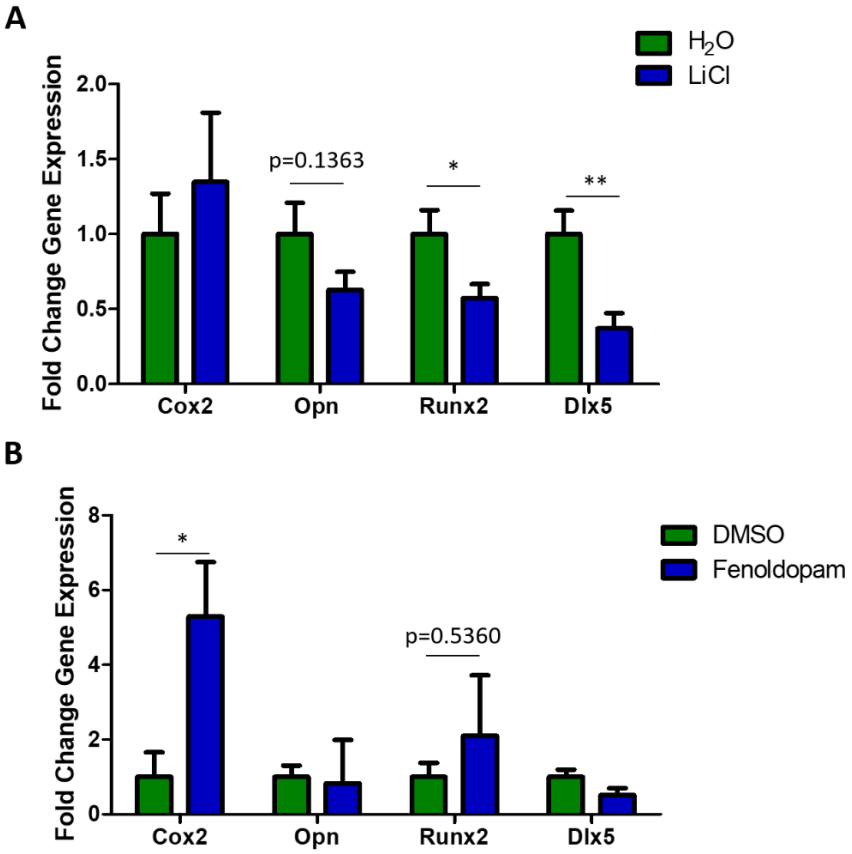

Figure 4.3: Effect of biochemical primary cilium elongation on osteogenic gene expression. *Cox2, Opn, Runx2* and *Dlx5* expression following 24 hours of **A** 100mM LiCl or **B** 50µM Fenoldopam treatment,

N=3, n=4-6. Bars illustrate mean±SEM, NS, not significant, *p<0.05, statistical analysis, unpaired two tailed t-test.

4.3.3.2 Mechanosensitivity

To investigate the influence of ciliotherapy treatments on the role of the cilium in MSC mechanosensitivity, the ciliotherapy treated MSCs were exposed to 2Pa fluid shear, oscillating at 2Hz for 2 hours and osteogenic gene expression was analysed. Strikingly, in both treatments the flow induced increase in *Cox2* was enhanced compared to vehicle controls (Figure 4.4A, E). There is a significant effect of fluid shear on *Cox2* expression in all cases (LiCl p<0.001, Fenoldopam p<0.05) however, the fold change compared to no flow controls increased following treatment, with a 6.65±1.55-fold increase in H_2O but a 9.31±2.63-fold increase following LiCl treatment and a 11.98±6.52-fold change in DMSO but a 22.48±7.93-fold increase following fenoldopam treatment. Despite the increase in basal no flow *Cox2* levels with DMSO, elongation of the cilium correlates with an increased *Cox2* response to flow. Fluid shear induced an upregulation in *Opn* in both treatment groups (Figure 4.4B- 1.31±0.38-fold, Figure 4.4F-1.63±1.00 fold) but the shear conditions applied here didn't significantly affect *Runx2* and resulted in a decrease in *Dlx5* (Figure 4.4D-p<0.01, Figure 4.4H p<0.01). As in basal conditions, LiCl treatment suppresses the expression of *Opn* (p<0.05), *Runx2* (0.57±0.09 fold) and *Dlx5* (p<0.001) and Fenoldopam didn't affect osteogenic markers. This therefore demonstrate that elongation of the primary cilium enhances MSC mechanosensitivity but in a gene dependent manner.

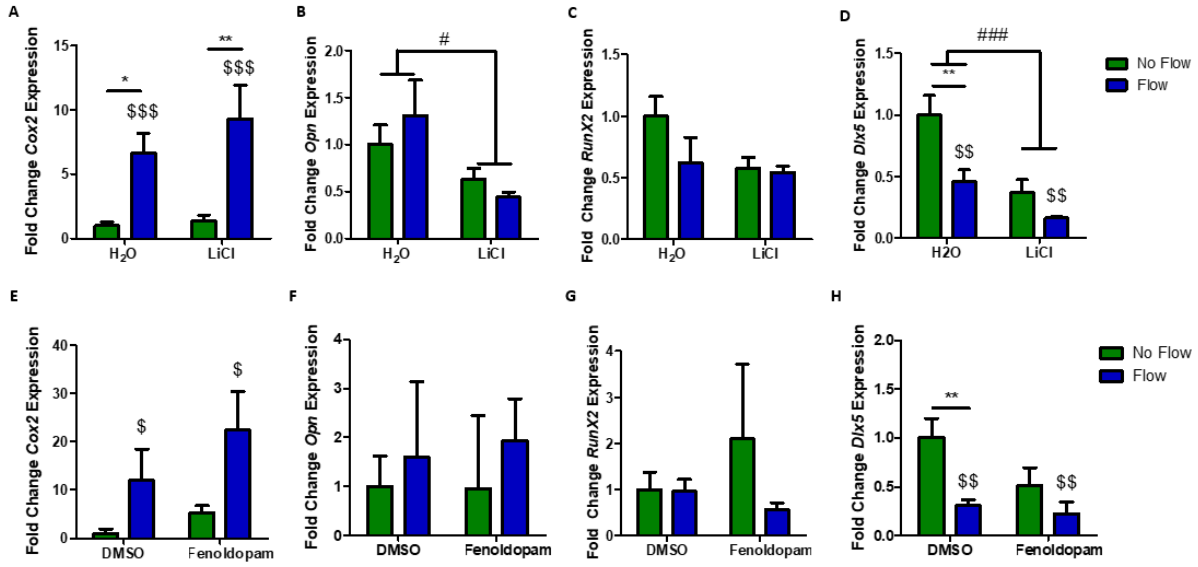

Figure 4.4: Osteogenic marker expression following 2 hours of 2Pa 2Hz OFF in each group A-D Lithium Chloride or vehicle, H2O and E-H Fenoldopam or vehicle, DMSO represented as Mean ±SEM, N=3, n=5-12, statistical analysis, 2 way ANOVA with Bonferroni post-hoc test; $$p<0.01, $$$p<0.001 effect of flow on gene expression, #p<0.05, ###p<0.001 effect of treatment on gene expression, *p<0.05, **p<0.01 effect of flow within individual treatment groups.

4.3.4 The effect of ciliotherapy treatment on biochemical induction of MSC osteogenic lineage commitment

Following the analysis of short term changes, the implications of ciliotherapy treatments on proliferation, via DNA quantification and full osteogenic differentiation, via osteogenic matrix formation were investigated over 21 days culture in osteogenic induction medium. DNA significantly decreased following LiCl treatment when compared to the vehicle controls, which is consistent with fewer cells visualised at day 21 following matrix staining ($p<0.05$, Figure 4.5A, C). Fenoldopam treatment does not influence cell proliferation (Figure 4.5B). Although total collagen and calcium deposition is decreased in LiCl ($p<0.001$, $p<0.01$ respectively) due to significantly fewer cells surviving in this group; relative to the DNA content, the collagen and calcium produced increases with LiCl ($p=0.0744$, $p<0.01$) (Figure 4.5E, I). Fenoldopam treatment had no considerable effect on collagen deposition and led to a slight but

significant decrease in the total quantity of calcium produced ($p<0.05$) (Figure 4.5F, J). Overall, treatment with LiCl increased the matrix deposition of the population of surviving cells, however due to significant cell death following this treatment the total quantity of bone tissue is dramatically reduced. Fenoldopam treated MSCs did not display any adverse effects on cell viability although no apparent increase in MSC osteogenic lineage commitment was observed following chemical induction.

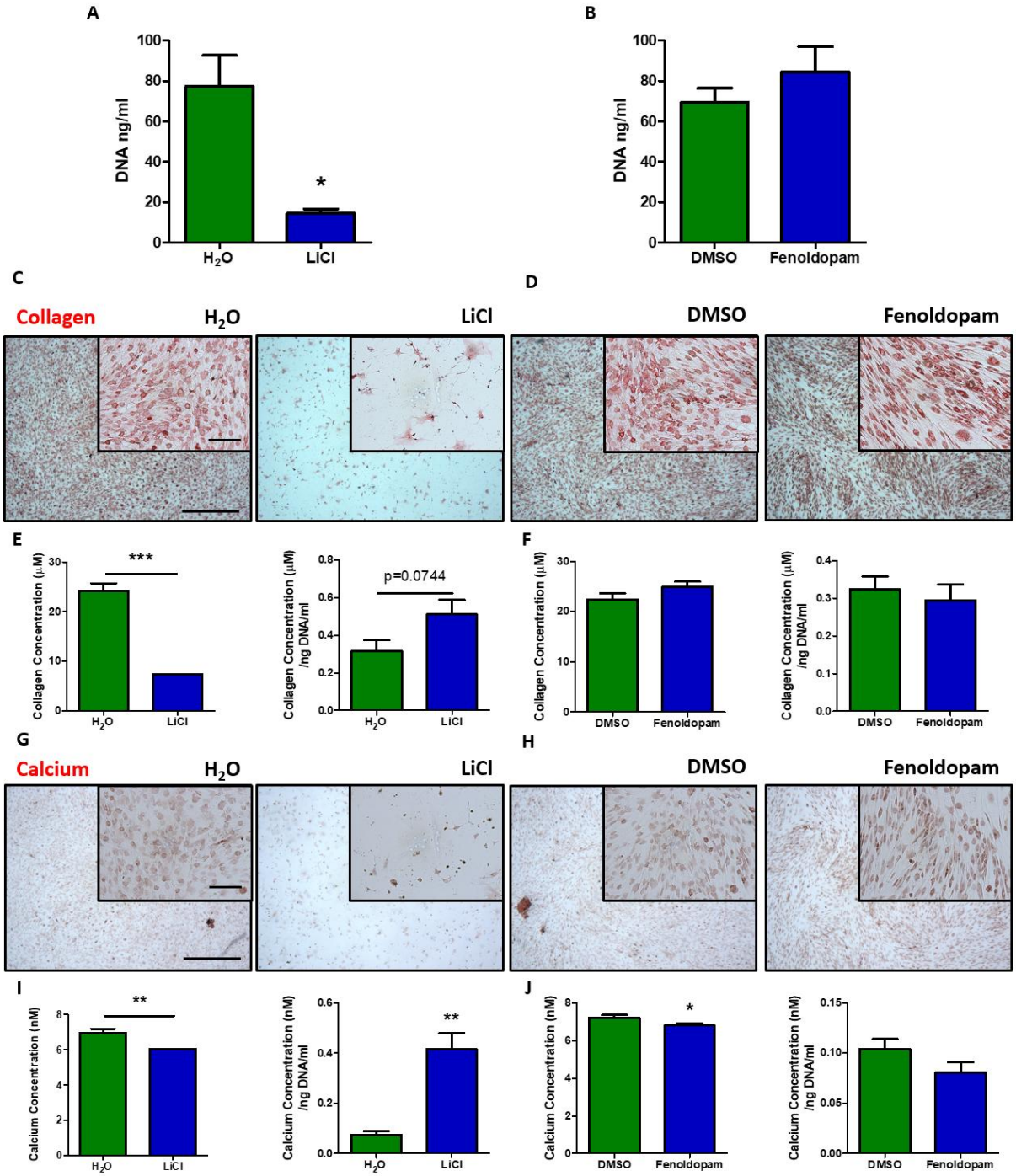

Figure 4.5: Quantification of DNA content following treatment with A 100mM LiCl or vehicle, H2O and B 50µM Fenoldopam or vehicle, DMSO for 21 days with full osteogenic supplements under static conditions. N=1, n=5-6, Mean±SEM, *p<0.05, student's t-test with Welch's correction. C, D, G, H Representative images of extracellular matrix staining C, D Picrosirius and G, H Alizarin Red, following treatment with C, G LiCl or vehicle, H2O and D, H Fenoldopam or vehicle, DMSO after 21 days culture in full osteogenic supplements, scale =500µm and 100µm in the inset. E, F, I, J Quantification of matrix staining E, I total collagen and collagen normalized to DNA content and F, J total calcium and calcium normalized to DNA content from each group, student's t-test, *p<0.05, **p<0.01, ***p<0.001.

4.3.5 The effect of ciliotherapy treatment on biophysical induction of MSC osteogenic lineage commitment.

Considering the influence of ciliotherapies in early adaptation to fluid shear (Figure 4), the impact on osteogenic commitment in response to fluid shear was analysed via matrix deposition. Fluid shear did not change the LiCl induced decrease in cell survival, however, under the influence of Fenoldopam cell proliferation was decreased with fluid shear which contrasts with the increase seen under flow in vehicle controls (Figure 4.7A). The fluid shear conditions applied were not sufficient to change total collagen concentration in response to flow in H_2O and caused a slight but significant decrease in collagen with DMSO ($p<0.05$) (Figure 4.6D, 7D). Interestingly, relative to DNA content the quantity of collagen significantly increased in response to flow ($p<0.05$, 1.76-fold change) (Figure 4.6F). A similar trend in normalized collagen per DNA is seen with Fenoldopam treatment (Figure 4.7F). The application of flow at these conditions increased overall calcium concentration in all samples (LiCl-$p<0.05$, Fenoldopam-$p<0.01$). While LiCl treatment significantly increased the calcium produced per cell in response to flow ($p<0.001$, 2.37-fold) Fenoldopam treatment increased the mechanoresponse both in terms of total calcium ($p<0.01$) and calcium per cell ($p<0.05$) (Figure 4.6G, 4.7E, G). In summary, MSCs treated with ciliotherapies LiCl or Fenoldopam exhibit an increased response to fluid shear in terms of bone matrix production, however due the poor effects of LiCl on cell viability, Fenoldopam is the recommended ciliotherapy to enhance MSC ciliogenesis, mechanosensitivity and osteogenesis.

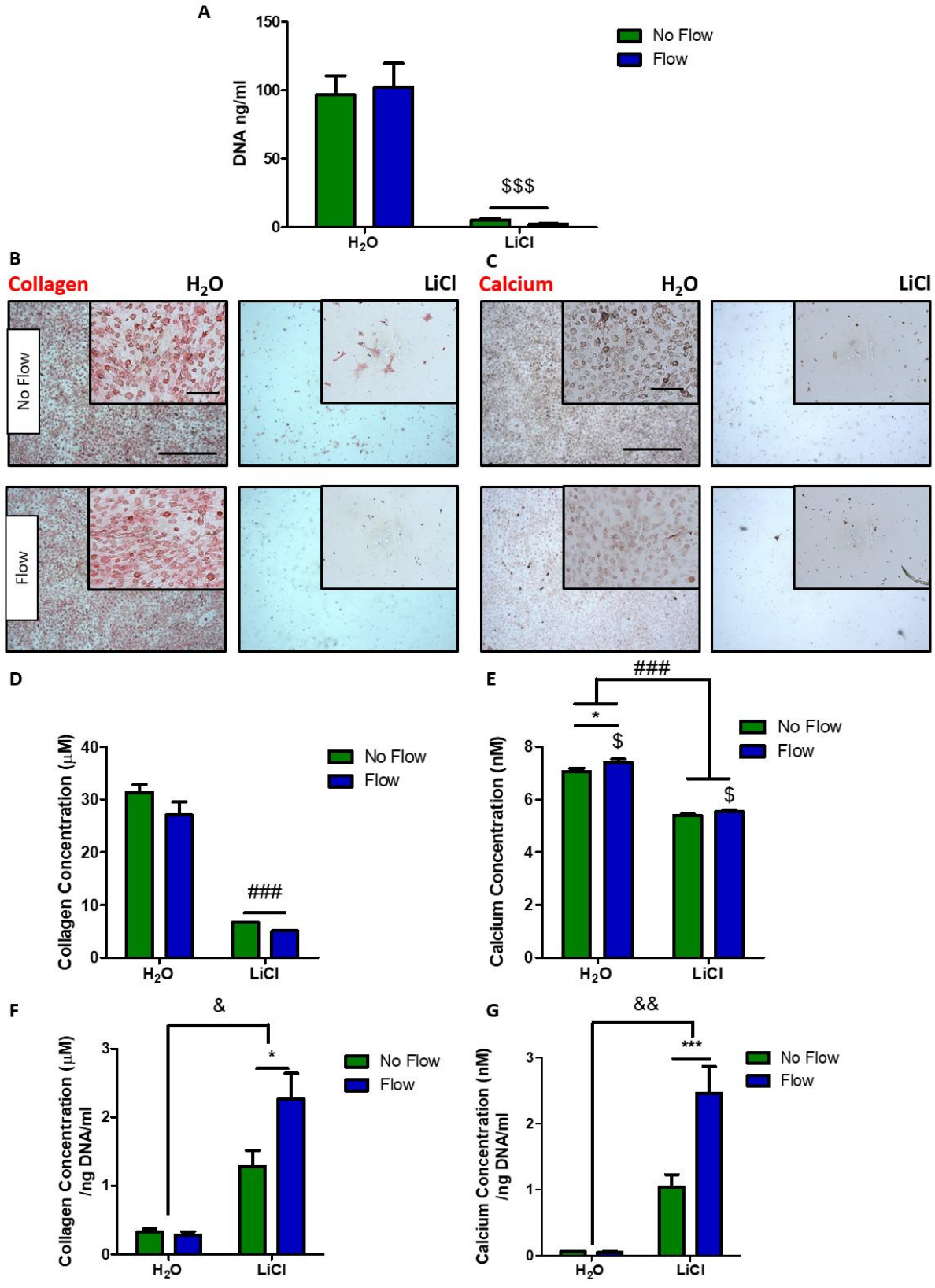

Figure 4.6: A, Quantification of DNA content following treatment with LiCl or vehicle, H2O for 21 days cultured in either static, No Flow, or mechanically stimulated, Flow. B, C Representative images of extracellular matrix staining B Picrosirius, C Alizarin Red staining, following treatment, scale =500µm and 100µm in the inset. D-G Quantification of matrix staining D, E total collagen and calcium concentration extracted from each group. F, G Extracellular matrix normalized to DNA quantification F collagen and G calcium, two-way ANOVA, $p<0.05, effect of flow on collagen and calcium

concentration. ###p<0.001 effect of treatment, *p<0.05, ***p<0.001 Bonferroni post test, effect of flow on individual treatment groups, &p<0.05, &&p<0.01 difference between the effect of flow in each treatment.

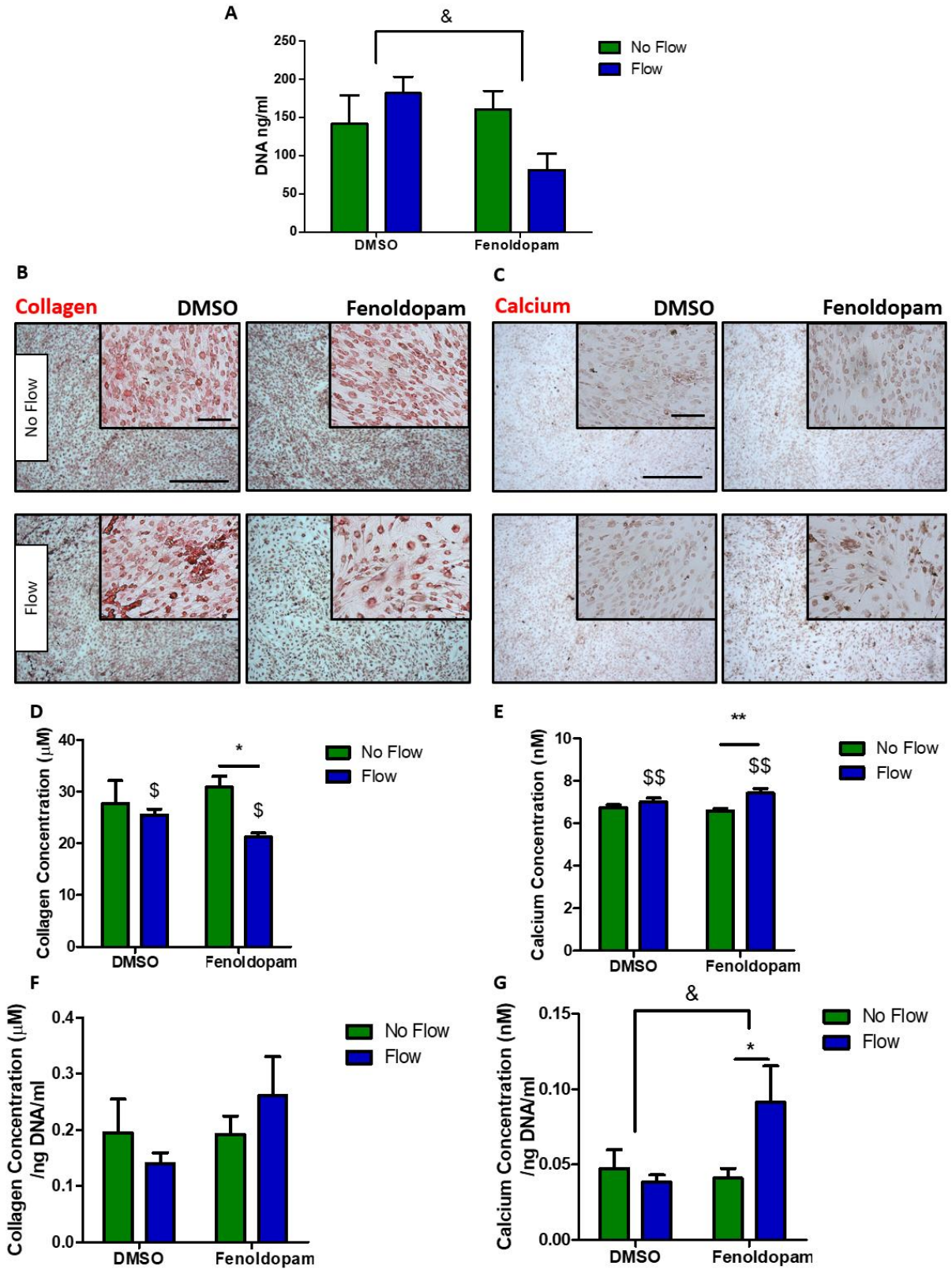

Figure 4.7: A, Quantification of DNA content following treatment with Fenoldopam or vehicle, DMSO for 21 days cultured in either static, No Flow, or mechanically stimulated, Flow. **B, C** Representative images of extracellular matrix staining **B** Picrosirius, **C** Alizarin Red staining, following treatment, scale

=500μm and 100μm in the inset. **D-G** Quantification of matrix staining **D, E** total collagen and calcium concentration extracted from each group. **F, G** Extracellular matrix normalized to DNA quantification **F** collagen and **G** calcium, two-way ANOVA, $p<0.05, $$p<0.01, effect of flow on collagen and calcium concentration.*p<0.05, **p<0.01 Bonferroni post test, effect of flow on individual treatment groups, &p<0.05, difference between the effect of flow in each treatment.

4.4 Discussion

New approaches to treat osteoporosis have focused on promoting bone formation through the targeting of osteoblasts and their progenitors, mesenchymal stem cells. The primary cilium is a singular cellular extension that represents a distinct cellular compartment known to play an important role in biochemical and biophysical osteogenic induction of MSCs. Defects in the cilium leading to alterations in its structure have been associated with a plethora of diseases, and thus targeting ciliary structure therapeutically, with ciliotherapies, has emerged as a potential new treatment modality. Therefore, given the important role of the MSC cilium in bone physiology, this study performed a comparison analysis on known ciliotherapies and their potential effects in mediating MSC osteogenic differentiation. Two established ciliotherapies, LiCl and Fenoldopam, were found to enhance MSC ciliogenesis to a similar degree but have diverse effects on cilia-associated signalling pathways and early osteogenic differentiation. LiCl significantly altered HH and Wnt signalling which was associated with inhibited osteogenic gene expression, while Fenoldopam demonstrated enhanced early osteogenesis. Long term treatment with both ciliotherapies did not enhance osteogenesis, however LiCl had detrimental effects on cell viability. Intriguingly both ciliotherapies enhanced MSC mechanosensitivity as demonstrated by augmented osteogenic gene expression in response to fluid shear, which over longer durations resulted in enhanced bone matrix deposition per cell. Therefore, known ciliotherapies can be utilised to enhance ciliogenesis in MSCs resulting in enhanced

mechanosensitivity, although based on our findings, only fenoldopam is a viable therapeutic option due to poor cell viability following long term LiCl treatment. Fenoldopam therefore represents a novel ciliotherapeutic option to enhance MSC osteogenesis and treat bone loss diseases such as osteoporosis.

Ciliogenesis in MSCs and the length of the ciliary axoneme can be significantly increased by the application of 100mM LiCl or 50μM Fenoldopam for 24 hours. Surprisingly, forskolin treatment did not increase cilium length at concentrations which were effective in collecting duct and kidney epithelial cells (Besschetnova et al., 2010, Sharma et al., 2011). Forskolin is an adenylyl cyclase activator which highlights a potential disparity in the cAMP-PKA pathway in kidney cells and MSCs. LiCl treatment elongated MSC primary cilia 1.21-fold which is in line with the 1.43-fold change seen in osteocytes and 2-fold change seen in chondrocytes (Spasic and Jacobs, 2017, Thompson et al., 2016). The modulation of cilia via LiCl is mediated by a downregulation in adenylate cyclase III according to mechanistic studies in synoviocytes, where LiCl has a similar effect on cilium length. Fenoldopam elicits a 1.18-fold change in MSC cilium length, similar to the effect displayed in osteocytes, 1.29-fold and vascular endothelial cells, 1.4-fold (Spasic and Jacobs, 2017, Kathem et al., 2014b). The target of fenoldopam is dopamine receptor 5 and is found expressed on the cilia of epithelial and endothelial cells (Upadhyay et al., 2014). Hence our data demonstrates that known ciliotherapies are effective at enhancing stem cell ciliogenesis through diverse mechanisms.

The identification of two regimes which significantly elongate cilia via distinct mechanisms presents a novel tool to study the role of axoneme length in ciliary function. Increasing cilia length, increases the surface area of the ciliary membrane which houses receptors probing the extracellular environment. In addition, the

mechanical properties of the ciliary axoneme, modelled most recently as a rotational spring, are altered with axoneme length. Increased length generates greater bending energy at the basal body promoting the movement of signalling molecules from within the ciliary membrane to the cytosol (Resnick, 2015, Downs et al., 2014b, Hoey et al., 2012c). Furthermore, the axoneme length increases by a similar magnitude in both treatments (LiCl 0.42μm, Fenoldopam 0.49μm) facilitating comparison of the effect of axoneme length on the response to stimuli. Despite similar increases in ciliary length, the Hedgehog and Wnt pathways were significantly altered following LiCl treatment, yet, Fenoldopam doesn't affect either of these cilia-associated pathways, demonstrating a diverse and potentially non-ciliary effect of these treatments. Moreover, LiCl treatment inhibited osteogenic gene expression, which is consistent with a decrease in HH signalling (Nakamura et al., 2015), while Fenoldopam enhances early MSC osteogenesis. The effect of Fenoldopam, a dopamine receptor agonist, on basal *Runx2* expression mirrors the early pro-osteogenic response of osteoblasts to dopamine (Lee et al., 2015a). Despite disparate effects on basal osteogenic gene expression, elongation of the primary cilium enhanced the fluid shear mediated increases in *Cox2* expression in all groups, demonstrating a consistent increase in mechanosensitivity in cells with longer primary cilia. This finding is consistent with the hypothesis that the cilium is a fluid shear mechanosensor, where it is hypothesised that enhanced bending due to a longer axoneme may activate mechanosensitive ion channels at the base of cilium (Corrigan et al., 2018). *Cox2* is required to produce PGE2 and has roles in MSC osteogenesis, loading-induced bone formation and fracture repair (Zhang et al., 2002). Previous studies have linked the primary cilium to fluid shear-induced *Cox2* upregulations among other early osteogenic markers (Hoey et al., 2012d, Stavenschi et al., 2017) and the increased mechano-regulated *Cox2* response is mirrored in osteocytes

treated to elongate cilia (Spasic and Jacobs, 2017). Taken together, the early response of MSCs with elongated cilia shows some support for ciliotherapies as a tool for promoting osteogenic differentiation, with fenoldopam showing the greatest promise.

Despite similar effects on MSC ciliogenesis, due to LiCl's detrimental effect on cell viability, Fenoldopam is the only examined ciliotherapy with potential for use as a skeletal targeted therapeutic. Completely different effects on cell viability were seen following 21 days of treatment, where LiCl had adverse effects while Fenoldopam had minimal influence. The effect of lithium may be attributed to the high concentrations applied to optimize cilium length as lithium treatments at 5mM has previously been shown to support MSC proliferation via gsk3beta inhibition (Zhu et al., 2014). Intuitively, the loss of cell numbers under the influence of LiCl leads to marked decreases in overall collagen and calcium production following long term treatment, even in the presence of osteogenic supplements, indicating that this ciliotherapy is not a viable option to enhance bone regeneration. However, the cells which survive and differentiate are more osteogenic in terms of collagen and calcium production per cell. Previously, LiCl treatment has demonstrated a pro-osteogenic effect (Zamani et al., 2009) which has been linked to the activation of β-catenin in analyses of bone tissue (Chen et al., 2007). Our findings indicate that LiCl does not impact MSCs in the same way. Previous applications of much lower, less than 20mM, LiCl to MSCs did not alter the production of Alizarin under the same biochemical supplements (Zhu et al., 2014). The influence of Fenoldopam on biochemical differentiation was subtle in terms of collagen and calcium, however total calcium concentration did unexpectedly decrease slightly. Normalising for the number of cells per sample, the calcium response of MSCs to fluid shear is greatly improved when treated with either ciliotherapy, which is consistent with early gene expression in response to fluid shear, demonstrating

enhanced mechanosensitivity. The collagen response is significantly upregulated with LiCl but the upward trend is not significant in Fenoldopam. This increase in calcium production in response to flow in both treatments supports a role for the primary cilium as a mechanosensor in fluid shear mediated osteogenesis. Furthermore, it suggests that the length of cilia is influential in this process. However, the suitability of these agents as a therapy to increase bone formation is disputable due to the non-ciliary and potential toxic effects of these drugs at high concentrations. The effect of lithium chloride on cell survival dissuades use past 2 hours in MSCs. Fenoldopam is currently used as an intervention to relieve high blood pressure so the implications that its application could have in other tissues pose considerable risk, particularly for individuals who suffer from low blood pressure.

4.5 Conclusion

This study demonstrates that known ciliotherapies, LiCl and Fenoldopam, can be utilised to enhance ciliogenesis in mesenchymal stem cells. Both cilium enhancing treatments increase the sensitivity of MSCs to fluid shear induced by physical exercise in terms of mRNA and matrix deposition. However, the impact to Hedgehog and Wnt signaling mediated by LiCl, as well as its impact on cell viability doesn't support its use as a therapy to enhance MSC osteogenesis. However, despite minimal effects of fenoldopam on biochemical osteogenic induction of MSCs, this ciliotherapy is effective at enhancing biophysical induction through enhanced mechanosensitivity and thus represents a novel ciliotherapeutic option to enhance MSC osteogenesis and treat bone loss diseases such as osteoporosis.

Chapter 5:

Human bone marrow MSCs isolated from osteoporotic patients demonstrate abnormal recruitment, mechanosensitivity, and osteogenic matrix deposition.

5.1 Introduction

Osteoporosis is a debilitating bone disease characterised by low bone density, quality, and strength, leading to an increased risk of fracture, and represents a leading global medical challenge (Melton et al., 1992, Melton et al., 1998). Osteoporotic fractures result in a loss of independence and dramatic increases in mortality rates (Keene et al., 1993). Aside from the clear devastating human cost, osteoporosis is a major public health problem, with an enormous social and economic impact. Furthermore, due to a growing, ageing population this problem is only escalating. Therefore, due to the overwhelming personal and financial impact of osteoporosis, a greater understanding of the aetiology of the disease resulting in the development of more effective treatments is required.

Osteoporosis arises when there is an imbalance between bone formation (mediated by the mesenchymal derived osteoblast) and bone resorption (mediated by the hematopoietic derived osteoclast). Current osteoporosis therapeutics target receptors known to inhibit resorption, but in some cases are associated with side effects including increased risk of atypical fracture, osteonecrosis of the jaw, oesophageal cancer and

atrial fibrillation (Kennel and Drake, 2009). An emerging alternative approach to treatment is to enhance bone formation through the targeting of osteoblasts and their precursor, mesenchymal stem cells (MSC). Teriparatide, a low dose analogue of parathyroid hormone, is currently the only clinically approved anabolic therapy for osteoporosis, however it is only effective for 2 years (Bodenner et al., 2007). Although other anabolic therapies in the form of the sclerostin targeting antibody romosozumab are emerging (McClung, 2017), deficiencies in anabolic therapies may arise due to an inherent defect in the osteoblast and osteoprogenitors in the osteoporotic environment.

Continued bone formation requires the replenishment of the osteoblast from a progenitor or stem cell population. Bone marrow contains a multitude of cellular populations, one of which is the multipotent progenitor of fat, cartilage and bone among other tissues, traditionally called a 'mesenchymal stem cell' (MSC) (Caplan, 1991). The nomenclature and definition of these cells has undergone extensive debate lately (Robey, 2017, Bianco and Robey, 2015, Zhou et al., 2014, Chan et al., 2018). However, we will use the nomenclature MSC here to denote the cells isolated from marrow for *in vitro* culture capable of self-renewal and differentiation towards the adipogenic, chondrogenic and osteogenic lineages as per the guidelines set out by the International Society for Cellular Therapy (Dominici et al., 2006). In response to an anabolic biochemical (Brady et al., 2015, Jaiswal et al., 1997) or biophysical (Hoey et al., 2012d, Stavenschi et al., 2018a, Chen et al., 2016a, Stavenschi et al., 2017) stimulus it is hypothesised that MSCs are recruited from the niche to the site of bone deposition, proliferate to maintain supply, and undergo differentiation towards the osteoblastic lineage, to facilitate the deposition of new matrix in form of collagen and mineral (Kristensen et al., 2014, Chen et al., 2016a, Turner et al., 1998). However, how this

process occurs and whether this is altered in the osteoporotic environment is poorly understood.

Several often-conflicting studies demonstrate altered behaviour in cells isolated from osteoporotic bone (Antebi et al., 2014, Veronesi et al., 2011). There is some disagreement over the quantity and proliferative capacity of osteoprogenitors present in osteoporosis. Some studies observe a reduction in MSC number and growth capacity in osteoporosis while others see no change (D'Ippolito et al., 1999, Rodríguez et al., 1999, Stenderup et al., 2001). In a recent study, transplanted osteoporotic MSCs showed significantly reduced homing to a fracture site demonstrating an inhibited chemotactic capacity (Tewari et al., 2015). Furthermore, osteoporotic hMSCs reveal reduced migration upon stimulation with BMPs *in vitro* (Haasters et al., 2014). Dysregulation of differentiation has been observed in studies of osteoporotic MSCs with adipogenic activity increasing (Rodríguez et al., 2000, Moerman et al., 2004). Both osteoclast and osteoblast progenitor colony forming units, are increased in the estrogen deficient environment post menopause (Manolagas and Jilka, 1995), however, the number of mineralising progenitors, demonstrated by alkaline phosphatase production, decrease in women with aging (Muschler et al., 2001). While there has been some investigation of alterations in biochemically induced differentiation in osteoporotic MSCs, the changes in biophysical induction are almost completely lacking (Jing et al., 2016, Donoso et al., 2015, Valenti et al., 2011).

Therefore, in this study we aim to isolate, characterise and compare MSCs from healthy and osteoporotic donors in terms of recruitment, proliferation and biophysical and biochemical induced osteogenic differentiation potential. This new understanding of the MSC behaviour may contribute to our understanding of the aetiology of osteoporosis,

which will better inform the development of new anabolic therapies and regenerative strategies to enhance bone repair in the osteoporotic environment.

5.2 Methods

5.2.1 Human bone marrow sample acquisition

Bone marrow aspirates were obtained from patients undergoing a hemiarthroplasty or total hip arthroplasty at University Hospital Limerick or the Midwestern Orthopaedic Hospital, Croom. Ethical approval was obtained from the Health Service Executive and the University of Limerick and all patients gave informed consent. Osteoporotic female patients were identified following the diagnosis of a femoral neck fragility fracture. Osteoporosis was clinically diagnosed as per the National Osteoporosis Foundation Guidelines which state that 'a clinical diagnosis can be made in at risk individuals who sustain a low trauma fracture (Cosman et al., 2014). Healthy female patients were identified following the diagnosis of a femoral neck fracture where the mechanism of injury was considered significant in causing the fracture, i.e trauma. Healthy patients had no history of osteoporosis. Exclusion criteria included patients unable to consent to the procedure, active malignancy or patients receiving osteoporotic medications prior to admission. Bone marrow aspirates were taken from the pelvis intraoperatively during the exposure of the acetabulum, prior to the insertion of the prosthesis. A Jamshidi needle (Stryker) and a 50ml luer lock syringe were used to withdraw 30ml of bone marrow aspirate, which was transferred to a sterile container and transported to the laboratory at room temperature. Supplemental samples of bone marrow from healthy female donors were purchased from Lonza (www.lonza.com)

5.2.2 Human bone marrow mesenchymal stem cell (hMSC) isolation and culture

Whole bone marrow was divided into 5ml aliquots and washed in 35ml of PBS (Sigma) before centrifugation at 900g for 10 minutes. The pellets were resuspended in PBS and pooled, an aliquot was diluted 1:1 in 4% acetic acid (Sigma) to lyse red blood cells before counting. The cells were seeded at 250,000/cm^2 in DMEM (Sigma-Aldrich) supplemented with 10% fetal bovine serum (FBS) (Labtech), 1% penicillin streptomycin (PS) (Sigma) and 5ng/ml bFGF2 (Prospec). On day 5 of culture the medium was removed and flasks were washed with PBS to dislodge red blood cells before feeding with fresh medium. Following this the medium was changed every 3-4 days and trypsinised once colonies of cells were seen to adhere to the plastic. The adherent cells were seeded at 4000-5000/cm^2 and grown to 70% confluency for characterisation and experimentation at passage 3-7.

5.2.3 Validation of hMSC Isolation

The cells isolated were tested in accordance with the standards of the International Society for Cellular Therapy (Dominici et al., 2006). Briefly, fibroblast-like, plastic adherent cells were characterised for surface marker expression using flow cytometry (Accuri C6, BD), with >95% expression of positive markers (CD105, CD90, CD73 and CD44) and <2% expression of negative markers (CD34 and CD45) (Abcam) meeting ISCT guidelines. Differentiation capacity down the osteo-, adipo- and chondro-genic lineages was validated. MSCs were seeded at 25,000 cells/well in 6 well plates. When monolayers reached a confluency of 70% the medium was changed to either osteogenic supplemented medium (standard culture media + 100nM dexamethasone (Sigma), 0.05mM ascorbic acid (Sigma) and 10mM β-glycerophosphate (Sigma)) (Jaiswal et al.,

1997) or adipogenic supplemented medium (standard culture media + 0.5mM IBMX (Sigma), 50µM indomethacin (Sigma) and 100nM dexamethasone) (Janderová et al., 2003). For chondrogenesis, a pellet of 250,000 cells was formed by centrifugation at 2000rpm for 5 minutes and grown in basal medium (DMEM1.5mg/ml BSA (Sigma), PS, 0.04mg/ml L-proline (Sigma)). After 3 days the medium was supplemented with 1x ITS (Gibco), 10ng/ml TGFβ3 (Prospec), 100nM dexamethasone, 0.17mM ascorbic acid, and 4.7µg/ml linoleic acid (Sigma) (Mackay et al., 1998). Following 21 days culture the monolayers and pellets were rinsed in PBS and fixed in neutral buffered formalin (Sigma). Osteogenic staining (i.e. mineral and collagen deposition) was performed using 1% Alizarin Red (pH4.1) (Sigma) for 20 minutes and 1% Picrosirius Red (Sigma) staining for 1 hour at room temperature while gently shaking. Adipogenic staining (i.e. lipid formation) was performed using Oil Red O (Sigma) staining for 30 minutes at room temperature. Chondrogenic pellets were wax embedded and sliced before staining in Alcian Blue (pH1) (Sigma) with counterstaining in 0.1% Nuclear Fast Red (Sigma) for 5 minutes each. The stained monolayers and slices were imaged using 2x (NA 0.06) and 10x (NA 0.25) objectives for the monolayers and 4x (NA 0.10) and 10x (NA 0.25) for the sliced pellets on an Olympus BX41 (Olympus).

5.2.4 hMSC Migration

Chemotaxis towards 10% FBS was analysed using a modified Boyden chamber assay (24 wells Millicell inserts, 0.8 µm, Millipore). The inserts were placed in the wells of a 24 well plate in triplicate, with the wells containing 1.5ml serum free medium. 10,000 hMSCs were seeded into each insert and incubated for 4 hours to allow the cells to adhere. Then the inserts were transferred to a new plate with wells containing 10% FBS or a serum free control. After 18 hours the cells were moved to new wells of PBS for

rinsing, followed by fixation in 10% formalin for 10 minutes. The inserts were rinsed in distilled water and stained in hematoxylin (Sigma HHS32-1L) for 8 mins. After extensive rinsing, the inside of the inserts were cleaned using cotton buds. A fine forceps was then used to lift the membranes away from the insert for mounting in DPX mounting medium. Migration was quantified by counting the number of cells on the membrane in at least 8 different fields of view following bright field microscopy (BX41, Olympus) at 20x (NA 0.4).

5.2.5 hMSC gene Expression

TRI reagent (Sigma) was used to extract RNA per the manufacturer's protocol. The concentration of RNA in each sample was measured using a Nanodrop spectrophotometer and sample purity was checked via 260/280 and 260/230 absorbance ratios. A minimum of 200ng of RNA was reverse transcribed to cDNA using the High-Capacity cDNA Reverse Transcription Kit (Applied Biosystems). The efficiency of the reverse transcription was monitored by quantifying cDNA using a Qubit single stranded DNA assay (Invitrogen). Quantitative polymerase chain reactions (qPCR) were prepared for all samples using SYBR Select Master Mix with ROX passive dye (Applied Biosystems, 4472903) and custom designed primers (Sigma) for *18S, COX2, OPN, and RUNX2,* for amplification using the ABI 7500 real time PCR machine (Applied Biosystems) as outlined in Supplementary Table 5.1. To calculate the basal gene expression levels the quantity of each sample was calculated in ng from a standard curve created from a healthy human calibrator sample. These are expressed relative to the reference gene, *18S.* To analyse the response to fluid shear the relative quantity of each sample was calculated with reference to *18S* and expressed as fold change normalised to the control, no flow group.

5.2.6 Mechanical Stimulation

Parallel plate flow chambers, designed in house as described previously, were used for short term fluid shear application (Stavenschi et al., 2017). Briefly, hMSCs were seeded on fibronectin (10µg/ml) coated glass slides, assembled between two plates and attached to a programmable syringe pump (New Era Pump Systems). Oscillating fluid flow (OFF) was applied through a 10ml syringe (Becton Dickinson) at 104ml/min, subjecting cells to a shear stress of 2Pa, at a frequency of 2Hz. This stimulus was applied for 2 hours. The no flow controls were similarly assembled within the chambers but were not subjected to fluid shear.

5.2.7 Proliferation

Cell growth was monitored over 21 days by measuring the DNA content at 7 day intervals using a QuantIT Picogreen assay (Thermofisher) for dsDNA. Monolayers were rinsed in PBS and lysed in 0.2% v/v Triton X100 (Sigma), 10mM Tris pH8 (Sigma), 1mM EDTA (Sigma) for 20 minutes on ice. The monolayer was scraped for collection in microtubes before vortexing for 30 seconds and sonicating for 1 minute. The vortex and sonication steps were repeated 5 times at 10 minute intervals and samples were passed through a 21G needle 10 times before flash freezing samples in liquid nitrogen and storing at -80°C. Fluorescent reaction to picogreen reagent was excited at 480nm and read at 520nm. The DNA quantity was read from a standard curve of 0-200ng/ml.

5.2.8 Quantification of osteogenic matrix deposition

To quantify the formation of collagen matrix 1ml PBS was added to each Picrosirius Red stained well. The monolayers were removed using a cell scraper to a 1.5ml

microtube. The samples were centrifuged at 14000g for 10 minutes. The resulting pellet was dissolved in 0.5M NaOH and absorbance measured at 550nm. A standard curve was prepared using rat tail collagen (354249 Corning) incubated in Picrosirius Red for 30 minutes with gentle agitation, this stock was serial diluted in PBS. To quantify the formation of mineral, alizarin red stain was extracted via incubation in 10% acetic acid for 30 minutes under gentle agitation followed by heating at 85°C for 10 minutes. Cell debris was collected by centrifugation at 20,000g for 15 minutes and the pH adjusted to pH4.1-4.5 before measuring absorbance at 405nm. A standard curve was prepared from serial dilutions of the Alizarin Red S stock in distilled water, each standard was adjusted to pH 4.1-4.5.

5.2.9 Quantification of adipogenic matrix deposition

To quantify formation of lipids 750µl of IPA was added to each Oil Red O stained well and incubated for 15 minutes with gentle shaking. Solubilised lipids are removed to microtubes and diluted 1:2 in IPA. A standard is created from diluting freshly prepared Oil Red O stock in IPA at a dilution of 1:2. Sample absorbance is read at 490nm and the concentration of Oil Red O calculated from a standard curve.

5.2.10 Data Analysis

The percentage surface marker expression is the average of 3 replicates. All plots represent the mean and standard error of the mean. Comparisons between control and treatment of each sample or the pooled samples of one condition (i.e. healthy or osteoporotic) were analysed using an unpaired two-tailed student's t-test, with Welch's correction where the variances are unequal between groups. The effects of health or treatment on behaviour were tested using a two-way ANOVA with Bonferroni post-test.

5.3 Results

5.3.1 Human bone marrow mesenchymal stem cells were isolated from healthy and osteoporotic donors

Whole bone marrow was processed for the extraction of MSCs which were validated according to surface marker expression and trilineage differentiation potential (Dominici et al., 2006). Marrow was isolated from 4 female patients undergoing hip replacement surgery under informed consent, in collaboration with University Hospitals Limerick Group. 3 patients suffered a fracture of the femoral head following a low impact trauma and were undergoing a hip hemiarthroplasty. 1 patient suffered a significant trauma which resulted in a femoral head fracture and necessitated a total hip arthroplasty. A further 2 samples of whole bone marrow from healthy female donors were acquired commercially. All donors had good mobility and no significant orthopaedic history. Although there is considerable variation in the age of donors (age range-22-89 years) and considerable difference between the mean age of the healthy (38 years ±6.3) and osteoporotic (85 years ±1.5) cohorts these populations are deemed to be representative (Figure 5.1A). The preparation of each marrow sample resulted in plastic adherent cells by day 5 of culture. Flow cytometric analysis validated MSC surface marker identifiers. CD34 and CD45 were rarely expressed with only osteoporotic sample 3 demonstrating a slightly high CD34 expression at 2.1%. Positive markers CD73 and CD44 were highly expressed by all samples (>95%) (Figure 5.1B-F). Unexpectedly, two of the healthy and one of the osteoporotic samples had lower CD90 expression than guidelines from the ISCT would suggest of MSCs. Similarly, all samples except osteoporotic 3 fell below 95% expression of CD105, with the lowest expression levels in healthy 2 at 79.2%. Despite slightly reduced CD90 and CD105 expression, at passage 3 the extracted MSCs from all groups were capable of

differentiating down the adipogenic (Figure 5.7), chondrogenic (Supplementary Figure 5.1) and osteogenic lineages (Figure 5.5, 6). Adipogenesis was verified by positive staining for Oil Red O. Although there was lipid visible within hMSCs cultured in growth medium, there was considerable increases in lipid formation in adipogenic differentiation medium (Figure 5.7B, C). Regarding chondrogenesis, 5 of the 6 samples stained positively for Alcian blue following pellet culture for 21 days. Osteoporotic 1 and 3 formed a pellet in culture but were considerably smaller than all other samples (Supplementary Figure 5.1). As a result, the fixed pellets for osteoporotic 1 were lost during the slicing process. Osteoporotic 3 has some peripheral cells stained blue which is likely due to the small pellet size. Finally, all samples stained positively for calcium by Alizarin Red following growth in osteogenic medium for 21 days (Figure 5.6A, B).

A

Patient	Gender	Age	Diagnosis	Orthopaedic History	Mobility
Healthy 1	Female	59	Trauma	Nil	Independent
Healthy 2	Female	22	Donor	Nil	Independent
Healthy 3	Female	33	Donor	Nil	Independent
Osteoporotic 1	Female	86	Fragility	Trauma, age 20	Independent
Osteoporotic 2	Female	80	Fragility	Nil	Assisted
Osteoporotic 3	Female	89	Fragility	Nil	Independent

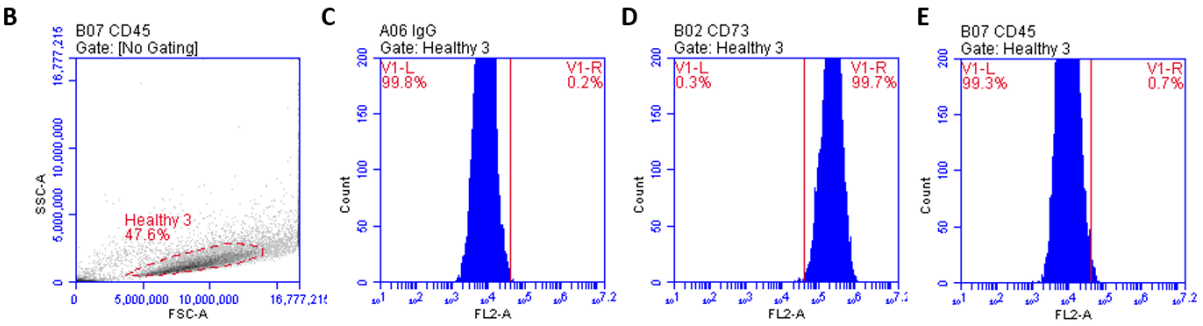

F

	Healthy			Osteoporotic		
	1	**2**	**3**	**1**	**2**	**3**
CD34	2.0%	0.5%	1.1%	1.2%	1.5%	*2.1%*
CD45	1.7%	0.5%	1.3%	1.7%	1.1%	1.5%
CD90	96.3%	*92.5%*	*94.9%*	99.3%	98.5%	*92.3%*
CD73	99.8%	99.6%	99.7%	99.4%	99.3%	99.7%
CD105	*91.3%*	*79.2%*	*81.0%*	*93.2%*	*92.5%*	95.5%
CD44	97.6%	99.8%	100.0%	98.8%	97.7%	98.0%

Figure 5.1: Details of MSC donors and immunophenotypic analyses of extracted MSCs **A** Donor age and orthopaedic health. **B** Representative forward and side scatter dot plot illustrating the selection of a gate to define the MSC population. **C-E** Representative plots of phycoerythrin fluorescence magnitude against the count of events, gated for healthy 3 defined in **B**. **C** IgG control to quantify background fluorescence of the cells, marked by vertical red line, **D** CD73 positive events detected in 99.7% overall, **E** CD45 positive events detected in 0.7% of the gated population. **F** Percentage population expressing stem cell specific surface markers, negative markers (shaded orange) should not exceed 2.0% expression in an MSC population and positive markers (shaded green) should exceed 95.0% expression to adhere to International Society for Cellular Therapy guidelines for defining an MSC population. n=3. Blue dashed line highlights readings outside of ISCT guidelines.

5.3.2 Osteoporotic hMSCs have defective chemotaxis

Healthy MSCs demonstrate significant chemotactic properties in the presence of 10% FBS which is absent in MSCs isolated from osteoporotic patients. In healthy MSCs the average number of cells migrating is greater in 10% FBS in each patient, whereas only one of the osteoporotic MSCs show this same trend (Figure 5.2A). Considerable individual patient variability is evident in the number of cells migrating even in the absence of a chemotactic stimulus. This variability increases in the osteoporotic population, with a mean of 9.22 cells migrating and a standard deviation of 3.94 compared to the healthy population of 8.63±1.05. Pooling the data of the healthy and osteoporotic patients shows significant chemotaxis in healthy MSCs ($p<0.05$) that is absent in osteoporotic hMSCs (Figure 5.2B), which is suggestive of defective hMSC recruitment in osteoporotic bone.

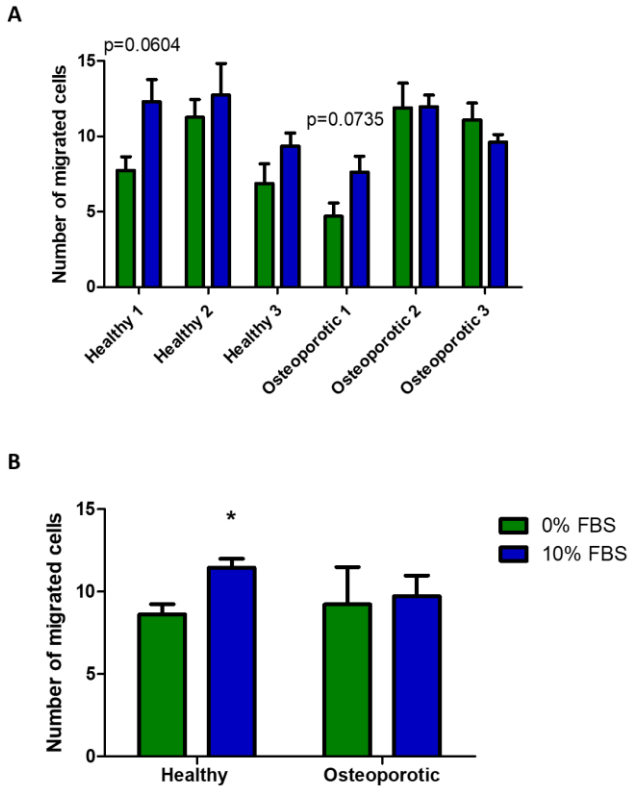

Figure 5.2: Migratory capacity of hMSC samples in the presence of 10% FBS. A Number of cells in each individual samples migrating upon exposure to 10% FBS, Mean±SEM, n>3, students unpaired t-test comparing 0% to 10% FBS in each sample, lowest p values, less than 0.1 listed. B Number of cells migrating to 10% FBS pooled from the healthy and osteoporotic groups, Mean±SEM, student's unpaired t-test, *$p<0.05$.

5.3.3 Osteoporotic hMSCs have reduced mechanosensitivity when compared to healthy controls

Osteoporotic MSCs express less *COX2* than healthy counterparts but comparable levels of *OPN* and *RUNX2*. Furthermore, the upregulation in *COX2* and *OPN* in response to fluid shear in osteoporotic MSCs is significantly inhibited compared to healthy counterparts. Although the basal expression levels of *COX2* varies considerably between individuals, osteoporotic patients show a trend towards reduced expression compared to healthy counterparts ($p=0.0506$) (Figure 5.3A). The basal expression of *OPN* and *RUNX2* show no significant difference between healthy and osteoporotic hMSCs (Figure 5.3B, C). Similarly, the upregulation in early osteogenic markers elicited by fluid shear is changeable from one patient to the next, demonstrating a patient specific degree of mechanosensitivity. Each of the hMSCs isolated from healthy donors elicit a fold increase in *COX2* greater than 11.89 following oscillatory fluid shear. Only osteoporotic 2 has a comparable mechanoresponse, responding significantly to the flow stimulus ($p<0.001$) (Figure 5.3D). There is a trend of increased *OPN* and *RUNX2* expression following fluid shear which is more evident in healthy hMSCs (Figure 5.3E, F). Pooling the average mechanoresponse of healthy and osteoporotic MSCs clearly demonstrates a diminished mechanosensitivity within the osteoporotic population (Figure 5.3G-I). The robust upregulation in *COX2* following fluid shear seen in healthy hMSCs (14.18-fold, $p<0.001$) is dramatically reduced in osteoporotic MSCs (8.42-fold, $p<0.05$), with this reduction in mechanoresponse approaching significance ($p=0.1225$). The *OPN* response to fluid shear in healthy hMSCs is 2.04 ± 0.44 fold but significantly less at 0.62 ± 0.40 in the osteoporotic cohort ($p<0.05$). Again the change in the *RUNX2* response in osteoporosis follows the trend seen in *OPN* and *COX2* ($p=0.0540$) further illustrating the lack of osteogenic response in osteoporosis. Taken

together, this data demonstrates that osteoporotic hMSCs have a reduced mechanosensitivity which may be a contributing factor to the osteoporotic phenotype.

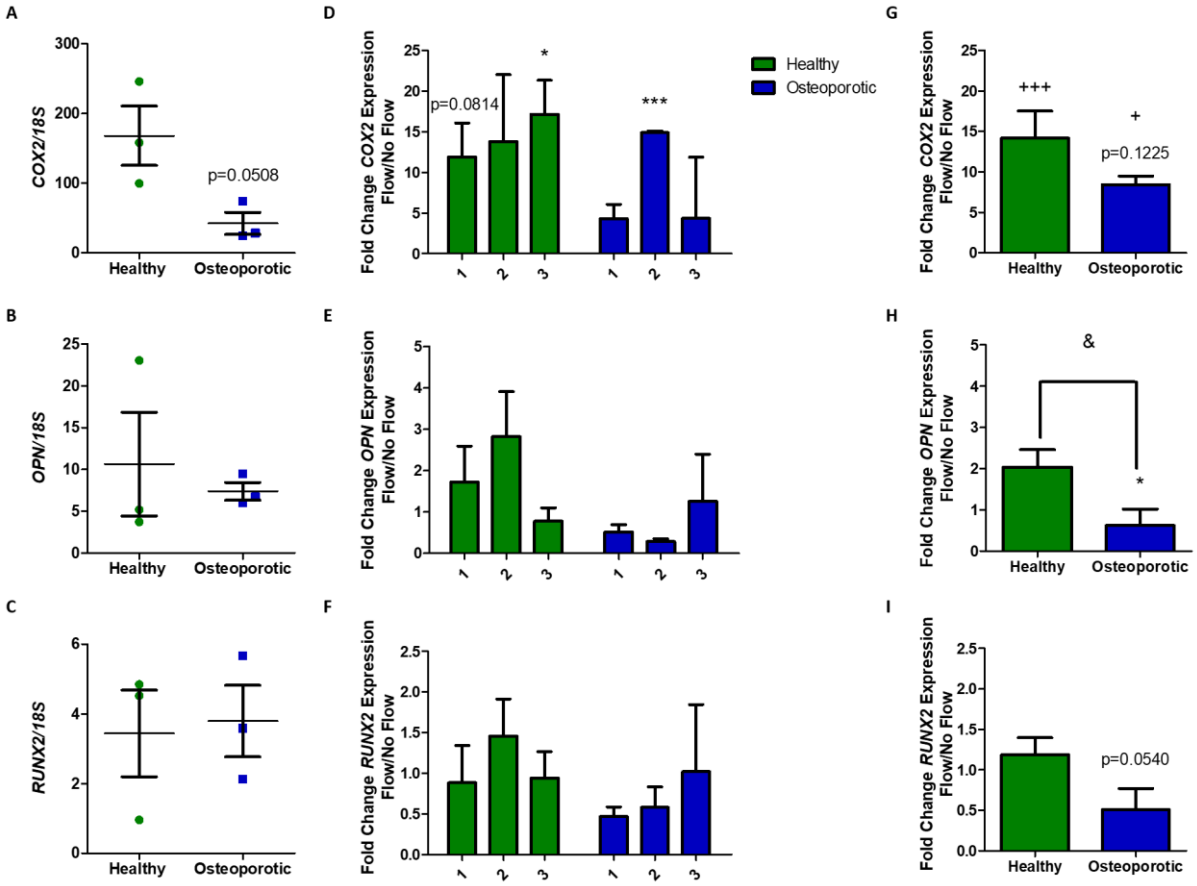

Figure 5.3: Expression of genes associated with early osteogenic differentiation in each sample **A** *COX2* **B** *OPN* **C** *RUNX2* relative to *18S*, Mean ± SEM, n=3-7, student's t-test, p values <0.15 are shown. Fold change gene expression response to 2Pa, 2Hz fluid shear applied for 2 hours. **D, E, F** Response of individual patients, Mean ±SEM, n=3-5, two-way ANOVA, not significant. **G, H, I** Comparison of healthy or osteoporotic samples pooled, Mean±SEM, n=3, two-way ANOVA comparing effect of flow and effect of MSC health, &p<0.05 effect of flow is different in healthy and osteoporotic, Bonferroni post test showing effect of flow in individual groups, +p<0.05, +++p<0.001, students t-test comparing fold change expression in healthy and osteoporotic MSCs, p values <0.15 are shown.

5.3.4 Osteoporotic hMSCs exhibit reduced cell growth when compared to healthy controls

Osteoporotic samples demonstrate reduced cell growth at day 7, 14, and 21 compared to the healthy cohort following initial seeding at the same density. The quantity of DNA is significantly affected by patient health according to a 2 way ANOVA of all 6 samples (Figure 5.4A), highlighting the importance of considering the outcomes of further measurements normalised for the cellular content, represented here by DNA. Furthermore, quantification of DNA in each group in growth medium reveals a significant growth in healthy MSCs between day 7 and 14 which does not continue out to day 21, however the number of osteoporotic MSCs is not significantly changed over the same time frame (Figure 5.4B). Overall, there is an inhibited capacity for growth in the healthy MSCs.

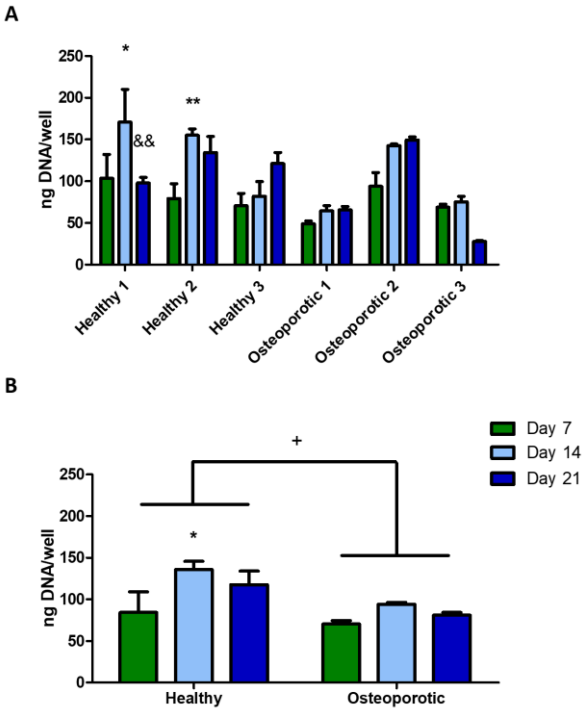

Figure 5.4: Quantification of proliferative activity, at 7 day intervals for 3 weeks, via picogreen assay for DNA content. A Individual patients DNA content, Mean±SEM, n=3-4, two-way ANOVA *p<0.05, **p<0.01 significant increase between day 7 and 14, &&p<0.01 significant increase between day 14 and 21. **B** Average DNA content in samples of healthy and osteoporotic patients, Mean±SEM, N=3, n=12, two-way ANOVA with Bonferroni post test, +p<0.05 significant effect of health on DNA content, p<0.05 significant difference between days (not shown), *p<0.05 significant increase at day 14 in healthy samples.

5.3.5 Osteoporotic MSCs deposit abnormal and reduced osteogenic matrix when compared to controls

Biochemically-induced osteogenic differentiation of osteoporotic MSCs is dysregulated resulting in abnormal matrix deposition when compared to healthy MSCs. Osteogenic differentiation media enhanced MSC proliferation in healthy samples (Healthy 1 $p<0.01$, Healthy 2 $p<0.05$), but did not affect any of the osteoporotic samples ($p>0.05$) (Figure 5.5A).

Biochemical stimulation of healthy and osteoporotic MSCs leads to significant ($p<0.001$) increase in collagen deposition in only 2 of the 6 donors examined, one healthy and one osteoporotic (Figure 5.5D). The quantity of collagen produced in different patients is varied, for example, healthy 1 produces the greatest quantities in growth medium but elicits very little difference in differentiation medium. Osteoporotic 1 produces the least collagen of all 6 samples in either growth or osteogenic differentiation medium. Pooling the collagen produced in healthy and osteoporotic samples shows little difference in deposition quantities, independent of media supplements used or the condition of donors. Interestingly, although quantities were not altered, the quality of the collagen matrix produced in all 3 osteoporotic samples undergoing differentiation is visually atypical (Figure 5.5C). The deposited collagen matrix does not cover the entire surface of the culture dish in osteoporotic MSCs cultured in osteogenic supplemented media. Quantification of the collagen area reveals matrix coverage can be as low as 19.30% in osteoporotic samples but remains at greater than 89% coverage in the healthy cohort and greater than 75% in all samples in growth medium, demonstrating this artefact is a feature of hMSC osteogenic differentiation but not hMSC growth (Supplementary Figure 5.2). Normalising the quantity of collagen to DNA per sample indicates the strongest production of collagen occurs in osteoporotic 2,

in fact osteogenic medium leads to a decrease in collagen per DNA in healthy 1 ($p<0.001$) and osteoporotic 3 ($p<0.05$) (Figure 5.5F) which may indicate a patient specific collagen production deficit.

The production of mineral in growth medium is minimal but similar between all samples, yet there is significant variability between the mineral produced following osteogenic induction (Figure 5.6C). Healthy 2 produces the most calcium of all 6 samples. Within healthy 2 there is some areas of the culture dish which are left unstained; the darker staining and denser cell packing at the periphery of these spots indicates they are the product of contraction as the matrix matures and deposits matrix in overlapping layers. Pooling the data reveals an increase in mineral deposition in the healthy cohort following osteogenic differentiation that is diminished in the osteoporotic donor population, but due to donor variability this is not significant. However, the quantity of calcium produced per cell in healthy hMSCs is significantly greater following 21 days in osteogenic medium ($p<0.01$), while osteoporotic MSCs do not respond to osteogenic supplements with enhanced mineral deposition (Figure 5.6F), further demonstrating a defect in hMSC osteogenesis in osteoporosis which may be an underlying factor leading to a reduction in bone mass and quality.

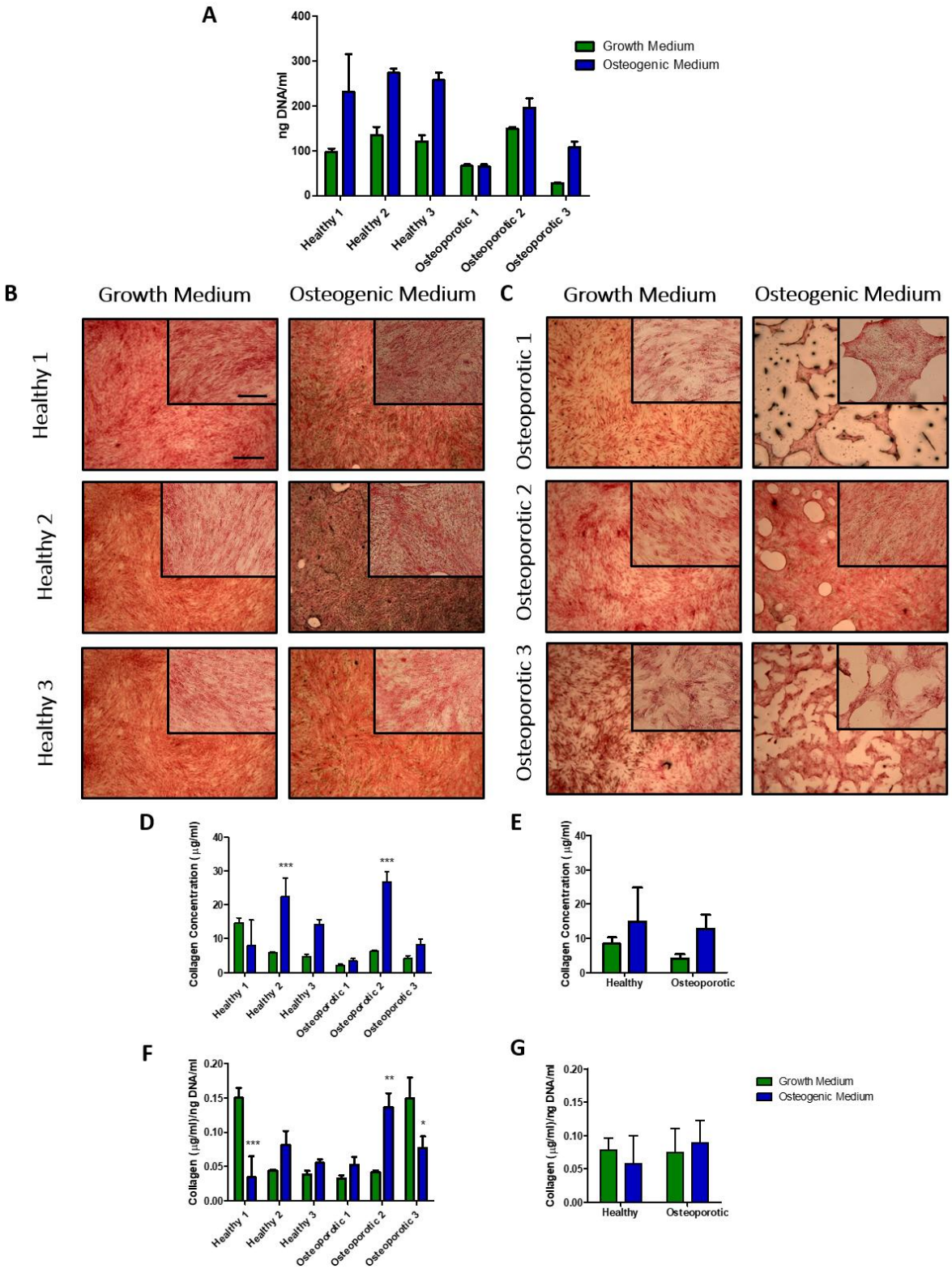

Figure 5.5: A Quantification of DNA content following 21 days in growth medium or osteogenic medium, Mean±SEM, n=4, two-way ANOVA with Bonferroni post test **B, C** Representative images of Picrosirius Red stained monolayers of **B** Healthy and **C** Osteoporotic samples following 21 days culture in growth or osteogenic differentiation medium, 2x scale bar=1000µm, inset at 10x scale bar=200µm, n=3. **D-G** Quantification of osteogenic matrix in each sample **D, E** concentration of collagen extracted from **D** individual samples and **E** samples pooled based on health (µg/ml), Mean±SEM, n=4, two-way ANOVA with Bonferroni post test, ***p<0.001, differentiation medium effects the samples differently

p<0.001 (interaction effect. **F, G** Collagen concentration normalized to DNA content (ng/ml) for **F** each sample and **G** pooled concentration of collagen in healthy and osteoporotic samples, N=3, two-way ANOVA with Bonferroni post test, ***p<0.001, **p<0.01,*p<0.05.

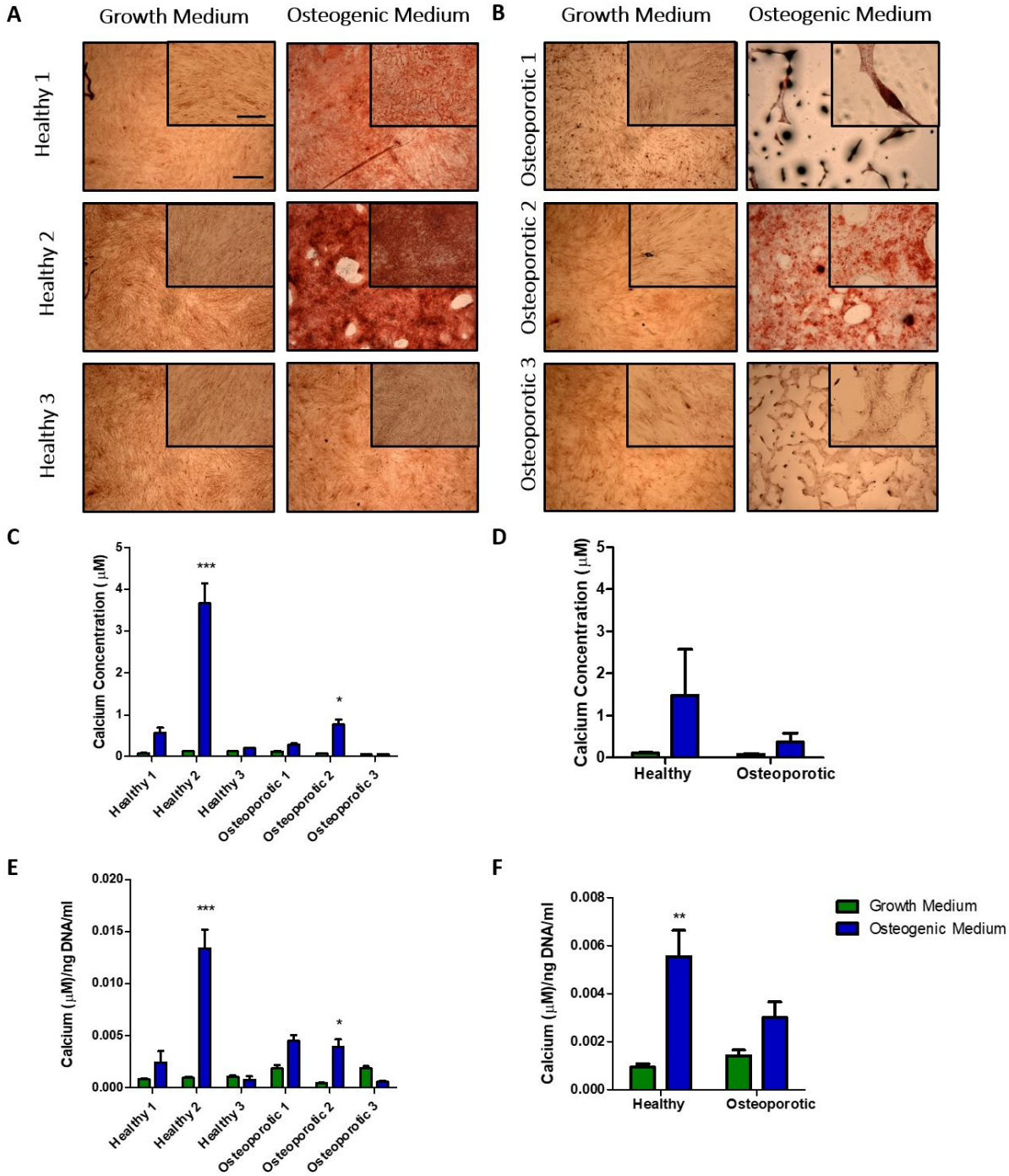

Figure 5.6: A, B Representative images of Alizarin Red stained monolayers of **A** Healthy and **B** Osteoporotic samples following 21 days culture in growth or osteogenic differentiation medium, 2x scale bar=1000μm, inset at 10x scale bar=200μm, n=3. **C-F** Quantification of osteogenic matrix in each sample **C, D** concentration of calcium extracted from C individual samples and **D** samples pooled based on health (μg/ml), Mean±SEM, two-way ANOVA with Bonferroni post test, ***p<0.001, differentiation medium effects the samples differently p<0.001 (interaction effect), n=4. **E, F** Calcium concentration normalized to DNA content (ng/ml) for **E** each sample and **F** pooled concentration of calcium in healthy and osteoporotic samples, N=3.

5.3.6 Defective hMSC osteogenic differentiation in osteoporosis does not lead to a shift to enhanced adipogenesis

Given the demonstrated defect in hMSC osteogenesis, we next investigated whether this decrease in osteogenic potential may result in a shift in adipogenesis, potentially contributing to the increase in adipose tissue in osteoporosis. We therefore quantified adipogenesis in each of the hMSCs samples isolated from healthy and osteoporotic donors. Interestingly, adipogenic differentiation medium has the opposite effect on cell growth to that seen with osteogenic supplements, where there is significantly less DNA in 2 healthy and 1 osteoporotic samples following treatment for 21 days (Figure 5.7A). Further examination of adipogenic differentiation as measured by Oil Red O staining demonstrated significant adipogenesis in all hMSC samples isolated from healthy donors. Interestingly, no osteoporotic donor underwent adipogenic differentiation, demonstrating an inhibited differentiation capability (Figure 5.7B-D). This finding is further emphasised after pooling data where there is a significant inhibition of adipogenesis in the osteoporotic cohort when compared to heathy controls (Figure 5.7E). This trend of reduced lipid formation in the osteoporotic cohort is also evident when comparing lipid formation per cell (Figure 5.7F-G). Notably, adipogenic differentiation of osteoporotic hMSCs did not result in the fragmented monolayer seen in osteogenesis. This therefore demonstrates that hMSC isolated from osteoporotic patients have a reduced differentiation potential that is not specific to lineage.

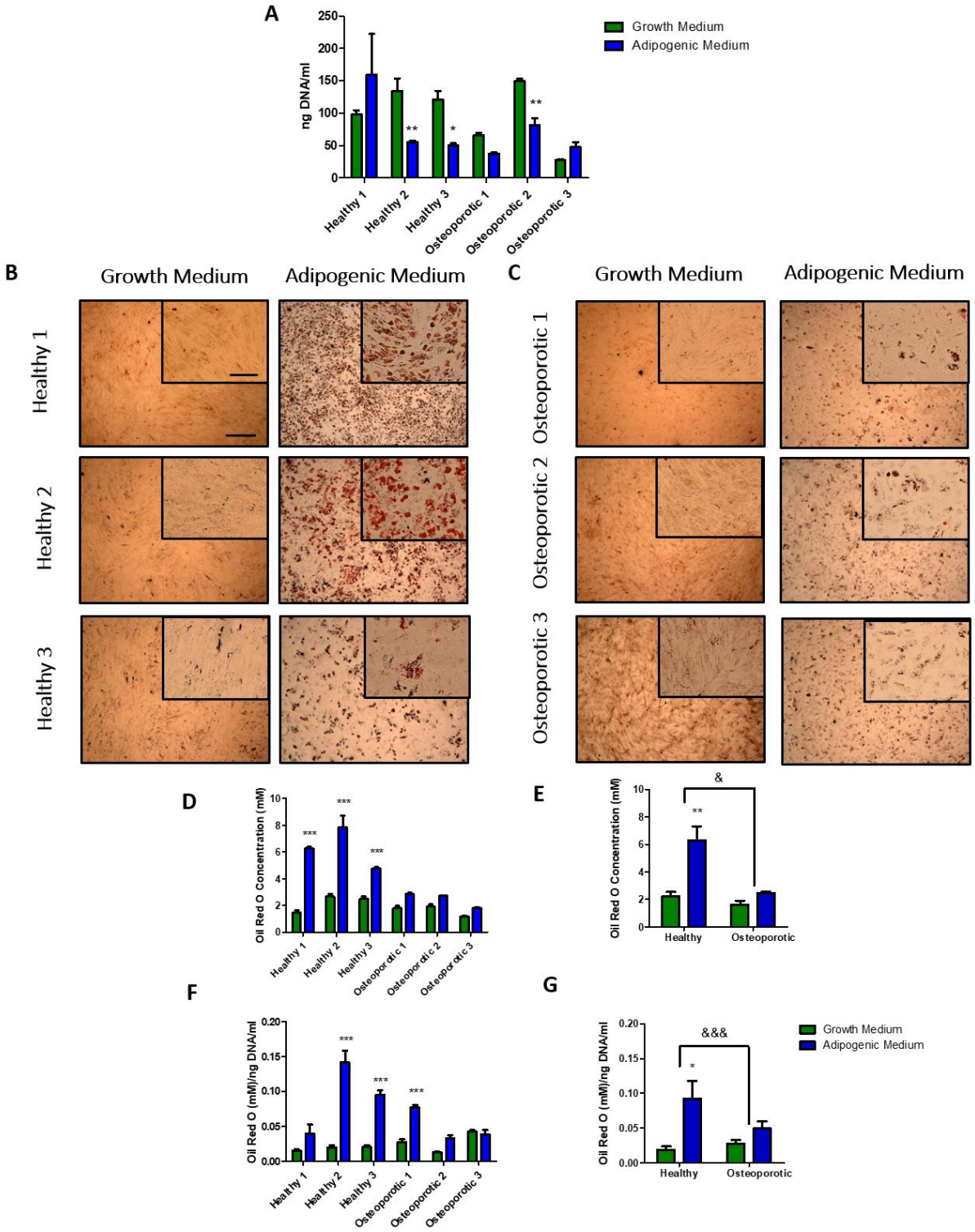

Figure 5.7: A Quantification of DNA content following 21 days in growth medium or adipogenic, Mean±SEM, n=4, two-way ANOVA with Bonferroni post test **B, C** Representative images of Oil Red O stained monolayers of **B** Healthy and **C** Osteoporotic samples following 21 days culture in growth or adipogenic differentiation medium, 2x scale bar=1000µm, inset at 10x scale bar=200µm, n=3. **D-G** Quantification of adipogenic matrix in each sample **D, E** concentration of lipid extracted from **D** individual samples and **E** samples pooled based on health (µg/ml), n=4. **F, G** Oil Red O concentration normalized to DNA content (ng/ml) for **F** each sample and **G** pooled concentration of collagen in healthy and osteoporotic samples, N=3, Mean±SEM, two-way ANOVA with Bonferroni post test, *p<0.05,

***p<0.001, differentiation medium effects the samples differently &p<0.05, &&&p<0.001 interaction effect.

5.4 Discussion

Bone formation requires the replenishment of the osteoblast from a progenitor or stem cell population, which must be recruited, expanded and differentiated to ensure continued anabolism. How this process occurs and whether this is altered in the osteoporotic environment is poorly understood. Furthermore, given that emerging treatments for osteoporosis are targeting this osteoprogenitor population, it is critical to determine the regenerative capacity of this cell type in the setting of osteoporosis. Herein, MSCs from a cohort of osteoporotic female patients were compared to MSCs isolated from healthy donors. Although considerable donor variability is present across samples, hMSCs isolated from healthy donors demonstrate good recruitment, mechanosensitivity, proliferation, and differentiation capacity as determined by both osteogenic and adipogenic differentiation. Contrastingly, hMSCs isolated from osteoporotic patients had significantly diminished regenerative potential. Osteoporotic hMSCs no longer respond to chemokine gradients directing recruitment. They have become desensitised to mechanical stimulation, have reduced proliferative potential and importantly demonstrate an attenuated differentiation capability with reduced mineral deposition and lipid formation following osteogenic and adipogenic induction respectively. Interestingly, during osteogenesis, despite minimal differences in the quantity of deposited collagen, the distribution of collagen was dramatically altered in the osteoporotic donors, suggesting a potential defect in matrix quality. This trend was also evident when considering mineral deposition. Taken together this study has demonstrated that hMSC isolated from osteoporotic patients demonstrate significantly

reduced regenerative potential, which must be considered during the development of new anabolic therapies targeting this cell population.

hMSCs isolated from healthy and osteoporotic donors demonstrate considerable variability that is not clearly dependent on age or surface marker expression. With the youngest donor being 22 years old, all donors have reached skeletal maturity (Barreto et al., 2017, Nahhas et al., 2013). Older donors were not available to donate healthy bone marrow; furthermore there is a healthy patient sample of post-menopausal age when osteoporosis is prevalent. While age is associated with reduced regenerative capacity (Ahmed et al., 2017), Healthy 1 is 59 years of age and displays the strongest chemotactic response, shows strong proliferation, is mechanoresponsive and can undergo osteogenic and adipogenic differentiation, on par with the younger donors. This would indicate that age is not a major contributor to the variability in our findings specifically within the healthy cohort. It must be noted that the osteoporotic donors are older with an average age of 85 and these additional years are likely to contribute to the loss in stem cell regenerative potential compared to the healthy group (Muschler et al., 2001). All the samples studied here were capable of producing lipid, collagen and calcified matrix under biochemical treatment and although differences between the healthy and osteoporotic samples have been identified these differences may also be reflective of the influence of aging. Interestingly the expression of CD105 was consistently lower than 95% in 5 of the 6 donors and CD90 is expressed below expected levels in 2 healthy and 1 osteoporotic donors. Recent studies of skeletal progenitor populations suggest low CD105 expression could be indicative of osteogenic potential (Anderson et al., 2013, Levi et al., 2011). This is consistent with our findings where Osteoporotic 3, being the only donor with CD105 expression above the recommended ISCT 95%, demonstrated the lowest mineral deposition following

osteogenic induction. Despite this slight reduction in CD105, surface marker expression alone or age were not reliable indicators of MSC regenerative potential in our donor cohort.

hMSCs isolated from osteoporotic donors have a reduced recruitment and proliferative capacity, which is indicative of reduced osteoprogenitor numbers at sites of fracture and bone remodelling in osteoporosis (Oryan et al., 2017). This reduced chemotactic response is consistent with previous studies demonstrating impaired MSC migration to BMP-2/-7 and SDF-1 in osteoporosis that are linked to a decreases in integrin (Haasters et al., 2014) and CXCR4 expression (Sanghani-Kerai et al., 2017) respectively. Our results suggest that this impaired migration may not be factor specific but rather a wider defect in chemotaxis which is in agreement with reduced homing of transplanted osteoporotic MSCs to a bone fracture site (Tewari et al., 2015). Moreover, regardless of MSC ability to reach the site of formation, the proliferative capacity of osteoporotic MSCs is also significantly inhibited which would further the complication of reduced osteoprogenitor numbers. Taken together this data indicates that a contributing factor to reduced bone formation, leading to remodelling imbalances, and bone loss in osteoporosis could be attributed to defective homing and proliferation of mesenchymal stem cells. This therefore highlights recruitment and proliferation as potential areas for therapeutic development.

Osteoporotic hMSCs have a diminished osteogenic signature and have become desensitised to mechanical stimulation. The basal level of COX2 expressed in osteoporotic MSCs is considerably lower than healthy MSCs. COX2-/- mice have defective bone repair and a MSC population that demonstrate inhibited osteoblastogenesis (Zhang et al., 2002). This important role for COX2 in MSC osteogenesis was further demonstrated in human MSCs, where COX-2 inhibitors

resulted in a blunting of osteogenesis. In addition to this diminished basal osteogenic signalling, the COX-2 expression cannot be rescued by a biophysical stimulus, with osteoporotic hMSCs demonstrating reduced mechanosensitivity. COX-2 is a known mechanosensitive gene which is consistently upregulated ~15-fold in response to fluid shear in the healthy donor cohort. While osteoporotic hMSCs can still respond to fluid shear with a significant increase in COX-2, this upregulation is considerably dampened. This reduced mechanosensitivity is clearly demonstrated when considering RUNX2 and OPN expression where the response to fluid shear is significantly reduced. This reduction in mechanically-induced osteogenesis may be another contributor to reduced bone formation in osteoporosis and highlights another potential avenue for therapeutic development.

hMSCs isolated from osteoporotic donors have an inhibited differentiation potential with reduced and abnormal matrix deposition that is lineage dependent. Despite significant variability in collagen deposition across all donors, there was no significant difference in the quantity of collagen deposited both in standard growth medium and following osteogenic induction. Interestingly, the quality of collagen deposition following osteogenic induction, in terms of area covered, is dramatically altered in the osteoporotic patient cohort. Slight contraction of deposited collagen, as seen in healthy 2, has been demonstrated in the literature, however the collagen deposited by osteoporotic donors only covered a fraction of the culture area. Given that collagen acts as a template for mineral deposition, it is not surprising that this defect in collagen spatial deposition continues to mineral deposition, with similarly abnormal mineral spatial organisation and quantity (Katsimbri, 2017). The reduction in calcium deposition have been demonstrated in osteoporotic MSCs previously (Prall et al., 2013, Rodríguez et al., 1999), but our data demonstrates that mineral organisation is also

significantly altered, potentially as a result of abnormal collagen organisation. Osteogenically differentiated cells form clusters around deposits of mineral (Shima et al., 2015). The lack of matrix coverage in osteoporotic samples may be due to weaker adhesion as multi-layered aggregates of cells are still visible within nodules of mineral. Studies of surface treatments for the functionalisation of biomaterials supports this hypothesis where the strength of the adhesion mechanisms effect the matrix formation (Phillips et al., 2010). Moreover, the same work found that the lineage that MSCs differentiate down effects the monolayer formation. This hypothesis is also consistent with altered integrin expression identified in osteoporotic hMSCs (Haasters et al., 2014). Interestingly, the osteoporotic cohort also demonstrated reduced adipogenesis but no defect in spatial organisation of lipids. This indicates a loss of differentiation capacity of MSCs regardless of lineage. While it is widely appreciated that adipocyte numbers increase in the marrow with aging, MSC adipogenesis is believed to become dysregulated in osteoporosis (Pino et al., 2012b, Astudillo et al., 2008). In summary, osteoporotic hMSCs demonstrate reduced multilineage potential and abnormal osteogenic matrix deposition. This therefore indicates a further defect in hMSC behaviour during osteoporosis which may contribute to the aetiology of osteoporosis.

5.0 Conclusion

Bone formation requires the recruitment, proliferation and differentiation of osteoprogenitors. How this process occurs and whether this is altered in the osteoporotic environment is poorly understood. Herein, we demonstrate that human MSCs from a cohort of osteoporotic female patients demonstrate defective recruitment, mechanosensitivity, proliferation, and differentiation capacity as determined by both

osteogenic and adipogenic differentiation when compare to MSCs isolated from healthy donors. This study has therefore demonstrated that osteoporotic hMSCs demonstrate significantly reduced regenerative potential, which must be considered during the development of new anabolic therapies targeting this cell population.

Chapter 6:

Targeting primary cilia and associated mechanosensitive channels as a therapeutic strategy to enhance human MSC osteogenesis in osteoporosis.

6.1 Introduction

Osteoporosis occurs when bone density and quality decreases to the extent that the skeleton becomes prone to fracture at low impact. The devastating impact of osteoporosis is ever increasing with our aging population, with hip fracture incidence predicted to increase by 310% in men and 240% in women between 1990 and 2050 (Gullberg et al., 1997). Although fracture risk is reduced following bisphosphonate treatment, the side effects which include atypical fractures deter long term use (Kling et al., 2014). Furthermore, this reduction in fracture risk is limited at sites prone to impact such as the hip (Cosman et al., 2014). Bisphosphonates act through an inhibition of osteoclast activity, where osteoclasts are the cells responsible for resorbing damaged or surplus bone during the remodeling cycle. An alternative approach which is garnering much interest is to target osteoblasts or their precursors to promote bone formation rather than inhibit resorption (Khosla and Hofbauer, 2017, Uihlein and Leder, 2012).

Bone tissue is exquisitely mechanosensitive, responding to mechanical loads encountered during exercise and daily activities by increasing the formation rate of

mineralized matrix. This bone mechanoadaptation is most obvious comparing the arms of a tennis player where the humerus of the serving arm is significantly larger compared to the contralateral limb (Haapasalo et al., 2000). This loading-induced increase in bone formation is believed to require the differentiation of mesenchymal stem cells (MSCs) towards the osteoblastic lineage. During exercise, the marrow is displaced in an oscillating motion resulting in shear stress on resident cells (Li et al., 2004, Metzger et al., 2015b, Gurkan and Akkus, 2008). The application of shear stresses to MSCs at magnitudes predicted to occur in the marrow elicits an increase in osteogenic differentiation (Stavenschi et al., 2017). Moreover, in osteoporosis MSC behaviour is dysregulated, with stem cells demonstrating reduced mechanosensitivity and differentiation capacity (Chapter 5)(Rodríguez et al., 2004). Therefore, novel pharmacological options to enhance MSC differentiation towards osteoblastogenesis could improve bone mass.

The mechanisms by which MSCs sense mechanical stimuli and the pathways transducing such activity into a bone forming response could be targeted to increase MSC osteogenesis and bone density in osteoporosis. Of particular interest are the sites on the cell membrane exposed to fluid shear. In bone, among other tissues, a rapid response to fluid flow is mediated by calcium signaling and mechanosensitive ion channels such as TRPV4 (Lee et al., 2015c). Previously, we delineated the role of the calcium channel TRPV4 in fluid shear-induced osteogenic differentiation of MSCs (Corrigan et al., 2018). Moreover, TRPV4 expressed along the primary cilium was found to be important in mediating the osteogenic response. The primary cilium is a microtubule based antennae-like extension of the cell membrane (Satir et al., 2010). The primary cilium has an important role in transducing fluid shear stimuli in MSCs leading to an osteogenic response (Hoey et al., 2012d). Furthermore, defects in primary

cilium formation or function result in a range of skeletal pathologies indicating a role for the cilium and associated signaling in bone formation (Zhang et al., 2018). Supporting and enhancing ciliogenesis has been found to increase MSC mechanosensitivity and we have previously optimized a pharmacological treatment to enhance cilium incidence and length in MSCs (Corrigan et al. 2018). By therapeutically targeting TRPV4 and the primary cilium it is envisaged that fluid shear-induced MSC osteogenesis could be mimicked therapeutically.

The overall objective of this study was to enhance MSC osteogenesis and matrix deposition in the setting of osteoporosis, through the potential targeting of the primary cilium and associated mechanosensitive calcium channel TRPV4. Initially, given the previously demonstrated defect in mechanosensitivity in osteoporotic MSC, TRPV4 expression and the primary cilium structure was investigated in both healthy and osteoporotic MSCs. TRPV4 activity was enhanced using the biochemical agonist, GSK101, and ciliogenesis was increased using fenoldopam treatment. Healthy and osteoporotic MSCs were treated with fenoldopam, GSK101 or a combination of both and MSC osteogenesis and matrix deposition was investigated at early and late time points respectively, to determine whether targeting the cilium and associated mechanosensitive channels is a viable therapeutic strategy to enhance human MSC mediated bone formation in the setting of osteoporosis.

6.2 Methods

6.2.1 Bone marrow mesenchymal stem cell isolation and culture

Human mesenchymal stem cells were isolated from the whole bone marrow of healthy and osteoporotic patients and validated according to ISCT guidelines as outlined in

chapter 5. Each of the 6 MSC samples, 3 osteoporotic and 3 healthy were cultured in DMEM, 10% FBS, 1% P/S at 37°C and grown to passage 3 before experimentation. MSCs were not used beyond passage 7. For long term studies MSCs were supplemented with 10mM β-glycerophosphate (Sigma) and 0.05mM ascorbic acid (Sigma) as well as dexamethasone (Sigma) at 10nM (minimal supplements) to provide the components necessary for osteogenic matrix formation.

6.2.2 Biochemical treatments to promote TRPV4 activity and primary ciliogenesis

TRPV4 was activated via the specific agonist GSK1016790A (Abcam). MSCs were treated with GSK101 at 10nM for 2 hours before gene expression and immunocytochemistry analysis. Primary cilium incidence and length was targeted using fenoldopam mesylate (Sigma). MSCs were treated with fenoldopam at 50µM for 24 hours before gene expression and immunocytochemistry analysis. The suitability of these agents for targeting TRPV4 and ciliogenesis was validated previously in murine MSCs, where the concentration and application times were optimized (Corrigan et al., 2018). Vehicle controls consisted of 0.2% DMSO for each set up. For long term cell culture DMSO, GSK101, and fenoldopam were applied at the same concentrations and maintained throughout the culture period via supplementation of the medium which was changed every 3 days.

6.2.3 Immunocytochemistry

hMSCs were seeded on fibronectin coated glass coverslips for 24 hours before serum starvation in DMEM low glucose, 0.5% FBS, 1% P/S for 48 hours. After fixation in neutral buffered formalin for 10 minutes (Sigma), coverslips were permeabilised in

0.1% Triton X-100 for a further 10 minutes and non-specific binding sites were blocked using 1% w/v BSA (Sigma) in PBS for 2 hours at room temperature. The primary antibody targeting TRPV4 (TRPV4, ab74738, Abcam) or the primary cilium (acetylated α tubulin, ab24610, Abcam) was applied overnight at 4°C, diluted 1:1000 and 1:1500 respectively in blocking solution. For characterizing ciliogenesis this was followed by the application of the primary antibody targeting pericentrin (ab448, Abcam) for 1 hour at room temperature at a dilution of 1:1000. Alexa 488 secondary antibody was applied to all coverslips for 1 hour at room temperature at 1:500. For primary cilium staining Alexa 594 secondary antibody was applied in tandem under the same conditions. Finally, phalloidin (rhodamine phalloidin, VWR) was applied to the TRPV4 stained samples for 20 minutes at a dilution of 1:500. DAPI (Sigma) was applied for 5 minutes in PBS prior to sample mounting on glass slides using Prolong gold mounting medium (Invitrogen). Imaging was performed on an Olympus IX83 (Olympus) epifluorescent microscope at 100x (N.A. 1.40 Oil). For imaging the primary cilium z-stacks were acquired, taking the first slice when the acetylated α tubulin stain came into focus and the last when it was no longer in focus at any point along the axoneme. The distance between slices was maintained at 0.25µm.

6.2.4 Measurement of primary cilium incidence and length

Primary cilium incidence was defined as positive staining for acetylated α tubulin on a cord protruding from two centrosomes stained by pericentrin. The length of the cilium was calculated by constructing a right-angled triangle to capture the length that may lie within multiple planes between the coverslip and slide as outlined in Rowson *et al.* (Rowson et al., 2016). Briefly, the number of slices in the z direction and the thickness of each slice were taken as one side, the length of the cilium in a maximum projection

of all slices was taken as another side, and the length of the cilium was calculated as the hypotenuse of the triangle formed by these two sides.

6.2.5 Measurement of TRPV4 intensity

TRPV4 intensity was measured by creating a mask for the cytoskeleton using the phalloidin stained area in the red channel, limiting both the intensity and size of this region of interest (Image J). Mean fluorescence intensity was corrected for background, the mean intensity in an identical area outside the phalloidin stained area.

6.2.6 Gene expression

TRI reagent (Sigma) was used to extract RNA per the manufacturer's protocol. The concentration of RNA in each sample was measured using a Nanodrop spectrophotometer and sample purity was checked via 260/280 and 260/230 absorbance ratios. A minimum of 200ng of RNA was reverse transcribed to cDNA using the High-Capacity cDNA Reverse Transcription Kit (Applied Biosystems). The efficiency of the reverse transcription was monitored by quantifying cDNA using a Qubit single stranded DNA assay (Invitrogen). Quantitative polymerase chain reactions (qPCR) were prepared for all samples using SYBR Select Master Mix with ROX passive dye (Applied Biosystems, 4472903) and custom designed primers (Sigma) for *18S, COX2, OPN, RUNX2, TRPV4* and *IFT88* for amplification using the ABI 7500 real time PCR machine (Applied Biosystems) as outlined in Supplementary Table 6.1. The relative quantity of each sample was calculated with reference to *18S* and expressed as fold change normalised to the healthy control.

6.2.7 Mechanical Stimulation

Parallel plate flow chambers, designed in house as described previously, were used for short term fluid shear application (Stavenschi et al., 2017). Briefly, MSCs were seeded on fibronectin (10µg/ml) coated glass slides, assembled between two plates and attached to a programmable syringe pump (New Era Pump Systems). Oscillating fluid flow (OFF) was applied through a 10ml syringe (Becton Dickinson) at 104ml/min, subjecting cells to a shear stress of 2Pa, at a frequency of 2Hz. This stimulus was applied for 2 hours. The no flow controls were similarly assembled within the chambers but were not subjected to fluid shear. For long term studies an orbital shaker (Roth) was used to apply a spatiotemporal fluid shear of minimum 0.3Pa, exceeding 1Pa at the edge of the well, across the wells of a 6 well plate containing 1.8ml of medium as previously demonstrated in (Salek et al., 2012). Shear stress was applied for 2 hours/day, 5 days/week for 21 days.

6.2.8 Staining and quantification of osteogenic matrix deposition

To investigate osteogenic matrix formation, cells were fixed in formalin following 21 days in culture. Collagen deposition was stained using 1% picrosirius red (Sigma) under gentle agitation at room temperature, after 1 hour all wells were rinsed twice in 0.5% acetic acid and distilled H_2O. Calcium staining was performed using alizarin red S at 1% for 20 minutes at room temperature and rinsed in distilled H_2O until the background was clear of stain. Images were acquired using 2x (NA 0.06) and 10x (NA 0.25) objectives. Collagen deposition was quantified by scraping picrosirius stain from each well in PBS and centrifuging at 14000g for 10 minutes. The pellet collected was dissolved in 0.5M NaOH and absorbance measured at 550nm. Calcium stain was extracted via incubation in 10% acetic acid for 30 minutes under gentle agitation

followed by heating at 85°C for 10 minutes. Cell debris was collected by centrifugation at 20,000g for 15 minutes and the pH adjusted to pH4.1-4.5 before measuring absorbance at 405nm.

6.2.9 DNA Quantification

The DNA content was measured at the end of the 21 day study using a QuantIT Picogreen assay (Thermofisher) for dsDNA. Monolayers were rinsed in PBS and lysed in 0.2% v/v Triton X100, 10mM Tris pH8, 1mM EDTA for 20 minutes on ice. The monolayer was scraped for collection in microtubes before vortexing for 30 seconds and sonicating for 1 minute. The vortex and sonicate cycle was repeated 5 times at 10 minute intervals and samples were passed through a 21G needle 10 times before flash freezing samples in liquid nitrogen and storing at -80°C. Fluorescent reaction to picogreen reagent excited at 480nm and read at 520nm. The DNA quantity was read from a standard curve of 0-200ng/ml.

6.2.10 Data Analysis

Box plots used for cilium length and TRPV4 intensity illustrate the 25th and 75th percentile values, whiskers represent 5th and 95th percentile values and the line is at the median, black dots represent points outside of the 5th and 95th percentile. A two-way ANOVA was used to test the effect of treatment on cilium formation and TRPV4 intensity, a one-way ANOVA was used to test the effect on cilium length. All other plots represent the mean and standard error of the mean. The effects of health or treatment on behaviour were tested using a two-way ANOVA with Bonferroni post-test to compare the performance of control to each treatment.

6.3 Results

6.3.1 Osteoporotic hMSCs demonstrate similar TRPV4 expression but inhibited TRPV4 mechanoregulation when compared to healthy controls

The expression of TRPV4 at the gene and protein level is similar in healthy and osteoporotic MSCs. Basal gene expression shows little variation across all hMSCs isolated from healthy and osteoporotic donors (Figure 6.1A). Furthermore, immunocytochemical staining of TRPV4 shows the channel expressed throughout the cell membrane of both healthy and osteoporotic MSCs (Figure 6.1B). The average intensities calculated were similar for all samples except healthy 1, which was significantly higher than all other samples ($p<0.001$) (Figure 6.1C). However, a change in TRPV4 intensity in healthy MSCs is not reflected in the average intensity calculated across pooled healthy and osteoporotic samples (Figure 6.1 D). Exposing MSCs to oscillatory fluid shear stress results in a markedly different response in osteoporotic MSCs compared to healthy controls. While there is an increasing trend in *TRPV4* expression in healthy 2 and no significant change in healthy 1 or healthy 3, the osteoporotic samples all respond with an average fold change less than 1 (Figure 6.1E). In fact, donor health plays a significant role in response to flow ($p<0.05$). Analyzing the average response of the healthy and osteoporotic cohorts confirms that there is an increase in *TRPV4* with fluid shear ($p<0.05$) in healthy MSCs but the response in the osteoporotic cohort is significantly reduced ($p<0.01$) (Figure 6.1F). This is consistent with a reduced mechanosensitivity in the setting of osteoporosis.

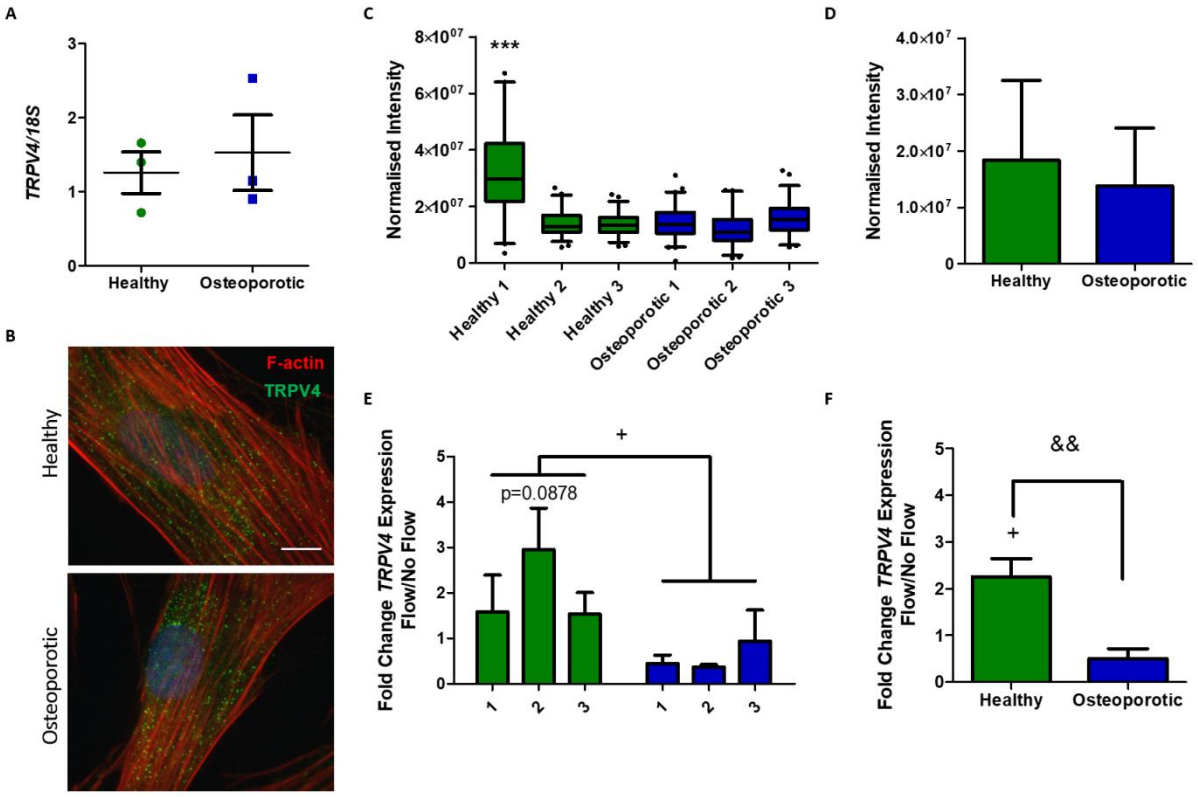

Figure 6.1: Expression of TRPV4 in healthy and osteoporotic MSCs. A TRPV4 relative to 18S, Mean± SEM, n=3-7, student's t-test. B Representative images of TRPV4 expression on healthy and osteoporotic hMSCs at 100x fluorescence (red channel- F-actin, green channel- TRPV4 and DAPI) (scale bar 10µm). C Quantification of cell wide TRPV4 intensity in individual hMSC samples, 25-75th percentile shown in box, whiskers mark 5-95 percentile, outliers marked in black points, one way anova shows healthy 1 is significantly more intense than all other samples, ***p<0.001. D Pooled TRPV4 intensity for healthy and osteoporotic samples, Mean ±SEM, n=3, student's t-test, not significant. E, F Fold change TRPV4 expression in response to 2Pa, 2Hz fluid shear applied for 2 hours. E Response of individual patients, Mean ±SEM, n=3-6, two-way ANOVA, +p<0.05 effect of osteoporosis. F Comparison of healthy and osteoporotic samples pooled, Mean±SEM, n=3, two-way ANOVA with Bonferroni post test, comparing effect of flow and effect of MSC health, &&p<0.01 effect of flow is different in healthy and osteoporotic, +p<0.05 effect of flow in healthy compared to no flow healthy.

6.3.2 Osteoporotic hMSCs have reduced cilium incidence and cilium length when compared to healthy controls

Primary cilium formation is impaired in osteoporotic MSCs in both incidence and length despite little variation in the expression of *IFT88*. The quantity of *IFT88* expressed in MSCs is variable in healthy samples but the average quantity does not differ from osteoporotic samples (Figure 6.2A). Despite this, there are fewer cilia found on osteoporotic MSCs compared to healthy counterparts (p<0.05), with this effect being consistent through individual samples and analyzing the average across the cohort

(Figure 6.2C, D). Moreover, the length of the primary cilium is consistently shorter in osteoporotic MSCs (Figure 6.2E). The average length found in healthy MSCs is 2.61±0.05 µm while osteoporotic MSCs display an average cilium length of 1.87±0.05µm which is a significant reduction ($p<0.001$) (Figure 6.2F). In response to fluid shear there is little change in *IFT88* expression. Fluid shear results in a significant decrease in *IFT88* in osteoporotic 2 ($p<0.05$) but on average flow has no effect on *IFT88* expression and this holds true in osteoporotic MSCs (Figure 6.2G, H).

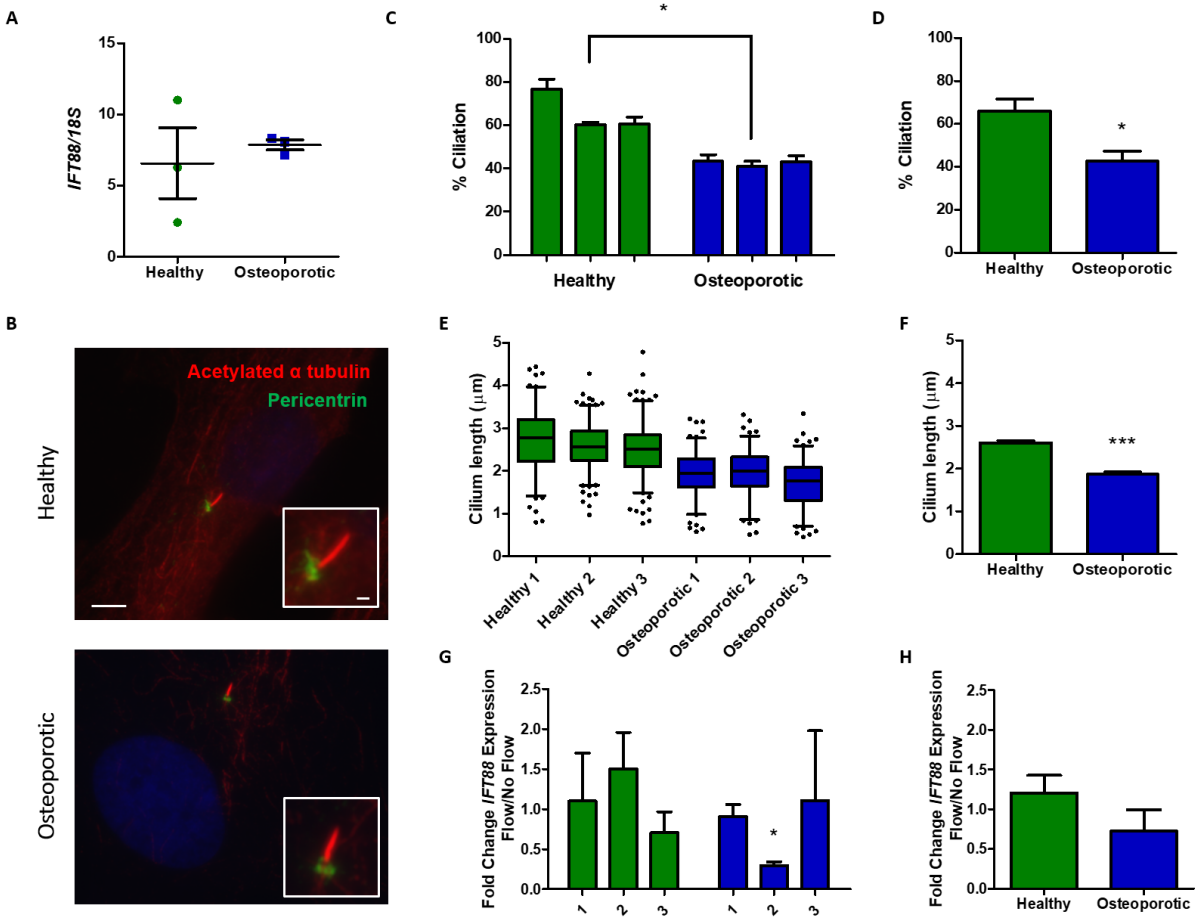

Figure 6.2: Expression of IFT88 in healthy and osteoporotic MSCs. **A** IFT88 relative to 18S, Mean± SEM, n=3-7, student's t-test. **B** Representative images of the primary cilium on healthy and osteoporotic hMSCs at 100x fluorescence (red channel- acetylated alpha tubulin, green channel- pericentrin and DAPI) (scale bar 10µm), inset shows zoom on cilium (scale bar 1µm). **C** % ciliation in individual samples shown as Mean ±SEM, n=3, two-way ANOVA, $p<0.05$ the variation in cilium incidence is significantly different in osteoporosis. **D** Pooled % ciliation for healthy and osteoporotic patients, Mean ±SEM, n=3, student's t-test, $p<0.05$. **E** Cilium length 25-75th percentile shown in box, whiskers mark 5-95th percentile, outliers marked in black points, one way anova shows each healthy sample is significantly different to each osteoporotic sample $p<0.001$, healthy 1 and healthy 3 are significantly different $p<0.05$, osteoporotic 3 is significantly shorter than osteoporotic 1 and 2 $p<0.05$. **F** Pooled cilium length, Mean ±SEM, n=3, student's t-test, $p<0.001$. **G, H** Fold change IFT88 expression in response to

2Pa, 2Hz fluid shear applied for 2 hours. **G** Response of individual patients, Mean ±SEM, n=3-6, two-way ANOVA, not significant, t-test to compare No flow to Flow for each individual sample, *p<0.05. **H** Comparison of healthy and osteoporotic samples pooled, Mean±SEM, n=3, students t-test, not significant.

6.3.3 The effect of TRPV4 agonist (GSK101) and ciliotherapy (fenoldopam) treatment on TRPV4 expression and primary cilia structure in healthy and osteoporotic hMSCs

Based on demonstrated defects in proliferation, migration, and differentiation (Chapter 5), and defects in cilium structure (Figure 6.2), in hMSCs isolated from osteoporotic donors, Osteoporotic Sample 3 was brought forward as a model of osteoporosis and Healthy Sample 2 was brought forward as a control in all future experiments.

Biochemical treatment with GSK101, fenoldopam or a combination of both either resulted in no change or a slight reduction in TRPV4 expression. TRPV4 expression at the mRNA level is not significantly altered by any treatment (Figure 6.3A). However, at the protein level, although TRPV4 expression is not significantly altered in healthy hMSCs with any treatment compared to vehicle controls, it is significantly reduced in the osteoporotic hMSCs following fenoldopam treatment or the combined fenoldopam and GSK101 ($p<0.01$) (Figure 6.3B, C).

Primary cilia on osteoporotic MSCs can be significantly elongated by treatment with fenoldopam or a combination of fenoldopam and GSK101, but in healthy MSCs primary cilia are only affected by GSK101. The expression of *IFT88* at the mRNA level is unchanged by any of the conditions investigated (Figure 6.4A). Interestingly cilium incidence in the osteoporotic donor is greater than the healthy donor across all treatments including vehicle control ($p<0.001$) (Figure 6.4C), despite a previous analysis demonstrating defective ciliary structure in the osteoporotic sample (Figure 6.2). This therefore indicates that DMSO is having a considerable effect on cilia

structure with the osteoporotic sample being more perturbed. Independent of DMSO, fenoldopam treatment resulted in an increasing but insignificant trend in cilium incidence in both healthy and osteoporotic MSCs. The average length of primary cilia in both healthy and osteoporotic MSCs can be increased by biochemical treatment. Although fenoldopam marginally increases median length in the healthy MSCs (+0.22µm), it is surprising that in this donor GSK101 was the only treatment that had a significant effect ($p<0.05$) increasing median cilia length from 1.98 to 2.15µm. The length of cilia is increased in the osteoporotic donor by fenoldopam ($p<0.01$) and the combined treatments ($p<0.05$) significantly increasing median length from 2.17 to 2.56µm (Figure 6.4D).

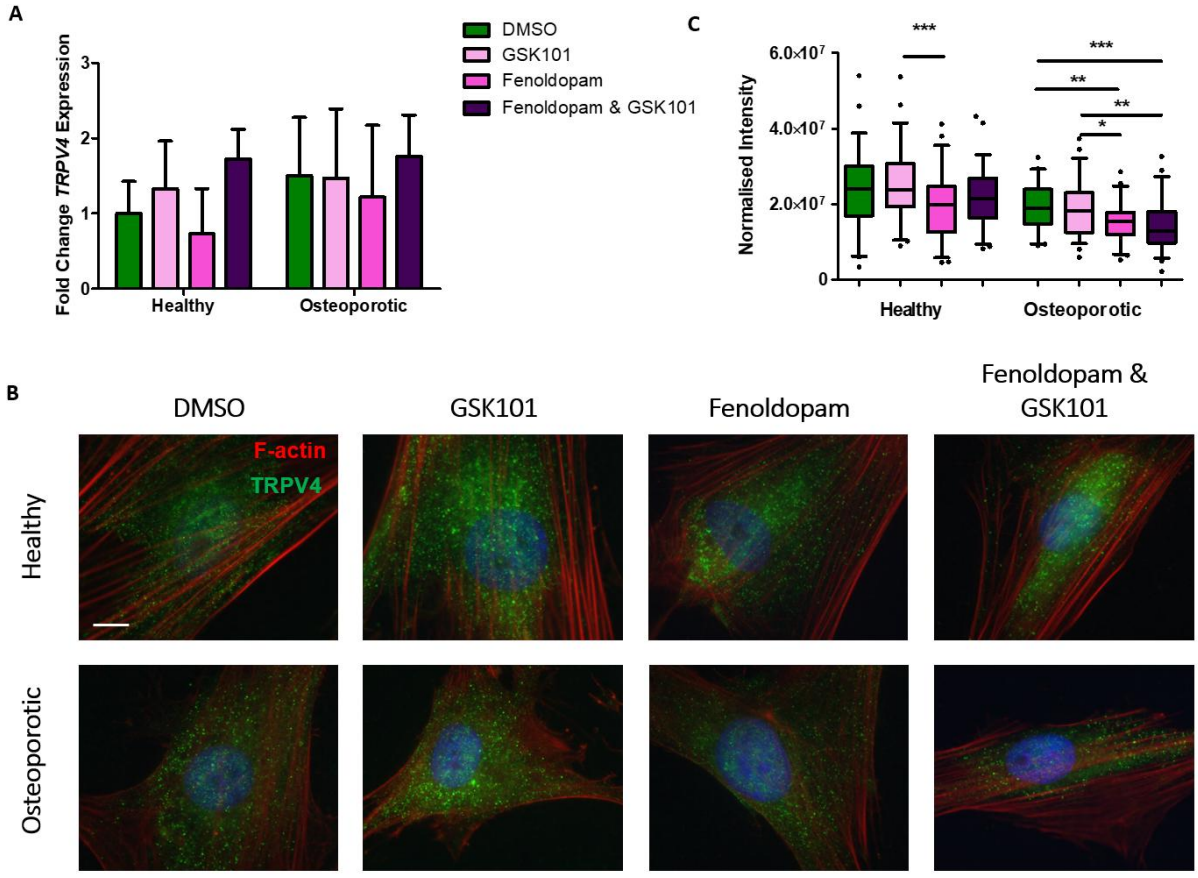

Figure 6.3: Characterisation of short term treatment of healthy and osteoporotic hMSCs with vehicle (DMSO), GSK101, Fenoldopam or Fenoldopam and GSK101 on TRPV4. **A** Fold change TRPV4 expression relative to vehicle control, Mean ±SEM, n=3-8, two-way ANOVA, not significant. **B** Representative images of TRPV4 on healthy and osteoporotic hMSCs at 100x fluorescence (red channel- F-actin, green channel- TRPV4 and DAPI) (scale bar 10µm). **C** Quantification of cell wide TRPV4

intensity in treated healthy and osteoporotic hMSCs, 25-75th percentile shown in box, whiskers mark 5-95th percentile, outliers marked in black points, n=52-59, one-way ANOVA $p<0.001$ healthy hMSCs treated with GSK101 express significantly more TRPV4 than Fenoldopam treated samples. Osteoporotic hMSCs treated with GSK101 express more TRPV4 $p<0.05$, relative to fenoldopam, those treated with fenoldopam express less TRPV4 compared to vehicle controls, $p<0.01$. Treatment with Fenoldopam & GSK101 decreases TRPV4 relative to DMSO, $p<0.001$ and relative to GSK101, $p<0.01$.

6.3.4 The effect of GSK101 and fenoldopam treatment on early osteogenesis in healthy and osteoporotic hMSCs

To determine whether cilia-targeted mechanotherapeutics could enhance early osteogenesis in human MSCs, we next treated healthy and osteoporotic hMSCs with GSK101, Fenoldopam or a combination of both and investigated their effect on early osteogenic gene expression. Treatment with fenoldopam for 24 hours to elongate primary cilia, followed by GSK101 for 2 hours to activate TRPV4, results in an upward trend in the expression of early osteogenic markers, with some positive but variable effects with GSK101 or fenoldopam alone. *COX2* expression gives the most convincing evidence for the use of these therapies, with increases in expression following GSK101 and fenoldopam in both healthy and osteoporotic samples. This increase was augmented following dual treatment, reaching significance in the osteoporotic hMSCs (4.73±1.29-fold increase, $p<0.05$) (Figure 6.5A). The combined treatments result in the most effective changes in *OPN* expression also, although this is not significant. The changes in *OPN* are variable but fenoldopam and the combination treatment increase expression by 2.61±0.84 and 3.37±1.53 fold respectively in healthy MSCs. Although basal *OPN* expression is somewhat higher in osteoporotic MSCs, the combined treatment demonstrates the most favorable response (Figure 6.5B). Surprisingly, the osteoporotic MSCs have significantly less basal *RUNX2* expression compared to the healthy MSCs ($p<0.001$). There are minor but insignificant increases in *RUNX2* in healthy MSCs following the combined treatments (1.43±0.72-fold) (Figure 6.5C). Taken together, this

data suggests these therapies hold promise for enhancing hMSC osteogenesis, with simultaneous targeting of the cilium structure and localized calcium channels being the optimal strategy.

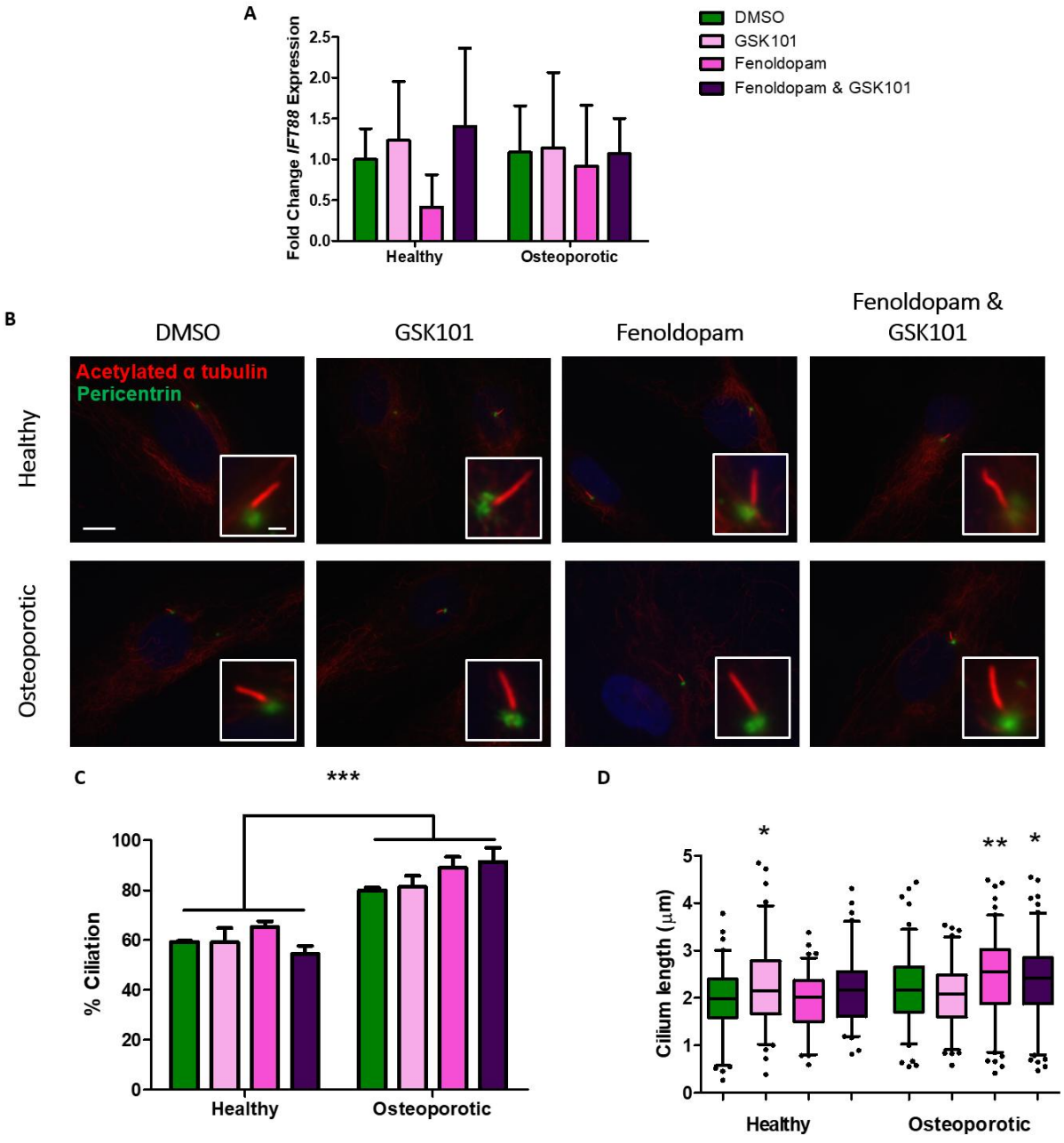

Figure 6.4: Characterisation of short term treatment of healthy and osteoporotic hMSCs with vehicle (DMSO), GSK101, Fenoldopam or Fenoldopam and GSK101 on primary cilia. A Fold change IFT88 expression relative to vehicle control, Mean ±SEM, n=3-8, two-way ANOVA, not significant. B Representative images of the primary cilium on healthy and osteoporotic hMSCs at 100x fluorescence (red channel- acetylated alpha tubulin, green channel- pericentrin and DAPI) (scale bar 10μm), inset shows zoom on cilium (scale bar 1μm). C % Ciliation Mean ±SEM, n=3, two-way ANOVA, ***p<0.01 effect of health. D Cilium length 25-75th percentile shown in box, whiskers mark 5-95 percentile, outliers

marked in black points, n=81-124, one way anova shows GSK101 induces a significant increase in length in healthy ($p<0.05$) and in osteoporotic ($p<0.01$) hMSCs compared to Fenoldopam treatment , Fenoldopam & GSK101 treatment induces a significant increase in osteoporotic hMSCs, $p<0.05$.

6.3.5 The effect of GSK101 and fenoldopam treatment on proliferation in healthy and osteoporotic hMSCs

The combination treatment elicits a significant increase in proliferation in both healthy and osteoporotic MSCs. The proliferation of healthy MSCs is not affected by treatment with GSK101 or fenoldopam separately but a combined treatment regime elicits significant increases in proliferation after 21 days ($p<0.001$). In addition to the application of cilia-targeted therapies, mechanical stimulation was also applied to determine whether treatments would increase cellular mechanosensitivity. Following mechanical stimulation there is no change in proliferation in the healthy hMSCs and the therapies have the same effect under mechanical stimulation (Figure 6.6A). As was previously demonstrated, osteoporotic hMSC have a reduced proliferative capacity when compared to healthy controls (Figure 6.6A, B). In the osteoporotic hMSC cohort, GSK101 has no effect but there is a trend of inhibition of proliferation following fenoldopam treatment. Following fenoldopam treatment DNA content is decreased from 25.58±4.36ng/well to 14.92±3.27ng/well under static conditions and significantly from 37.33±22.87ng/well to 11.33±0.52ng/well under fluid flow. The combined treatments support proliferation in osteoporotic MSCs as in healthy, increasing DNA to 71.74±9.43 in static conditions ($p<0.001$) and showing a similar but more variable trend under fluid flow where DNA reaches 58.90±17.8ng/well (Figure 6.6B). Interestingly, the combined treatment in the setting of osteoporosis (71.74±9.43ng/well) brings the level of proliferation close to that seen in healthy controls (104.89±24.99ng/well). Mechanical stimulation has no effect on proliferation in the osteoporotic MSCs nor does it increase any therapy induced affect.

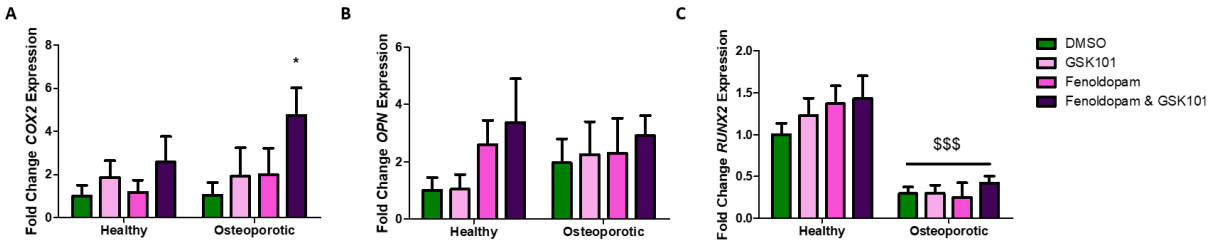

Figure 6.5: Gene expression following short term treatment with vehicle (DMSO), GSK101, Fenoldopam or Fenoldopam and GSK101 in a healthy and osteoporotic hMSCs. A COX2 B OPN C RUNX2 fold change expression relative to vehicle control, Mean ±SEM, n=3-8, two-way ANOVA, with Bonferroni post test, COX2 effect of treatment p=0.0821, *p<0.05 significant effect of Fenoldopam & GSK101 on COX2 expression.

6.3.6 The effect of GSK101 and fenoldopam treatment on the osteogenic lineage commitment and matrix deposition of healthy and osteoporotic hMSCs

Interestingly, the application of GSK101 had no effect on collagen deposition, while fenoldopam, either alone or in combination with GSK101, significantly reduced collagen deposition. In healthy MSCs, fenoldopam significantly reduced total collagen concentration ($p<0.001$), but the reduction per cell was not significant, changing from 2.20±0.54µg/ng DNA in DMSO to 1.40±0.47µg/ng DNA in fenoldopam (Figure 6.6C, E, G). The combined treatments diminished the total collagen concentration and the quantity produced per cell in healthy MSCs ($p<0.001$). Mechanical stimulation also had a negative influence on collagen deposition which furthered the decline in collagen following fenoldopam treatments.

The production of collagen in osteoporotic MSCs in static conditions is reduced compared to healthy counterparts. A reduced collagen monolayer is visible comparing picrosirius staining of the osteoporotic MSCs to healthy MSCs (Figure 6.6C, D) in the vehicle (DMSO) control. Quantification of the extracted monolayer confirms that the total concentration of collagen in the osteoporotic sample is lower, at 62.42±10.66µg/ml, than the healthy sample at 230.35±14.18µg/ml (Figure 6.6E, F),

which is consistent with previous findings (Chapter 5). However, normalizing collagen to DNA content per sample indicates similar collagen production per cell in healthy MSCs, at 2.20±0.54µg/ng DNA, and osteoporotic MSCs, at 2.44±0.58 µg/ng DNA MSCs under static conditions (Figure 6.6G, H), indicating that cell proliferation may be a key factor contributing to overall matrix production. Under mechanical stimulation, collagen concentration was also decreased in the osteoporotic sample ($p<0.05$) but this effect was less pronounced than that seen in the healthy controls (Figure 6.6E, F). Following treatment with GSK101 under static conditions osteoporotic MSCs were unchanged. There was a similar response to fenoldopam treatment in osteoporotic MSCs where total collagen concentration was diminished by fenoldopam ($p<0.001$) but the change normalized to DNA was not significant reaching 1.98±0.84µg/ng DNA following treatment. Here, the matrix formed was an incomplete layer, with patches where the monolayer had contracted and failed to completely cover the well surface as it does in healthy and vehicle control wells (Figure 6.6D). The combined treatments diminished the total collagen concentration and the quantity produced per cell in osteoporotic MSCs ($p<0.01$) under static conditions (figure 6.6E-H). In contrast, there were some differences in how MSCs from the osteoporotic donor responded to treatments when applied in concert with a mechanical stimulus. While fenoldopam resulted in a decreasing trend in total collagen concentration from 25.86±4.35µg/ml in DMSO to 12.99±2.43µg/ml in fenoldopam, the quantity normalized to DNA is actually slightly greater in fenoldopam at 1.15±0.22 µg/ng DNA compared to DMSO at, 0.69±0.44 µg/ng DNA. In mechanically stimulated osteoporotic MSCs GSK101 increased collagen concentration overall ($p<0.05$) and when normalized to DNA ($p<0.05$). The combined treatments show the same decreasing trend in flow conditions

but the effect is not significant changing from 0.69±0.44 µg/ng DNA in DMSO to 0.28±0.11 µg/ng DNA in fenoldopam and GSK101.

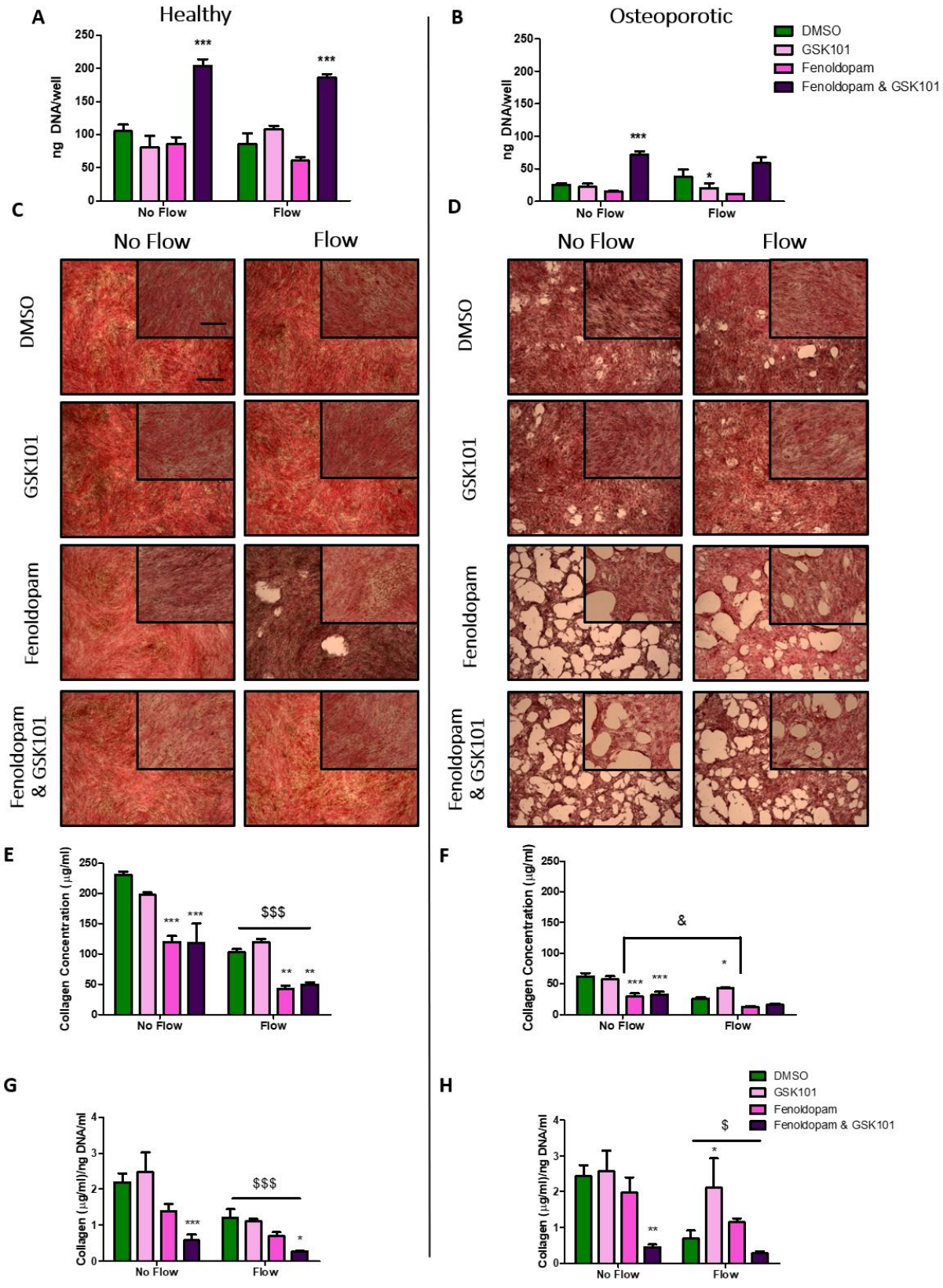

Figure 6.6: Quantification of DNA content in A Healthy and B Osteoporotic samples following 21 days culture in osteogenic differentiation medium containing either vehicle (DMSO), GSK101, Fenoldopam or Fenoldopam & GSK101 and exposed to static (No Flow) or mechanical stimulation (Flow), ng DNA/well, Mean±SEM, n=4-6, two-way ANOVA with Bonferroni post test, ***p<0.001, *p<0.05 significant difference between vehicle and treatment. Representative images of Picrosirius Red stained monolayers of C Healthy and D Osteoporotic samples following 21 days culture in osteogenic differentiation medium containing either vehicle (DMSO), GSK101, Fenoldopam or Fenoldopam & GSK101 and exposed to static (No Flow) or mechanical stimulation (Flow) 2x scale bar=1000µm, inset at 10x scale bar=200µm, n=4-6. C-F Quantification of osteogenic matrix in each sample E, F concentration of collagen extracted from E Healthy and F Osteoporotic samples (µg/ml), Mean±SEM, n=4-6. G, H Collagen concentration normalized to DNA content (ng/ml) for G Healthy and H Osteoporotic samples n=4-6, two-way ANOVA $$$ p<0.001 effect of flow, & p<0.05 effect of treatment is different under the influence of flow, with Bonferroni post test, ***p<0.001, **p<0.01, *p<0.05 significant difference between vehicle and treatment.

In terms of mineral deposition, the application of mechanotherapeutics to healthy MSCs in static conditions had no significant effect on calcium deposition but there is a decreasing trend in calcium normalized to DNA following the combined treatments decreasing from 0.023±0.011µm/ng DNA to 0.003±0.000±0.44µM/ng DNA. Interestingly, the effect of treatment was changed when applied under mechanical stimulation. Fenoldopam significantly increased calcium deposition in healthy MSCs ($p<0.01$) both the total concentration and the quantity normalized to DNA. GSK101 did not elicit a change in calcium and the combined treatments resulted in a trend of inhibition of calcium as seen in the static counterparts (Figure 6.7C, E).

Surprisingly, the deposition of calcium was higher in the osteoporotic MSCs than the healthy counterparts, both in total calcium concentration and the calcium quantity normalized to DNA where healthy MSCs had 0.02±0.01µM/ng DNA compared to 0.28±0.05µM/ng DNA (Figure 7C-F). In osteoporotic MSCs there was less calcium deposited following treatment with GSK101 ($p<0.001$) and the combination of both drugs ($p<0.001$). The 2x images show weaker staining in these conditions, this relationship is true of calcium normalized to DNA also. Contrastingly, the fenoldopam treated osteoporotic MSCs have stronger staining than GSK101 or the combined treatments but it is not uniformly spread as seen in the DMSO control or in healthy counterparts; some areas of the well are not covered by monolayer (Figure 6.7B).

Although total calcium isn't changed, the quantity normalized to DNA shows an increased trend at 0.41±0.09µM/ng DNA compared to the DMSO control at 0.28±0.05µM/ng DNA. In response to mechanical stimulation, fenoldopam resulted in decreased calcium concentration in osteoporotic MSCs ($p<0.001$). The images indicate that alizarin staining is restricted to discrete pockets of the well. Although total calcium concentration is reduced following GSK101 treatment of mechanically stimulated osteoporotic MSCs ($p<0.01$) the quantity normalized to DNA is variable but displays an increasing trend at 0.02±0.01µM/ng DNA in DMSO compared to 0.06±0.05µM/ng DNA in GSK101. Similar to healthy cells and static controls the combined treatments decreased the calcium concentration ($p<0.001$) and demonstrated a similar trend in values normalized to DNA.

In summary, although the treatments, particularly in combination, can enhance early osteogenesis and proliferation of hMSCs, no treatment regime elicited a significantly positive effect on osteogenic matrix deposition.

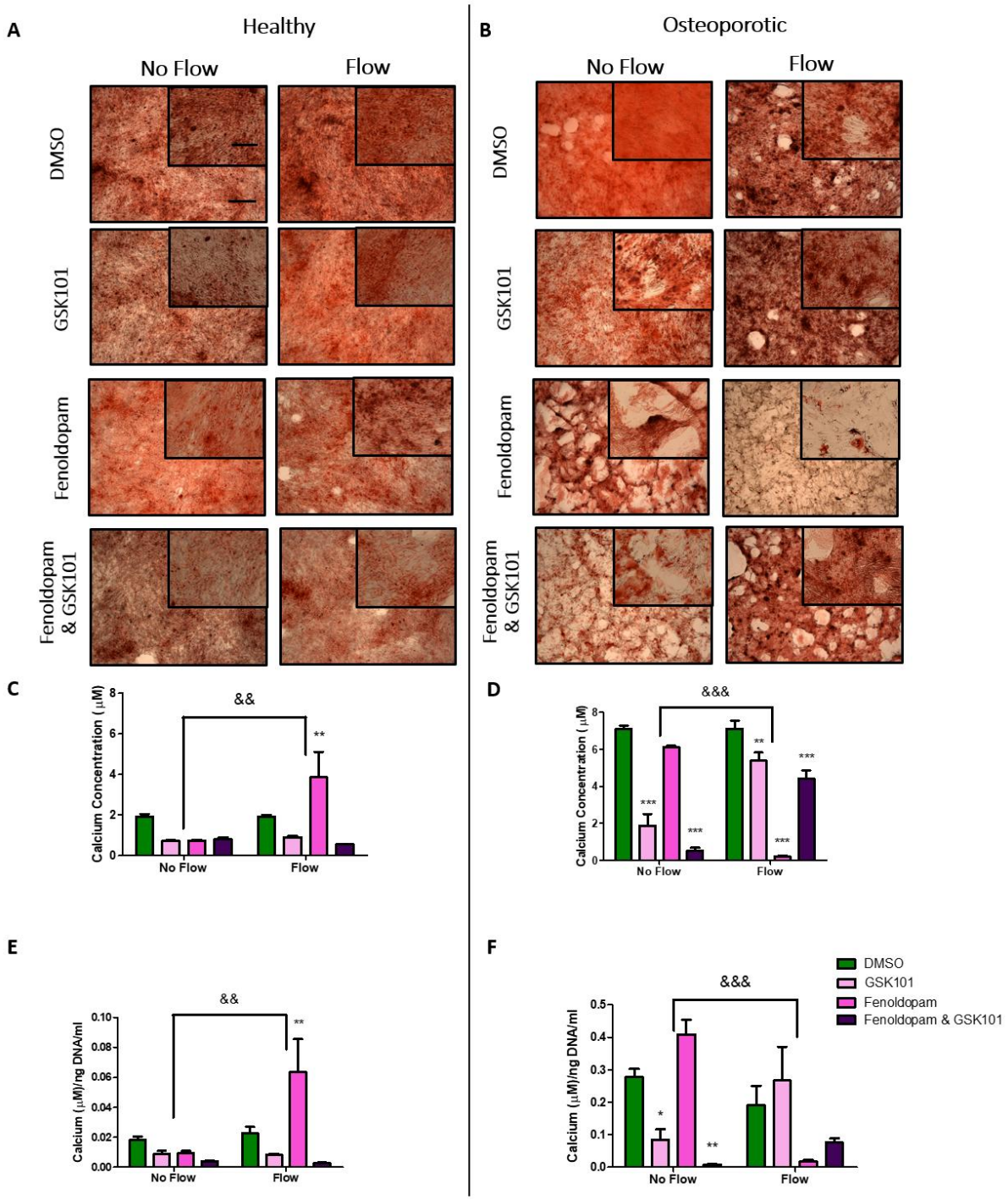

Figure 6.7: Representative images of Alizarin Red stained monolayers of **A** Healthy and **B** Osteoporotic samples following 21 days culture in osteogenic differentiation medium containing either vehicle (DMSO), GSK101, Fenoldopam or Fenoldopam & GSK101 and exposed to static (No Flow) or mechanical stimulation (Flow) 2x scale bar=1000μm, inset at 10x scale bar=200μm, n=4-6. **C-F** Quantification of osteogenic matrix in each sample **C, D** concentration of calcium extracted from **C** Healthy and **D** Osteoporotic samples (μM), Mean±SEM, n=4-6. **E, F** Calcium concentration normalized to DNA content (ng/ml) for **E** Healthy and **F** Osteoporotic samples n=4-6, two-way ANOVA with Bonferroni post test, ***p<0.001, **p<0.01, *p<0.05 significant difference between vehicle and treatment; &&p<0.01, &&&p<0.001 interaction effect.

6.4 Discussion

Osteoporosis presents a major clinical challenge; it places massive pressure on orthopaedic services, costs approximately €37 billion across Europe and threatens the quality of life of our aging population (Hernlund et al., 2013). Current therapies are limited by adverse side effects and effective treatment times. Therefore, novel therapeutic approaches are moving away from inhibiting resorption of bone and more towards the enhancement of new bone. Mesenchymal stem cells are the precursor to osteoblasts, which deposit new osteogenic matrix to maintain healthy bone density and quality. MSC osteogenic differentiation is mediated by mechanical loading and this anabolic process is a key component of bone mechanoadaptation (Stavenschi et al., 2017). Previously, we have demonstrated the role of the calcium channel TRPV4 in MSC mechanotransduction and particularly the significance of its localisation to the primary cilium (Corrigan et al., 2018), and have also demonstrated the role of ciliogenesis in mediating the mechanically induced osteogenic responses in MSCs (Corrigan et al., 2019). Furthermore, we have shown that mechanosensitivity and MSC osteogenesis is defective in osteoporosis (Chapter 5). This study therefore aimed to understand whether cilium and/or TRPV4 were altered in osteoporosis and whether they could be targeted therapeutically to enhance MSC osteogenesis in this disease setting. MSCs, from healthy and osteoporotic patients, were found to express similar levels of TRPV4 but osteoporotic MSCs had consistently lower cilium incidence and shorter axoneme length. Targeting TRPV4 via GSK101 treatment induced a trend of upregulation in *COX2* expression and following treatment for 21 days GSK101 supported the deposition of collagen, particularly in the mechanically stimulated osteoporotic MSCs. Fenoldopam elongated the primary cilia of osteoporotic MSCs. However, despite an upward trend in the expression of *OPN* and *RUNX2* and an

upregulation of calcium deposition in mechanically stimulated healthy MSCs, fenoldopam did not positively influence osteoporotic hMSC osteogenesis. Interestingly, the combined treatments led to an increase in osteoporotic hMSC cilium length and increase in proliferation but unfortunately a decrease in osteogenic matrix deposition in static and mechanically stimulated groups. Overall, although combinatory treatments can enhance early osteogenesis and proliferation of hMSCs, no treatment regime elicited a significantly positive effect on osteogenic matrix deposition.

Although TRPV4 expression is not altered in osteoporosis, the incidence of the primary cilium and its length are significantly reduced, suggesting that that osteoporosis may be an environmental ciliopathy. Investigating the activity of TRPV4 at the gene and protein level, no difference was found in osteoporotic MSCs compared to healthy MSCs. Interestingly, the fluid shear induced increase in *TRPV4* that is seen in healthy MSCs was significantly depleted in osteoporotic counterparts. This indication of a diminished mechanosensitivity agrees with previous findings in Chapter 5. Characterization of ciliogenesis in osteoporotic MSCs revealed inhibited cilium incidence and decreased cilium length. The identification of dysfunctional cilia in osteoporosis is intriguing because there are several ciliopathies that are associated with skeletal malformation, and indicates that osteoporosis may be classified as an environmental ciliopathy (Waters and Beales, 2011). Given the critical role for the cilium in regulating major pathways such as Hedgehog and Wnt, which are important for osteogenic differentiation, an attractive therapeutic approach may be to target ciliogenesis. Following the characterization of MSC properties, the samples with the strongest and weakest osteogenic capacity based on chapter 5, healthy 2 and osteoporotic 3, were further investigated. Healthy 2 had 60.31±1.96% ciliation and a median cilium length of 2.59±0.04μm while osteoporotic 3 had 43.33±4.8% ciliation

and a median cilium length of 1.77±0.05µm facilitating comparison of the effect of treatments on ciliogenesis and osteogenic capacity.

TRPV4 activation with 10nM GSK101 does not significantly influence TRPV4 levels or enhance osteogenic matrix deposition by healthy or osteoporotic human MSCs. Following short term treatment there were positive trends in early osteogenic markers in both healthy and osteoporotic MSCs. However, following long term treatment, despite a positive effect on collagen deposition in the mechanically activated osteoporotic MSCs, TRPV4 activation had minimal or even negative effects on calcium deposition. The results seen in this study indicate that GSK101 may support TRPV4 mediated osteogenic activity but that the concentration of application needs to be optimized for human MSCs. Higher concentrations of GSK101 may mediate a more robust activation of TRPV4 and facilitate greater TRPV4 mediated osteogenic signaling. While work to date on the role of TRPV4 in osteoporosis is limited, there is evidence for its role in the regulation of bone remodeling based on murine models (Mizoguchi et al., 2008). Previous investigations suggest that mutations in *TRPV4* lead to increased non-vertebral fracture risk in male but not females (van der Eerden et al., 2013). This indicates a sex specific role for TRPV4 and encourages the investigation of TRPV4 activity and potential therapeutic targeting in hMSCs isolated from male donors.

Fenoldopam at 50µM concentration can support ciliogenesis in human MSCs resulting in a positive trend on cilium length in the healthy donor MSCs where median length was increased by 0.04µm. However, significant increases in ciliogenesis in the osteoporotic donor MSCs are seen following treatment with median length increasing by 0.39µm. The % ciliation data from the osteoporotic patient was surprising as the values in the vehicle control were much higher than those found in the original characterization data in Figure 2. Although it is unclear why this has occurred, it may

possibly be due to DMSO treatment used as a vehicle control. DMSO is known to influence ciliogenesis, via microtubule stabilization, and this may have altered cilia length and incidence to a greater degree in our osteoporotic cohort (Robinson and Engelborghs, 1982). Regardless of the altered basal cilia structural parameters, fenoldopam treatment could significantly increase cilia length in osteoporotic hMSCs demonstrating ciliotherapy potential. Fenoldopam treatment elicited an increasing trend in *OPN* and *RUNX2* in healthy MSCs but not in the osteoporotic sample. The long-term outcome of fenoldopam treatment was condition dependent. Although fenoldopam negatively influenced collagen deposition in all conditions, healthy MSCs under mechanical stimulation had significantly higher calcium deposition in fenoldopam but there was no effect in static conditions. Exercise is a vital part of maintaining bone health but gentle exercise, which limits the risk of fall and fractures, isn't effective alone at increasing bone density (Cavanaugh and Cann, 1988, Prince et al., 1991). This encourages the targeting of primary cilium mediated mechanotransduction to generate a robust osteogenic response from limited physical activity. However, it must be stated that this effect of fenoldopam and mechanical treatment in osteoporosis resulted in significantly reduced calcium deposition. Interestingly, despite positive effects on early osteogenesis, the combined treatments had no positive influence on long-term matrix deposition. Therefore, further optimization is required to fully validate the potential use of these therapies in the setting of osteoporosis.

6.5 Conclusion

The need for new anabolic therapeutic targets to treat osteoporosis is a driving factor in research deciphering the mechanism of osteogenic lineage commitment. Osteogenic

differentiation of MSCs is mechanically influenced and two mechanisms involved in this process have been previously identified and biochemically targeted. This study has examined the performance of these mechanisms in healthy and osteoporotic MSCs and activated those using pharmacological agents. Osteoporotic MSCs have reduced *TRPV4* mediated fluid shear responses and have a reduced cilium incidence and length, demonstrating possible defects in mechanotransduction machinery. Targeting the primary cilium and associated TRPV4 can positively influence early osteogenic signaling and proliferation but it is currently unclear whether long term treatments can have beneficial effects. Therefore, these results encourage further optimization of these treatments and other mechanotransduction mechanisms to direct the bone forming response of MSCs.

Chapter 7:

Discussion and Conclusion

7.1 Summary

Driven by the demand for new anabolic therapies for osteoporosis, the objective of this thesis was to delineate the molecular mechanisms involved in biophysically-induced MSC osteogenesis in order to direct bone regeneration (Figure 7.1). Given the important role of calcium as a second messenger in the mechanobiology of lineage committed bone and cartilage cells (Lee et al., 2015c, O'Conor et al., 2014, You et al., 2001), initially the role of this second messenger in fluid shear induced osteogenesis of MSCs was explored. While it was known that physical loading induces an influx of calcium in MSCs, the mediating channels and source of calcium are poorly understood (Riddle et al., 2006). Chapter 3 found that TRPV4 is predominant in mediating the fluid shear induced calcium response in MSCs and the membrane localisation of TRPV4 implies that this signal is transported from the extracellular environment. Moreover, the TRPV4-mediated calcium signal is involved in the upregulation of early osteogenic markers in response to loading. The biochemical agonist GSK101, specific to TRPV4, could recapitulate the calcium signal and osteogenic gene expression response under static conditions. Although TRPV4 is expressed throughout the cell membrane, striking colocalization to the primary cilium was observed and the loss of cilium localised TRPV4 activity disrupted TRPV4-mediated osteogenic activity. This highlights TRPV4 as a target for therapeutic direction of MSC osteogenic lineage commitment. Following on from the role found for primary cilium localised TRPV4 in mediating osteogenic signals and previous literature which determined an essential role for the primary cilium

in the response of MSCs to fluid shear, the potential of the cilium as a therapeutic target was next explored (Hoey et al., 2012d). Recently treatments have been designed to enhance the signal processing activity at the primary cilium via elongation of its axoneme (Thompson et al., 2016, Kathem et al., 2014a). Chapter 4 optimised such treatments, termed ciliotherapies, for the promotion of ciliogenesis in MSCs and found that fenoldopam was the most appropriate agent for supporting enhanced mechanosensitivity and osteogenesis. In fenoldopam, a protocol was optimised which elongates the cilium significantly and also enhances early osteogenic gene expression as well as increasing the osteogenic matrix deposition in response to fluid shear. Therefore, the first part of this thesis identifies two components of MSC mechanotransduction, which could be targeted therapeutically as a potentially novel anabolic therapies for osteoporosis.

The second part of this project examined the suitability of these targets for influencing the behaviour of human osteoporotic MSCs, particularly to enhance osteogenic activity and contribute to the bone adaptation response to mechanical loading. Previous studies have identified alterations to the adipogenic differentiation process in osteoporosis but the osteogenic response of osteoporotic MSCs under physical loading is poorly understood. MSCs were isolated from the bone marrow of a cohort of osteoporotic and healthy patients for characterisation. MSCs adipogenic, chondrogenic and osteogenic lineage potential were found to have impaired migration towards FBS, inhibited proliferation, and decreased production of adipogenic and osteogenic matrix in the osteoporotic cohort (Chapter 5). Furthermore, the osteogenic gene expression response to fluid shear was stunted in osteoporosis. These findings supported the development of a mechanotherapeutic approach to increase MSC osteogenesis and bone formation in osteoporosis. The final study (chapter 6) attempted to mimic the osteogenic response of

MSCs to physical activity by biochemically activating the mechanotransduction mechanisms delineated in chapter 3 and 4 (Figure 7.1). The application of GSK101, to activate TRPV4, and fenoldopam, to enhance ciliogenesis at the concentrations and durations optimised in earlier studies partially supported MSC osteogenesis and bone formation. In fact, GSK101 treatment increased the mechanically induced collagen deposition in osteoporotic MSCs whereas fenoldopam treatment increased the mechanically induced calcium deposition in healthy MSCs. The combined treatment with GSK101 and fenoldopam elicited an increase in *COX2* expression and upregulated proliferation under static conditions. Taken together, these findings demonstrate defective mechanotransduction and regenerative potential of osteoporotic MSCs but the developed mechanotherapeutics show promise in targeting mechanotransduction mechanisms to increase MSC osteogenesis for the treatment of osteoporosis, however further optimisation in human MSCs is required.

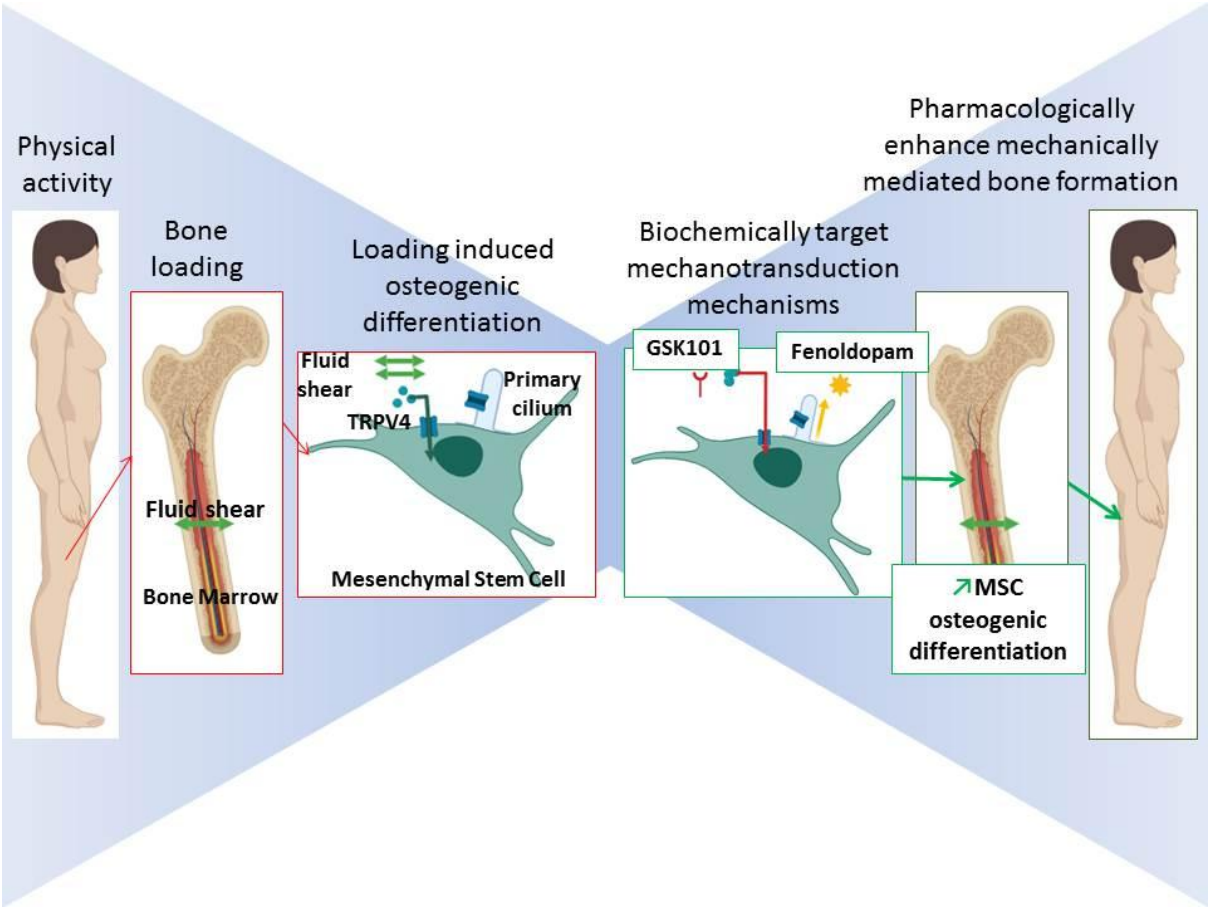

Figure 7.1: Overview of the mechanisms researched in this thesis and their application for therapeutic design. Initially the mechanical environment of bone marrow during physical activity was modelled in vitro and two MSC mechanotransduction mechanisms were delineated, calcium signalling via TRPV4 and primary cilium mediated osteogenesis. Protocols developed to biochemically activate the mechanisms identified were applied to human MSCs to enhance bone modelling activity (Aoki et al., 2019).

7.2 Delineation of MSC mechanotransduction mechanisms

The role of MSCs in the anabolic response of bone to mechanical loading is widely appreciated and the role of calcium as a second messenger in MSCs has been indicated previously. The mechanisms mediating mechanotransduction could form novel therapeutic targets and the first study investigates the role of the mechanosensitive

calcium channel TRPV4, previously characterised in chondrocytes and osteocytes, in the MSC response to fluid shear. The specific antagonism of TRPV4 activity completely prevents calcium signalling in response to fluid shear while GSK101 successfully mimics the fluid shear induced calcium flux, indicating TRPV4 is the primary mediator of the calcium response to fluid shear in MSCs. TRPV4 is heavily expressed along the cilium axoneme and treatment of MSCs, without a primary cilium, with GSK101 results in impaired *Cox2* expression and augmented *Opn* expression compared to control ciliated cells, demonstrating a regulatory role of the primary cilium in TRPV4 signal transduction. The influence of the cilium in the response to TRPV4 activation encourages investigation into calcium signalling within the ciliary microdomain. The optimisation of GSK101 in this study was successful at mimicking the response fluid shear induced *Cox2* and *Opn* upregulation. Furthermore, GSK101 treatment enhances both collagen and calcium matrix deposition, demonstrating the importance of TRPV4-mediated calcium in downstream osteogenic differentiation and the potential to biochemically target mechanically activated signalling mechanisms.

Given its importance in MSC mechanotransduction and in TRPV4 mediated signalling, the primary cilium has the potential to be a therapeutic target, where the osteogenic response could be triggered biochemically. Treatments which elongate the cilium axoneme have been identified and used for the therapeutic influence of cilium localised activity in polycystic kidney disease and osteoarthritis models (Thompson et al., 2016, Kathem et al., 2014a). The second study optimised a ciliotherapy treatment for MSCs significantly elongating the axoneme via two different treatments, 100mM LiCl and 50µM fenoldopam. The concentrations of LiCl required to elongate MSC cilia also decreased expression of osteogenic markers and long term treatment effected cell survival and proliferation. The identification of a ciliotherapy capable of improving

osteogenic matrix formation in response to loading is a substantial development in attempts to establish new anabolic therapeutic targets in osteoporotic bone. In addition, the modulation of cilium length can be used to further delineate the role of cilium-localised activity in MSC mechanotransduction by increasing the ciliary membrane surface area where membrane bound channels and receptors access the extracellular environment. Moreover, the behaviour of elongated MSC cilia supports the previously suggested hypothesis that the additional axoneme length results in an increased membrane strain under the influence of extracellular fluid flow (Schwartz et al., 1997, Spasic and Jacobs, 2017). The findings of this work could be explained by either hypothesis of the positive effect of cilium length, identifying the mechanism of the change in behaviour could aid in ciliotherapy development and direct treatment optimisation. If the change in ciliary mechanics is of significant effect then the effect of treatment on microtubule structure should be studied. This could be tested by disrupting the cytoskeletal components of the cilium biochemically. The positive influence of cilium elongation on mechanosensitivity in osteocytes and preliminary data from murine osteoporotic models treated systemically with fenoldopam encourages further investigation into fenoldopam as a therapeutic strategy to increase bone formation (Spasic et al., 2018). However, it can be concluded that cilium length can be altered biochemically in MSCs and that this is an effective target to modulate cell mechanosensitivity.

7.3 Human osteoporotic MSC treatment

To effectively target the mechanotransduction mechanisms delineated in the first two studies as a therapeutic strategy, knowledge of the mechanoadaptation activity within

MSCs of osteoporotic patients is required. Indeed, a thorough understanding of alterations in MSC behaviour in osteoporosis is important in determining effective therapeutic targets. Previous findings on the proliferative and migratory capacity of MSCs in osteoporosis are conflicting and the impairment observed in the patient cohort recorded here as well as donor variability encourages expansion of the study to a larger sample size (Veronesi et al., 2011). Comparison of the osteoporotic donor cohort to healthy MSCs used in this study revealed impaired basal *COX2* expression and decreased *COX2*, *OPN* and *RUNX2* expression in response to fluid shear. This is the first study to demonstrate a decrease in the mechanosensitivity of MSCs in osteoporosis. Furthermore, as MSCs were induced to differentiate to the adipogenic and osteogenic lineages the formation of extracellular matrix was defective in comparison to healthy counterparts. Lipid formation was significantly lower in osteoporotic MSCs and the significant increase in mineralised matrix in response to biochemical induction seen in healthy MSCs was impaired in osteoporosis. The pattern of deposition of calcium observed in osteoporotic MSCs, in irregular contracted patches suggests a deficit in the adhesion and spreading of the differentiating MSCs (Phillips et al., 2010). These findings emphasise the MSC as an important player in the osteoporotic disease mechanism which will be important to consider as therapeutic design moves towards targeting bone formation activity as is being introduced in teriparatide and romosozumab (Khosla and Hofbauer, 2017).

Given the loss in mechanosensitivity discovered in osteoporosis, targeting this deficit becomes a more attractive therapeutic avenue. The delineation of the role of TRPV4 in transducing physiological loads into osteogenic activity via MSC calcium signalling as well as the determination of an effective biochemical TRPV4 activation protocol directed the investigation of TRPV4 activity in osteoporosis. Furthermore, the influence

of cilium length, which can be significantly modulated by fenoldopam, on mechanosensitivity and upregulation of mechanically induced osteogenic matrix formation promoted investigation into ciliogenesis in osteoporosis. There is an urgent and growing demand for osteoporotic therapies, and as the attempts to target sclerostin have been presented concerning side effects, novel therapeutic targets are required (Khosla and Shane, 2016). The mechanotherapeutic approach, designed to target the osteogenic activity mediated by TPRV4 and the primary cilium in response to mechanical load, presents an innovative development in osteoporotic therapy design. It is envisioned that the support of the mechanoadaptation response could reduce fracture risk and facilitate osteoporotic patients in benefiting from the positive influence of physical activity on skeletal health (Cavanaugh and Cann, 1988). Osteoporotic MSCs have an inhibited *TRPV4* upregulation in response to fluid shear but have comparable expression of the TRPV4 channel to healthy counterparts. Interestingly, the incidence and length of primary cilia in osteoporotic MSCs is consistently less than that in healthy MSCs. The application of GSK101, fenoldopam or a combination of both to human MSCs can significantly increase the length of primary cilia and GSK101 but not fenoldopam can maintain but not increase TRPV4 expression. Nevertheless, GSK101 treatment increased collagen production of osteoporotic MSCs under mechanical stimulation while fenoldopam treatment increased calcium deposition in mechanically stimulated healthy MSCs. The positive effects seen on osteogenic matrix deposition in this study support the expansion of this investigation in MSCs from more donors, in addition to further optimisation of treatment strategies in a human model. The promising effects seen with this mechanotherapeutic design, where the mechanoadaptive bone modelling effect of loading is enhanced, suggests this route should be pursued for osteoporosis.

7.4 Limitations and future directions

The initial studies, chapter 3 and 4, were carried out using the murine cell line C3H10T1/2. Although often used as a model for mesenchymal stem cells these cells are embryonic in origin and may behave differently to bone marrow progenitors found in the marrow (Reznikoff et al., 1973, James, 2013). The results of the studies carried out in C3H10T1/2s are promising and in each case the osteogenic potential of the cell line is demonstrated under biochemical induction. However, the human MSCs isolated from fresh bone marrow aspirates and characterised according to the International Society for Cellular Therapy's guidelines did not respond to treatments conditions optimised in C3H10T1/2 (Dominici et al., 2006). Although there was some influence of treatment, such as the partial change in *COX2* expression with GSK101 treatment, the changes are weak and variable. Human and mouse MSCs differ in size and surface marker expression which indicates the regulation of the responses to environmental changes may differ (Jones and Schäfer, 2015). Moreover, while immortalised mesenchymal stem cells have maintained their differentiation potential *in vitro* for neuronal regenerative medicine the immortalisation process and culture of the cell line through multiple passages removes the model further from the conditions which are relevant to the study, living bone marrow (Gong et al., 2011). Given the potential differences in behaviour in murine immortalised MSCs a continuation of this study should optimise the activation of TRPV4 using GSK101 and the elongation of primary cilia using fenoldopam in human primary bone marrow derived MSCs.

Another limitation arises from the study of MSC behaviour in two-dimensional cell culture when the native environment of MSCs would facilitate adhesion and spreading in three dimensions. The culture surfaces are coated in fibronectin for MSC culture but

beneath that a flat plastic surface, of uniform elasticity, facilitates growth of a monolayer of MSCs. *In vivo* the MSC would experience the trabeculae of cancellous bone at the bone-marrow interface, the ECM surrounding sinusoids, and the viscous fluid of marrow which is densely populated with cells. The development of a three dimensional culture system for MSCs would allow more accurate modelling of the dynamic mechanical cues generated in bone marrow as well as the spatial arrangement of cells and the receptors and signals interacting between them (Edmondson et al., 2014). The comparison of cells cultured in two or three dimensions has observed differences in cell proliferation and gene expression. The studies described in this thesis provide valuable and relevant data on the expression and activity of the calcium channel TRPV4 in MSCs as well as the response of MSCs to ciliotherapies. It is envisaged that a next step in continuation of this study would create a culture system to allow the application of fluid flow mediated shear stress to a three-dimensional scaffold seeded with MSCs (Michael Delaine-Smith et al., 2015). This will require MSC numbers, growth factor quantities and bioreactor development beyond the scope of this project.

Throughout these studies the behaviour of MSCs under short term and long term mechanical loading is investigated. Using parallel plate flow chambers a uniform precisely controlled shear stress can be applied to glass slides and our studies apply a shear stress of 2Pa oscillating at 2Hz using custom built chambers that were optimised in house to model physiologically relevant osteogenic fluid shear signals (Stavenschi et al., 2017). However, for long term studies and the investigation into multiple biochemical modulators, including GSK101 and fenoldopam, the glass slides were not suitable. An orbital shaker was used to displace the medium in cell culture well plates as a high throughput alternative which facilitated long term culture requirements including multiple medium changes and daily phase contrast imaging. Based on

computational models carried out to quantify the fluid shear experienced at the surface of a 6 well plate when the medium of a height of 1.8cm is displaced by a shaker with a radius of gyration of 9.5mm moving at 100rpm the MSCs experienced an average of 0.3Pa shear stress over the entire well and in excess of 1Pa at a maximum (Salek et al., 2012). While both the orbital shaker and parallel plate flow chambers apply physiologically relevant fluid shear, the stimulus achieved by the orbital shaker may not be robust enough to generate an osteogenic response in MSCs. Fluid shear in the marrow is difficult to measure and predict because of the difficulties in measuring the native viscosity of marrow tissue, however even with low magnitude high frequency vibration the best models have predicted that most of the marrow experiences 0.5Pa shear stress. Furthermore, the levels can be much higher at the interface of bone and marrow and during more intensive loading greater pressure gradients could produce shear stress in excess of 24Pa (Metzger et al., 2015b, Coughlin and Niebur, 2012). Overall, there may be some limitation in the mechanoadaptation response observed in the studies described here because of a minimal fluid shear stimulus, however the behaviour observed encourage further investigation into the response to a higher shear stress stimulus.

In chapter 5 studying the behaviour of human patient samples was challenged by considerable individual donor variability. Although efforts were made to reduce the factors influencing behaviour by choosing only female donors and limiting samples to as close an age range as could be obtained, major differences between samples were observed within the healthy and osteoporotic cohorts. For example the osteogenic matrix deposited by healthy 2 is approximately 7 fold higher than that seen in healthy 1 (Figure 5.6C). Nonetheless significant differences in differentiation and mechanosensing capacities of osteoporotic MSCs were observed in the populations

studied. These interesting results suggest the pursuit of this study with a larger population of female donors which will require the time and collaboration with an orthopaedic surgery department for access to consenting donors. Furthermore, the discovery of altered mechanosensation capacity in the characterisation of female osteoporotic MSCs encourages the study of this factor in male osteoporotic patients. The findings collected here promote the scale up of such a characterisation of mechanotransduction mechanisms in the osteoporotic disease state.

A striking observation was made of the properties of matrix deposited from osteoporotic donors, apart from the incomplete coverage of the cell culture surface, stained matrix was concentrated in small patches or islands which appeared to have contracted and separated over time (Figure 6.6 and 6.7). This was only apparent in the osteoporotic samples where mechanosensitivity was also compromised. Further investigation is required to identify the possible cause of this outcome and the first steps should evaluate the adhesive properties of osteoporotic MSCs. To inform this integrin, gap junction activity, and cell behaviour on a range of protein coatings should be tested. The characterisation of mature matrix formation in differentiating osteoporotic samples is important in designing effective therapies to support bone formation and this finding highlights characteristics of osteoporotic MSCs which must be considered.

7.5 Conclusion

- TRPV4 plays an essential role in mediating a calcium signal in MSCs responding to fluid shear and TRPV4 mediated signalling increases the expression of early osteogenic genes and the deposition of osteogenic matrix downstream.
- TRPV4 expression is localised to the primary cilium of MSCs and its activity at the cilium modulates the expression of early osteogenic genes, upregulating *Cox2* and decreasing *Opn*.
- Fluid shear mediated osteogenic activity, both early osteogenic marker expression and enhanced osteogenic matrix deposition, can be mimicked via biochemical activation of TRPV4 with GSK101.
- The MSC primary cilium can be elongated using LiCl or fenoldopam and increasing primary cilium length increases mechanosensitivity, increasing the *Cox2* and osteogenic matrix upregulation in response to fluid shear.
- Fenoldopam treatment is more suitable for directing MSC lineage commitment towards osteogenesis as it does not affect hedgehog or Wnt activity and is supportive of early osteogenic marker expression.
- A biobank of human MSCs were isolated from bone marrow aspirates of 3 healthy and 3 osteoporotic donors, all donors were skeletally mature and female. The MSCs isolated were characterised according to ISCT guidelines (Dominici et al., 2006).
- In osteoporosis, MSCs display impaired chemotactic migratory capacity, impaired proliferation and impaired differentiation towards the adipogenic and

osteogenic lineages as evaluated by matrix quantity and quality respectively in comparison to healthy MSC behaviour.

- The mechanosensitivity of osteoporotic MSCs is diminished and fluid shear mediated upregulations in *COX2* and *OPN* display a decreasing trend while the upregulation of *RUNX2* is significantly reduced compared to healthy counterparts.
- The mechanotransduction mechanism of osteoporotic MSCs is weakened as *TRPV4* is not upregulated in response to fluid shear as in healthy MSCs and primary cilium incidence and length is significantly depleted compared to healthy counterparts.
- Biochemically activating the TRPV4 and cilium mediated mechanotransduction mechanisms can improve the mechanically induced osteogenic matrix deposition in a patient specific manner and presents a novel target to develop anabolic therapies for osteoporosis.

Supplementary Material:

Supplementary Figure 3.1

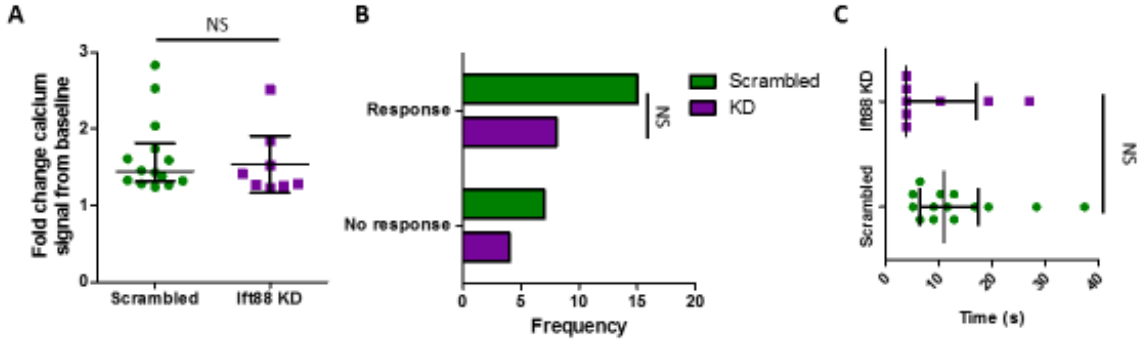

Supplementary Figure 3.1: (A) Median and interquartile range of fold increase in calcium at first peak following application of GSK101 in cells transfected with scrambled siRNA or siRNA targeting IFT88, Mann Whitney test, NS p>0.05. (B) Frequency of calcium response in MSCs exposed to GSK101, Fisher's exact test, NS p>0.05. (C) Time to first peak for individual cells following application of GSK101 at time 0s. Bars mark Median and interquartile range, Scrambled N=4, n= 20, IFT88 KD N=4, n=12, Mann Whitney test, NS p>0.05.

Supplementary Table 3.1:

Primer sequences and concentrations employed in quantitative PCR analysis

Gene	Tm (°C)	Primer concentration	Sequence	Amplicon Size
18S	60	400 nM	5'-GTAACCCGTTGAACCCCATT-3'	151bp
			3'-CCATCCAATCGGTAGTAGCG-5'	
Cox2	60	400 nM	5'-ACTCATAGGAGAGACTATCAAG-3'	147bp
			3'-GAGTGTGTTGAATTCAGAGG-5'	
Opn	60	400 nM	5'-GGATGAATCTGACGAATCTC-3'	188bp
			3'-GCATCAGGATACTGTTCATC-5'	
TRPV4	60	1x	Mm00499025_m1	56bp

Supplementary Figure 4.1

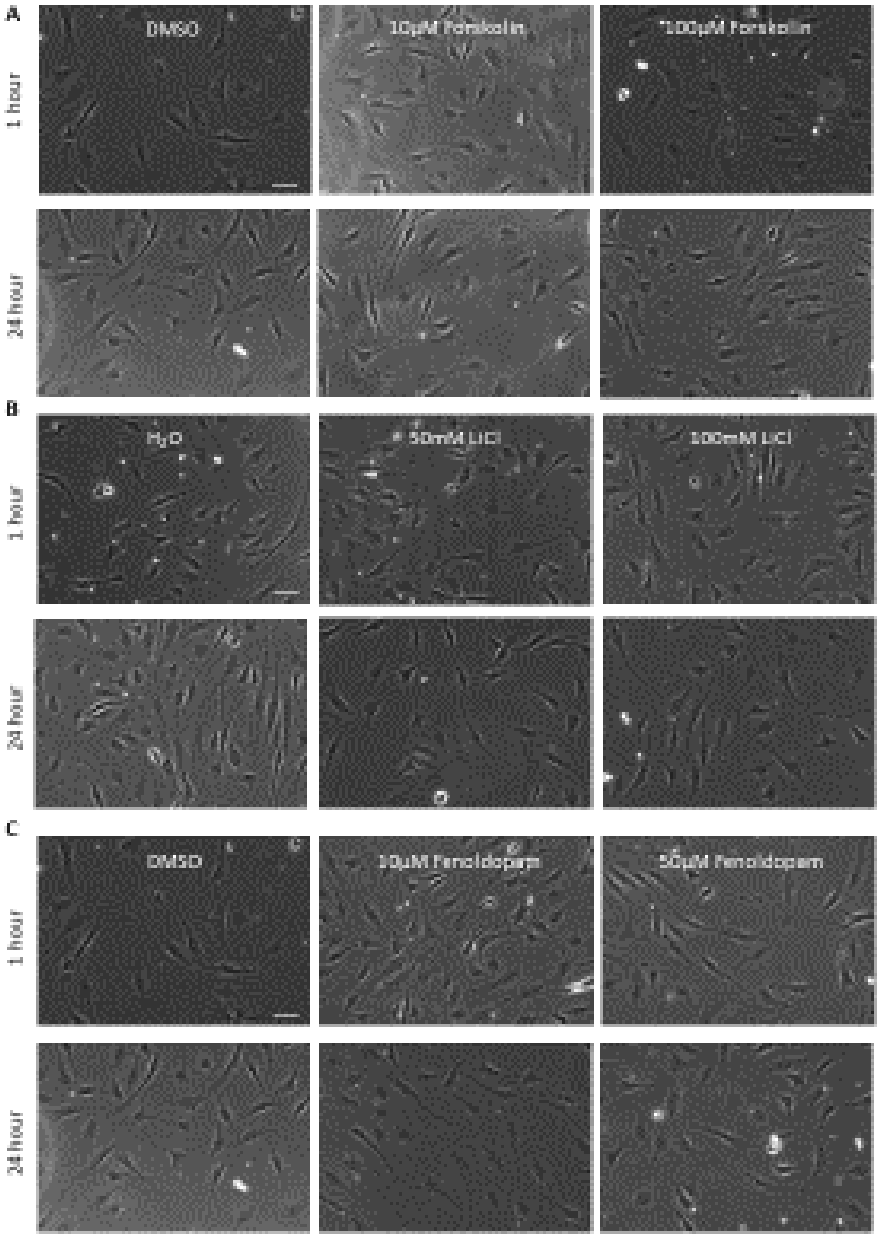

Supplementary Figure 4.1: Representative images of MSCs following treatment with A Forskolin, B LiCl or C Fenoldopam or vehicle, DMSO or H2O, control for 1 hour and 24 hours in 4x phase contrast (scale bar 200μm).

Supplementary Figure 4.2

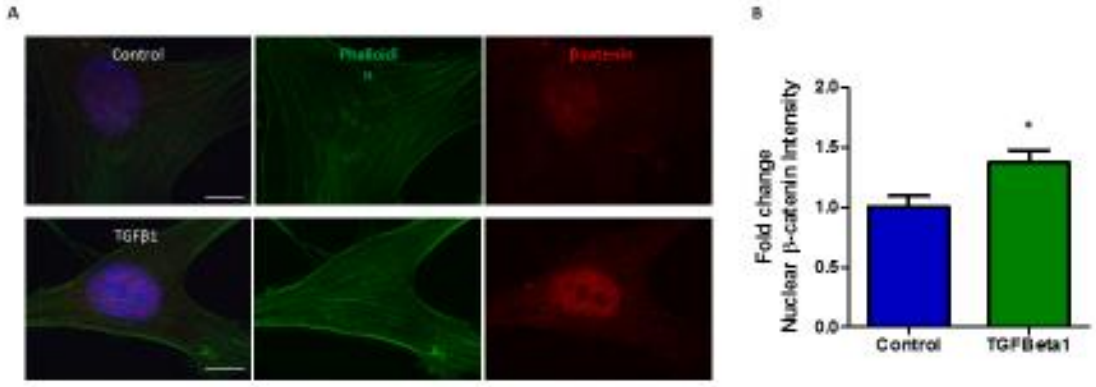

Supplementary Figure 4.2: Positive Control for β-catenin localization to the nucleus A representative images of immunofluorescent staining at 100x fluorescence (red channel- β-catenin, green channel-phalloidin and DAPI (scale bar 10μm) following treatment with 2ng/ml TGF-β1 or vehicle, 4mM HCl 1mg/ml BSA, control for 2 hours. B Quantification of nuclear intensity of β-catenin in each condition, statistical analysis, two-tailed t-test, *$p<0.05$.

Supplementary Table 4.1

The sequences of the primers used to quantify gene expression in MSC

Gene	Tm (^{o}C)	Primer concentration	Sequence	Amplicon Size
18s	60	400 nM	5'-GTAACCCGTTGAACCCCATT-3'	151bp
			3'-CCATCCAATCGGTAGTAGCG-5'	
Cox2	60	400 nM	5'-ACTCATAGGAGAGACTATCAAG-3'	147bp
			3'-GAGTGTGTTGAATTCAGAGG-5'	
Opn	60	400 nM	5'-GGATGAATCTGACGAATCTC-3'	188bp
			3'-GCATCAGGATACTGTTCATC-5'	
Axin2	60	400nM	5'-CAGCCCAAGAACCGGGAAAT-3'	117bp
			3'-AGCCTCCTCTCTTTTACAGCAA-5'	
Ptch1	60	400nM	5'-TGTGGCTGAGAGCGAAGTTT-3'	179bp
			3'-CACTCGTCCACCAACTTCCA-5'	
Gli1	60	400nM	5'-CAGCATGGGAACAGAAGGACT-3'	177bp
			3'-GAGAGAGCCCGCTTCTTTGT-5'	
Runx2	60	300nM	5'-ACAAGGACAGAGTCAGATTAC-3'	196bp
			3'-CAGTGTCATCATCTGAAATACG-5'	
Dlx5	60	400nM	5'-AGAGAAGGTTTCAGAAGAC-3'	93bp
			3'-GCAAACACAGGTGAAAATCT-5'	

Supplementary Table 5.1:

The sequences of the primers used to quantify gene expression in MSCs

Gene	Forward Primer	Reverse Primer
18S	ATCGGGGATTGCAATTATTC	CTCACTAAACCATCCAATCG
COX2	AAGCAGGCTAATACTGATAGG	TGTTGAAAAGTAGTTCTGGG
OPN	GACCAAGGAAAACTCACTAC	CTGTTTAACTGGTATGGCAC
RUNX2	GCAGTATTTACAACAGAGGG	TCCCAAAAGAAGTTTTGCTG
TRPV4	GATCTTTCAGCACATCATCC	GGTCATAAAGCGAGGAATAC

Supplementary Methods 5.2:

Quantification of coverage of culture surface by stained monolayer

The surface area covered by positively stained monolayer was quantified by limiting the threshold of 8-bit images between 135 and 255 in Image J, so as to highlight stain free regions. Areas below threshold were selected and the sum of the areas of these regions was calculated. The below threshold area was subtracted from the total area of each image to calculate the area covered by stained matrix, the data was converted to percentage for presentation in Supplementary Figure 2. For each healthy and osteoporotic sample of MSCs % coverage was measured for one representative image.

Supplementary Figure 5.1:

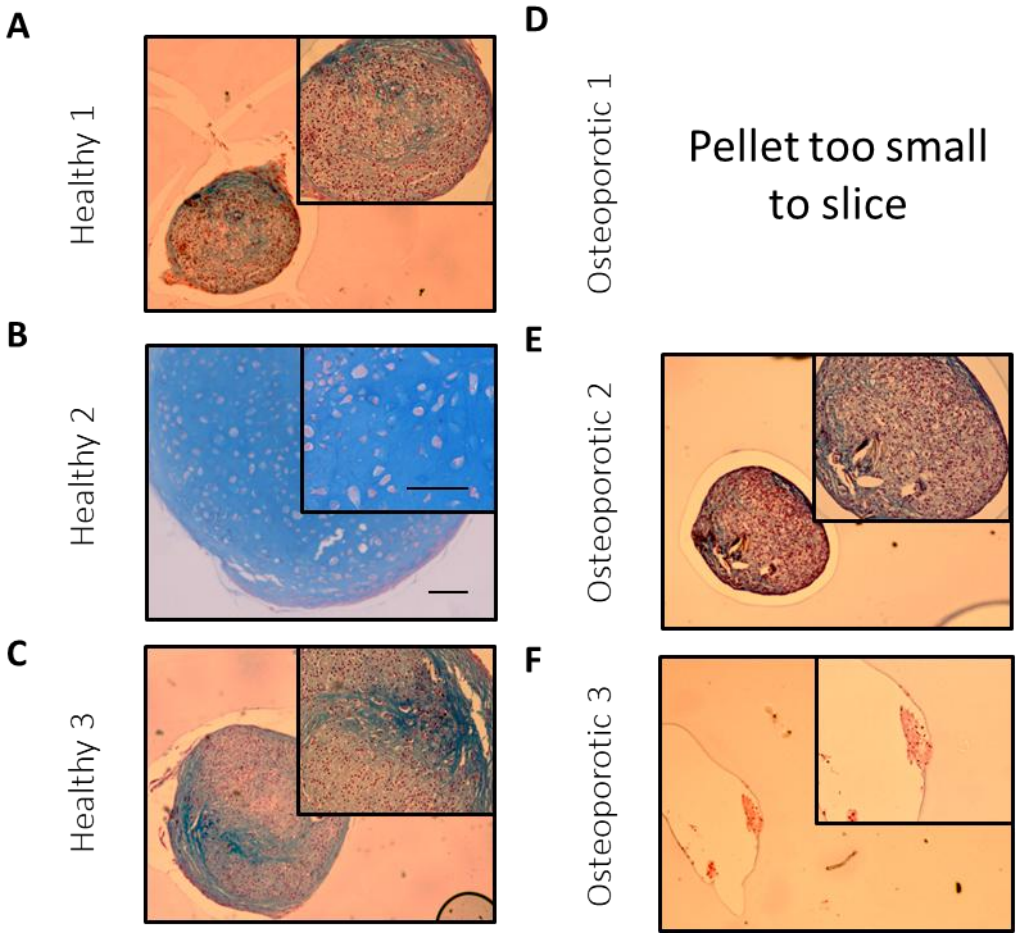

Supplementary Figure 5.1: Representative images of Alcian blue stained pellet cultures of each sample following 21 days culture in chondrogenic differentiation medium, 4x scale bar =500µm, inset is at 10x, scale bar =100µm, n=2-4.

Supplementary Figure 5.2:

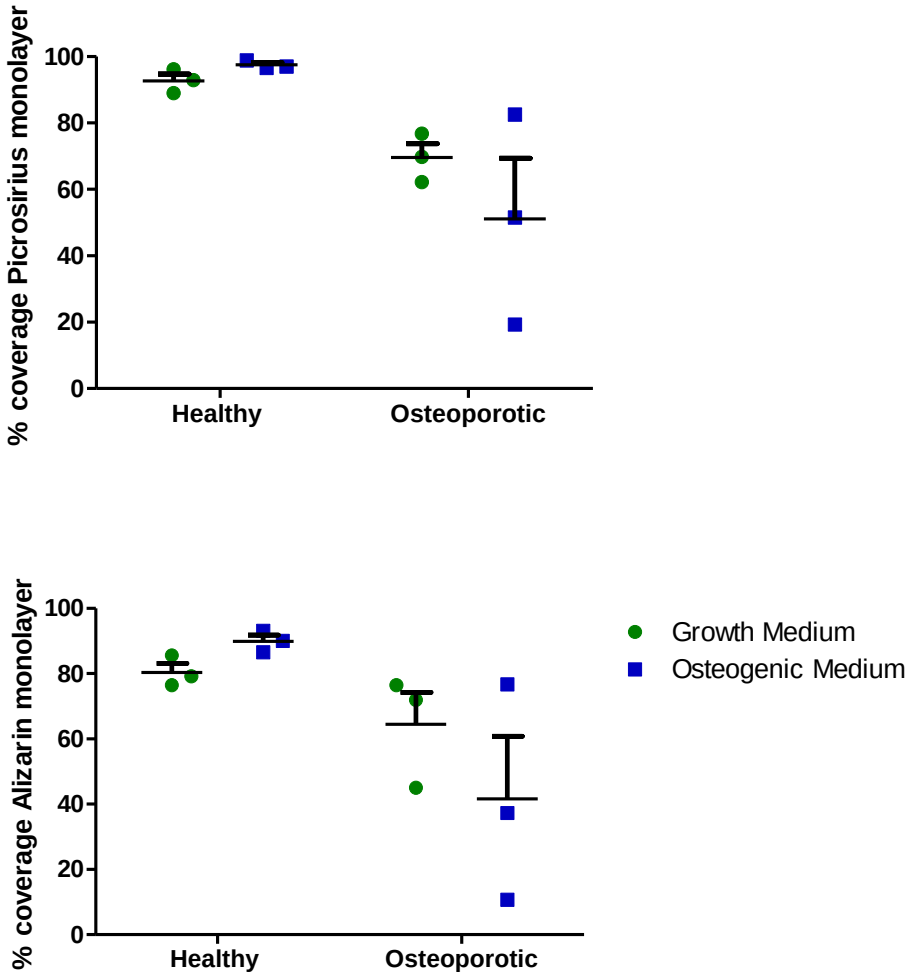

Supplementary Figure 5.2: % of the surface area covered by Picrosirius (top) and Alizarin (bottom) stained monolayer in healthy and osteoporotic MSCs in growth or osteogenic medium, n=3, Mean +/- SEM.

Supplementary Table 6.1:

The sequences of the primers used to quantify gene expression in MSC

Gene	Tm (^{o}C)	Primer Concentration	Sequence	Amplicon Size (bp)
18S	60	300nM	5'-ATCGGGGATTGCAATTATTC-3'	130
			3'-GCTAACCTACCAAATCACTC-5'	
COX2	60	400nM	5'-AAGCAGGCTAATACTGATAGG-3'	113
			3'-GGGTCTTGATGAAAAGTTGT-5'	
OPN	60	400nM	5'-GACCAAGGAAAACTCACTAC-3'	84
			3'-CACGGTATGGTCAATTTGTC-5'	
RUNX2	60	400nM	5'-GCAGTATTTACAACAGAGGG-3'	112
			3'-GTCGTTTTGAAGAAAACCCT-5'	
TRPV4	60	400nM	5'-GATCTTTCAGCACATCATCC-3'	110
			3'-CATAAGGAGCGAAATACTGG-5'	
IFT88	60	400nM	5'-ATGTCTGCGTTTCTTAGTTC-3'	82
			3'-GGTCTTTTGACTTCTCCAAC-5'	

Supplementary Table 6.2:

Comparison of the performance of each MSC sample characterized in terms of migration, osteogenic gene expression under fluid shear, proliferation, collagen and calcium deposition in osteogenic supplements for 21 days

		Healthy 1	Healthy 2	Healthy 3	Osteoporotic 1	Osteoporotic 2	Osteoporotic 3
Migration		↗↗↗	↗	↗↗	↗↗	↙↙	↙↙↙
Fluid shear Response	*COX2*	↗↗	↗↗↗	↗↗↗	↗	↗↗↗	↗
	OPN	↗↗	↗↗↗	↙	↙	↙↙	↗↗
	RUNX2	↙	↗↗	↙	↙↙	↙	↗
Proliferation		↗↗↗	↗↗↗	↗	↗	↗↗	↗
Collagen		↙↙↙	↗↗	↗	↗	↗↗↗	↙↙
Calcium		↗	↗↗↗	↙	↗	↗	↙

Migration: Change in number of cells migrating in 10% FBS >4 ↗↗↗, >2 ↗↗, >1 ↗, <0 ↙↙, <-1 ↙↙↙

Fluid shear response: Fold change *COX2* >12 ↗↗↗, >8 ↗↗, >4 ↗; fold change *OPN* >2 ↗↗↗, >1.5 ↗↗, >1 ↗, <1 ↙, <0.5 ↙↙; fold change *RUNX2* >1.5 ↗↗, >1 ↗, <1 ↙, <0.5 ↙↙

Proliferation: Change in ng DNA/well from day 7 to 14, <30ng ↗, <54ng ↗↗, <78ng ↗↗↗

Collagen: Change in collagen production (µg/ml per ng DNA) in osteogenic differentiation medium >0.02 ↗, >0.04 ↗↗, >0.08 ↗↗↗, <0.04 ↙↙, <0.08 ↙↙↙

Calcium: Change in calcium production (µM per ng DNA) in osteogenic differentiation medium <0.004 ↗, <0.008 ↗↗, <0.012 ↗↗↗, <0 ↙

References:

ADAMS, M. 2010. The Primary Cilium: An Orphan Organelle Finds a Home. *Nature Education,* 3.

AHMED, A. S., SHENG, M. H., WASNIK, S., BAYLINK, D. J. & LAU, K. W. 2017. Effect of aging on stem cells. *World J Exp Med,* 7**,** 1-10.

ALENGHAT, F. J. & INGBER, D. E. 2002. Mechanotransduction: all signals point to cytoskeleton, matrix, and integrins. *Sci STKE,* 2002**,** pe6.

ANDERSON, P., CARRILLO-GÁLVEZ, A. B., GARCÍA-PÉREZ, A., COBO, M. & MARTÍN, F. 2013. CD105 (endoglin)-negative murine mesenchymal stromal cells define a new multipotent subpopulation with distinct differentiation and immunomodulatory capacities. *PLoS One,* 8**,** e76979.

ANTEBI, B., PELLED, G. & GAZIT, D. 2014. Stem cell therapy for osteoporosis. *Curr Osteoporos Rep,* 12**,** 41-7.

AOKI, S., SHTEYN, K. & MARIAN, R. 2019. *Biorender.com* [Online]. [Accessed].

ARMAS, L. A. & RECKER, R. R. 2012. Pathophysiology of osteoporosis: new mechanistic insights. *Endocrinol Metab Clin North Am,* 41**,** 475-86.

ARNSDORF, E. J., TUMMALA, P., KWON, R. Y. & JACOBS, C. R. 2009. Mechanically induced osteogenic differentiation--the role of RhoA, ROCKII and cytoskeletal dynamics. *J Cell Sci,* 122**,** 546-53.

ASTUDILLO, P., RÍOS, S., PASTENES, L., PINO, A. M. & RODRÍGUEZ, J. P. 2008. Increased adipogenesis of osteoporotic human-mesenchymal stem cells (MSCs) characterizes by impaired leptin action. *J Cell Biochem,* 103**,** 1054-65.

BALLANE, G., CAULEY, J. A., LUCKEY, M. M. & FULEIHAN, G. L.-H. 2014. Secular trends in hip fractures worldwide: opposing trends East versus West. *J Bone Miner Res,* 29**,** 1745-55.

BANCROFT, G. N., SIKAVITSAS, V. I., VAN DEN DOLDER, J., SHEFFIELD, T. L., AMBROSE, C. G., JANSEN, J. A. & MIKOS, A. G. 2002. Fluid flow increases mineralized matrix deposition in 3D perfusion culture of marrow stromal osteoblasts in a dose-dependent manner. *Proc Natl Acad Sci U S A,* 99**,** 12600-5.

BARON, R. & HESSE, E. 2012. Update on Bone Anabolics in Osteoporosis Treatment: Rationale, Current Status, and Perspectives. *Journal of Clinical Endocrinology & Metabolism,* 97**,** 311-325.

BARRETO, S., GONZALEZ-VAZQUEZ, A., CAMERON, A. R., CAVANAGH, B., MURRAY, D. J. & O'BRIEN, F. J. 2017. Identification of the mechanisms by which age alters the mechanosensitivity of mesenchymal stromal cells on substrates of differing stiffness: Implications for osteogenesis and angiogenesis. *Acta Biomater,* 53**,** 59-69.

BATTLE, C., OTT, C. M., BURNETTE, D. T., LIPPINCOTT-SCHWARTZ, J. & SCHMIDT, C. F. 2015. Intracellular and extracellular forces drive primary cilia movement. *Proc Natl Acad Sci U S A,* 112**,** 1410-5.

BESSCHETNOVA, T. Y., KOLPAKOVA-HART, E., GUAN, Y., ZHOU, J., OLSEN, B. R. & SHAH, J. V. 2010. Identification of signaling pathways regulating primary cilium length and flow-mediated adaptation. *Curr Biol,* 20**,** 182-7.

BETTS, G. J., DESAIX, P., JOHNSON, E., JOHNSON, J. E., KOROL, O., KRUSE, D., POE, B., WISE, J. A., WOMBLE, M. & YOUNG, K. A. 2018. Anatomy and Physiology. *In:* PROJECT, B. O. T. (ed.). PressBooks.

BIANCO, P. & ROBEY, P. G. 2015. Skeletal stem cells. *Development,* 142**,** 1023-7.

BINDERMAN, I., ZOR, U., KAYE, A. M., SHIMSHONI, Z., HARELL, A. & SÖMJEN, D. 1988. The transduction of mechanical force into biochemical events in bone cells may involve activation of phospholipase A2. *Calcif Tissue Int,* 42**,** 261-6.

BIRMINGHAM, E., NIEBUR, G. L., MCHUGH, P. E., SHAW, G., BARRY, F. P. & MCNAMARA, L. M. 2012. Osteogenic differentiation of mesenchymal stem cells is regulated by osteocyte and osteoblast cells in a simplified bone niche. *Eur Cell Mater,* 23**,** 13-27.

BODENNER, D., REDMAN, C. & RIGGS, A. 2007. Teriparatide in the management of osteoporosis. *Clin Interv Aging,* 2**,** 499-507.

BODINE, P. V. & KOMM, B. S. 2006. Wnt signaling and osteoblastogenesis. *Rev Endocr Metab Disord,* 7**,** 33-9.

BRADY, R. T., O'BRIEN, F. J. & HOEY, D. A. 2015. Mechanically stimulated bone cells secrete paracrine factors that regulate osteoprogenitor recruitment, proliferation, and differentiation. *Biochem Biophys Res Commun,* 459**,** 118-23.

BROWN, J. P., JOSSE, R. G. & CANADA, S. A. C. O. T. O. S. O. 2002. 2002 clinical practice guidelines for the diagnosis and management of osteoporosis in Canada. *CMAJ,* 167**,** S1-34.

BRYANT, J. D. 1983. The effect of impact on the marrow pressure of long bones in vitro. *J Biomech,* 16**,** 659-65.

CAIROLI, E., ELLER-VAINICHER, C., ULIVIERI, F. M., ZHUKOUSKAYA, V. V., PALMIERI, S., MORELLI, V., BECK-PECCOZ, P. & CHIODINI, I. 2014. Factors associated with bisphosphonate treatment failure in postmenopausal women with primary osteoporosis. *Osteoporos Int,* 25**,** 1401-10.

CAPLAN, A. I. 1991. Mesenchymal stem cells. *J Orthop Res,* 9**,** 641-50.

CASTILLO, A. B. & JACOBS, C. R. 2010. Mesenchymal stem cell mechanobiology. *Curr Osteoporos Rep,* 8**,** 98-104.

CAVANAUGH, D. J. & CANN, C. E. 1988. Brisk walking does not stop bone loss in postmenopausal women. *Bone,* 9**,** 201-4.

CHAN, C. K., SEO, E. Y., CHEN, J. Y., LO, D., MCARDLE, A., SINHA, R., TEVLIN, R., SEITA, J., VINCENT-TOMPKINS, J., WEARDA, T., LU, W. J., SENARATH-YAPA, K., CHUNG, M. T., MARECIC, O., TRAN, M., YAN, K. S., UPTON, R., WALMSLEY, G. G., LEE, A. S., SAHOO, D., KUO, C. J., WEISSMAN, I. L. & LONGAKER, M. T. 2015. Identification and specification of the mouse skeletal stem cell. *Cell,* 160**,** 285-98.

CHAN, C. K. F., GULATI, G. S., SINHA, R., TOMPKINS, J. V., LOPEZ, M., CARTER, A. C., RANSOM, R. C., REINISCH, A., WEARDA, T., MURPHY, M., BREWER, R. E., KOEPKE, L. S., MARECIC, O., MANJUNATH, A., SEO, E. Y., LEAVITT, T., LU, W. J., NGUYEN, A., CONLEY, S. D., SALHOTRA, A., AMBROSI, T. H., BORRELLI, M. R., SIEBEL, T., CHAN, K., SCHALLMOSER, K., SEITA, J., SAHOO, D., GOODNOUGH, H., BISHOP, J., GARDNER, M., MAJETI, R., WAN, D. C., GOODMAN, S., WEISSMAN, I. L., CHANG, H. Y. & LONGAKER, M. T. 2018. Identification of the Human Skeletal Stem Cell. *Cell,* 175**,** 43-56 e21.

CHEN, J. C., HOEY, D. A., CHUA, M., BELLON, R. & JACOBS, C. R. 2015. Mechanical signals promote osteogenic fate through a primary cilia-mediated mechanism. *Faseb j*.

CHEN, J. C., HOEY, D. A., CHUA, M., BELLON, R. & JACOBS, C. R. 2016a. Mechanical signals promote osteogenic fate through a primary cilia-mediated mechanism. *FASEB J,* 30**,** 1504-11.

CHEN, Q., SHOU, P., ZHENG, C., JIANG, M., CAO, G., YANG, Q., CAO, J., XIE, N., VELLETRI, T., ZHANG, X., XU, C., ZHANG, L., YANG, H., HOU, J., WANG, Y. & SHI, Y. 2016b. Fate decision of mesenchymal stem cells: adipocytes or osteoblasts? *Cell Death Differ,* 23**,** 1128-39.

CHEN, Y., WHETSTONE, H. C., LIN, A. C., NADESAN, P., WEI, Q., POON, R. & ALMAN, B. A. 2007. Beta-catenin signaling plays a disparate role in different phases of fracture repair: implications for therapy to improve bone healing. *PLoS Med,* 4**,** e249.

CHERIAN, P. P., CHENG, B., GU, S., SPRAGUE, E., BONEWALD, L. F. & JIANG, J. X. 2003. Effects of mechanical strain on the function of Gap junctions in osteocytes are mediated through the prostaglandin EP2 receptor. *J Biol Chem,* 278**,** 43146-56.

CHERIAN, P. P., SILLER-JACKSON, A. J., GU, S., WANG, X., BONEWALD, L. F., SPRAGUE, E. & JIANG, J. X. 2005. Mechanical strain opens connexin 43 hemichannels in osteocytes: a novel mechanism for the release of prostaglandin. *Mol Biol Cell,* 16**,** 3100-6.

CHUBINSKIY-NADEZHDIN, V. I., VASILEVA, V. Y., PUGOVKINA, N. A., VASSILIEVA, I. O., MORACHEVSKAYA, E. A., NIKOLSKY, N. N. & NEGULYAEV, Y. A. 2017. Local calcium signalling is mediated by mechanosensitive ion channels in mesenchymal stem cells. *Biochem Biophys Res Commun,* 482**,** 563-568.

CLAPHAM, D. E. 2007. Calcium signaling. *Cell,* 131**,** 1047-58.

COMPSTON, J. 2011. Age-related changes in bone remodelling and structure in men: histomorphometric studies. *J Osteoporos,* 2011**,** 108324.

COOPER, C., ATKINSON, E. J., JACOBSEN, S. J., O'FALLON, W. M. & MELTON, L. J. 1993. Population-based study of survival after osteoporotic fractures. *Am J Epidemiol,* 137**,** 1001-5.

CORN, D. J., KIM, Y., KREBS, M. D., MOUNTS, T., MOLTER, J., GERSON, S., ALSBERG, E., DENNIS, J. E. & LEE, Z. 2013. Imaging early stage osteogenic differentiation of mesenchymal stem cells. *J Orthop Res,* 31**,** 871-9.

CORRAL, D. A., AMLING, M., PRIEMEL, M., LOYER, E., FUCHS, S., DUCY, P., BARON, R. & KARSENTY, G. 1998. Dissociation between bone resorption and bone formation in osteopenic transgenic mice. *Proc Natl Acad Sci U S A,* 95**,** 13835-40.

CORRIGAN, M. A., FERRADAES, T. M., RIFFAULT, M. & HOEY, D. A. 2019. Ciliotherapy Treatments to Enhance Biochemically- and Biophysically-Induced Mesenchymal Stem Cell Osteogenesis: A Comparison Study. *Cellular and Molecular Bioengineering,* 12**,** 53-67.

CORRIGAN, M. A., JOHNSON, G. P., STAVENSCHI, E., RIFFAULT, M., LABOUR, M. N. & HOEY, D. A. 2018. TRPV4-mediates oscillatory fluid shear mechanotransduction in mesenchymal stem cells in part via the primary cilium. *Sci Rep,* 8**,** 3824.

COSMAN, F., DE BEUR, S. J., LEBOFF, M. S., LEWIECKI, E. M., TANNER, B., RANDALL, S., LINDSAY, R. & FOUNDATION, N. O. 2014. Clinician's Guide to Prevention and Treatment of Osteoporosis. *Osteoporos Int,* 25**,** 2359-81.

COUGHLIN, T. R. & NIEBUR, G. L. 2012. Fluid shear stress in trabecular bone marrow due to low-magnitude high-frequency vibration. *J Biomech,* 45**,** 2222-9.

COUGHLIN, T. R., VOISIN, M., SCHAFFLER, M. B., NIEBUR, G. L. & MCNAMARA, L. M. 2015. Primary cilia exist in a small fraction of cells in trabecular bone and marrow. *Calcif Tissue Int,* 96**,** 65-72.
COWIN, S. C. 1986. Wolff's law of trabecular architecture at remodeling equilibrium. *J Biomech Eng,* 108**,** 83-8.
CROCKETT, J. C., ROGERS, M. J., COXON, F. P., HOCKING, L. J. & HELFRICH, M. H. 2011. Bone remodelling at a glance. *J Cell Sci,* 124**,** 991-8.
CURRAN, G. & RAVINDRAN, A. 2014. Lithium for bipolar disorder: a review of the recent literature. *Expert Rev Neurother,* 14**,** 1079-98.
D'IPPOLITO, G., SCHILLER, P. C., RICORDI, C., ROOS, B. A. & HOWARD, G. A. 1999. Age-related osteogenic potential of mesenchymal stromal stem cells from human vertebral bone marrow. *J Bone Miner Res,* 14**,** 1115-22.
DALBAY, M. T., THORPE, S. D., CONNELLY, J. T., CHAPPLE, J. P. & KNIGHT, M. M. 2015. Adipogenic Differentiation of hMSCs is Mediated by Recruitment of IGF-1r Onto the Primary Cilium Associated With Cilia Elongation. *Stem Cells,* 33**,** 1952-61.
DE VERNEJOUL, M. C. 1989. Bone remodelling in osteoporosis. *Clin Rheumatol,* 8 Suppl 2**,** 13-5.
DELAINE-SMITH, R. M. & REILLY, G. C. 2012. Mesenchymal stem cell responses to mechanical stimuli. *Muscles Ligaments Tendons J,* 2**,** 169-80.
DELAISSE, J. M. 2014. The reversal phase of the bone-remodeling cycle: cellular prerequisites for coupling resorption and formation. *Bonekey Rep,* 3**,** 561.
DELMAS, P. 2004. Polycystins: from mechanosensation to gene regulation. *Cell,* 118**,** 145-8.
DEMONTIERO, O., VIDAL, C. & DUQUE, G. 2012. Aging and bone loss: new insights for the clinician. *Ther Adv Musculoskelet Dis,* 4**,** 61-76.
DENG, Z., PAKNEJAD, N., MAKSAEV, G., SALA-RABANAL, M., NICHOLS, C. G., HITE, R. K. & YUAN, P. 2018. Cryo-EM and X-ray structures of TRPV4 reveal insight into ion permeation and gating mechanisms. *Nat Struct Mol Biol,* 25**,** 252-260.
DOMINICI, M., LE BLANC, K., MUELLER, I., SLAPER-CORTENBACH, I., MARINI, F., KRAUSE, D., DEANS, R., KEATING, A., PROCKOP, D. & HORWITZ, E. 2006. Minimal criteria for defining multipotent mesenchymal stromal cells. The International Society for Cellular Therapy position statement. *Cytotherapy,* 8**,** 315-7.
DOMINICI, M., PRITCHARD, C., GARLITS, J. E., HOFMANN, T. J., PERSONS, D. A. & HORWITZ, E. M. 2004. Hematopoietic cells and osteoblasts are derived from a common marrow progenitor after bone marrow transplantation. *Proc Natl Acad Sci U S A,* 101**,** 11761-6.
DONOSO, O., PINO, A. M., SEITZ, G., OSSES, N. & RODRÍGUEZ, J. P. 2015. Osteoporosis-associated alteration in the signalling status of BMP-2 in human MSCs under adipogenic conditions. *J Cell Biochem,* 116**,** 1267-77.
DOWNEY, D. J., SIMKIN, P. A. & TAGGART, R. 1988. The effect of compressive loading on intraosseous pressure in the femoral head in vitro. *J Bone Joint Surg Am,* 70**,** 871-7.
DOWNS, M. E., NGUYEN, A. M., HERZOG, F. A., HOEY, D. A. & JACOBS, C. R. 2014a. An experimental and computational analysis of primary cilia deflection under fluid flow. *Comput Methods Biomech Biomed Engin,* 17**,** 2-10.
DOWNS, M. E., NGUYEN, A. M., HERZOG, F. A., HOEY, D. A. & JACOBS, C. R. 2014b. An experimental and computational analysis of primary cilia deflection

under fluid flow. *Computer Methods in Biomechanics and Biomedical Engineering,* 17**,** 2-10.
DRAKE, M. T., CLARKE, B. L. & KHOSLA, S. 2008. Bisphosphonates: mechanism of action and role in clinical practice. *Mayo Clin Proc,* 83**,** 1032-45.
DUCHER, G., JAFFRÉ, C., ARLETTAZ, A., BENHAMOU, C. L. & COURTEIX, D. 2005. Effects of long-term tennis playing on the muscle-bone relationship in the dominant and nondominant forearms. *Can J Appl Physiol,* 30**,** 3-17.
DUMMER, A., POELMA, C., DERUITER, M. C., GOUMANS, M. J. & HIERCK, B. P. 2016. Measuring the primary cilium length: improved method for unbiased high-throughput analysis. *Cilia,* 5**,** 7.
DUNCAN, R. L. & TURNER, C. H. 1995. Mechanotransduction and the functional response of bone to mechanical strain. *Calcif Tissue Int,* 57**,** 344-58.
DUQUE, G. & TROEN, B. R. 2008. Understanding the mechanisms of senile osteoporosis: new facts for a major geriatric syndrome. *J Am Geriatr Soc,* 56**,** 935-41.
EASTELL, R., ROBINS, S. P., COLWELL, T., ASSIRI, A. M., RIGGS, B. L. & RUSSELL, R. G. 1993. Evaluation of bone turnover in type I osteoporosis using biochemical markers specific for both bone formation and bone resorption. *Osteoporos Int,* 3**,** 255-60.
EDMONDSON, R., BROGLIE, J. J., ADCOCK, A. F. & YANG, L. J. 2014. Three-Dimensional Cell Culture Systems and Their Applications in Drug Discovery and Cell-Based Biosensors. *Assay and Drug Development Technologies,* 12**,** 207-218.
EL HAJ, A. J., WALKER, L. M., PRESTON, M. R. & PUBLICOVER, S. J. 1999. Mechanotransduction pathways in bone: calcium fluxes and the role of voltage-operated calcium channels. *Med Biol Eng Comput,* 37**,** 403-9.
ESPINHA, L. C., HOEY, D. A., FERNANDES, P. R., RODRIGUES, H. C. & JACOBS, C. R. 2014. Oscillatory fluid flow influences primary cilia and microtubule mechanics. *Cytoskeleton (Hoboken),* 71**,** 435-45.
EVENEPOEL, P., D'HAESE, P. & BRANDENBURG, V. 2014. Romosozumab in Postmenopausal Women with Osteopenia. *New England Journal of Medicine,* 370**,** 1664-1664.
FARAJI, A., ABTAHI, S., GHADERI, A. & SAMSAMI DEHAGHANI, A. 2016. Transforming Growth Factor β1 (TGF-β1) in the Sera of Postmenopausal Osteoporotic Females. *Int J Endocrinol Metab,* 14**,** e36511.
FIEDLER, J., RÖDERER, G., GÜNTHER, K. P. & BRENNER, R. E. 2002. BMP-2, BMP-4, and PDGF-bb stimulate chemotactic migration of primary human mesenchymal progenitor cells. *J Cell Biochem,* 87**,** 305-12.
FORSYTH, J. J. & DAVEY, R. C. 2008. Bone Health. *In:* BUCKLEY, J. P. (ed.) *Exercise Physiology in Special Populations.* Churchill Livingstone.
FORWOOD, M. R. 1996. Inducible cyclo-oxygenase (COX-2) mediates the induction of bone formation by mechanical loading in vivo. *J Bone Miner Res,* 11**,** 1688-93.
FROST, H. M. 1987. Bone "mass" and the "mechanostat": a proposal. *Anat Rec,* 219**,** 1-9.
FROST, H. M. 1990. Skeletal structural adaptations to mechanical usage (SATMU): 1. Redefining Wolff's law: the bone modeling problem. *Anat Rec,* 226**,** 403-13.
FROST, H. M. 1992. The role of changes in mechanical usage set points in the pathogenesis of osteoporosis. *J Bone Miner Res,* 7**,** 253-61.

FROST, H. M. 2003. Bone's mechanostat: a 2003 update. *Anat Rec A Discov Mol Cell Evol Biol,* 275**,** 1081-101.
FYHRIE, D. P. & CHRISTIANSEN, B. A. 2015. Bone Material Properties and Skeletal Fragility. *Calcif Tissue Int,* 97**,** 213-28.
GENNARI, L., MERLOTTI, D. & NUTI, R. 2010. Selective estrogen receptor modulator (SERM) for the treatment of osteoporosis in postmenopausal women: focus on lasofoxifene. *Clin Interv Aging,* 5**,** 19-29.
GIACHELLI, C. M. & STEITZ, S. 2000. Osteopontin: a versatile regulator of inflammation and biomineralization. *Matrix Biol,* 19**,** 615-22.
GIULIANI, N., LISIGNOLI, G., MAGNANI, M., RACANO, C., BOLZONI, M., DALLA PALMA, B., SPOLZINO, A., MANFERDINI, C., ABATI, C., TOSCANI, D., FACCHINI, A. & AVERSA, F. 2013. New insights into osteogenic and chondrogenic differentiation of human bone marrow mesenchymal stem cells and their potential clinical applications for bone regeneration in pediatric orthopaedics. *Stem Cells Int,* 2013**,** 312501.
GONG, M., BI, Y., JIANG, W., ZHANG, Y., CHEN, L., HOU, N., LIU, Y., WEI, X., CHEN, J. & LI, T. 2011. Immortalized mesenchymal stem cells: an alternative to primary mesenchymal stem cells in neuronal differentiation and neuroregeneration associated studies. *J Biomed Sci,* 18**,** 87.
GREGORY, C. A., YLOSTALO, J. & PROCKOP, D. J. 2005. Adult bone marrow stem/progenitor cells (MSCs) are preconditioned by microenvironmental "niches" in culture: a two-stage hypothesis for regulation of MSC fate. *Sci STKE,* 2005**,** pe37.
GUIMARÃES-CAMBOA, N., CATTANEO, P., SUN, Y., MOORE-MORRIS, T., GU, Y., DALTON, N. D., ROCKENSTEIN, E., MASLIAH, E., PETERSON, K. L., STALLCUP, W. B., CHEN, J. & EVANS, S. M. 2017. Pericytes of Multiple Organs Do Not Behave as Mesenchymal Stem Cells In Vivo. *Cell Stem Cell,* 20**,** 345-359.e5.
GULLBERG, B., JOHNELL, O. & KANIS, J. A. 1997. World-wide projections for hip fracture. *Osteoporos Int,* 7**,** 407-13.
GURKAN, U. A. & AKKUS, O. 2008. The mechanical environment of bone marrow: a review. *Ann Biomed Eng,* 36**,** 1978-91.
HAAPASALO, H., KONTULAINEN, S., SIEVÄNEN, H., KANNUS, P., JÄRVINEN, M. & VUORI, I. 2000. Exercise-induced bone gain is due to enlargement in bone size without a change in volumetric bone density: a peripheral quantitative computed tomography study of the upper arms of male tennis players. *Bone,* 27**,** 351-7.
HAASTERS, F., DOCHEVA, D., GASSNER, C., POPOV, C., BÖCKER, W., MUTSCHLER, W., SCHIEKER, M. & PRALL, W. C. 2014. Mesenchymal stem cells from osteoporotic patients reveal reduced migration and invasion upon stimulation with BMP-2 or BMP-7. *Biochem Biophys Res Commun,* 452**,** 118-23.
HADJIDAKIS, D. J. & ANDROULAKIS, I. I. 2006. Bone remodeling. *Ann N Y Acad Sci,* 1092**,** 385-96.
HAMMETT-STABLER, C. A. 2004. *Osteoporosis: From Pathophysiology to Treatment : Special Topics in Diagnostic Testing,* AACC Press.
HARDING, A. T. & BECK, B. R. 2017. Exercise, Osteoporosis, and Bone Geometry. *Sports (Basel),* 5.
HART, N. H., NIMPHIUS, S., RANTALAINEN, T., IRELAND, A., SIAFARIKAS, A. & NEWTON, R. U. 2017. Mechanical basis of bone strength: influence of bone

material, bone structure and muscle action. *J Musculoskelet Neuronal Interact,* 17**,** 114-139.
HAYCRAFT, C. J., ZHANG, Q., SONG, B., JACKSON, W. S., DETLOFF, P. J., SERRA, R. & YODER, B. K. 2007. Intraflagellar transport is essential for endochondral bone formation. *Development,* 134**,** 307-16.
HE, X., WANG, H., JIN, T., XU, Y., MEI, L. & YANG, J. 2016. TLR4 Activation Promotes Bone Marrow MSC Proliferation and Osteogenic Differentiation via Wnt3a and Wnt5a Signaling. *PLoS One,* 11**,** e0149876.
HENSTOCK, J. R., ROTHERHAM, M. & EL HAJ, A. J. 2018. Magnetic ion channel activation of TREK1 in human mesenchymal stem cells using nanoparticles promotes osteogenesis in surrounding cells. *J Tissue Eng,* 9**,** 2041731418808695.
HERNLUND, E., SVEDBOM, A., IVERGÅRD, M., COMPSTON, J., COOPER, C., STENMARK, J., MCCLOSKEY, E. V., JÖNSSON, B. & KANIS, J. A. 2013. Osteoporosis in the European Union: medical management, epidemiology and economic burden. A report prepared in collaboration with the International Osteoporosis Foundation (IOF) and the European Federation of Pharmaceutical Industry Associations (EFPIA). *Arch Osteoporos,* 8**,** 136.
HESS, R., PINO, A. M., RÍOS, S., FERNÁNDEZ, M. & RODRÍGUEZ, J. P. 2005. High affinity leptin receptors are present in human mesenchymal stem cells (MSCs) derived from control and osteoporotic donors. *J Cell Biochem,* 94**,** 50-7.
HILDEBRANDT, F., BENZING, T. & KATSANIS, N. 2011. Mechanisms of Disease: Ciliopathies. *New England Journal of Medicine,* 364**,** 1533-1543.
HILGENDORF, K. I., JOHNSON, C. T. & JACKSON, P. K. 2016. The primary cilium as a cellular receiver: organizing ciliary GPCR signaling. *Curr Opin Cell Biol,* 39**,** 84-92.
HOEY, D. A., CHEN, J. C. & JACOBS, C. R. 2012a. The primary cilium as a novel extracellular sensor in bone. *Front Endocrinol (Lausanne),* 3**,** 75.
HOEY, D. A., DOWNS, M. E. & JACOBS, C. R. 2012b. The mechanics of the primary cilium: an intricate structure with complex function. *J Biomech,* 45**,** 17-26.
HOEY, D. A., DOWNS, M. E. & JACOBS, C. R. 2012c. The mechanics of the primary cilium: An intricate structure with complex function. *Journal of Biomechanics,* 45**,** 17-26.
HOEY, D. A., TORMEY, S., RAMCHARAN, S., O'BRIEN, F. J. & JACOBS, C. R. 2012d. Primary cilia-mediated mechanotransduction in human mesenchymal stem cells. *Stem Cells,* 30**,** 2561-70.
HU, K., SUN, H., GUI, B. & SUI, C. 2017. TRPV4 functions in flow shear stress induced early osteogenic differentiation of human bone marrow mesenchymal stem cells. *Biomed Pharmacother,* 91**,** 841-848.
HUANG, H., KIM, H. J., CHANG, E. J., LEE, Z. H., HWANG, S. J., KIM, H. M., LEE, Y. & KIM, H. H. 2009. IL-17 stimulates the proliferation and differentiation of human mesenchymal stem cells: implications for bone remodeling. *Cell Death Differ,* 16**,** 1332-43.
HUANG, W. & OLSEN, B. R. 2015. Skeletal defects in Osterix-Cre transgenic mice. *Transgenic Res,* 24**,** 167-72.
HUBER, C. & CORMIER-DAIRE, V. 2012. Ciliary disorder of the skeleton. *Am J Med Genet C Semin Med Genet,* 160C**,** 165-74.
HUSE, M. 2017. Mechanical forces in the immune system. *Nat Rev Immunol,* 17**,** 679-690.

INGBER, D. E. 2006. Cellular mechanotransduction: putting all the pieces together again. *FASEB J,* 20**,** 811-27.
IRIANTO, J., RAMASWAMY, G., SERRA, R. & KNIGHT, M. M. 2014. Depletion of chondrocyte primary cilia reduces the compressive modulus of articular cartilage. *J Biomech,* 47**,** 579-82.
JACOBS, C. R., YELLOWLEY, C. E., DAVIS, B. R., ZHOU, Z., CIMBALA, J. M. & DONAHUE, H. J. 1998. Differential effect of steady versus oscillating flow on bone cells. *J Biomech,* 31**,** 969-76.
JAISWAL, N., HAYNESWORTH, S. E., CAPLAN, A. I. & BRUDER, S. P. 1997. Osteogenic differentiation of purified, culture-expanded human mesenchymal stem cells in vitro. *J Cell Biochem,* 64**,** 295-312.
JAMES, A. W. 2013. Review of Signaling Pathways Governing MSC Osteogenic and Adipogenic Differentiation. *Scientifica (Cairo),* 2013**,** 684736.
JANDEROVÁ, L., MCNEIL, M., MURRELL, A. N., MYNATT, R. L. & SMITH, S. R. 2003. Human mesenchymal stem cells as an in vitro model for human adipogenesis. *Obes Res,* 11**,** 65-74.
JANSEN, K. A., DONATO, D. M., BALCIOGLU, H. E., SCHMIDT, T., DANEN, E. H. & KOENDERINK, G. H. 2015. A guide to mechanobiology: Where biology and physics meet. *Biochim Biophys Acta,* 1853**,** 3043-52.
JING, H., LIAO, L., AN, Y., SU, X., LIU, S., SHUAI, Y., ZHANG, X. & JIN, Y. 2016. Suppression of EZH2 Prevents the Shift of Osteoporotic MSC Fate to Adipocyte and Enhances Bone Formation During Osteoporosis. *Mol Ther,* 24**,** 217-229.
JONES, D. B., NOLTE, H., SCHOLÜBBERS, J. G., TURNER, E. & VELTEL, D. 1991. Biochemical signal transduction of mechanical strain in osteoblast-like cells. *Biomaterials,* 12**,** 101-10.
JONES, E. & SCHÄFER, R. 2015. Where is the common ground between bone marrow mesenchymal stem/stromal cells from different donors and species? *Stem Cell Res Ther,* 6**,** 143.
JONES, H. H., PRIEST, J. D., HAYES, W. C., TICHENOR, C. C. & NAGEL, D. A. 1977. Humeral hypertrophy in response to exercise. *J Bone Joint Surg Am,* 59**,** 204-8.
KAHLES, F., FINDEISEN, H. M. & BRUEMMER, D. 2014. Osteopontin: A novel regulator at the cross roads of inflammation, obesity and diabetes. *Mol Metab,* 3**,** 384-93.
KANG, S. S., SHIN, S. H., AUH, C. K. & CHUN, J. 2012. Human skeletal dysplasia caused by a constitutive activated transient receptor potential vanilloid 4 (TRPV4) cation channel mutation. *Experimental and Molecular Medicine,* 44**,** 707-722.
KANIS, J. A. 2007. Assessment of osteoporosis at the primary health-care level. Technical Report. University of Shefflied, UK: World Health Organization Collaborating Centre for Metabolic Bone Diseases.
KANIS, J. A. & JOHNELL, O. 2005. Requirements for DXA for the management of osteoporosis in Europe. *Osteoporos Int,* 16**,** 229-38.
KANIS, J. A., JOHNELL, O., DE LAET, C., JOHANSSON, H., ODEN, A., DELMAS, P., EISMAN, J., FUJIWARA, S., GARNERO, P., KROGER, H., MCCLOSKEY, E. V., MELLSTROM, D., MELTON, L. J., POLS, H., REEVE, J., SILMAN, A. & TENENHOUSE, A. 2004. A meta-analysis of previous fracture and subsequent fracture risk. *Bone,* 35**,** 375-82.

KANIS, J. A., JOHNELL, O., ODEN, A., SEMBO, I., REDLUND-JOHNELL, I., DAWSON, A., DE LAET, C. & JONSSON, B. 2000. Long-term risk of osteoporotic fracture in Malmö. *Osteoporos Int,* 11**,** 669-74.

KANIS, J. A., MELTON, L. J., CHRISTIANSEN, C., JOHNSTON, C. C. & KHALTAEV, N. 1994. The diagnosis of osteoporosis. *J Bone Miner Res,* 9**,** 1137-41.

KATHEM, S., MOHIELDIN, A., ABDUL-MAJEED, S., ISMAIL, S., ALTAEI, Q., ALSHIMMARI, I., ALSAIDI, M., KHAMMAS, H., NAULI, A., JOE, B. & NAULI, S. 2014a. Ciliotherapy: a novel intervention in polycystic kidney disease. *Journal of Geriatric Cardiology,* 11**,** 63-73.

KATHEM, S. H., MOHIELDIN, A. M., ABDUL-MAJEED, S., ISMAIL, S. H., ALTAEI, Q. H., ALSHIMMARI, I. K., ALSAIDI, M. M., KHAMMAS, H., NAULI, A. M., JOE, B. & NAULI, S. M. 2014b. Ciliotherapy: a novel intervention in polycystic kidney disease. *J Geriatr Cardiol,* 11**,** 63-73.

KATSIMBRI, P. 2017. The biology of normal bone remodelling. *Eur J Cancer Care (Engl),* 26.

KAUFMANN, J., LEMASTER, M., MATERN, P., MORRISON-GRAHAM, K., QUICK, D. & RUNYEON, J. 2018. *Anatomy & Physiology,* OpenStax

KEENE, G. S., PARKER, M. J. & PRYOR, G. A. 1993. Mortality and morbidity after hip fractures. *BMJ,* 307**,** 1248-50.

KENNEL, K. A. & DRAKE, M. T. 2009. Adverse effects of bisphosphonates: implications for osteoporosis management. *Mayo Clin Proc,* 84**,** 632-7; quiz 638.

KHOSLA, S. & HOFBAUER, L. C. 2017. Osteoporosis treatment: recent developments and ongoing challenges. *Lancet Diabetes Endocrinol,* 5**,** 898-907.

KHOSLA, S. & SHANE, E. 2016. A Crisis in the Treatment of Osteoporosis. *J Bone Miner Res,* 31**,** 1485-7.

KLEIN-NULEND, J., BACABAC, R. G. & BAKKER, A. D. 2012. Mechanical loading and how it affects bone cells: the role of the osteocyte cytoskeleton in maintaining our skeleton. *Eur Cell Mater,* 24**,** 278-91.

KLING, J. M., CLARKE, B. L. & SANDHU, N. P. 2014. Osteoporosis prevention, screening, and treatment: a review. *J Womens Health (Larchmt),* 23**,** 563-72.

KNIGHT, M. N. & HANKENSON, K. D. 2013. Mesenchymal Stem Cells in Bone Regeneration. *Adv Wound Care (New Rochelle),* 2**,** 306-316.

KOMM, B. S., MORGENSTERN, D., L, A. Y. & JENKINS, S. N. 2015. The safety and tolerability profile of therapies for the prevention and treatment of osteoporosis in postmenopausal women. *Expert Rev Clin Pharmacol,* 8**,** 769-84.

KOTTGEN, M., BUCHHOLZ, B., GARCIA-GONZALEZ, M. A., KOTSIS, F., FU, X., DOERKEN, M., BOEHLKE, C., STEFFL, D., TAUBER, R., WEGIERSKI, T., NITSCHKE, R., SUZUKI, M., KRAMER-ZUCKER, A., GERMINO, G. G., WATNICK, T., PRENEN, J., NILIUS, B., KUEHN, E. W. & WALZ, G. 2008. TRPP2 and TRPV4 form a polymodal sensory channel complex. *J Cell Biol,* 182**,** 437-47.

KREKE, M. R., HUCKLE, W. R. & GOLDSTEIN, A. S. 2005. Fluid flow stimulates expression of osteopontin and bone sialoprotein by bone marrow stromal cells in a temporally dependent manner. *Bone,* 36**,** 1047-55.

KRISTENSEN, H. B., ANDERSEN, T. L., MARCUSSEN, N., ROLIGHED, L. & DELAISSE, J. M. 2014. Osteoblast recruitment routes in human cancellous bone remodeling. *Am J Pathol,* 184**,** 778-89.

KRØLNER, B., TOFT, B., PORS NIELSEN, S. & TØNDEVOLD, E. 1983. Physical exercise as prophylaxis against involutional vertebral bone loss: a controlled trial. *Clin Sci (Lond),* 64**,** 541-6.

KUMAR, S., DAVIS, P. R. & PICKLES, B. 1979. Bone-marrow pressure and bone strength. *Acta Orthop Scand,* 50**,** 507-12.

KWON, R. Y., TEMIYASATHIT, S., TUMMALA, P., QUAH, C. C. & JACOBS, C. R. 2010. Primary cilium-dependent mechanosensing is mediated by adenylyl cyclase 6 and cyclic AMP in bone cells. *FASEB J,* 24**,** 2859-68.

KÖTTGEN, M., BUCHHOLZ, B., GARCIA-GONZALEZ, M. A., KOTSIS, F., FU, X., DOERKEN, M., BOEHLKE, C., STEFFL, D., TAUBER, R., WEGIERSKI, T., NITSCHKE, R., SUZUKI, M., KRAMER-ZUCKER, A., GERMINO, G. G., WATNICK, T., PRENEN, J., NILIUS, B., KUEHN, E. W. & WALZ, G. 2008. TRPP2 and TRPV4 form a polymodal sensory channel complex. *J Cell Biol,* 182**,** 437-47.

LABOUR, M. N., RIFFAULT, M., CHRISTENSEN, S. T. & HOEY, D. A. 2016a. TGF beta 1-induced recruitment of human bone mesenchymal stem cells is mediated by the primary cilium in a SMAD3-dependent manner. *Scientific Reports,* 6.

LABOUR, M. N., RIFFAULT, M., CHRISTENSEN, S. T. & HOEY, D. A. 2016b. TGFbeta1 - induced recruitment of human bone mesenchymal stem cells is mediated by the primary cilium in a SMAD3-dependent manner. *Sci Rep,* 6**,** 35542.

LABOUR, M. N., RIFFAULT, M., CHRISTENSEN, S. T. & HOEY, D. A. 2016c. TGFβ1 - induced recruitment of human bone mesenchymal stem cells is mediated by the primary cilium in a SMAD3-dependent manner. *Sci Rep,* 6**,** 35542.

LEE, D. J., TSENG, H. C., WONG, S. W., WANG, Z., DENG, M. & KO, C. C. 2015a. Dopaminergic effects on in vitro osteogenesis. *Bone Res,* 3**,** 15020.

LEE, E. U., KIM, D. J., LIM, H. C., LEE, J. S., JUNG, U. W. & CHOI, S. H. 2015b. Comparative evaluation of biphasic calcium phosphate and biphasic calcium phosphate collagen composite on osteoconductive potency in rabbit calvarial defect. *Biomater Res,* 19**,** 1.

LEE, K. L., GUEVARRA, M. D., NGUYEN, A. M., CHUA, M. C., WANG, Y. & JACOBS, C. R. 2015c. The primary cilium functions as a mechanical and calcium signaling nexus. *Cilia,* 4**,** 7.

LEVI, B., WAN, D. C., GLOTZBACH, J. P., HYUN, J., JANUSZYK, M., MONTORO, D., SORKIN, M., JAMES, A. W., NELSON, E. R., LI, S., QUARTO, N., LEE, M., GURTNER, G. C. & LONGAKER, M. T. 2011. CD105 protein depletion enhances human adipose-derived stromal cell osteogenesis through reduction of transforming growth factor β1 (TGF-β1) signaling. *J Biol Chem,* 286**,** 39497-509.

LI, L., YAO, X. L., HE, X. L., LIU, X. J., WU, W. C., KUANG, W. & TANG, M. 2013. Role of mechanical strain and estrogen in modulating osteogenic differentiation of mesenchymal stem cells (MSCs) from normal and ovariectomized rats. *Cell Mol Biol (Noisy-le-grand),* Suppl 59**,** OL1889-93.

LI, Y. J., BATRA, N. N., YOU, L., MEIER, S. C., COE, I. A., YELLOWLEY, C. E. & JACOBS, C. R. 2004. Oscillatory fluid flow affects human marrow stromal cell proliferation and differentiation. *J Orthop Res,* 22**,** 1283-9.

LIU, C., ZHAO, Y., CHEUNG, W. Y., GANDHI, R., WANG, L. & YOU, L. 2010a. Effects of cyclic hydraulic pressure on osteocytes. *Bone,* 46**,** 1449-56.

LIU, J., ZHAO, Z., LI, J., ZOU, L., SHULER, C., ZOU, Y., HUANG, X., LI, M. & WANG, J. 2009. Hydrostatic pressures promote initial osteodifferentiation with ERK1/2 not p38 MAPK signaling involved. *J Cell Biochem,* 107**,** 224-32.

LIU, L., YUAN, W. & WANG, J. 2010b. Mechanisms for osteogenic differentiation of human mesenchymal stem cells induced by fluid shear stress. *Biomech Model Mechanobiol,* 9**,** 659-70.

LIU, Y. S., LIU, Y. A., HUANG, C. J., YEN, M. H., TSENG, C. T., CHIEN, S. & LEE, O. K. 2015. Mechanosensitive TRPM7 mediates shear stress and modulates osteogenic differentiation of mesenchymal stromal cells through Osterix pathway. *Sci Rep,* 5**,** 16522.

LUND, S. A., GIACHELLI, C. M. & SCATENA, M. 2009. The role of osteopontin in inflammatory processes. *J Cell Commun Signal,* 3**,** 311-22.

LUO, N., CONWELL, M. D., CHEN, X., KETTENHOFEN, C. I., WESTLAKE, C. J., CANTOR, L. B., WELLS, C. D., WEINREB, R. N., CORSON, T. W., SPANDAU, D. F., JOOS, K. M., IOMINI, C., OBUKHOV, A. G. & SUN, Y. 2014. Primary cilia signaling mediates intraocular pressure sensation. *Proc Natl Acad Sci U S A,* 111**,** 12871-6.

LYONS, J. S., JOCA, H. C., LAW, R. A., WILLIAMS, K. M., KERR, J. P., SHI, G., KHAIRALLAH, R. J., MARTIN, S. S., KONSTANTOPOULOS, K., WARD, C. W. & STAINS, J. P. 2017. Microtubules tune mechanotransduction through NOX2 and TRPV4 to decrease sclerostin abundance in osteocytes. *Sci Signal,* 10.

MACKAY, A. M., BECK, S. C., MURPHY, J. M., BARRY, F. P., CHICHESTER, C. O. & PITTENGER, M. F. 1998. Chondrogenic differentiation of cultured human mesenchymal stem cells from marrow. *Tissue Eng,* 4**,** 415-28.

MACKIE, E. J., AHMED, Y. A., TATARCZUCH, L., CHEN, K. S. & MIRAMS, M. 2008. Endochondral ossification: how cartilage is converted into bone in the developing skeleton. *Int J Biochem Cell Biol,* 40**,** 46-62.

MANOLAGAS, S. C. & JILKA, R. L. 1995. Bone marrow, cytokines, and bone remodeling. Emerging insights into the pathophysiology of osteoporosis. *N Engl J Med,* 332**,** 305-11.

MARTINAC, B. 2004. Mechanosensitive ion channels: molecules of mechanotransduction. *J Cell Sci,* 117**,** 2449-60.

MATHIEU, P. S. & LOBOA, E. G. 2012. Cytoskeletal and focal adhesion influences on mesenchymal stem cell shape, mechanical properties, and differentiation down osteogenic, adipogenic, and chondrogenic pathways. *Tissue Eng Part B Rev,* 18**,** 436-44.

MATIC, I., MATTHEWS, B. G., WANG, X., DYMENT, N. A., WORTHLEY, D. L., ROWE, D. W., GRCEVIC, D. & KALAJZIC, I. 2016. Quiescent Bone Lining Cells Are a Major Source of Osteoblasts During Adulthood. *Stem Cells,* 34**,** 2930-2942.

MATTHEWS, B. D., THODETI, C. K., TYTELL, J. D., MAMMOTO, A., OVERBY, D. R. & INGBER, D. E. 2010. Ultra-rapid activation of TRPV4 ion channels by mechanical forces applied to cell surface beta1 integrins. *Integr Biol (Camb),* 2**,** 435-42.

MCCLUNG, M. R. 2017. Sclerostin antibodies in osteoporosis: latest evidence and therapeutic potential. *Ther Adv Musculoskelet Dis,* 9**,** 263-270.

MCMAHON, L. A., CAMPBELL, V. A. & PRENDERGAST, P. J. 2008. Involvement of stretch-activated ion channels in strain-regulated glycosaminoglycan

synthesis in mesenchymal stem cell-seeded 3D scaffolds. *J Biomech,* 41**,** 2055-9.
MCMURRAY, R. J., DALBY, M. J. & TSIMBOURI, P. M. 2015. Using biomaterials to study stem cell mechanotransduction, growth and differentiation. *J Tissue Eng Regen Med,* 9**,** 528-39.
MCMURRAY, R. J., WANN, A. K., THOMPSON, C. L., CONNELLY, J. T. & KNIGHT, M. M. 2013. Surface topography regulates wnt signaling through control of primary cilia structure in mesenchymal stem cells. *Sci Rep,* 3**,** 3545.
MCNAMARA, L. M. 2010. Perspective on post-menopausal osteoporosis: establishing an interdisciplinary understanding of the sequence of events from the molecular level to whole bone fractures. *J R Soc Interface,* 7**,** 353-72.
MEHTA, N. M., MALOOTIAN, A. & GILLIGAN, J. P. 2003. Calcitonin for osteoporosis and bone pain. *Curr Pharm Des,* 9**,** 2659-76.
MELTON, L. J., ATKINSON, E. J., O'CONNOR, M. K., O'FALLON, W. M. & RIGGS, B. L. 1998. Bone density and fracture risk in men. *J Bone Miner Res,* 13**,** 1915-23.
MELTON, L. J., CHRISCHILLES, E. A., COOPER, C., LANE, A. W. & RIGGS, B. L. 1992. Perspective. How many women have osteoporosis? *J Bone Miner Res,* 7**,** 1005-10.
METZGER, T. A., KREIPKE, T. C., VAUGHAN, T. J., MCNAMARA, L. M. & NIEBUR, G. L. 2015a. The in situ mechanics of trabecular bone marrow: the potential for mechanobiological response. *J Biomech Eng,* 137.
METZGER, T. A., SCHWANER, S. A., LANEVE, A. J., KREIPKE, T. C. & NIEBUR, G. L. 2015b. Pressure and shear stress in trabecular bone marrow during whole bone loading. *J Biomech,* 48**,** 3035-43.
MICHAEL DELAINE-SMITH, R., JAVAHERI, B., HELEN EDWARDS, J., VAZQUEZ, M. & RUMNEY, R. M. 2015. Preclinical models for in vitro mechanical loading of bone-derived cells. *Bonekey Rep,* 4**,** 728.
MINISOLA, S., CIPRIANI, C., OCCHIUTO, M. & PEPE, J. 2017. New anabolic therapies for osteoporosis. *Intern Emerg Med,* 12**,** 915-921.
MIRZA, F. & CANALIS, E. 2015. Management of endocrine disease: Secondary osteoporosis: pathophysiology and management. *Eur J Endocrinol,* 173**,** R131-51.
MIYANISHI, K., TRINDADE, M. C., LINDSEY, D. P., BEAUPRÉ, G. S., CARTER, D. R., GOODMAN, S. B., SCHURMAN, D. J. & SMITH, R. L. 2006. Effects of hydrostatic pressure and transforming growth factor-beta 3 on adult human mesenchymal stem cell chondrogenesis in vitro. *Tissue Eng,* 12**,** 1419-28.
MIYOSHI, K., KASAHARA, K., MIYAZAKI, I. & ASANUMA, M. 2011. Factors that influence primary cilium length. *Acta Med Okayama,* 65**,** 279-85.
MIZOGUCHI, F., MIZUNO, A., HAYATA, T., NAKASHIMA, K., HELLER, S., USHIDA, T., SOKABE, M., MIYASAKA, N., SUZUKI, M., EZURA, Y. & NODA, M. 2008. Transient receptor potential vanilloid 4 deficiency suppresses unloading-induced bone loss. *J Cell Physiol,* 216**,** 47-53.
MIZOGUCHI, T., PINHO, S., AHMED, J., KUNISAKI, Y., HANOUN, M., MENDELSON, A., ONO, N., KRONENBERG, H. M. & FRENETTE, P. S. 2014. Osterix marks distinct waves of primitive and definitive stromal progenitors during bone marrow development. *Dev Cell,* 29**,** 340-9.
MOERMAN, E. J., TENG, K., LIPSCHITZ, D. A. & LECKA-CZERNIK, B. 2004. Aging activates adipogenic and suppresses osteogenic programs in mesenchymal marrow stroma/stem cells: the role of PPAR-gamma2

transcription factor and TGF-beta/BMP signaling pathways. *Aging Cell,* 3**,** 379-89.
MOORE, E. M., RYU, H. S., ZHU, Y. X. & JACOBS, C. R. 2018a. Adenylyl cyclases and TRPV4 mediate Ca2+/ cAMP dynamics to enhance fluid flow-induced osteogenesis in osteocytes. *Journal of Molecular Biochemistry,* 7**,** 48-59.
MOORE, E. R., ZHU, Y. X., RYU, H. S. & JACOBS, C. R. 2018b. Periosteal progenitors contribute to load-induced bone formation in adult mice and require primary cilia to sense mechanical stimulation. *Stem Cell Res Ther,* 9**,** 190.
MULVIHILL, B. M., MCNAMARA, L. M. & PRENDERGAST, P. J. 2008. Loss of trabeculae by mechano-biological means may explain rapid bone loss in osteoporosis. *J R Soc Interface,* 5**,** 1243-53.
MUSCHLER, G. F., NITTO, H., BOEHM, C. A. & EASLEY, K. A. 2001. Age- and gender-related changes in the cellularity of human bone marrow and the prevalence of osteoblastic progenitors. *J Orthop Res,* 19**,** 117-25.
NAHHAS, R. W., SHERWOOD, R. J., CHUMLEA, W. C., TOWNE, B. & DUREN, D. L. 2013. Predicting the timing of maturational spurts in skeletal age. *Am J Phys Anthropol,* 150**,** 68-75.
NAKAKURA, T., ASANO-HOSHINO, A., SUZUKI, T., ARISAWA, K., TANAKA, H., SEKINO, Y., KIUCHI, Y., KAWAI, K. & HAGIWARA, H. 2015. The elongation of primary cilia via the acetylation of alpha-tubulin by the treatment with lithium chloride in human fibroblast KD cells. *Med Mol Morphol,* 48**,** 44-53.
NAKAMURA, T., NARUSE, M., CHIBA, Y., KOMORI, T., SASAKI, K., IWAMOTO, M. & FUKUMOTO, S. 2015. Novel Hedgehog Agonists Promote Osteoblast Differentiation in Mesenchymal Stem Cells. *Journal of Cellular Physiology,* 230**,** 922-929.
NAULI, S. M., ALENGHAT, F. J., LUO, Y., WILLIAMS, E., VASSILEV, P., LI, X., ELIA, A. E., LU, W., BROWN, E. M., QUINN, S. J., INGBER, D. E. & ZHOU, J. 2003. Polycystins 1 and 2 mediate mechanosensation in the primary cilium of kidney cells. *Nat Genet,* 33**,** 129-37.
NAYLOR, K. E., BRADBURN, M., PAGGIOSI, M. A., GOSSIEL, F., PEEL, N. F. A., MCCLOSKEY, E. V., WALSH, J. S. & EASTELL, R. 2018. Effects of discontinuing oral bisphosphonate treatments for postmenopausal osteoporosis on bone turnover markers and bone density. *Osteoporos Int,* 29**,** 1407-1417.
NILIUS, B. & OWSIANIK, G. 2011. The transient receptor potential family of ion channels. *Genome Biol,* 12**,** 218.
NORDIN, B. E., AARON, J., SPEED, R. & CRILLY, R. G. 1981. Bone formation and resorption as the determinants of trabecular bone volume in postmenopausal osteoporosis. *Lancet,* 2**,** 277-9.
O'CONOR, C. J., GRIFFIN, T. M., LIEDTKE, W. & GUILAK, F. 2013. Increased susceptibility of Trpv4-deficient mice to obesity and obesity-induced osteoarthritis with very high-fat diet. *Ann Rheum Dis,* 72**,** 300-4.
O'CONOR, C. J., LEDDY, H. A., BENEFIELD, H. C., LIEDTKE, W. B. & GUILAK, F. 2014. TRPV4-mediated mechanotransduction regulates the metabolic response of chondrocytes to dynamic loading. *Proc Natl Acad Sci U S A,* 111**,** 1316-21.
ORYAN, A., KAMALI, A., MOSHIRI, A. & BAGHABAN ESLAMINEJAD, M. 2017. Role of Mesenchymal Stem Cells in Bone Regenerative Medicine: What Is the Evidence? *Cells Tissues Organs,* 204**,** 59-83.

OU, Y., RUAN, Y., CHENG, M., MOSER, J. J., RATTNER, J. B. & VAN DER HOORN, F. A. 2009. Adenylate cyclase regulates elongation of mammalian primary cilia. *Exp Cell Res,* 315**,** 2802-17.

PARFITT, A. M. 1982. The coupling of bone formation to bone resorption: a critical analysis of the concept and of its relevance to the pathogenesis of osteoporosis. *Metab Bone Dis Relat Res,* 4**,** 1-6.

PELLEGRIN, S. & MELLOR, H. 2007. Actin stress fibres. *J Cell Sci,* 120**,** 3491-9.

PERRINI, S., NATALICCHIO, A., LAVIOLA, L., CIGNARELLI, A., MELCHIORRE, M., DE STEFANO, F., CACCIOPPOLI, C., LEONARDINI, A., MARTEMUCCI, S., BELSANTI, G., MICCOLI, S., CIAMPOLILLO, A., CORRADO, A., CANTATORE, F. P., GIORGINO, R. & GIORGINO, F. 2008. Abnormalities of insulin-like growth factor-I signaling and impaired cell proliferation in osteoblasts from subjects with osteoporosis. *Endocrinology,* 149**,** 1302-13.

PHAN, M. N., LEDDY, H. A., VOTTA, B. J., KUMAR, S., LEVY, D. S., LIPSHUTZ, D. B., LEE, S. H., LIEDTKE, W. & GUILAK, F. 2009. Functional characterization of TRPV4 as an osmotically sensitive ion channel in porcine articular chondrocytes. *Arthritis Rheum,* 60**,** 3028-37.

PHILLIPS, J. E., PETRIE, T. A., CREIGHTON, F. P. & GARCÍA, A. J. 2010. Human mesenchymal stem cell differentiation on self-assembled monolayers presenting different surface chemistries. *Acta Biomater,* 6**,** 12-20.

PINGGUAN-MURPHY B. & M.M., K. 2008. Mechanosensitive Purinergic Calcium Signalling in Articular Chondrocytes. *In:* KAMKIN A., K. I. (ed.) *Mechanosensitive Ion Channels. Mechanosensitivity in Cells and Tissues.* Dordrecht: Springer.

PINO, A. M., ROSEN, C. J. & RODRIGUEZ, J. P. 2012a. In Osteoporosis, differentiation of mesenchymal stem cells (MSCs) improves bone marrow adipogenesis. *Biological Research,* 45**,** 279-287.

PINO, A. M., ROSEN, C. J. & RODRÍGUEZ, J. P. 2012b. In osteoporosis, differentiation of mesenchymal stem cells (MSCs) improves bone marrow adipogenesis. *Biol Res,* 45**,** 279-87.

PISANI, P., RENNA, M. D., CONVERSANO, F., CASCIARO, E., DI PAOLA, M., QUARTA, E., MURATORE, M. & CASCIARO, S. 2016. Major osteoporotic fragility fractures: Risk factor updates and societal impact. *World J Orthop,* 7**,** 171-81.

PITTENGER, M. F., MACKAY, A. M., BECK, S. C., JAISWAL, R. K., DOUGLAS, R., MOSCA, J. D., MOORMAN, M. A., SIMONETTI, D. W., CRAIG, S. & MARSHAK, D. R. 1999. Multilineage potential of adult human mesenchymal stem cells. *Science,* 284**,** 143-7.

POCHYNYUK, O., ZAIKA, O., O'NEIL, R. G. & MAMENKO, M. 2013. Novel insights into TRPV4 function in the kidney. *Pflugers Archiv-European Journal of Physiology,* 465**,** 177-186.

PRAETORIUS, H. A. & SPRING, K. R. 2001. Bending the MDCK cell primary cilium increases intracellular calcium. *J Membr Biol,* 184**,** 71-9.

PRAETORIUS, H. A. & SPRING, K. R. 2003. Removal of the MDCK cell primary cilium abolishes flow sensing. *J Membr Biol,* 191**,** 69-76.

PRALL, W. C., HAASTERS, F., HEGGEBÖ, J., POLZER, H., SCHWARZ, C., GASSNER, C., GROTE, S., ANZ, D., JÄGER, M., MUTSCHLER, W. & SCHIEKER, M. 2013. Mesenchymal stem cells from osteoporotic patients

feature impaired signal transduction but sustained osteoinduction in response to BMP-2 stimulation. *Biochem Biophys Res Commun,* 440**,** 617-22.
PRINCE, R. L., SMITH, M., DICK, I. M., PRICE, R. I., WEBB, P. G., HENDERSON, N. K. & HARRIS, M. M. 1991. Prevention of postmenopausal osteoporosis. A comparative study of exercise, calcium supplementation, and hormone-replacement therapy. *N Engl J Med,* 325**,** 1189-95.
RAUNER, M., SIPOS, W., GOETTSCH, C., WUTZL, A., FOISNER, R., PIETSCHMANN, P. & HOFBAUER, L. C. 2009. Inhibition of lamin A/C attenuates osteoblast differentiation and enhances RANKL-dependent osteoclastogenesis. *J Bone Miner Res,* 24**,** 78-86.
REICH, K. M. & FRANGOS, J. A. 1993. Protein kinase C mediates flow-induced prostaglandin E2 production in osteoblasts. *Calcif Tissue Int,* 52**,** 62-6.
RESNICK, A. 2015. Mechanical properties of a primary cilium as measured by resonant oscillation. *Biophys J,* 109**,** 18-25.
REZNIKOFF, C. A., BERTRAM, J. S., BRANKOW, D. W. & HEIDELBERGER, C. 1973. Quantitative and qualitative studies of chemical transformation of cloned C3H mouse embryo cells sensitive to postconfluence inhibition of cell division. *Cancer Res,* 33**,** 3239-49.
RHO, J. Y., KUHN-SPEARING, L. & ZIOUPOS, P. 1998. Mechanical properties and the hierarchical structure of bone. *Med Eng Phys,* 20**,** 92-102.
RIDDLE, R. C., TAYLOR, A. F., GENETOS, D. C. & DONAHUE, H. J. 2006. MAP kinase and calcium signaling mediate fluid flow-induced human mesenchymal stem cell proliferation. *Am J Physiol Cell Physiol,* 290**,** C776-84.
RIEHL, B. D., LEE, J. S., HA, L. & LIM, J. Y. 2015. Fluid-flow-induced mesenchymal stem cell migration: role of focal adhesion kinase and RhoA kinase sensors. *J R Soc Interface,* 12.
ROBEY, P. 2017. "Mesenchymal stem cells": fact or fiction, and implications in their therapeutic use. *F1000Res,* 6.
ROBINSON, J. & ENGELBORGHS, Y. 1982. Tubulin polymerization in dimethyl sulfoxide. *J Biol Chem,* 257**,** 5367-71.
RODRÍGUEZ, J. P., GARAT, S., GAJARDO, H., PINO, A. M. & SEITZ, G. 1999. Abnormal osteogenesis in osteoporotic patients is reflected by altered mesenchymal stem cells dynamics. *J Cell Biochem,* 75**,** 414-23.
RODRÍGUEZ, J. P., MONTECINOS, L., RÍOS, S., REYES, P. & MARTÍNEZ, J. 2000. Mesenchymal stem cells from osteoporotic patients produce a type I collagen-deficient extracellular matrix favoring adipogenic differentiation. *J Cell Biochem,* 79**,** 557-65.
RODRÍGUEZ, J. P., RÍOS, S., FERNÁNDEZ, M. & SANTIBAÑEZ, J. F. 2004. Differential activation of ERK1,2 MAP kinase signaling pathway in mesenchymal stem cell from control and osteoporotic postmenopausal women. *J Cell Biochem,* 92**,** 745-54.
ROHATGI, R., MILENKOVIC, L. & SCOTT, M. P. 2007. Patched1 regulates hedgehog signaling at the primary cilium. *Science,* 317**,** 372-6.
ROSS, T. D., COON, B. G., YUN, S., BAEYENS, N., TANAKA, K., OUYANG, M. & SCHWARTZ, M. A. 2013. Integrins in mechanotransduction. *Curr Opin Cell Biol,* 25**,** 613-8.
ROWSON, D., KNIGHT, M. M. & SCREEN, H. R. 2016. Zonal variation in primary cilia elongation correlates with localized biomechanical degradation in stress deprived tendon. *J Orthop Res,* 34**,** 2146-2153.

RUBIN, C. T., CAPILLA, E., LUU, Y. K., BUSA, B., CRAWFORD, H., NOLAN, D. J., MITTAL, V., ROSEN, C. J., PESSIN, J. E. & JUDEX, S. 2007. Adipogenesis is inhibited by brief, daily exposure to high-frequency, extremely low-magnitude mechanical signals. *Proc Natl Acad Sci U S A,* 104**,** 17879-84.

RUDMAN, K. E., ASPDEN, R. M. & MEAKIN, J. R. 2006. Compression or tension? The stress distribution in the proximal femur. *Biomed Eng Online,* 5**,** 12.

RYDHOLM, S., ZWARTZ, G., KOWALEWSKI, J. M., KAMALI-ZARE, P., FRISK, T. & BRISMAR, H. 2010. Mechanical properties of primary cilia regulate the response to fluid flow. *Am J Physiol Renal Physiol,* 298**,** F1096-102.

RÁLIS, Z. A., RÁLIS, H. M., RANDALL, M., WATKINS, G. & BLAKE, P. D. 1976. Changes in shape, ossification and quality of bones in children with spina bifida. *Dev Med Child Neurol Suppl***,** 29-41.

SACCHETTI, B., FUNARI, A., REMOLI, C., GIANNICOLA, G., KOGLER, G., LIEDTKE, S., COSSU, G., SERAFINI, M., SAMPAOLESI, M., TAGLIAFICO, E., TENEDINI, E., SAGGIO, I., ROBEY, P. G., RIMINUCCI, M. & BIANCO, P. 2016. No Identical "Mesenchymal Stem Cells" at Different Times and Sites: Human Committed Progenitors of Distinct Origin and Differentiation Potential Are Incorporated as Adventitial Cells in Microvessels. *Stem Cell Reports,* 6**,** 897-913.

SALEK, M. M., SATTARI, P. & MARTINUZZI, R. J. 2012. Analysis of fluid flow and wall shear stress patterns inside partially filled agitated culture well plates. *Ann Biomed Eng,* 40**,** 707-28.

SAMBROOK, P. & COOPER, C. 2006. Osteoporosis. *Lancet,* 367**,** 2010-8.

SANGHANI-KERAI, A., COATHUP, M., SAMAZIDEH, S., KALIA, P., SILVIO, L. D., IDOWU, B. & BLUNN, G. 2017. Osteoporosis and ageing affects the migration of stem cells and this is ameliorated by transfection with CXCR4. *Bone Joint Res,* 6**,** 358-365.

SATIR, P., PEDERSEN, L. B. & CHRISTENSEN, S. T. 2010. The primary cilium at a glance. *J Cell Sci,* 123**,** 499-503.

SCAGLIONE, S., WENDT, D., MIGGINO, S., PAPADIMITROPOULOS, A., FATO, M., QUARTO, R. & MARTIN, I. 2008. Effects of fluid flow and calcium phosphate coating on human bone marrow stromal cells cultured in a defined 2D model system. *J Biomed Mater Res A,* 86**,** 411-9.

SCHAFFLER, M. B. & KENNEDY, O. D. 2012. Osteocyte signaling in bone. *Curr Osteoporos Rep,* 10**,** 118-25.

SCHUIT, S. C., VAN DER KLIFT, M., WEEL, A. E., DE LAET, C. E., BURGER, H., SEEMAN, E., HOFMAN, A., UITTERLINDEN, A. G., VAN LEEUWEN, J. P. & POLS, H. A. 2004. Fracture incidence and association with bone mineral density in elderly men and women: the Rotterdam Study. *Bone,* 34**,** 195-202.

SCHWARTZ, E. A., LEONARD, M. L., BIZIOS, R. & BOWSER, S. S. 1997. Analysis and modeling of the primary cilium bending response to fluid shear. *Am J Physiol,* 272**,** F132-8.

SEEFRIED, L. A. E. R. A. M.-D. S. A. K. B. A. K. M. A. L. A. A. I. A. A. J. F. 2010. Mechanotransduction in aging and osteoporosis. *Osteologie,* 19**,** 232-239.

SHAMSEER, L., STEVENS, A., SKIDMORE, B., TURNER, L., ALTMAN, D. G., HIRST, A., HOEY, J., PALEPU, A., SIMERA, I., SCHULZ, K. & MOHER, D. 2012. Does journal endorsement of reporting guidelines influence the completeness of reporting of health research? A systematic review protocol. *Syst Rev,* 1**,** 24.

SHARMA, N., KOSAN, Z. A., STALLWORTH, J. E., BERBARI, N. F. & YODER, B. K. 2011. Soluble levels of cytosolic tubulin regulate ciliary length control. *Mol Biol Cell,* 22**,** 806-16.
SHIH, Y. R., TSENG, K. F., LAI, H. Y., LIN, C. H. & LEE, O. K. 2011. Matrix stiffness regulation of integrin-mediated mechanotransduction during osteogenic differentiation of human mesenchymal stem cells. *J Bone Miner Res,* 26**,** 730-8.
SHIMA, W. N., ALI, A. M., SUBRAMANI, T., MOHAMED ALITHEEN, N. B., HAMID, M., SAMSUDIN, A. R. & YEAP, S. K. 2015. Rapid growth and osteogenic differentiation of mesenchymal stem cells isolated from human bone marrow. *Exp Ther Med,* 9**,** 2202-2206.
SIBONGA, J. D. 2013. Spaceflight-induced bone loss: is there an osteoporosis risk? *Curr Osteoporos Rep,* 11**,** 92-8.
SINGLA, V. & REITER, J. F. 2006. The primary cilium as the cell's antenna: signaling at a sensory organelle. *Science,* 313**,** 629-33.
SONAM, S., SATHE, S. R., YIM, E. K., SHEETZ, M. P. & LIM, C. T. 2016. Cell contractility arising from topography and shear flow determines human mesenchymal stem cell fate. *Sci Rep,* 6**,** 20415.
SONG, B., HAYCRAFT, C. J., SEO, H. S., YODER, B. K. & SERRA, R. 2007. Development of the post-natal growth plate requires intraflagellar transport proteins. *Dev Biol,* 305**,** 202-16.
SPASIC, M. & JACOBS, C. R. 2017. Lengthening primary cilia enhances cellular mechanosensitivity. *Eur Cell Mater,* 33**,** 158-168.
SPASIC, M. S., DELP, Q. C. & JACOBS, C. R. 2018. Drug screening of primary cilia-targeted therapies for in vivo osteoporosis treatment. *Cellular and Molecular Bioengineering Conference 2018.* Key Largo, Florida.
STANDRING, S. 2015. *Gray's Anatomy International Edition: The Anatomical Basis of Clinical Practice*, Elsevier Health Sciences.
STAVENSCHI, E., CORRIGAN, M. A., JOHNSON, G. P., M., R. & D.A., H. 2018a. Physiological cyclic hydrostatic pressure induces osteogenic lineage commitment of human bone marrow stem cells: a systematic study. *Stem Cell Research and Therapy*.
STAVENSCHI, E., CORRIGAN, M. A., JOHNSON, G. P., RIFFAULT, M. & HOEY, D. A. 2018b. Physiological cyclic hydrostatic pressure induces osteogenic lineage commitment of human bone marrow stem cells: a systematic study. *Stem Cell Res Ther,* 9**,** 276.
STAVENSCHI, E. & HOEY, D. A. 2018. Pressure-induced mesenchymal stem cell osteogenesis is dependent on intermediate filament remodeling. *FASEB J***,** fj201801474RR.
STAVENSCHI, E., LABOUR, M. N. & HOEY, D. A. 2017. Oscillatory fluid flow induces the osteogenic lineage commitment of mesenchymal stem cells: The effect of shear stress magnitude, frequency, and duration. *J Biomech,* 55**,** 99-106.
STENDERUP, K., JUSTESEN, J., ERIKSEN, E. F., RATTAN, S. I. & KASSEM, M. 2001. Number and proliferative capacity of osteogenic stem cells are maintained during aging and in patients with osteoporosis. *J Bone Miner Res,* 16**,** 1120-9.
STERCK, J. G., KLEIN-NULEND, J., LIPS, P. & BURGER, E. H. 1998. Response of normal and osteoporotic human bone cells to mechanical stress in vitro. *Am J Physiol,* 274**,** E1113-20.
STEWARD, A. J. & KELLY, D. J. 2015. Mechanical regulation of mesenchymal stem cell differentiation. *J Anat,* 227**,** 717-31.

STEWARD, A. J., WAGNER, D. R. & KELLY, D. J. 2014. Exploring the roles of integrin binding and cytoskeletal reorganization during mesenchymal stem cell mechanotransduction in soft and stiff hydrogels subjected to dynamic compression. *J Mech Behav Biomed Mater,* 38**,** 174-82.

STEWART, A., GUAN, H. & YANG, K. 2010. BMP-3 promotes mesenchymal stem cell proliferation through the TGF-beta/activin signaling pathway. *J Cell Physiol,* 223**,** 658-66.

SU, P., TIAN, Y., YANG, C., MA, X., WANG, X., PEI, J. & QIAN, A. 2018. Mesenchymal Stem Cell Migration during Bone Formation and Bone Diseases Therapy. *Int J Mol Sci,* 19.

TAKAO, D. & KAMIMURA, S. 2017. Simulation of intra-ciliary diffusion suggests a novel role of primary cilia as a cell-signaling enhancer. *Dev Growth Differ*.

TANG, Y., WU, X., LEI, W., PANG, L., WAN, C., SHI, Z., ZHAO, L., NAGY, T. R., PENG, X., HU, J., FENG, X., VAN HUL, W., WAN, M. & CAO, X. 2009. TGF-beta1-induced migration of bone mesenchymal stem cells couples bone resorption with formation. *Nat Med,* 15**,** 757-65.

TEITELBAUM, S. L. 2000. Bone resorption by osteoclasts. *Science,* 289**,** 1504-8.

TELLA, S. H. & GALLAGHER, J. C. 2014. Prevention and treatment of postmenopausal osteoporosis. *J Steroid Biochem Mol Biol,* 142**,** 155-70.

TEWARI, D., KHAN, M. P., SAGAR, N., CHINA, S. P., SINGH, A. K., KHERUKA, S. C., BARAI, S., TEWARI, M. C., NAGAR, G. K., VISHWAKARMA, A. L., OGECHUKWU, O. E., BELLARE, J. R., GAMBHIR, S. & CHATTOPADHYAY, N. 2015. Ovariectomized Rats with Established Osteopenia have Diminished Mesenchymal Stem Cells in the Bone Marrow and Impaired Homing, Osteoinduction and Bone Regeneration at the Fracture Site. *Stem Cell Rev,* 11**,** 309-21.

THODETI, C. K., MATTHEWS, B., RAVI, A., MAMMOTO, A., GHOSH, K., BRACHA, A. L. & INGBER, D. E. 2009. TRPV4 channels mediate cyclic strain-induced endothelial cell reorientation through integrin-to-integrin signaling. *Circ Res,* 104**,** 1123-30.

THOMPSON, C. L., WILES, A., POOLE, C. A. & KNIGHT, M. M. 2016. Lithium chloride modulates chondrocyte primary cilia and inhibits Hedgehog signaling. *FASEB J,* 30**,** 716-26.

TOMKINSON, A., REEVE, J., SHAW, R. W. & NOBLE, B. S. 1997. The death of osteocytes via apoptosis accompanies estrogen withdrawal in human bone. *J Clin Endocrinol Metab,* 82**,** 3128-35.

TSANGARI, H., FINDLAY, D. M., KULIWABA, J. S., ATKINS, G. J. & FAZZALARI, N. L. 2004. Increased expression of IL-6 and RANK mRNA in human trabecular bone from fragility fracture of the femoral neck. *Bone,* 35**,** 334-42.

TUMMALA, P., ARNSDORF, E. J. & JACOBS, C. R. 2010. The Role of Primary Cilia in Mesenchymal Stem Cell Differentiation: A Pivotal Switch in Guiding Lineage Commitment. *Cell Mol Bioeng,* 3**,** 207-212.

TURNER, C. H. 1998. Three rules for bone adaptation to mechanical stimuli. *Bone,* 23**,** 399-407.

TURNER, C. H., OWAN, I., ALVEY, T., HULMAN, J. & HOCK, J. M. 1998. Recruitment and proliferative responses of osteoblasts after mechanical loading in vivo determined using sustained-release bromodeoxyuridine. *Bone,* 22**,** 463-9.

TZIMA, E., DEL POZO, M. A., SHATTIL, S. J., CHIEN, S. & SCHWARTZ, M. A. 2001. Activation of integrins in endothelial cells by fluid shear stress mediates Rho-dependent cytoskeletal alignment. *EMBO J,* 20**,** 4639-47.

UIHLEIN, A. V. & LEDER, B. Z. 2012. Anabolic therapies for osteoporosis. *Endocrinol Metab Clin North Am,* 41**,** 507-25.

UPADHYAY, V. S., MUNTEAN, B. S., KATHEM, S. H., HWANG, J. J., ABOUALAIWI, W. A. & NAULI, S. M. 2014. Roles of dopamine receptor on chemosensory and mechanosensory primary cilia in renal epithelial cells. *Front Physiol,* 5**,** 72.

VALENTI, M. T., GARBIN, U., PASINI, A., ZANATTA, M., STRANIERI, C., MANFRO, S., ZUCAL, C. & DALLE CARBONARE, L. 2011. Role of ox-PAPCs in the differentiation of mesenchymal stem cells (MSCs) and Runx2 and PPARγ2 expression in MSCs-like of osteoporotic patients. *PLoS One,* 6**,** e20363.

VAN DE PEPPEL, J., STRINI, T., TILBURG, J., WESTERHOFF, H., VAN WIJNEN, A. J. & VAN LEEUWEN, J. P. 2017. Identification of Three Early Phases of Cell-Fate Determination during Osteogenic and Adipogenic Differentiation by Transcription Factor Dynamics. *Stem Cell Reports,* 8**,** 947-960.

VAN DER EERDEN, B. C., OEI, L., ROSCHGER, P., FRATZL-ZELMAN, N., HOENDEROP, J. G., VAN SCHOOR, N. M., PETTERSSON-KYMMER, U., SCHREUDERS-KOEDAM, M., UITTERLINDEN, A. G., HOFMAN, A., SUZUKI, M., KLAUSHOFER, K., OHLSSON, C., LIPS, P. J., RIVADENEIRA, F., BINDELS, R. J. & VAN LEEUWEN, J. P. 2013. TRPV4 deficiency causes sexual dimorphism in bone metabolism and osteoporotic fracture risk. *Bone,* 57**,** 443-54.

VAUGHAN, T. J., MULLEN, C. A., VERBRUGGEN, S. W. & MCNAMARA, L. M. 2014. Bone cell mechanosensation of fluid flow stimulation: a fluid-structure interaction model characterising the role integrin attachments and primary cilia. *Biomech Model Mechanobiol*.

VERBRUGGEN, S. W., MC GARRIGLE, M. J., HAUGH, M. G., VOISIN, M. C. & MCNAMARA, L. M. 2015. Altered mechanical environment of bone cells in an animal model of short- and long-term osteoporosis. *Biophys J,* 108**,** 1587-1598.

VERMA, S., RAJARATNAM, J. H., DENTON, J., HOYLAND, J. A. & BYERS, R. J. 2002. Adipocytic proportion of bone marrow is inversely related to bone formation in osteoporosis. *J Clin Pathol,* 55**,** 693-8.

VERONESI, F., TORRICELLI, P., BORSARI, V., TSCHON, M., RIMONDINI, L. & FINI, M. 2011. Mesenchymal Stem Cells in the Aging and Osteoporotic Population. *Critical Reviews in Eukaryotic Gene Expression,* 21**,** 363-377.

VIA, A. G., FRIZZIERO, A. & OLIVA, F. 2012. Biological properties of mesenchymal Stem Cells from different sources. *Muscles Ligaments Tendons J,* 2**,** 154-62.

WAGNER, D. R., LINDSEY, D. P., LI, K. W., TUMMALA, P., CHANDRAN, S. E., SMITH, R. L., LONGAKER, M. T., CARTER, D. R. & BEAUPRE, G. S. 2008. Hydrostatic pressure enhances chondrogenic differentiation of human bone marrow stromal cells in osteochondrogenic medium. *Ann Biomed Eng,* 36**,** 813-20.

WANG, Y., MCNAMARA, L. M., SCHAFFLER, M. B. & WEINBAUM, S. 2007. A model for the role of integrins in flow induced mechanotransduction in osteocytes. *Proc Natl Acad Sci U S A,* 104**,** 15941-6.

WATERS, A. M. & BEALES, P. L. 2011. Ciliopathies: an expanding disease spectrum. *Pediatr Nephrol,* 26**,** 1039-56.

WEINBAUM, S., COWIN, S. C. & ZENG, Y. 1994. A model for the excitation of osteocytes by mechanical loading-induced bone fluid shear stresses. *J Biomech,* 27**,** 339-60.

WEN, L., WANG, Y., WANG, H., KONG, L. M., ZHANG, L., CHEN, X. & DING, Y. 2012. L-type calcium channels play a crucial role in the proliferation and osteogenic differentiation of bone marrow mesenchymal stem cells. *Biochemical and Biophysical Research Communications,* 424**,** 439-445.

WHITE, J. P., CIBELLI, M., URBAN, L., NILIUS, B., MCGEOWN, J. G. & NAGY, I. 2016. TRPV4: Molecular Conductor of a Diverse Orchestra. *Physiol Rev,* 96**,** 911-73.

WHITFIELD, J. F. 2008. The solitary (primary) cilium--a mechanosensory toggle switch in bone and cartilage cells. *Cell Signal,* 20**,** 1019-24.

WITKOWSKA-ZIMNY, M., WROBEL, E. & PRZYBYLSKI , J. 2010. THE MOST IMPORTANT TRANSCRIPTIONAL

FACTORS OF OSTEOBLASTOGENESIS. *Advances in Cell Biology,* 2**,** 17-28.

WORTHLEY, D. L., CHURCHILL, M., COMPTON, J. T., TAILOR, Y., RAO, M., SI, Y., LEVIN, D., SCHWARTZ, M. G., UYGUR, A., HAYAKAWA, Y., GROSS, S., RENZ, B. W., SETLIK, W., MARTINEZ, A. N., CHEN, X., NIZAMI, S., LEE, H. G., KANG, H. P., CALDWELL, J. M., ASFAHA, S., WESTPHALEN, C. B., GRAHAM, T., JIN, G., NAGAR, K., WANG, H., KHEIRBEK, M. A., KOLHE, A., CARPENTER, J., GLAIRE, M., NAIR, A., RENDERS, S., MANIERI, N., MUTHUPALANI, S., FOX, J. G., REICHERT, M., GIRAUD, A. S., SCHWABE, R. F., PRADERE, J. P., WALTON, K., PRAKASH, A., GUMUCIO, D., RUSTGI, A. K., STAPPENBECK, T. S., FRIEDMAN, R. A., GERSHON, M. D., SIMS, P., GRIKSCHEIT, T., LEE, F. Y., KARSENTY, G., MUKHERJEE, S. & WANG, T. C. 2015. Gremlin 1 identifies a skeletal stem cell with bone, cartilage, and reticular stromal potential. *Cell,* 160**,** 269-84.

WU, X. Y., PENG, Y. Q., ZHANG, H., XIE, H., SHENG, Z. F., LUO, X. H., DAI, R. C., ZHOU, H. D., WU, X. P. & LIAO, E. Y. 2013. Relationship between Serum Levels of OPG and TGF- β with Decreasing Rate of BMD in Native Chinese Women. *Int J Endocrinol,* 2013**,** 727164.

XIAO, E., YANG, H. Q., GAN, Y. H., DUAN, D. H., HE, L. H., GUO, Y., WANG, S. Q. & ZHANG, Y. 2015. Brief reports: TRPM7 Senses mechanical stimulation inducing osteogenesis in human bone marrow mesenchymal stem cells. *Stem Cells,* 33**,** 615-21.

YOU, J., REILLY, G. C., ZHEN, X., YELLOWLEY, C. E., CHEN, Q., DONAHUE, H. J. & JACOBS, C. R. 2001. Osteopontin gene regulation by oscillatory fluid flow via intracellular calcium mobilization and activation of mitogen-activated protein kinase in MC3T3-E1 osteoblasts. *J Biol Chem,* 276**,** 13365-71.

YOU, J., YELLOWLEY, C. E., DONAHUE, H. J., ZHANG, Y., CHEN, Q. & JACOBS, C. R. 2000. Substrate deformation levels associated with routine physical activity are less stimulatory to bone cells relative to loading-induced oscillatory fluid flow. *J Biomech Eng,* 122**,** 387-93.

YOUREK, G., MCCORMICK, S. M., MAO, J. J. & REILLY, G. C. 2010. Shear stress induces osteogenic differentiation of human mesenchymal stem cells. *Regen Med,* 5**,** 713-24.

YUAN, X., SERRA, R. A. & YANG, S. 2015. Function and regulation of primary cilia and intraflagellar transport proteins in the skeleton. *Ann N Y Acad Sci,* 1335**,** 78-99.

ZAHEER, S., LEBOFF, M. & LEWIECKI, E. M. 2015. Denosumab for the treatment of osteoporosis. *Expert Opin Drug Metab Toxicol,* 11**,** 461-70.

ZAMANI, A., OMRANI, G. R. & NASAB, M. M. 2009. Lithium's effect on bone mineral density. *Bone,* 44**,** 331-4.

ZHANG, W., TAYLOR, S. P., ENNIS, H. A., FORLENZA, K. N., DURAN, I., LI, B., SANCHEZ, J. A. O., NEVAREZ, L., NICKERSON, D. A., BAMSHAD, M., LACHMAN, R. S., KRAKOW, D., COHN, D. H. & GENOMICS, U. O. W. C. F. M. 2018. Expanding the genetic architecture and phenotypic spectrum in the skeletal ciliopathies. *Hum Mutat,* 39**,** 152-166.

ZHANG, X., SCHWARZ, E. M., YOUNG, D. A., PUZAS, J. E., ROSIER, R. N. & O'KEEFE, R. J. 2002. Cyclooxygenase-2 regulates mesenchymal cell differentiation into the osteoblast lineage and is critically involved in bone repair. *J Clin Invest,* 109**,** 1405-15.

ZHENG, B., JIANG, J., LUO, K., LIU, L., LIN, M., CHEN, Y. & YAN, F. 2015. Increased osteogenesis in osteoporotic bone marrow stromal cells by overexpression of leptin. *Cell Tissue Res,* 361**,** 845-56.

ZHOU, B. O., YUE, R., MURPHY, M. M., PEYER, J. G. & MORRISON, S. J. 2014. Leptin-receptor-expressing mesenchymal stromal cells represent the main source of bone formed by adult bone marrow. *Cell Stem Cell,* 15**,** 154-68.

ZHU, Z., YIN, J., GUAN, J., HU, B., NIU, X., JIN, D., WANG, Y. & ZHANG, C. 2014. Lithium stimulates human bone marrow derived mesenchymal stem cell proliferation through GSK-3beta-dependent beta-catenin/Wnt pathway activation. *FEBS J,* 281**,** 5371-89.

ZUO, C., HUANG, Y., BAJIS, R., SAHIH, M., LI, Y. P., DAI, K. & ZHANG, X. 2012. Osteoblastogenesis regulation signals in bone remodeling. *Osteoporos Int,* 23**,** 1653-63.